

TECHNISCHE UNIVERSITÄT MÜNCHEN



Lehrstuhl für Experimentelle Genetik

**SDR and AKR enzymes as a target of rational inhibitor
development and research on functions of new SDR members**

Dorota Patrycja Kowalik

Vollständiger Abdruck der von der Fakultät Wissenschaftszentrum Weihenstephan für
Ernährung Landnutzung und Umwelt der Technischen Universität München
zur Erlangung des akademischen Grades eines

Doktors der Naturwissenschaften

genehmigte Dissertation.

Vorsitzender: Univ.-Prof. Dr. Martin Hrabe de Angelis

Prüfer der Dissertation:

1. apl. Prof.Dr. Jerzy Adamski
2. Univ.-Prof. Dr. Johannes Buchner

Die Dissertation wurde am 09.05.2016 bei der Technischen Universität München eingereicht
und durch die Fakultät für Wissenschaftszentrum Weihenstephan für Ernährung Landnutzung
und Umwelt der Technischen Universität München am 25.11.2016 angenommen.

Zusammenfassung

Hydroxysteroiddehydrogenasen (HSDs) spielen eine bedeutende Rolle in Regulierung der Biosynthese von Steroidhormonen und gehören zur zwei großen Familien der Enzymen: short chain dehydrogenases (SDR) und der aldo-keto reductases (AKR). Die Fehlregulierung einiger HSD-Aktivitäten führt zu verschiedenen schweren Störungen wie Alzheimer Syndrom oder hormonabhängigem Krebs. Deshalb stellen die HSDs schon seit vielen Jahren interessante Ziele für die pharmazeutische Industrie für die Entwicklung neuer spezifischer Inhibitoren dar. Zwei der 17 β -Hydroxysteroid dehydrogenasen, die 17 β -Hydroxysteroiddehydrogenase Typ 3 (zur Familie der short chain dehydrogenases (SDRs) gehörend) und die 17 β -Hydroxysteroid Dehydrogenase Typ 5 (eine Aldo-Keto Reduktase (AKR)), katalysieren die Testosteron Biosynthese und ihre Überaktivität wird assoziiert mit einigen Krankheiten wie Prostatakrebs.

Die Fortschritte in der Bioinformatik und Computer-basierten Methoden für Molekulare Modellierung ermöglichen Hochdurchsatz-Screening Methoden und erleichtern erheblich die systematische Entwicklung neuer enzym-spezifischer Liganden mit den gewünschten Eigenschaften, die später als Medikamente dienen könnten. Kooperierende Forscher der pharmazeutische Firma BioNetWorks und eines Forschungsteams der Universität Innsbruck entwickelten zwei Ligand- und Struktur -basiert Pharmakophormodelle und wendeten diese an, um neue mögliche Inhibitoren gegen die Aktivitäten der 17 β -Hydroxysteroiddehydrogenasen Typ 3 und 5 zu identifizieren. In der vorliegenden Arbeit wurden dann 35 verschiedene, durch das *in silico* Screening ausgewählte Chemikalien zur biologischen Prüfung und Bewertung untersucht. Aus dieser Gruppe wurden einige zukunftssträchtige Substanzen als 17 β -HSD3 oder 5 Inhibitoren für weitere mehr detailliert biologische Prüfungen identifiziert. Einer der Inhibitor-Kandidaten gegen die reduktive Aktivität der 17 β -HSD5 zeigte sogar eine Hemmwirkung im nanomolaren Bereich und wurde daher detaillierter untersucht. Ein Ki von 180 nM und IC₅₀ Werte in Bereich zwischen 140nM und 290nM, abhängig von der Sorte der enzymatischen Assay, wurden ermittelt.

Darüber hinaus wurden 3 in der Forschungsliteratur kaum annotierte humane SDR-Enzyme, die einige Ähnlichkeiten zu gut bekannten Hydroxysteroiddehydrogenasen zeigen, in dieser Doktorarbeit detaillierter charakterisiert: Hydroxysteroiddehydrogenase Typ 8 (HSD17B8), SDR-O (SDR-Orphan) und die Hydroxysteroiddehydrogenase like 2 (HSDL2). Um die Bedeutung für die mögliche Funktionen der Enzyme im Menschen zu erfassen wurden Experimente wie z.B. subzelluläre Lokalisierung durchgeführt, sowie enzymatische Tests zur Überprüfung der Aktivität mit Steroiden und Retinoiden. Während das bevorzugte Vorkommen für zwei der Enzyme einwandfrei festgestellt werden konnte, HSD17B8 findet man in Mitochondrien und HSDL2 in den Peroxisomen oder Mitochondrien, bleibt es für SDR-O ungeklärt. Von den drei Enzymen zeigte nur HSD17B8 eine enzymatische Aktivität mit einem Steroidsubstrat, dem Estradiol, und nur SDR-O eine schwache Aktivität mit einem Retinoid, dem Retinal in Gegenwart von NADH.

Abstract

Hydroxysteroid dehydrogenases (HSDs) play a key role in the regulation of the steroid hormone metabolism and belong to two protein superfamilies the short-chain dehydrogenases/reductases (SDR) and the aldo-keto reductases (AKR). Up-regulation of their enzymatic activity can be involved in pathogenesis of many serious disorders in humans like Alzheimer's disease or hormone-dependent cancers. Thus, since many years HSDs constitute interesting targets for the development of specific inhibitors which could be applied as potent therapeutic drugs. Two of the 17 β -hydroxysteroid dehydrogenases, the 17 β -hydroxysteroid dehydrogenase type 3 belonging to the SDRs and 17 β -hydroxysteroid dehydrogenase type 5 (belonging to the aldoketo reductases (AKRs)), catalyze reactions of the testosterone biosynthesis and an enhanced activity of the enzymes is linked to several androgen-related illnesses such as for example prostate cancer.

Nowadays due to advances in bioinformatics as well computational methods of molecular modelling high throughput rational approaches for designing new enzyme-specific inhibitors are available. Co-operating researchers of the company BioNetWorks and the University Innsbruck developed two ligand- and structure-based pharmacophore models and applied those to identify potential inhibitors for 17 β HSD3 and 5. By this *in silico* screen, 35 chemically diverse compounds we found as potent candidate inhibitors. In this PhD work here the 35 candidate compounds were subjected to biological evaluation. This allowed to discover some promising compounds, which could be lead structures for further researching or pharmacological tools in future projects. One of the compounds against the reductive activity of 17 β HSD5 even displayed an inhibitory activity in the nanomolar range and therefore was characterized in more detail. For this compound a K_i of 180 nM and IC_{50} values ranging between 140nM and 290nM, were found, depending on the kind of enzymatic assay applied.

Moreover, not all recently identified SDRs have been analyzed in detail yet. Three barely annotated human SDR candidates, which reveal some similarities to known hydroxysteroid dehydrogenases, were chosen in this PhD work for further characterization: hydroxysteroid dehydrogenase type 8 HSD17B8, an orphan SDR (SDR-O) and hydroxysteroid dehydrogenase like 2 (HSDL2). In search for their potent functions in human results for e.g., subcellular localization, bioinformatics studies based on sequence analysis of primary amino acid structure as well enzymatic tests checking the activities towards steroid and retinoid substrates are here presented. Two of the enzyme could be assigned to cellular compartments, HSD17B8 to mitochondria, HSDL2 to peroxisomes or mitochondria, while the preferred location of SDR-O remains unclear. Of the three enzymes only HSD17B8 showed an enzymatic activity with a steroid substrate, in that case estradiol, and only SDR-O was able to metabolize a retinoid compound, i.e., weak activity towards retinaldehyde in the presence of NADH as cofactor was observed with the human SDR-O gene.

List of Abbreviations

AKR	aldo-keto reductase
APS	ammoniumperoxodisulfat
cDNA	complementary deoxyribonucleic acid
DAPI	4',6-Diamidino-2-phenylindole,dihydrochlorid
DMSO	dimethylsulfoxid
DNA	deoxyribonucleic acid
dNTP	desoxyribonucleoside triphosphate
ds	double strand
EDTA	ethylendiamintetraacetat
ER	endoplasmatic retikulum
EST	expressed sequence tag
et al.	et alteri
FBS	fetal bovine serum
GFP	green fluorescent protein
GST	gluthation-S-transferase
HMGU	Helmholtz Zentrum München – Deutsches Forschungszentrum für Gesundheit und Umwelt
HPLC	High Pressure Liquid Chromatography
HRP	Horse raddish peroxidase
HSD	Hydroxysteroid dehydrogenase
HSD17BX	17 β -Hydroxysteroid dehydrogenase Type X
IPTG	isopropyl- β -D-thiogalactoside
IEG	Institute of Experimental Genetics
kb	kilobase paar
kDa	kilodalton
λ	lambda, wavelength
NAD ⁺	nicotinamide adenine dinucleotide, oxidized
NADH	nicotinamide adenine dinucleotide, reduced
NADP	nicotinamide adenine dinucleotide phosphate, oxidized
NADPH	nicotinamide adenine dinucleotide phosphate, reduced
OD	optical density
ORF	open reading frame
PBS	phosphate buffered saline
PCR	polymerase chain reaction
PDB	protein data bank
RDH	retinol dehydrogenase
RNA	ribonucleic acid
rpm	rotation per minute
SDR	short-chain dehydrogenase/reductase
SDS-PAGE	sodium dodecyl sulfat - polyacrylamide gel electrophoresis
TEMED	tetramethylethylendiamine

1	INTRODUCTION	1
1.1	Introduction into SDR protein superfamily	1
1.1.1	Structural aspects of SDRs	1
1.1.2	Classification criteria of SDR families	3
1.1.3	Enzymatic activities and substrate specificity	4
1.1.4	Mechanism of catalyzed reaction	6
1.2	Short introduction into AKR enzyme superfamily	8
1.3	Control of biological processes	10
1.3.1	Mechanism of hormone action	11
1.3.1.1	Hormone receptors	12
1.3.1.2	Steroid hormone receptors	13
1.3.1.3	Classical intracellular mechanism of hormone action	14
1.3.1.4	Non-genomic mechanisms of hormone action	16
1.3.2	Steroid hormone metabolism	16
1.3.2.1	Steroid hormone classes	17
1.3.2.2	Steroid hormone biosynthesis	19
1.3.3	Hydroxysteroid dehydrogenases	21
1.3.3.1	3 α -hydroxysteroid dehydrogenases	21
1.3.3.2	3 β -hydroxysteroid dehydrogenases/isomerases	22
1.3.3.3	11 β -hydroxysteroid dehydrogenases	23
1.3.3.4	20 α -hydroxysteroid dehydrogenases	24
1.3.3.5	17 β -hydroxysteroid dehydrogenases	25
1.3.4	Short overview of SDR role on retinol metabolism in human	28
1.3.5	Short overview of SDR role in fatty acid metabolism	31
1.3.6	Orphan SDR proteins reminding hydroxysteroid dehydrogenases	35
1.4	Medical implications of SDRs	35
1.4.1	SDR/HSDs as potent targets for inhibitor development in treatment of hormone-related disease 37	
1.4.2	17 β -HSDs as drug targets in treatment of hormone cancers	37
1.4.2.1	Pathogenesis of hormone -related cancers	38
1.4.2.2	Short overview of sex hormone metabolism. Role of 17 β -HSDs	38
1.4.2.3	Role of 17 β -HSD enzymes in androgen metabolism	40
1.4.2.4	Changes in 17 β -HSD expression in hormone related cancers	41
1.4.2.5	Role of 17 β -HSD3 and 17 β -HSD5 as inhibitor targets in prostate cancer (PCa) therapy	42
1.4.3	Naturally occurring inhibitors of steroidogenesis	44
1.5	Aims of the study	46
2	RESULTS	48
2.1	Inhibitor studies	48
2.1.1	Expression of human 17 β -HSD3	48
2.1.1.1	Establishing the 17 β -HSD3 enzymatic activity	48
2.1.2	Expression of human 17 β -HSD5 (AKR1C3)	48
2.1.2.1	Human 17 β -HSD5 purification and <i>in vitro</i> assay optimization	49
2.1.3	Inhibitor screening results on 17 β -HSD3 and 17 β -HSD5	51
2.1.3.1	1 st round of inhibitor screening	51
2.1.3.2	2 nd round of inhibitor screening	53

2.1.4	Further biological tests with identified inhibitors.....	55
2.1.4.1	IC ₅₀ evaluation and selection of the best inhibitor.....	56
2.1.4.2	Specificity assay among other 17β-HSDs for selected inhibitor.....	57
2.1.5	Optimization of <i>in vitro</i> enzymatic assay by use of 96-well plates.....	57
2.1.5.1	Development of assays based on UV-Vis or fluorescent detection method.....	58
2.1.5.2	Enzymatic assays based on NADH/NADPH detection. Time progress curves.....	60
2.1.5.3	Optimization of <i>in vitro</i> test on 96-well plates with use of artificial fluorescent substrate for 17β-HSD5.....	62
2.1.5.4	In vitro IC ₅₀ estimation for assays with artificial substrate.....	63
2.1.6	Determination of Ki and inhibition mechanism of 2-9 compound.....	64
2.1.7	<i>Ex vivo</i> inhibitor studies.....	66
2.1.7.1	Searching for the best cell line model effectively converting androstenedione by HSD17B5.....	66
2.1.7.2	Optimization of in vivo assays testing the conversion of androstenedione to testosterone by HSD17B5.....	68
2.1.7.3	<i>Ex vivo</i> IC ₅₀ determination.....	71
2.1.7.4	Cell viability tests.....	71
2.2	Studies on partly characterized new SDR candidates.....	73
2.2.1	Cloning and expression of human SDR candidates.....	73
2.2.1.1	Human HSD17B8 expression.....	73
2.2.1.2	Human SDR-O expression.....	74
2.2.1.3	Human HSDL2 expression.....	75
2.2.2	Characterization and function prediction by use of bioinformatics tools basing on primary amino acid sequence.....	76
2.2.2.1	Secondary structure and SDR motives of HSD17B8, SDR-O and HSDL2.....	77
2.2.2.2	Cofactor preference prediction (SDR-O, HSDL2).....	81
2.2.2.3	Amino acid sequence analysis in the context of earlier phylogenetic studies and the sequence homology search (ProDom).....	82
2.2.3	Subcellular localization studies.....	88
2.2.3.1	Preparation of tagged version of studied proteins. Negative control.....	88
2.2.3.2	Subcellular localization studies on human HSD17B8.....	89
2.2.3.3	Subcellular localization studies on human SDR-O.....	90
2.2.3.4	Subcellular localization studies on human HSDL2.....	92
2.2.4	In search for enzymatic activity.....	93
2.2.4.1	Control of transfection procedure.....	93
2.2.4.2	Steroid substrate screening.....	94
2.2.4.3	Retinoid substrate screening.....	96
3	METHODS.....	99
3.1	Bacteria techniques.....	99
3.1.1	Media for bacteria cultures.....	99
3.1.2	Preparation the antibiotic selection media.....	99
3.1.3	Bacteria inoculation.....	100
3.1.4	Bacteria cultivation and harvesting.....	100
3.1.5	Bacteria growth control.....	100
3.1.6	Glycerol stock preparation.....	101
3.1.7	Induction of fusion-protein expression by bacteria.....	101
3.1.8	Bacteria transformation with plasmid DNA.....	102
3.1.9	Bacteria clones analysis.....	102
3.1.10	Preparation of bacteria pellets and homogenated bacteria lysates for enzymatic assays.....	102
3.2	Cell culture techniques.....	103

3.2.1	Cell culture media.....	103
3.2.2	Cell cultivation	104
3.2.2.1	Cell splitting.....	104
3.2.2.2	Cell Counting.....	104
3.2.2.3	Cell freezing.....	105
3.2.2.4	Cell thawing.....	105
3.2.2.5	Cell pelleting.....	105
3.2.3	Cell viability tests.....	105
3.2.4	Cell transfection	106
3.2.5	Stable transfected cell line.....	106
3.3	Methods with proteins.....	107
3.3.1	Isolation of protein fraction from bacteria pellets.....	107
3.3.2	Isolation of protein fraction from mammalian cells	107
3.3.3	SDS-Polyacrylamide Gel Electrophoresis (SDS-PAGE)	108
3.3.4	Western-blot.....	109
3.3.5	Purification of GST-fusion protein	112
3.4	DNA -based methods.....	114
3.4.1	DNA gel agar electrophoresis.....	114
3.4.2	Plasmid DNA isolation from E.coli	115
3.4.3	Purification of dsDNA fragments from agar gel or from reaction assays.....	115
3.4.4	Quality and quantity measurements of nucleic acids by optical density (OD)	116
3.4.5	DNA amplification (PCR method).....	116
3.4.6	Mutagenesis method	117
3.4.7	DNA sequencing	118
3.4.8	Restriction analysis.....	118
3.5	RNA -based methods.....	118
3.5.1	Total RNA isolation from cell	118
3.5.2	mRNA isolation and cDNA synthesis	119
3.6	Cloning strategies	119
3.6.1	TOPO-TA cloning.....	119
3.6.2	Cloning <i>via</i> restriction sites.....	119
3.6.3	Control of proper cloning.....	120
3.7	Immunochemistry methods.....	121
3.7.1	Immunocytochemical and immunofluorescent methods for intracellular localization studies:	121
3.8	Enzyme activity measurements.....	124
3.8.1	<i>In vitro</i> radio-labeled steroid assays for HPLC analysis	124
3.8.2	<i>In vitro</i> substrate specificity screening assays for chosen SDR enzymes:	125
3.8.2.1	Enzymatic assays with ³ H labeled steroid substrates	125
3.8.2.2	Enzymatic assays with retinoid substrates	126
3.8.3	Extraction of radio-labeled steroids from enzymatic assay for HPLC analysis	126
3.8.4	Extraction of retinoids from enzymatic assays for HPLC analysis	127
3.8.5	HPLC measurement	127
3.8.6	<i>Ex vivo</i> inhibitor activity measurements	128
3.8.7	<i>In vitro</i> enzymatic assays based on UV-Vis, fluorescence spectrophotometry.....	129
3.8.7.1	Assay monitoring the oxidative HSD17B5 activity by measuring the changes in NAD(P)H/ NADH absorption or fluorescence:.....	129
3.8.7.2	Assays with application of fluorogenic substrate (8-acetyl-2,3,5,6-tetrahydro-1H, 4H-11-oxa-3a-aza-benzo[de]anthracen-10-one) for HSD17B5.....	129

3.8.8	Enzyme kinetic and inhibition analysis	130
3.8.8.1	Calculation of inhibition percentage	130
3.8.8.2	Determination of IC ₅₀ value for selected inhibitory compounds.....	130
3.8.8.3	Determination of Michaelis-Menten constants and maximum velocity of substrate conversion.....	131
3.8.8.4	Determination of K _i value and mechanism of inhibition (by use of fluorescence detecting methods) 131	
4	MATERIALS	133
4.1	Used bacteria strains	133
4.2	Used cell lines.....	133
4.3	Used plasmid vectors.....	133
4.4	List of utilized antibodies	134
E. Kremmer, Helmholtz Zentrum München		134
4.5	List of used primers (sequences) for PCR methods	135
4.6	List of used ³H-labeled substances	138
4.7	List of utilized enzymes	138
4.8	Kits	138
4.9	Solutions for cell staining	139
4.10	Chemicals, supplements, media	139
4.11	Bioinformatic tools, software.....	141
4.12	Laboratory equipment.....	141
5	DISCUSSION.....	143
5.1	Inhibitor studies.....	143
5.1.1.1	Composition of the enzymatic assay for new inhibitor screening.....	143
5.1.1.2	Choice of the method for measurement the enzymatic activity.....	145
5.1.1.3	In search for alternative, high throughput and non-radioactive enzymatic assay for inhibitor studies. Development of assays based on UV-Vis, fluorescence detection.....	147
5.1.1.4	IC ₅₀ and K _i as values describing the inhibitor potency.....	151
5.1.1.5	Inhibition mechanism for compound 2-9. Can the use of an artificial fluorescence substrate affect the results?	153
5.1.1.6	Evaluation of inhibitor potency in living cells cultures. Comparison of IC ₅₀ values depending on kind of enzymatic assay.....	156
5.1.1.7	Chances of selected 2-9 compound for further development as 17β-HSD5 inhibitor	158
5.1.2	Summary of inhibitor screening studies	161
5.2	Characterization of new SDR candidates	162
5.2.1	Further characterization of human HSD17B8 gene	162
5.2.1.1	Comparison of the results with the present state of knowledge	164

5.2.1.2	Meaning of mitochondrial localization of HSD17B8 in context of putative role in steroid or fatty acid metabolism.....	164
5.2.1.3	Human 17 β -HSD8 as potent inhibitor development target.....	166
5.2.2	In search of function of human SDR-O (SDR9C7).....	167
5.2.2.1	Subcellular localization of human SDR-O.....	167
5.2.2.2	Human SDR-O as retinaldehyde reductase? Confrontation with the present state of knowledge.....	171
5.2.2.3	Comments on SDR-O mRNA expression profile	172
5.2.3	In search of function of human HSDL2	173
5.2.3.1	Comparison of the results with the state of knowledge from literature.....	173
5.2.3.2	Enzymatic assay results	176
5.2.3.2	HSDL2 may be involved in cholesterol or fatty acid metabolism.....	179
5.2.4	Closing remarks on new SDR candidates characterization studies.....	179
6	LITERATURE.....	181
7	APPENDIX.....	198
7.1	Chemical structures of used compounds in screening assays as potent inhibitors of HSD17B3 and HSD17B5	198
7.1.1	1 st screening round.....	198
7.1.2	2 nd screening round.....	201
7.2	List of Figures	205
7.3	List of Tables.....	209
7.4	List of publications and presentations	210

1 Introduction

1.1 Introduction into SDR protein superfamily

Short chain alcohol dehydrogenases/reductases (SDR) form the enormous evolutionarily old enzyme family of a great functional and substrate diversity. The superfamily of short chain dehydrogenases/reductases (SDRs) today comprises over 47.000 members found in pro-and eukaryotes. Among them at least 82 SDR gens have been identified in human genome [1]. First identified enzymes exhibiting the SDR characteristics were a prokaryotic - dehydrogenase and insect alcohol dehydrogenase from *D. melanogaster*. Originally, the SDR protein family was established in 1981 since the discovery of fundamental differences between insect-type and liver-type alcohol dehydrogenases which were classified to 'short-chain alcohol dehydrogenases/reductases' and 'medium-chain alcohol dehydrogenases/reductases,' respectively [2]. Since then new SDR members were added or newly identified. The first identified human SDR member was 15-hydroxyprostaglandine dehydrogenase in 1990 [3] and next further human enzymes were classified to the SDR family such as known since 1950 17 β - hydroxysteroid dehydrogenases type 1 [4, 5]. Most of human SDRs identified up to now play an important role in metabolism of signaling molecules like hormones which activate specific intracellular receptors. Catalytic dysfunctions of chosen SDRs have been reported to be connected with some metabolic disorders in humans and they are involved in hormone-dependent cancers or Alzheimer's disease. Thereby this group of enzymes is considered as important metabolism regulators and thus potent targets for inhibitor development.

1.1.1 Structural aspects of SDRs

Typical SDR monomer is built from 250-400 amino acids. In the secondary structure they create alternately β -strands and α -helices. Proteins belonging to SDR family are characterized by few distinct sequence motifs [Table1] which allow distinguishing them from other functionally related enzyme families such as MDR (medium-chain alcohol dehydrogenases) or AKR (aldo-ketoreductases) [6]. Among them the most conserved of SDRs are a glycine motif (GxxxGxG) and the catalytic motif with the most conservative residues: tyrosine and lysine (YxxxK), where 'x' letter is corresponding to any free amino acid. In spite of low pair-wise sequence identity between SDR

Introduction

members (around 15-30%) they reveal high similarity in 3D structure and α/β folding patterns with the most conserved central β -sheet constituting the Rossmann-fold. Rossmann fold structure is common among proteins binding nucleotide and consists of α -helices and β -strand in the topological order β - α - β - α - β . SDR proteins which bind NAD(P)(H) as cofactor consist of doubled Rossmann fold composed of 6 to 7 β -strands which form a characteristic central β -sheet surrounded by 2 to 3 α -helices on each side [Figure 1][7]. N-terminal region of the SDR monomer containing the Rossmann folds and three glycine motifs is the part of the enzyme responsible for cofactor binding, whereas the C-terminal region comprising the catalytic center is important for substrate binding and product release. Variation in amino acid sequences in the substrate binding region among SDRs is responsible for substrate specificity. For full enzymatic activity SDRs require to form homodimers or homotetramers. Besides of at least one reported exception (case of CBR enzyme) monomers are not active [5, 6, 7, 8].

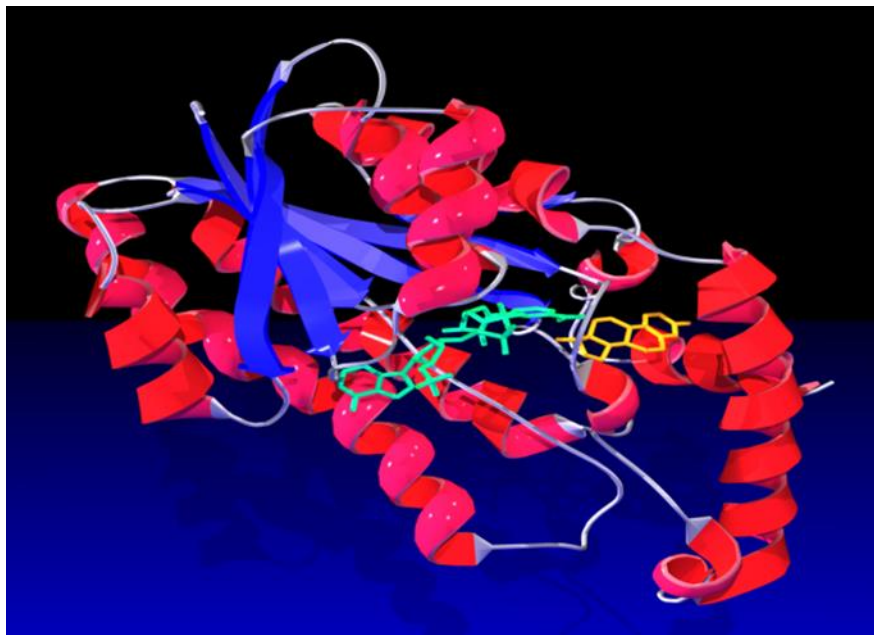


Figure 1 Ribbon diagram of human 17 β -Hydroxysteroid dehydrogenase type 1. β -strands (blue) and α -helices (red) compose two Rossmann folds enabling the cofactor NADP(H) (green) binding. The steroid substrate (estrone) is marked in yellow. Picture adapted from pdb, modified by J. Adamski.

Introduction

It is expected that formation of dimers or tetramers allow correct orientations of key catalytic residues in the active site towards substrate [7, 8].

Table 1 Conserved sequence motifs of SDR family [9].

Motif	Secondary structure localization	Function
TGxxxGxG	$\beta 1 + \alpha 1$	Coenzyme binding region
D	$\beta 3 + \alpha 3$	Stabilization of adenine ring pocket
NNAG	$\beta 4$	Structural role in stabilizing central β -sheet
N	$\alpha 4$	Part of active site (part of catalytic tetrad)
S - Y - K	$\beta 5 + \alpha 5$	Part of active site (part of catalytic tetrad)
N		Connection of the substrates binding loop and the active site
PG	$\beta 6$	Structural role, reaction direction
T		H-bonding to carboxamide of nicotinamide ring

1.1.2 Classification criteria of SDR families

At first classification trial there have been distinguished the 'classical' SDR enzymes with 250-odd residues and sharing the typical for SDR motifs [Table 1] from 'extended' ones which differed in glycine residue pattern in the coenzyme binding region as well in size of around 350 amino acid residues [2]. Next big-scale systematic classification was performed by use of multiple sequence alignment utilizing a hidden Markov model (HMM) in phylogenetic searching of all then existing in protein databases (Swissprot, KIND) SDR sequences and their putative members [1]. The project resulted in final subdivision into five families (types) which apart of 'classical' and 'extended' were created 'intermediate', 'divergent' and 'complex' [Table 2]. This new classification is based on specific SDR motif occurrence and their variations with conservative replacement [9].

Introduction

Table 2 Main differences between particular SDR subfamilies (Persson *et al.*, 2003); [9].

SDR types	Gly-motif	catalytic center	Seize
classical	TGxxxGxG	YxxxK	~250 aa
extended	TGxxxGhaG	YxxxK	~350 aa
intermediate	G/AxxGxxG/A	YxxxK	~250 aa
divergent	GxxxxxSxA	YxxMxxxK	
complex	TGxxxGxG	YxxxN	

Recently, on the basis of this classification updated with new identified sequences (by use of HMM approach) was developed a new nomenclature system of SDR enzymes allowing the division on families regarding the catalyzed substrates and which enables easy adaptation for new identified SDR sequences [10]. So far, over 300 SDR families have been identified including 47 SDR families in humans corresponding to 82 genes [1].

1.1.3 Enzymatic activities and substrate specificity

Enzymes belonging to the superfamily of SDR proteins are in the first instance NAD(P)H/NAD(P) – dependent oxidoreductases (EC 1.x.x.x) catalyzing the inter-conversion of hydroxyl- and keto-groups on many substrates [Figure 2].

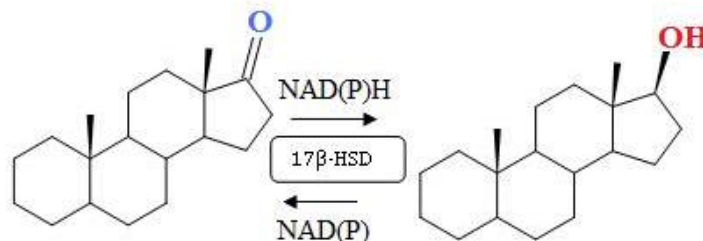


Figure 2 Oxido-reduction on example of 17 β -hydroxysteroid dehydrogenase type 1.

Thereby they play the significant role in various metabolic pathways of living organisms where the oxidation or reduction step is required. From among wide spectrum of utilized by SDRs substrates

Introduction

one can find sugars, fatty acids, steroids, retinoids, bile acids, prostaglandins, aliphatic alcohols, amino acids or xenobiotic [Table 3]. However, oxidoreductases constitute the majority some SDRs exhibit the enzymatic activity of other EC classes such as hydrolases (EC 3.x.x.x), isomerases (EC 4.x.x.x) or liases (EC 5.x.x.x). In humans, SDRs participate in many fundamental metabolic processes through providing the intermediates into numerous biochemical pathways. Among them first the most extensively studied human SDR members were enzymes connected with pathway of steroid hormone biosynthesis represented by 3 β -, 17 β -, 11 β -hydroxysteroid dehydrogenases. Hydroxysteroid dehydrogenases catalyze the inter-conversion of keto/hydroxyl residues on key position of steroid backbones and thus changing their potency of the hormones.

Table 3 Examples of substrates catalyzed by human SDR enzymes.

Type of substrate	substrate	Metabolism of	SDR member example	SDR family
sugar	UDP-galactose	galactose, glucose	UDP-galactose 4-epimerase [11]	SDR1E1-1
steroid	estradiol	17 β -steroid hormones	17 β -hydroxysteroid dehydrogenase 1 (HSD17B1) [12]	SDR28C1-1
steroid	cortisol	11 β -steroid hormones	11 β -hydroxysteroid dehydrogenase 1 (HSD17B1) [13]	SDR26C1
retinoid	all-trans-retinol, 13-cis-retinol	retinoids	Retinol dehydrogenase 16 (RODH-4) [14]	SDR9C8
prostaglandin	hydroxy-PGDH	prostaglandines	15-hydroxyprostaglandin dehydrogenase [NAD+] [15]	SDR36C1-1
amino acid	sepiapterine	neurotransmitters	Sepiapterine reductase (SPRE) [16]	SDR38C1-1
amino acid	dihydropteridine	neurotransmitters	Quinoid dihydropteridine reductase (QDPR) [17]	SDR33C1-2
fatty acid	2,4-dienoyl-CoA	unsaturated fatty acids	DECR 1 [18]	SDR18C1
fatty acid	saturated fatty acyl-CoA (C16-C18)	fatty alcohols, wax esters	Fatty acyl-CoA reductase 1 (FAR1) [19]	SDR10E1-1
Sterol	zymosterone	Cholesterol, bile acids	3-ketosteroid reductase (HSD17B7) [20]	SDR37C1-1

Introduction

1.1.4 Mechanism of catalyzed reaction

Classical reaction catalyzed by SDR enzyme is the redox process leading to inter-conversion of substrate with ketone group to its alcohol form and vice versa at the presence of NAD(P)/NAD(P)H as cofactors. Intensive studies on 3D-crystal structure of human 17 β -HSD1 in complex with ligand and cofactor [21] as well the structure of other SDRs [22] allowed to propose a model of molecular mechanism of reaction which is a general acid/base catalysis involving a catalytic triad of S-Y-K residues at the substrate binding site of enzyme [Figure 3]. Namely, in the considered mechanism tyrosine residue of the catalytic triad functions as the main catalytic base towards oxygen atom of reacting ketone group of the substrate, whereas serine stabilize the substrate *via* hydrogen bonds between reacted keto-oxygen of a substrate and thus probably stabilizes the transition state of the reaction and the proper orientation of a substrate in binding pocket. In turns, a protonated side chain of lysine (NH₃⁺) forms hydrogen bonds with the nicotinamide ribose hydroxyl groups (O2 and O3) enabling its proper position during catalysis and facilitate a proton transfer probably due to lowered pK_a of the hydroxyl group of tyrosine [6].

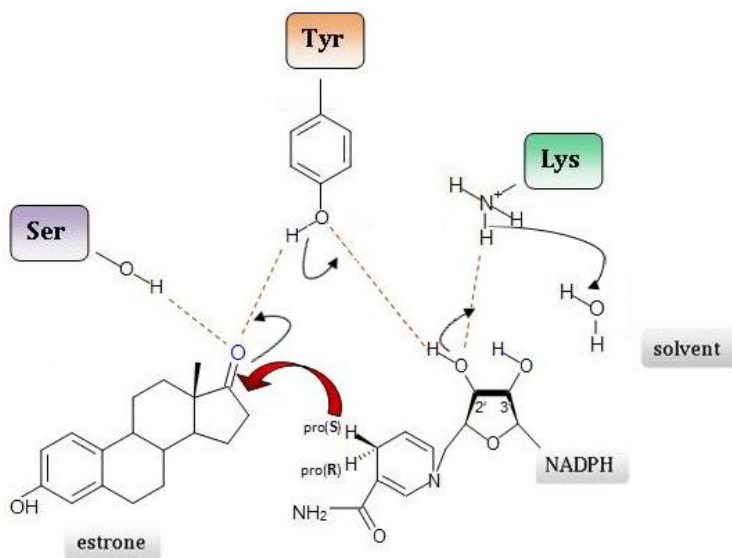


Figure 3 Reaction mechanism for the reduction of estrone to estradiol by human 17 β -HSD1 and the role of S-Y-K residues at catalytic center. Black arrows show hypothesized proton transfer during reaction; red arrow indicates the pro-S-hydrid transfer. Picture modified on base of a scheme at Deluca *et al.* 2004 [23].

Additionally, besides of conserved residues of catalytic tetrad essential role in the redox catalysis plays asparagine located N' terminally of the S-Y-K triad in really forming a catalytic tetrad N-S-Y-K

Introduction

in many SDR members. Asparagine of the proposed catalytic tetrad is suggested to be crucial for maintenance of the active site [7, 24]. Concerning the stereometry of hydride transfer between ketone/alcohol reacting group of the substrate and coenzyme, SDR enzymes seem to catalyze exclusively 4-pro-S hydride transfer in contrast to other functionally similar enzymes from other families like AKR or MDR catalyzing rather 4-pro-R hydride transfer [Figure 3 and 5][25].

Introduction

1.2 Short introduction into AKR enzyme superfamily

The aldo-keto reductases (AKRs) apart of SDRs and MDRs (Medium-chain dehydrogenases/reductases) are one of three enzyme superfamilies that perform NAD(P)(H) linked oxido-reduction on a wide variety of natural and foreign substrates [26]. Enzymes of this superfamily comprises fifteen different families containing over 150 members including at least 13 members in humans [26, 27]. Details for systematic nomenclature as well information and updates for new identified AKR family members are continuously provided on a web site: www.med.upenn.edu/akr maintained by Professor T. Penning at the University of Pennsylvania.

Primary function of AKRs is reducing of aldehydes and ketones to their corresponding primary and secondary alcohols [27]. Among variety of utilized physiological substrates there are lipids steroids, catecholamines, prostaglandins or retinoids. They can also catalyze the oxidation reactions on example of hydroxysteroids and trans-dihydrodiols of polycyclic aromatic hydrocarbons [26]. In human AKRs are involved in the metabolism of sugar aldehydes, reactive lipid aldehydes, ketoprostaglandins, ketosteroids and recently even more evidences indicate their role in the metabolism of xenobiotic substrates such as drugs or chemical carcinogens [27, 28].

Concerning structural aspects majority of AKRs are in contrast to SDRs soluble and monomeric proteins of approximately 320 amino acids and they share characteristic TIM barrel motif. This motif named so after the prototypical structure of triosephosphate isomerase (TIM) possess a characteristic protein fold built from eight α -helices alternating with eight β -strands in such a manner that β -strands lie parallel in a circular tilted array taking shape of barrel whereas α -helices surround it outside forming disordered loops [26,27,29][**Figure 4**]. The substrate-binding site of the enzyme is located in a large, deep elliptical and hydrophobic pocket at the C'-terminal end of the β -barrel with a bound NADPH in an extended conformation [30]. The loops at the back of the barrel may undergo a conformational change upon binding cofactor and the substrate carbonyl so that the correct sequences order in the processed reaction is preserved [27]. Flexibility of these loops explains also the broad substrate specificity in many AKR members.

Introduction

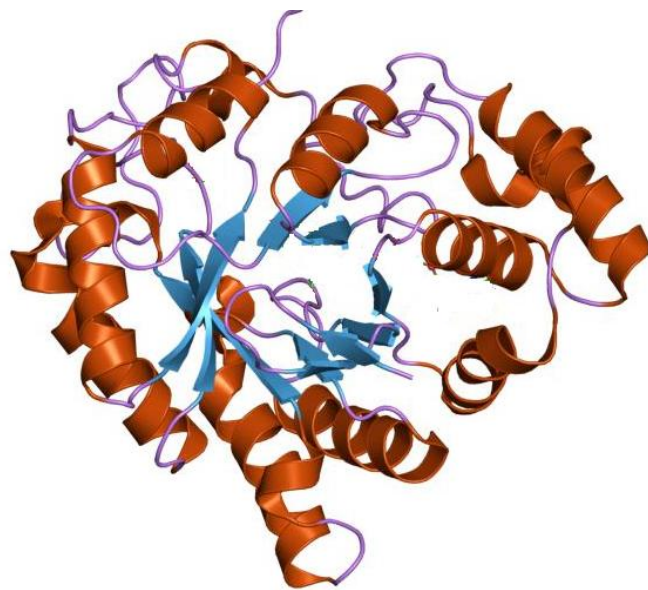


Figure 4 Ribbon diagram of human AKR1C3. Picture adopted from pdb (ID 1XF0).

Located at the base of the barrel active site of the AKR enzyme contains highly conserved catalytic tetrad consisting of **Y55**, **H117**, **D50** and **K84** (numbering according to AKR1C9) in which analogously to SDR enzymes the catalytic tyrosine (Y55) acts as the general acid/base [27]. However, in contrast to SDRs the position of catalytic tyrosine and histidine is the *re* face towards nicotinamide ring of the cofactor, which donates 4-*pro-R* hydride in AKR reactions [25].

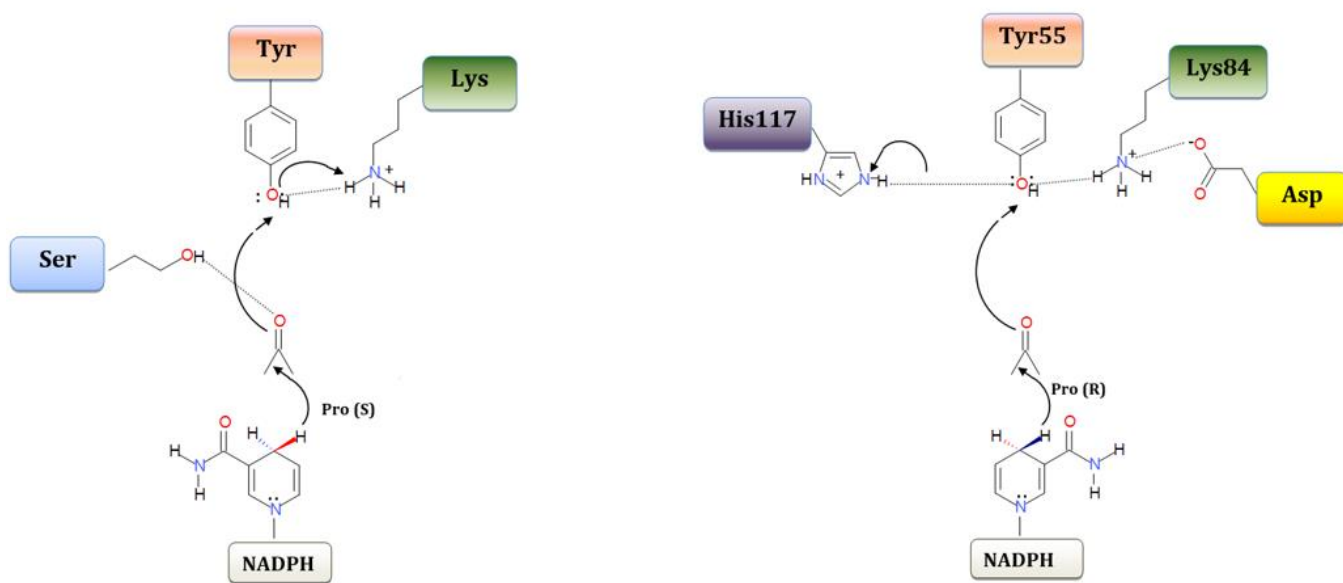


Figure 5 SDR catalytic amino acids (left) versus catalytic amino acids of AKRs (right) and hydride transfer on example of reduction reaction of carbonyl group. Picture modified on the base of the scheme after [25].

Introduction

Among AKR enzymes the special interest of pharmaceutical companies as a target for development of potent inhibitors is focused on human Aldo-ketoreductases from families AKR1C1-AKR1C4 and AKR1D1 since they play essential roles in the metabolism of all steroid hormones, biosynthesis of neurosteroids and bile acids. They catalyze reductions at the C3, C5, C17 and C20 positions on the steroid backbone and side chain [Figure 8]. Their activity has been reported to be implicated in pathogenesis of hormone dependent diseases including prostate, breast and endometrial cancers [31]. Recently, a new characterized human AKR enzyme from Aldo-keto reductases 1B family, named AKR1B15, has been reported to have an activity of retinaldehyde reductase [32] and 17 β hydroxysteroid dehydrogenase [33].

1.3 Control of biological processes

The homeostasis can be expressed as the ability to control or self-regulation of biological processes in multi-cellular organisms and it is essential for survival. The maintenance of homeostasis is possible owing to dynamic cooperation with different cells based on efficient systems of inter-cellular information exchange. Most often this information exchange is performed by use of chemical signals represented by different group of chemical compounds named generally as signaling molecules. Such a signaling compound after synthesis in a specialized cell can induce biochemical, physiological or genomic answer in the target cell. Whereas signaling molecules regulate the metabolism and functions on cellular level the term hormones describes rather signaling molecules which coordinate functions and metabolism of the whole organism. In human body hormones are important for proper homeostasis.

Among substrates catalyzed by SDRs there are many lipophilic compounds such as lipids, steroids, prostaglandins, retinoids or bile acids in which the latter can also act as signaling molecules. The mentioned here lipophilic hormones usually regulate the essential for survival and life continuity metabolisms and they will be further in the special interest of this work as potent substrate of SDR enzymes.

Introduction

1.3.1 Mechanism of hormone action

As mentioned above the general mechanism of hormones action relies on synthesizing and secretion of the signaling molecule from synthesizing cell and finally binding as a ligand with the specific hormone receptor and thus triggering the specific answer. However, considering the manners of hormones secretion and next achieving the receptor in a target cell there are distinguished few ways of hormone action [Figure 6]:

- **endocrine** - in which the hormone is secreted by cells of the endocrine gland directly into the blood before it reaches the target tissue and cell,
- **paracrine**- where secreted hormone has influence on cells in neighborhood,
- **autocrine**- where hormone exerted from a cell has an influence backwards on the same cell,
- **intracrine**- where hormones act within the same cells in which are synthesized,
- **juxtacrine**- where signal emitted by cell affects adjacent cells with those is in direct physical contact through connexons without crossing the cell membrane. In one of the three types of juxtacrine signal emitting relatively small molecules (for example acting as secondary messengers) can be transported *via* communication gaps [34].

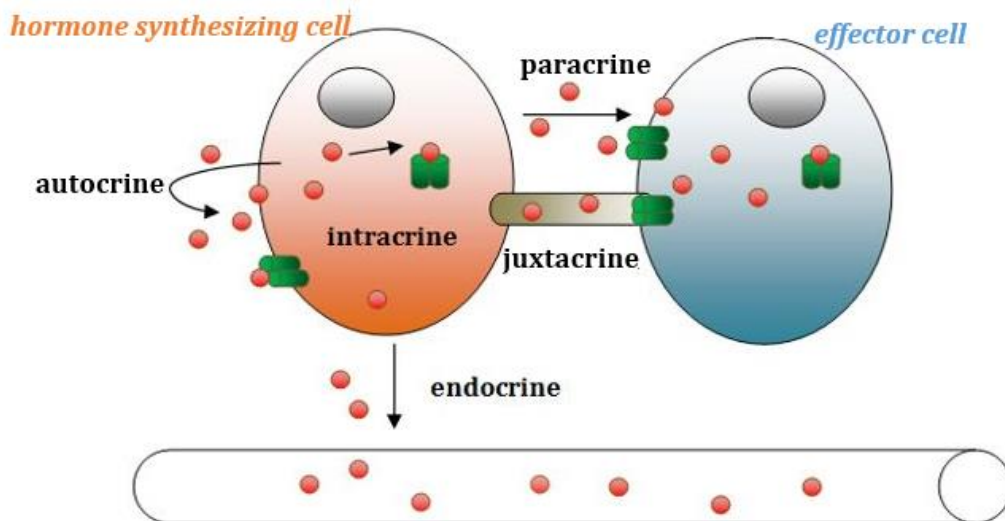


Figure 6 Simplified scheme for mechanisms of hormone action.

Introduction

Coming back to the term 'intracrine' one can describe with it the mechanism of hormones action inside the cells and usually it refers to either signaling molecules which can enter passively through the cell membrane and act inside on intracellular/nuclear receptors like steroid hormones or to some peptide/protein hormones which exhibit intracellular action apart of their classical signal transduction *via* membrane receptors. The whole process in which enzymes regulate the access of biologically active hormone to receptor and subsequent gene expression within the cell is named as the intracrine modulation. The term was first coined by Labrie *et al.* 1988 [35] in order to describe the action of sex steroid hormones [35, 36]. Many members of SDR family play a key role in modulation of intracrine hormone's metabolism.

1.3.1.1 Hormone receptors

Hormone specific receptors are proteins able to bind with ligand molecules of the hormone thus trigger the specific answer. Many of signaling molecules like protein or peptide hormones bind with plasma surface receptors such as:

- transmembrane receptors conjugated with ion channel, typical for neurotransmitters. for example receptor GABA_A in neuronal central system,
- transmembrane receptors bound through G protein with ion channel or system that transduces further the signal through enzymes activating the second messengers or
- transmembrane receptors bound with enzymes like: tyrosine kinase or serine-threonine kinases.

Another group of hormone receptors are intracellular receptors whose ligands are usually lipophilic and low weight signaling molecules potentially able to passively diffuse across the plasma membrane. Among them are nuclear receptors which can be located direct in nucleus or intracellular receptors first activated in cytoplasm and next trans-located into nuclear genome where act as transcription factor or as their co-activators (for instance signaling pathway with fatty acids and PPAR α receptors) [Table 4]. Such intracellular hormone receptors and induced pathways of gene activation are 'classical' (it means the best known and studied) for steroid hormones.

Introduction

Table 4 Examples of intracellular receptors and corresponding ligands being metabolites of SDR substrates

Nuclear receptors	ligand – being the SDR substrate
AR	testosterone, 5 α -DHT
ER α , ER β	estradiol
PR	progesterone
GR	cortisol, corticosterone
MR	aldosterone, cortisol
LXR	lipids, oxysterols
FXR	farnesoid, bile acids, androsterone
PXR	allopregnanolone
RAR	all-trans-retinoic acid
RXR	all-trans-retinoic acid, 9-cis-retinoic acid
PPAR α , PPAR γ	prostaglandins

1.3.1.2 Steroid hormone receptors

Steroid hormones can recognize nuclear receptors localized inside the target cell and what becomes more evidence, also the receptors associated with plasma membrane. Simultaneously, considering the studied intensively interrelations (cross-talk) between various intracellular signaling pathways the final response mediated by these two types of receptors may be both genomic and non-genomic. Classical nuclear receptors for steroid hormones constitute a steroid/thyroid hormone receptor family being a part of a big superfamily of nuclear receptors [37]. They share common structural elements such as characteristic helical sandwich structure around steroid ligand and they are transcription factors controlling the gene expression. Among them the 3rd subfamily classified as Estrogen Receptor-like comprises receptors for estrogens (ER α ER β), estrogen related receptors and 3-Ketosteroid receptors (GR, PR, MR, AR).

Nuclear receptors can be further distinguished on four different types concerning the mechanism of action and manner of binding to DNA [Table 5]. DNA sequence with which binds the receptor complex named as Hormone Specific Elements (HREs) consists of two usually palindromic arranged sites (direct and inverted repeats) often separated by a variable length of DNA. Type I and II mechanisms of action are principal for receptors binding with steroid hormones (GR, PR, MR, AR, ER) and retinoic acid (RXR, RAR), respectively [Figure 7].

Introduction

Table 5 Types of hormone intracellular action and activation of nuclear receptor. Table modified after [37] and [38].

	Mechanism of activated nuclear receptor action
Type I	nuclear receptor in the cytosol, ligand binding preceded by dissociation of heat shock proteins (Hsp) changing the ligand binding status of the receptor, homo-dimerization, translocation into nucleus, binding to specific sequence of DNA (Hormone Specific Elements, HREs). [Figure 7,A]
Type II	nuclear receptors localized in nucleus, ligand binding, hetero-dimerization, binding to HREs of DNA sequence often preceded with dissociation of co-repressor protein and recruitment of co-activators proteins. [Figure 7, B]
Type III	similar to type I receptors as they bind to DNA as homodimers. However in contrast to type I, bind to direct repeats instead of inverted repeats of the HREs
Type IV	nuclear receptors bind either as monomers or dimers, but only a single DNA binding domain of the receptor binds to a single half site HRE. Typical in most of the NR subfamilies.

1.3.1.3 Classical intracellular mechanism of hormone action

On example of two lipophilic signaling molecules: retinoic acid and endocrine sex steroid hormones the hormone molecules (often in the form of inactive pro-hormone such as retinol or DHEA, respectively) are first taken from blood where they are usually transported as bound with specific transport protein. In case of retinol the transporter proteins are Retinoid Binding Proteins (RBP) and in case of sex steroid hormones like DHT, testosterone, androstenediol, estradiol or estrone it is a specific Sex Hormone Binding Globulin (SHGB) or other non-specific plasma binding proteins. Next, the hormone molecule dissociate from the complex with protein and enter the target cell where are further subjected to intracrine modulations by enzymes (for example desulfatase enzymes in case of DHEA-S, E1S or Adione-S). Whereas in the cytoplasm retinol is immediately bound by specific Cellular Retinol Binding Proteins (CRBP) and subsequently converted by enzymes to it's the most potent form which is retinoic acid the activated by specific enzymes steroid hormones may recognize and bind directly with their specific intracellular receptors. The access to steroid receptors is then controlled by inter-converting enzymes such as hydroxysteroid dehydrogenases which act as switchers between active and not active forms of steroids thus changing their potency of binding to the receptor. Additionally, freely access to the steroid hormone receptors can be controlled by bound with receptors heat shock proteins which first have to dissociate from the complex with receptor before hormone bind, dimerize and next as homodimer complex is translocated into nucleus and activate DNA transcription by binding with HRE

Introduction

sequences of promoter regions. In turns, retinoic acid enter the nucleus in order to bind with its specific receptors (RARs) and the retinoid X receptors (RXRs) which themselves heterodimerize and bind to a sequence of DNA known as RARE (retinoic acid response element) activating the targeted gene expression. Although, here below [Figure 7] has been schemed only a simplified pathway of intracellular hormone action, in really for final gene activation induced by steroid hormone at least several binding proteins have to interact additionally with a steroid nuclear receptor such as steroid receptor co-activators (SRCs) or co-intergrations (CREB) among others that appropriately modulate stimulatory or inhibitory transcriptional effect.

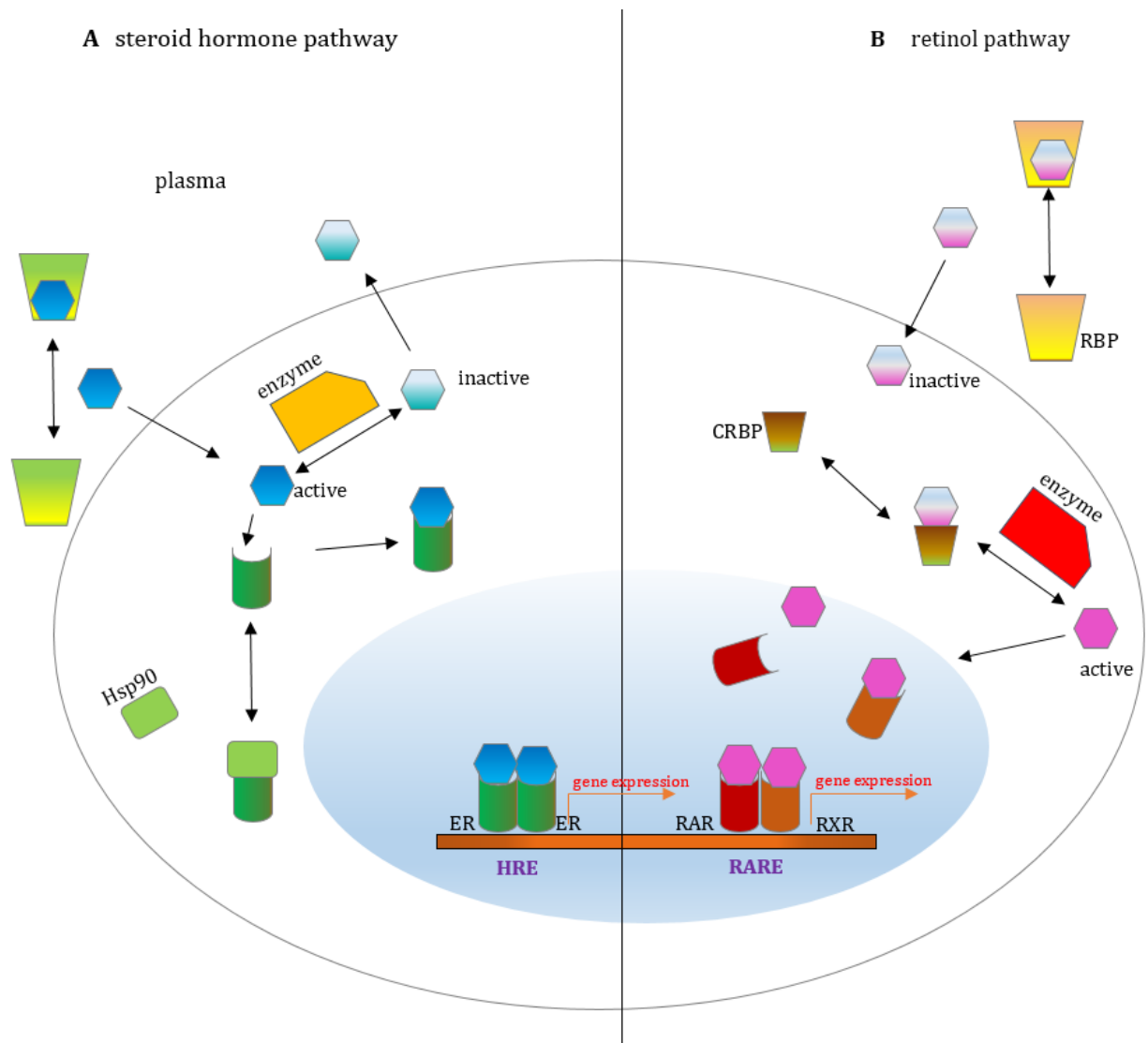


Figure 7 Simplified scheme of classical model for cellular mechanism of steroid hormone (A) and retinoid (B) action.

Introduction

1.3.1.4 Non-genomic mechanisms of hormone action

Apart of performed typical pathway of gene activation by steroids there are recognized also other ways of steroid hormone action usually by binding to membrane associated receptors or through direct triggering the given effector. Such the actions of steroid hormones are referred to as 'rapid actions' or 'non-genomic' actions [39]. As an example can serve the signal transduction through membrane aldosterone receptor [40] or inhibition of apoptosis by androgen [41]. Some of steroid hormones and their metabolites (for example neuroactive 3α -hydroxysteroids) can also act as allosteric modulators of neurotransmitter receptors like GABA_A [42]. Allopregnanolone and androsterone are examples of naturally occurring 3α -hydroxysteroids that act as positive allosteric regulators of γ -aminobutyric acid type A receptors [43]. These both are examples of steroid hormones which act through classical intracellular steroid hormone receptor or as allosteric modulators in GABA_A.

1.3.2 Steroid hormone metabolism

All naturally occurring in human organism steroid hormones are derivatives of cholesterol and pregnenolone as intermediate [chapter 1.3.2.2]. They share the same as cholesterol cyclopentanophenanthrene ring (tetracyclic skeleton) as well atomic numbering system [**Figure 8**]. Apart of pregnenolone and steroid hormones the cholesterol is precursor for bile acids and vitamine D group, another important for metabolism molecules which can also act as signaling molecules and interact with their corresponding nuclear receptors.

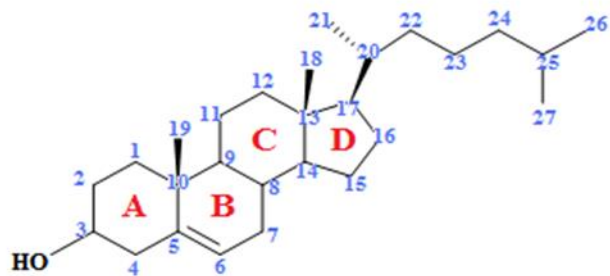


Figure 8 Numbering rule of steroids shown in cholesterol molecule

Introduction

Utilized for steroid biosynthesis cholesterol can be both derived dietary or synthesized *de novo*. The whole process of *de novo* synthesis which take a place usually in liver cells (but partially also in intestine, reproductive organs or adrenal glands) is then strictly regulated by level of cholesterol in organism. Biosynthesis of cholesterol is a multistep process of approximately 30 enzymatic reactions which starts in cytosol from one molecule of acetyl-CoA and one molecule of acetoacetyl-CoA. One can distinguish five major steps of cholesterol synthesis which are:

- formation of 3-hydroxy-3-methylglutaryl-CoA (HMG-CoA) from Acetyl-CoAs
- conversion of HMG-CoA to mevalonate
- conversion of mevalonate to isopentenyl pyrophosphate (IPP) with the concomitant loss of CO₂
- squalene formation from IPP
- conversion of squalene to cholesterol

Depending from catalyzing given step enzymes biosynthesis of cholesterol can be compartmentalized in the cytosol, ER or peroxisomes. Few of SDR enzymes are reported to participate in cholesterol biosynthesis in reduction reactions utilizing NADPH as cofactor.

1.3.2.1 Steroid hormone classes

Steroid hormones are ordered to five major classes according to their corresponding nuclear receptors with which they bind. There are:

Progestagens: group of steroid hormones whose steroid backbone consists of 21-carbones (C21 pregnane skeleton) involved in the female menstrual cycle and being essential for maintain of pregnancy among many other functions. Progesterone is the major naturally occurring human progestagen and at once the only one biologically active that bind with PR receptor. The hormone is produced by ovaries (in corpus luteus), adrenal glands and during the pregnancy in placenta. In endocrine pathway progestagens are transferred in blood as bound with transcortine proteins (CBG, Corticosteroid Bining Globulin) or as its sulfate for example pregnenolone which is precursor of neurosteroids. Since progesterone is an intermediate product for other steroids formation all tissues producing steroid hormones are naturally capable of progestagens synthesizing.

Glucocorticoids: together with mineralocorticoids are named generally as corticosteroids due to place of their endocrine production which is cortex of adrenal glands (*zona fasciculata*, *zona reticularis* are responsible for cortisol production apart of DHEA and DHEA-S). Similarly to progestagen corticosteroids contain a 21-carbone steroid backbone. Cortisol is the most

Introduction

biologically active glucocorticoid binding with GR receptor while cortisone is its inactive form. Glucocorticoids are key regulators of a whole-body homeostasis: they regulate the glucose metabolism (gluconeogenesis as well the formation of glycogens), enhance the degradation of fat and proteins as well they inhibit inflammatory response through down-regulation of pro-inflammatory proteins expression. Corticosteroids are synthesized from progesterone and can be further precursor for aldosterone formation. In blood they circulate usually as bound with CBG proteins or other nonspecific plasma globulin proteins.

Mineralocorticoids: are represented by aldosterone which binds with MR receptor. The receptor for mineralocorticoids can be also activated by cortisol which binds with MR receptor with equal potency as aldosterone. Aldosterone is produced in adrenal cortex (*zona glomerulosa*). It acts on distal tubules of the kidney to increase the reabsorption of Na^+ and the excretion of K^+ and H^+ thus control the electrolyte and water level. The hormone has also influence on blood volume and blood pressure in the body.

Androgens: 19-carbone steroids, which as hormones are responsible for development of male secondary sex characteristics. The most active of androgens which bind with AR receptor is 5α -DHT (5α -dihydrotestosterone) following by less potent testosterone. Many of androgens like DHEA (or DHEA sulfate, DHEA-S) androstenediol, androstenedione or androsterone are produced in adrenal cortex end excreted into blood as weak steroids or just precursors of their more potent forms. In production of active androgens are involved testis (Sertoli cells), ovaries, prostate gland (Wolfian ducts) and other tissues having active enzymes able to convert steroid precursors in the intracrine processes. Details for androgenic/estrogenic actions and metabolism will be described further in the chapter dedicated for their role in the pathogenesis of hormone sensitive cancers [chapter1.4.2].

Estrogens: are in turns 18-carbone steroids and they are responsible for development of female secondary sex characteristics. The most potent estrogen binding with ER receptor is estradiol (E2) whereas estrone is its less active form (E1). Estrone sulfonated further by sulfotransferase (SULT1E1) to estrone sulfate (E1S) is inactive form of the hormone. Estrogens are produced from androgenic precursors not only by ovaries (corpus luteum, granulosa cells) and placenta during pregnancy but also by adrenal glands, liver, fat cells or breast cells which are important source of local estrogens in postmenopausal women.

Introduction

1.3.2.2 Steroid hormone biosynthesis

Dietary or synthesized *de novo* cholesterol is transported with plasma into various cells like gonads or adrenal glands which can further convert it to appropriate steroid hormones. Transformation of containing 27 carbones cholesterol into 21-carbone pregnenolone is performed in three cleaving monooxygenase reactions catalyzed by mitochondrial P450_{scc} (side chain cleaving) enzyme in which the side chain at 20-carbone of steroid scaffold is removed. Pregnenolone is the primer progesterone and the precursore for further biosynthesis of glucocorticoids, mineralocortoids and androgens with estrogens [Figure 9].

Introduction

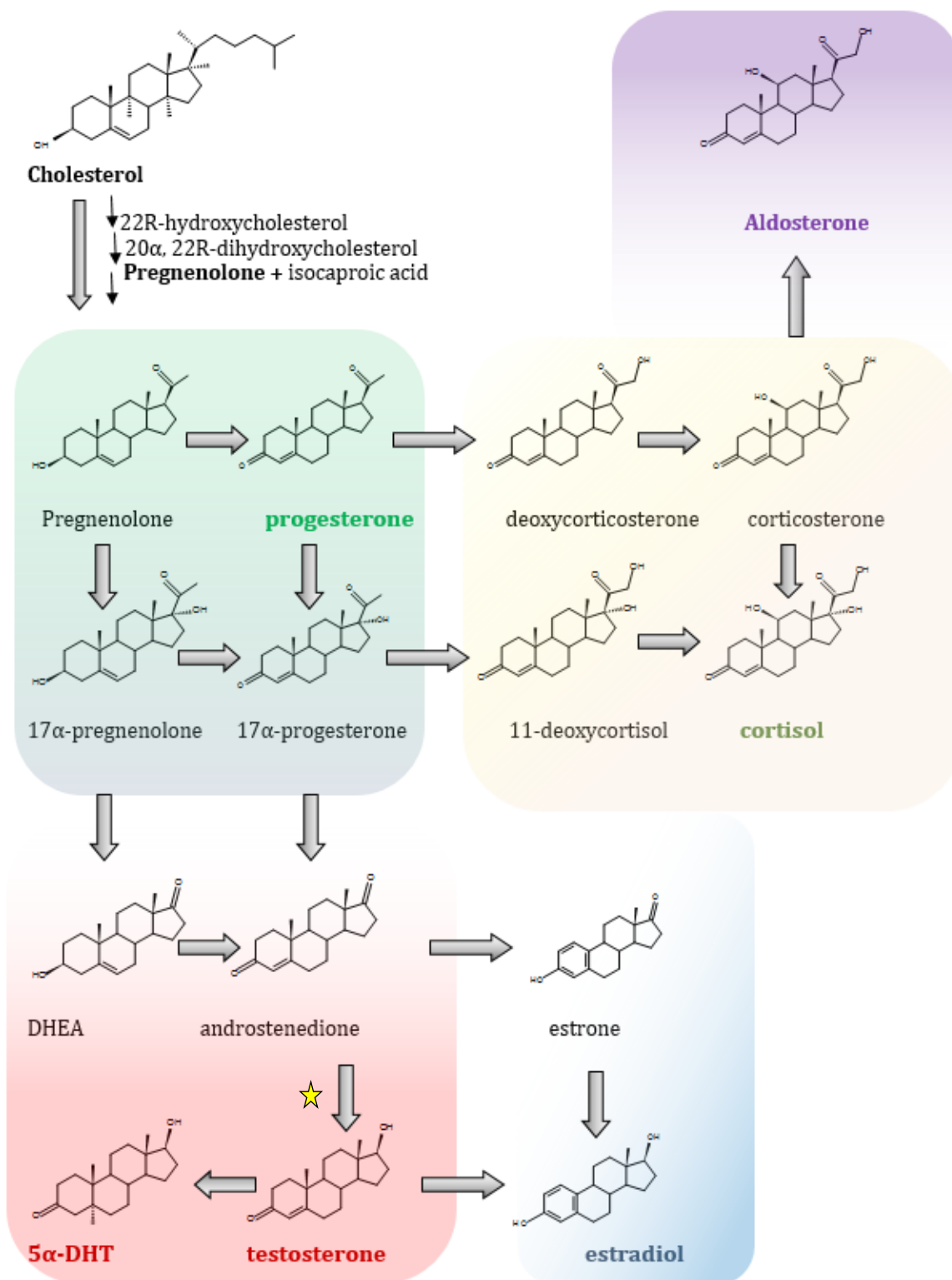


Figure 9 Scheme of steroid hormone biosynthesis. The yellow star shows the place of action of the enzymes: 17 β -HSD type 3 and 5, being of interest in the inhibitor project of this PhD.

Introduction

1.3.3 Hydroxysteroid dehydrogenases

Among proteins belonging to SDR superfamily intensively researched are hydroxysteroid dehydrogenases (HSDs). Functionally, they are a group of enzymes that in the target tissues catalyze oxido-reduction reactions on various position of steroid substrates utilizing NAD(P)H/NAD(P)⁺ as cofactor. They catalyze the reversible reaction of dehydrogenation of hydroxyl-steroid to the corresponding keto-steroids. They are playing a key role in steroid hormone metabolism and are responsible for the pre-receptor regulation of steroid hormone action by switching to biologically active form and reversely. Structurally HSDs belong into two enzymatic families: SDRs and AKRs.

1.3.3.1 3 α -hydroxysteroid dehydrogenases

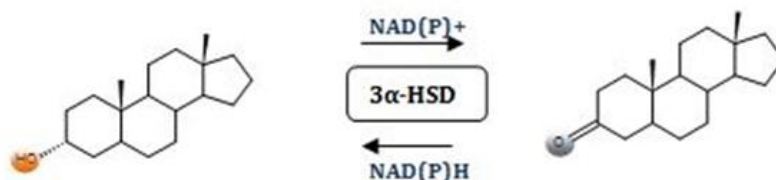


Figure 10 3 α -hydroxysteroid oxidoreduction

The enzymes with 3 α -HSD activity act at 3rd carbon of steroid scaffold and they convert the hydroxyl group at α -position to ketone in reversible oxidoreduction reaction. Most of well described human enzymes with 3 α -HSD activity belong to AKR superfamily [44, 45]. The examples are AKR1C isozymes such as AKR1C1, AKR1C2 or AKR1C3. Their substrates are androgens like 5 α -DHT which is reduced to not potent 3 α -androstenediol and androsterone to 5 α -androstenedione. They inactivate the circulating steroid hormones thereby in target tissue regulates the occupancy of steroid hormone receptor. In androgen metabolism they inactivate biologically active 5 α -DHT to 3 α -Androstenediol or indirectly by interconversion of 5 α -androstenedione to androsterone [Figure 19, chapter 1.4.2.3]. Among human proteins belonging to SDR superfamily 3 α -HSD activity *in vitro* reveal enzymes implicated with retinol metabolism (RODH-like group for example 11-cis retinol dehydrogenase, HSD17B6). However their physiological contribution in 3 α -hydroxysteroids

Introduction

metabolism is not completely known. They are active towards androgenic (C19) and neuroactive (C21) 3 α -hydroxysteroids.

1.3.3.2 3 β -hydroxysteroid dehydrogenases/isomerases

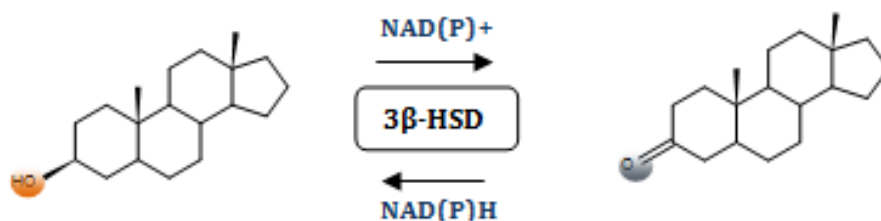


Figure 11 3 β -hydroxysteroid oxidoreduction

Among 3 β -HSDs in steroid hormone biosynthesis the important role plays 3 β -hydroxysteroid dehydrogenase/ Δ -5-4 isomerase which in human appears as two isozymes: 3 β -HSD/isomerase 1 and 3 β -HSD/isomerase 2. They are bifunctional enzymes and they differ in localization of expression in human tissues: whereas type 1 is expressed in placenta and peripheral tissues, the type 2 is expressed in the adrenal gland, ovary and testis. Both 3 β -HSD1 and 3 β -HSD2 catalyze the synthesis of progesterone from pregnenolone, 17-hydroxyprogesterone from 17-hydroxypregnenolone, androstenedione from dehydroepiandrosterone (DHEA) and androstenediol to testosterone in adrenal gland [46]. Their Δ 5- Δ 4 isomerase activity that reveals in the oxidative conversion of Δ 5-3 β -hydroxysteroid to the Δ 4-3keto form is essential for the biosynthesis of all classes of hormonal steroids as follows: progesterons, glucocorticoids, mineralocorticoids, androgens and estrogens [47] [Figure 12].

Introduction

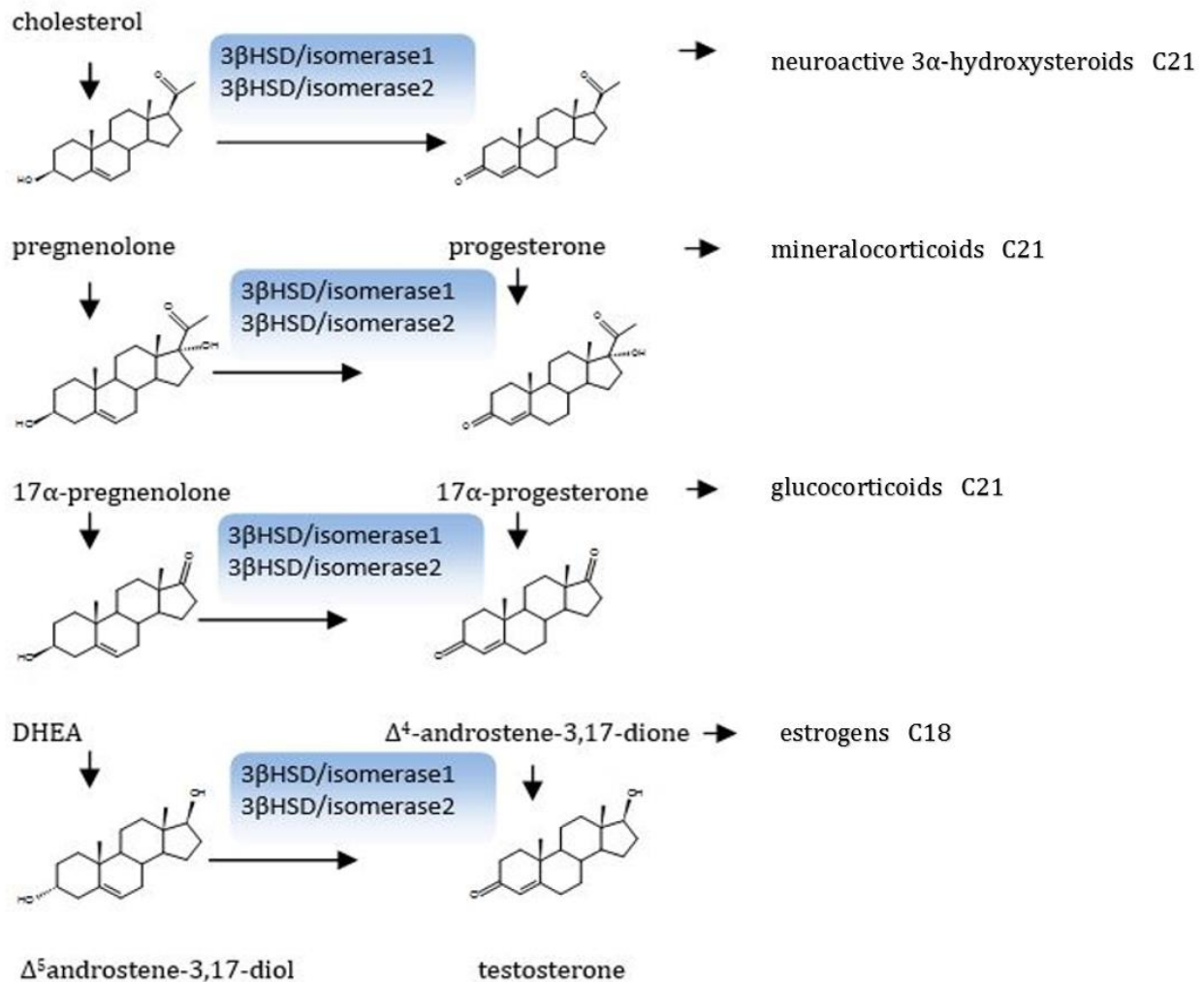


Figure 12 3β-hydroxysteroid dehydrogenases in steroidogenesis.

1.3.3.3 11β-hydroxysteroid dehydrogenases

11β-HSDs catalyze the conversion of inert 11 keto-products (cortisone) to active cortisol and *vice versa*. They regulate the final step of glucocorticoids biosynthesis and thus their access to the steroid receptors. There are two isoforms in human: 11β-HSD type 1 and 11β-HSD2. Whereas the 11β-HSD1 reduces the cortisone to biologically more potent cortisol, 11β-HSD2 inactivates cortisol by oxidation to cortisone [48]. 11β-HSD2 regulates also the activation of MR receptor in kidneys which is trans-activated with the similar affinity by cortisol and aldosterone [Figure 13].

Introduction

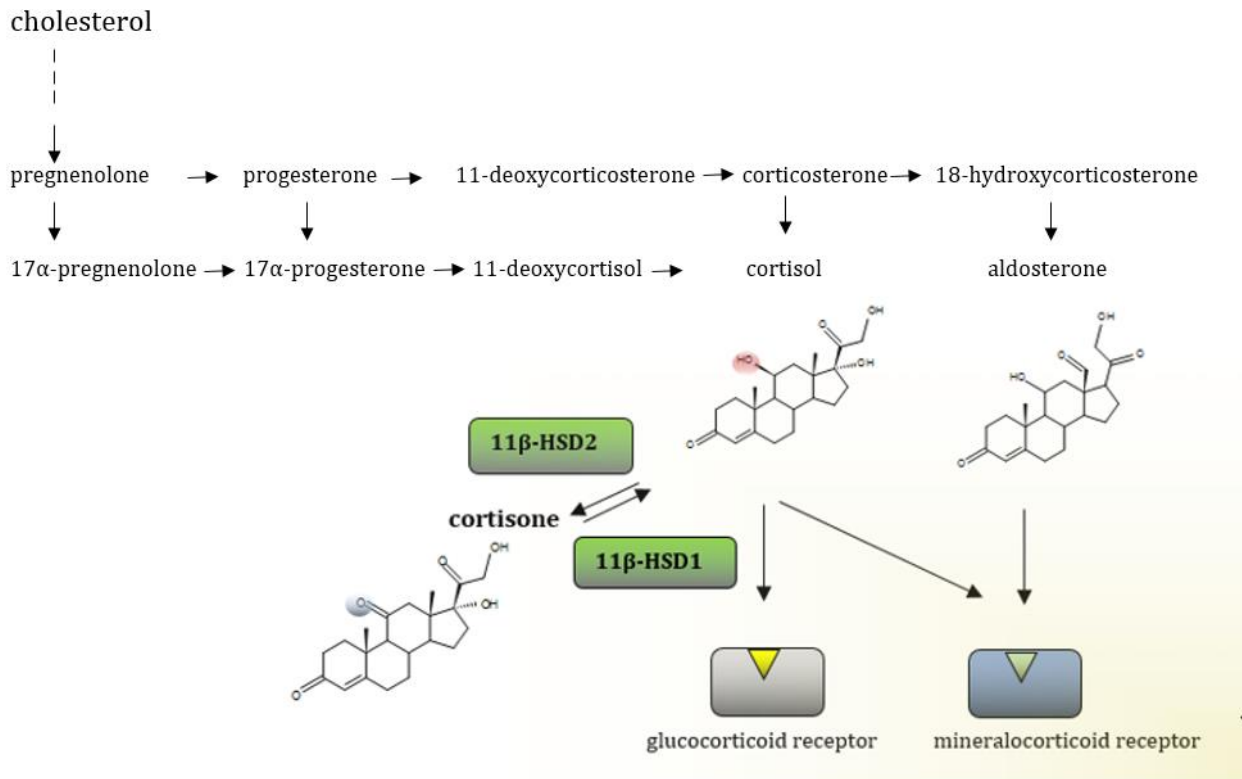


Figure 13 Corticosteroid biosynthesis pathway and 11β-hydroxysteroid oxidoreduction

1.3.3.4 20α-hydroxysteroid dehydrogenases

In human the best described 20α-HSDs belong to AKRs family. AKR1c1 which is also known as 20α(3α)-HSD acts an important role in regulating progesterone action converting the potent progestin: progesterone to its weak form 20α-progesterone [Figure 14].

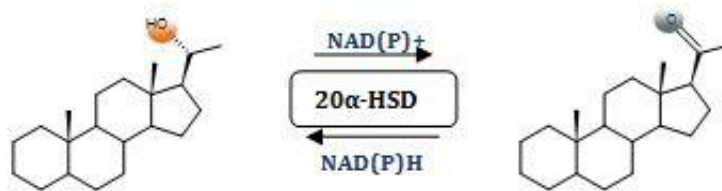


Figure 14 20α-hydroxysteroid oxidoreduction

Introduction

Among SDR proteins 20 α -HSD activity was described in DHRS9, 17 β -HSD1 and 17 β -HSD2. As progesterone and its metabolites are precursor for most biologically active steroid hormones the reduction of progesterone to its weak form 20 α -OH-progesterone is believed to protect before high level of steroids.

1.3.3.5 17 β -hydroxysteroid dehydrogenases

17 β -hydroxysteroid dehydrogenases play a key role in the final step of sex steroid formation acting as switchers between biologically less active 17-ketosteroids to more potent 17-hydroxysteroids and thus regulating the activation of androgen or estrogen receptors [Figure 2]. Up to now there were identified at least 15 types of this enzyme among them 14 in humans. The growing numbers at different 17 β -HSD types origin from the chronological order of their identification. Some of 17 β -hydroxysteroid dehydrogenases were first identified basing on DNA sequence similarity to known hydroxysteroid dehydrogenases and 17 β -HSD activity is not always their main function among other enzymatic activities. Among 17 β -HSDs only 17 β -HSD type 5 (AKR1c3) belongs to AKR superfamily whereas the rest are SDR proteins [49].

17 β -HSD type 1 (HSD17B1) was the first identified 17 β -HSD and was cloned from human placenta. 17 β -HSD1 is considered as the main enzyme that reduces estrone to its biologically active form estradiol among other 17 β -HSDs which also reveal the same substrate affinity *in vitro* [49]. Additionally, the enzyme show activity in reduction of DHEA to androstenediol and androstenedione to testosterone.

17 β -HSD type 2 (HSD17B2) is the next chronologically identified human 17 β -hydroxysteroid dehydrogenase and *in vivo* acts reversely to 17 β -HSD1 inactivating the estradiol to its estrone in various peripheral tissues including sex steroid target tissues. Similarly, it can also oxidase the androstenediol back to DHEA and testosterone to androstenedione. It activates also 20 α -hydroxyprogesterone to progesterone. Zhongyi *et al.* 2007 [50] suggested the role of 17 β -HSD2 in oxidation of retinoids in studies with transgenic mice expressing human HSD17B2 gene.

17 β -HSD type 3 (HSD17B3) was discovered as the third 17 β -HSD isozyme and was found to convert androstenedione to testosterone. The enzyme is active in male in testis. It is known to play role in testosterone biosynthesis from androtestosterone in testis and in male development. The

Introduction

enzyme is crucial for normal male sexual development, a complex process that requires the correct developmental interpretation of both genetic and hormonal signal. Genetic dysfunction of enzymatic genetic is known as male pseudohermaphroditism [51]. This inborn error of metabolism was originally described in 1971. 17 β -HSD3 is also called the microsomal enzyme and it is expressed as an integral membrane protein of the endoplasmic reticulum that uses NADPH as cofactor *in vivo*.

17 β -HSD type 4 (HSD17B4) is also called as multifunctional protein (MFP2). It is a three domain protein which is: SCAD domain (Short-Chain Alcohol Dehydrogenase), hydratase and SCP domain that refers to sterol carrier protein 2 (SCP2). Although the enzyme was first identified as 17 β -estradiol dehydrogenase [52, 53] it also shows the enoyl-CoA-hydratase and D-3-hydroxyacyl-CA dehydrogenase activity and is implicated with peroxisomal β -oxidation of fatty acids. Apart of steroid metabolism the enzyme participates in β -oxidation of fatty acids and bile acids synthesis. HSD17B4 acts as a catalyst for the formation of 3-ketoacyl-CoA intermediates from both straight-chain and 2-methyl-branched-chain fatty acids. Its 17 β -HSD activity appears in oxidation of estradiol to estrone. Mutations affecting the catalytic functions in this enzyme lead to many severe phenotypes like hypotonia, facial dysmorphism, psychomotor delay, neonatal seizure, neuronal migration defects and demyelination give an evidence how important is that enzyme for proper metabolism and development [54].

17 β -HSD type 5 is known also as AKR1C3 or 3 α -HSD2 or prostaglandin F synthase and represents the AKR superfamily. 17 β -HSD5 is an enzyme with a pleiotropic activity and plays a key function in androgen metabolism. Its 17 β -HSD activity appears in oxidoreduction in androgens and estrogens [55, 56]. More details about 17 β -HSD5 are here to found in the chapters 1.4.2.3-1.4.2.5 about androgen metabolism with a particular emphasis on its role on cancer development.

17 β -HSD type 6 (SDR9C6, RODH) in human was initially designated as 3(α - β) hydroxysteroid epimerase and was classified as 17 β -HSD6 in human due its (71, 4%) homology to rat 17 β -Hsd6 which oxidize steroids at 17 position [57]. It exhibits the oxidoreductase and epimerase activity in androgen catabolism. It oxidizes 3 α -Adiol to DHT (3 α -HSD activity) and due to its epimerase activity converts androsterone to DHEA [58]. This enzyme is also known as RoDH-like 3 α -HSD/RL-HSD and belongs to retinol metabolizing subgroup of SDR superfamily [53].

17 β -HSD type 7 (SDR37C1) however can reduce the estradiol to estrone its 17 β -HSD activity seems to not be a dominant role in human. The enzyme was found to reduce the estrone in mouse. 17 β -HSD7 was first characterized as prolactin receptor related protein as play a role in

Introduction

postsqualene cholesterol biosynthesis as 3-ketosteroid reductase in reduction of zymosterone to zymosterol. This enzyme was originally described as the protein associated with prolactin receptor in rats [59, 20].

17 β -HSD type 8 was first described as a Ke6 gene in mouse with recessive polycystic kidney disease (PKD). Ke6 was one of the two identified genes whose abnormal gene regulation was connected with development of this disease. Formitcheva *et al* [60] demonstrated first that the cloned from mouse and expressed in bacteria recombinant Ke6 reveals 17 β -activity oxidizing estradiol and with lower efficacy also testosterone and dihydrotestosterone *in vitro* with the preference to NAD⁺ over NADP⁺. Human Ke6 homolog gene was identified in the region of MHCII class genes and called HSD17B8 due to some sequence similarities with HSD17B4. There was also demonstrated that human recombinant protein expressed in *E. coli* as His tag fusion catalyzes estradiol, estrone, testosterone dihydrotestosterone and androstanediol (at the 2,4-5,9% that of estradiol oxidation)[61]. Human HSD17B8 mRNA was found in many tissues and organs like brain, cerebellum, heart, lung, kidney, liver, small intestine, ovary, testis, adrenals and placenta [61]. The latest evidences show the HSD17B8 is most likely involved in fatty acid metabolism rather than in steroid hormone regulation [62].

17 β -HSD type 9 (SDR9C5, RDH5) known as retinol dehydrogenase (11-cis, 9-cis) and similarly to 17 β -HSD6 belongs to the subgroup of SDR enzymes metabolizing retinoids/androgens/estrogens. The enzyme shows 17 β -HSD and 3 α -HSD activity towards 3 α -androstadiol [63, 64].

17 β -HSD type 10 is next multifunctional SDR enzyme with 17 β -HSD activity towards estrone which is only one of many others. The enzyme is a mitochondrial protein initially isolated from rat liver and shows homology to 17 β -HSD17B4. 17 β -HSD17B10 is known also under other synonym names which just reflect its multifunctionality like: short-chain L-3-hydroxyacyl coenzyme A dehydrogenase II (SCHAD/HCD2/HADH2), endoplasmic reticulum-associated binding protein (ERAB), amyloid β -peptide-binding alcohol dehydrogenase (ABAD), -methyl-3-hydroxy- butyryl-CoA dehydrogenase (MHBD). Other activities of the enzyme are 3 α -HSD, dehydrogenase 20 β -OH and 21-OH activity with C21 steroids. 17 β -HSD10 was found to be active towards cholic acid and oodeoxycholic acid [65].

17 β -HSD type 11 is known also as retSDR2 or DHRS8. It exhibits the 17 β -HSD activity in conversion of 5 α -Androstane-3 α ,17 β -diol to androsterone. Although it can bind retinoids, it has no retinoid metabolizing activity [66]. HSD17B11 gene is expressed in steroidogenic and non-

Introduction

steroidogenic tissues like pancreas, kidney, liver, lung, small intestine and heart. On cellular level human 17 β -HSD11 was found in lipid droplets of liver cells that accumulate in fatty liver diseases [67].

17 β -HSD type 12 (SDR12C1) is a protein in the ER that uses NADPH to reduce 3-ketoacyl-CoA to 3-hydroxyacyl-CoA thus playing a role in long fatty acid elongation acting as 3-ketoacyl reductase (KAR) which was the first identified activity of this enzyme [68]. Independently, by studying the sequence similarity to hsd17b3 gene a novel potent 17 β -HSD was identified (chronologically as 17 β -HSD12) and there was shown that the enzyme can effectively and selectively convert estrone to estradiol in ovarian mammary gland tissues [69].

17 β -HSD type 13 (SCDR9, SDR16C3) has been first cloned and characterized as SCDR9 gene and was isolated from human liver cDNA library. Subcellular localization studies showed in some sites cytoplasmatic localization but not in ER [70]. 17 β -HSD13 similar to 17 β -HSD11 has been identified as lipid droplet-associated protein [71].

17 β -HSD type 14 (DHRS10, SDR47C1) assayed *in vitro* converts estradiol, testosterone and 5-androstene-3 β , 17 β -diol at the presence of NAD⁺ as cofactor. Subcellular localization studies showed that the enzyme is localized in the cytoplasm [72].

1.3.4 Short overview of SDR role on retinol metabolism in human.

Retinol, commonly known as vitamin A, represents retinoids of molecular structure consisting of cyclic group, polyene side chain and a polar end group. It is a very important molecule obtained from diet (as carotenoids -provitamine A) required by humans for many physiological processes such as proper vision, cellular differentiation, epithelium growth, embryonic development, reproduction or immunity. Additionally, since few decades there are known evidences showing a significant role of retinoids in cancer development as well their promising results in application as therapeutic agents in cancer therapy [73, 74]. In humans, physiologically occurring retinoids are *all-trans*-retinol, *all-trans*-retinoic acid, 11-*cis*-retinal and 9-*cis*-retinoic acid [Figure 15]. While 11-*cis* retinoids actively participate in vision process as a universal chromophore of the visual pigment, *all-trans* and 9-*cis* physiologically retinoids act as hormones and can regulate the expression of target genes *via* activation of specific nuclear retinoid receptors. The most potent are final metabolites of retinol oxidation pathway: *all-trans* and 9-*cis* retinoid which bind to their specific

Introduction

receptors with the highest affinity. There are two classes of retinoid receptors: the retinoid acid receptors (RARs: α, β, γ) and the retinoid X receptors (RXRs: α, β, γ) that can dimerize appropriately in various combination. Nowadays is known that whereas the RARs receptors (α, β, γ) can be activated either by all-trans retinoic acid and 9-cis retinoic acid, RXR receptor are only activated by 9-cis retinoic acid.

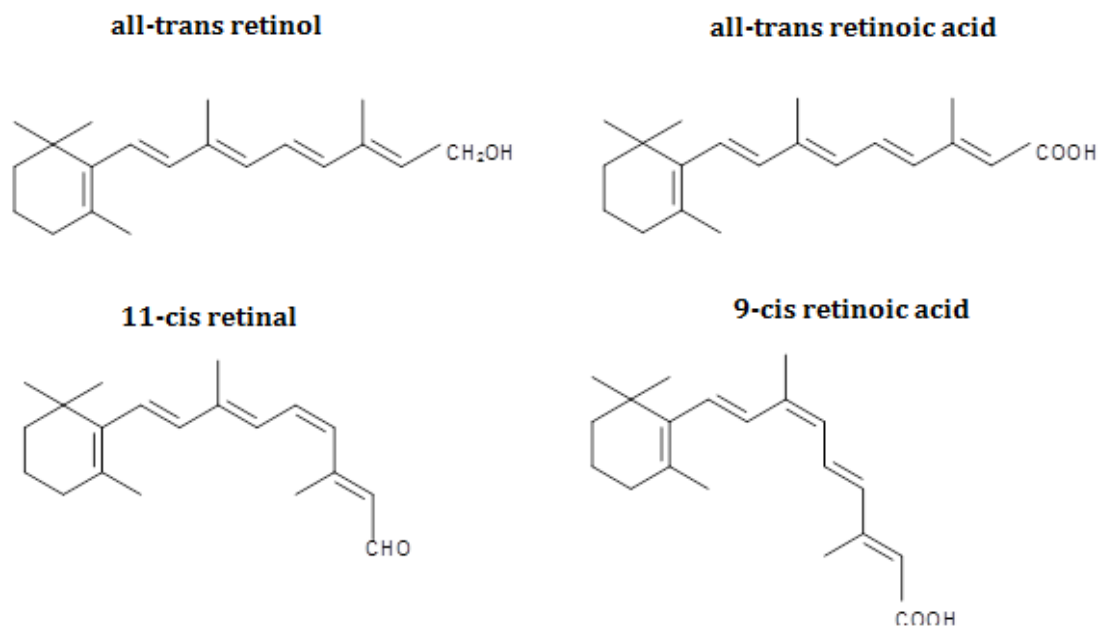


Figure 15 Physiologically occurring retinoids in humans.

Retinol is a basic precursor of 11-*cis*-retinal acting in vision process as well of *all-trans* and 9-*cis*-retinoid acids being the main agonist of retinoid acid receptors. Obtained dietary or derived from processed in liver (or partially in intestine) carotenoids retinol is excreted into blood (plasma) where is carried into targeted cells as complex with retinol binding protein (RBP) or as ester with lipoproteins. After entering the cell through the membrane retinol is then bound by CRBP proteins (Cellular Retinol Binding Proteins) which thereby control the amount of free retinol inside the cell. Inside the cell retinol is immediately oxidized to retinaldehyde and next to biologically potent retinoid acid [Figure 7; B]. Retinoic acid can be further metabolized by other oxidases (Cyp 26) into 13-*cis*-retinoid acid or into other not active retinoid esters.

Introduction

- **Human SDR members involved in retinol metabolism.**

In human organism are many enzymes able to catalyze the reactions of retinol metabolism such as ADH enzymes. Among SDR members involved in this process are enzymes reported mainly in the oxidation pathway of retinol and its stereoisomer [Figure 16]. However, reverse activity towards retinaldehyde is also observed. According to the new nomenclature system they were ordered into SDR7, SDR9 and SDR16 families of SDR superfamily [Table 6].

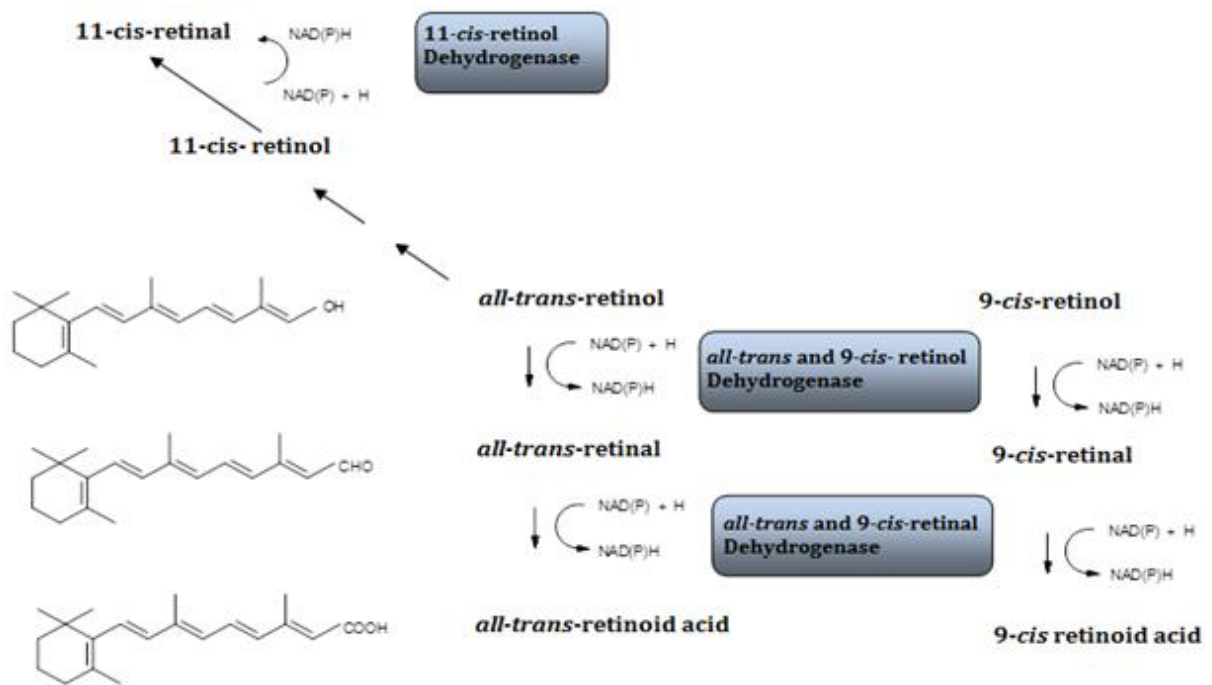


Figure 16 Main activities of SDR enzymes in retinol oxidation pathway

Additionally, SDR enzymes may differ considering the ability to recognizing of free or bound with CRBP retinol.

Introduction

Table 6 List of example human SDR enzymes involved in retinoid metabolism.

Human SDRs involved in retinoid metabolism	SDR family	Subcellular localization	Annotated activity in retinoid metabolism
RDH11	SDR7C1-1	ER	all-trans/9-cis-retinol dehydrogenase
RDH12	SDR7C2	ER	all-trans/9-cis-retinol dehydrogenase
RDH13	SDR7C3	ER	all-trans/9-cis-retinol dehydrogenase
RDH14	SDR7C4	ER	all-trans/9-cis/11-cis retinol dehydrogenase
RDH1 (HSD17B9,RDH5)	SDR9C5	ER	11-cis/9-cis-retinol dehydrogenase
RDH16 (RODH4)	SDR9C8	ER	all-trans/13-cis-retinol dehydrogenase
RDH10	SDR16C4	ER	all-trans-retinol dehydrogenase
retSDR2	SDR16C5	ER	all-trans-retinol dehydrogenase
RODH (HSD17B6)	SDR9C6	ER	all-trans-retinol dehydrogenase (<i>in vitro</i> [75])

1.3.5 Short overview of SDR role in fatty acid metabolism

Fatty acids and their derivatives fulfill pivotal physiological roles in living organism such as energy fuel and high caloric energy storage. They are also building components or can serve as hormones and intracellular messengers. Some of belonging to SDR protein family enzymes are involved in pathways of fatty acids metabolism usually serving as catalyzers in their NAD(P)/NAD(P)H dependent oxidation/reduction steps. Among them are enzymes direct engaged in cyclic processes of fatty acid biosynthesis and degradation as well SDR enzymes fulfilling an auxiliary role by providing fatty acid intermediates which are next handled by synthesis or breakdown enzyme system in cells. The latter group of SDRs which are indirectly involved in cyclic fatty acid metabolism seems to be the majority.

Introduction

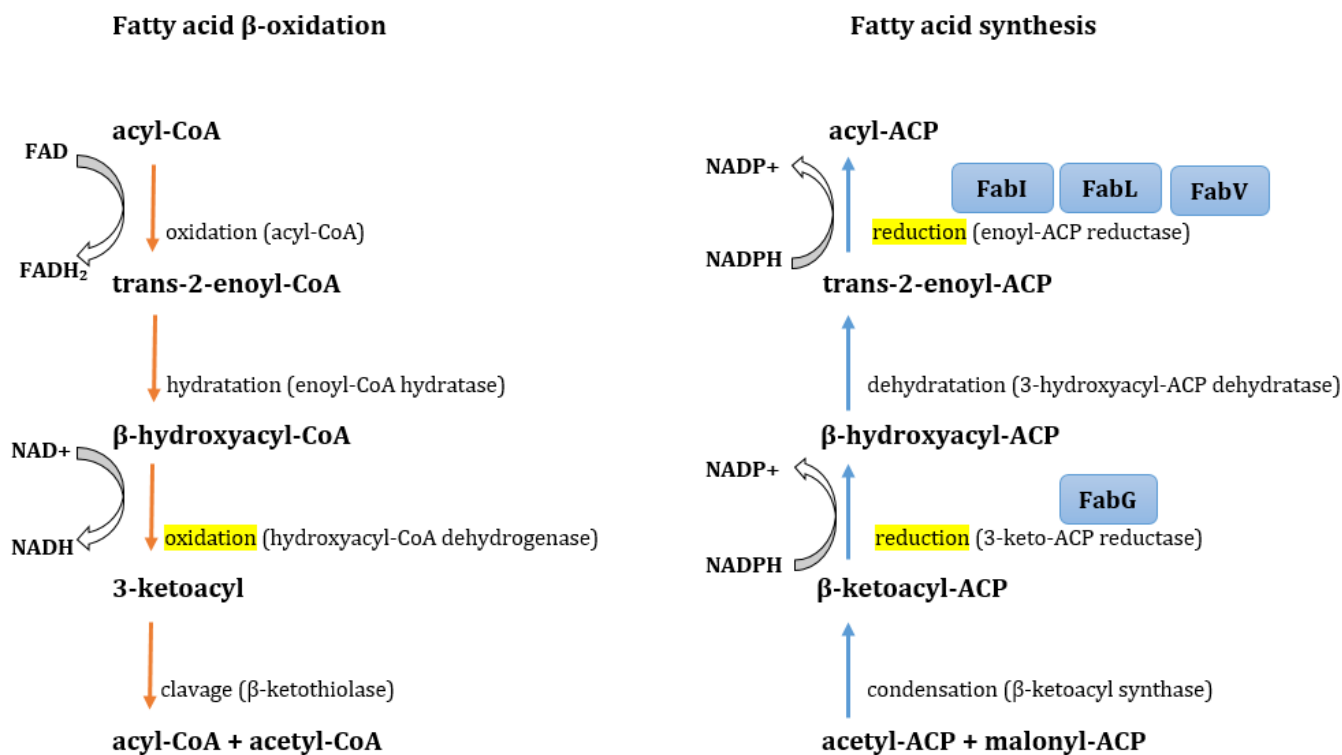


Figure 17 Simplified scheme of classical chemical reaction involved in cyclic processes of saturated fatty acids β -oxidation and synthesis. Possible catalytic activities of SDR enzymes are marked on yellow. Fab enzymes represented by SDR members.

Both processes of fatty acid synthesis and degradation are based on three classes of reverse to each other chemical reactions such as: carbon-carbon bond formation/cleavage, oxidation/reduction and hydration/dehydration [Figure 17]. The most extensively studied are pathways involved in mammalian (human) fatty acid β -oxidation localized in mitochondria and bacterial fatty acid biosynthesis known also as fatty acid synthesis type II (FAS II) where in both of them are involved discrete, separately encoded monofunctional enzymes in contrast to mammalian fatty acid synthesis type I (FAS I) or bacterial fatty acid breakdown which are catalyzed by multifunctional enzymes (MFEs) and associated enzyme complexes. In humans the biosynthesis of fatty acids take a place mainly in liver cells and is catalyzed by dimer of three-domain multifunctional fatty acid synthase. Apart of well-studied mitochondrial β -oxidation pathway eukaryotic organisms possess an alternative peroxisomal fatty acid β -oxidation pathway in which long chain fatty acids too long in order to be handled by mitochondria are initially shorten to octanyl CoA by use of peroxisomal specific enzymes.

Introduction

SDR enzymes are important components of the FAS II system found mostly in bacteria, plants and parasites. The individual enzymes catalyzing the particular steps of this the most studied fatty acid synthesis pathway in bacteria has been named as Fab enzymes. Among them the SDR protein family represent: FabG acting as NADPH-dependent β -ketoacyl-ACP-reductase as well as FabI, FabL and FabV which reduce trans-2-enoyl-ACP to acyl ACP. FabI together with FabL or FabV are atypical SDR members because of modified active center Y-xxxxxxx-K or Y-xxxxxxxx-K instead of typical Y-xxx-K [76, 77]. New identified proteins similar or corresponding to the enzymes of that pathway are initially named as Fab enzymes.

The latest evidences show that eukaryotic mitochondria possess also highly conserved pathway for fatty acid synthesis resembling the bacterial one (FAS II) and which is completely independent of the eukaryotic cytosolic FAS apparatus. Most probably the mitochondrial FAS is involved in synthesis of octanoic lipoic acid [78]. However the knowledge about of this pathway in humans as well the knowledge about the role of particular enzymes taking the part in this process is still not complete. Few of human SDRs are expected candidates to participate in this not completely explored pathway.

- **Human SDR members involved in fatty acid metabolism.**

Concerning the up to now identified human SDR enzymes participating in fatty acid metabolism they seem to play rather an auxiliary role at degradation or synthesis processes of saturated fatty acids. Moreover, they seem to be more engaged in alternative fatty acid metabolism pathways. For example, in human mitochondrial β -oxidation pathway the second NAD(P)⁺ dependent oxidation step is mainly catalyzed by human L-3-hydroxyacyl-CoA dehydrogenase (HADH) which convert (straight medium or short chain) L-3 hydroxyacyl CoA to 3-ketoacyl CoA. The similar activity shows mitochondrial 17 β -HSD10 which catalysis the oxidation of 2-methyl-3-hydroxybutyryl-CoA into 2-methylacetoacetyl-CoA thus fulfills a complementary role in degradation of branched fatty acid in mitochondria. Deficiency in the activity of this enzyme is involved with progress of Alzheimer disease [65].

Introduction

Table 7 List of example human SDR enzymes involved in fatty acid metabolism.

Human SDR genes coding the enzymes involved in fatty acid metabolism	SDR family	Subcellular localization	Activity in fatty acid metabolism
HSD17B4	SDR8C1	peroxisomes	D-3-hydroxyacyl-CoA DH, Enoyl-CoA-hydratase
HSD17B10	SDR5C1	mitochondria	hydroxyacyl-CoA DH type II
HSD17B8	SDR30C1	mitochondria	putative role in mit.FAS
DECR1	SDR18C1	mitochondria	2,4-dienoyl-CoA-reductase
DECR2	SDR17C1	peroxisomes	2,4-dienoyl-CoA-reductase
BDH1	SDR9C1	mitochondria	3-hydroxybutyrate DH
FAR1	SDR10E1	peroxisomes	Fatty acyl-CoA reductase
BDH2 (DHRS6)	SDR15C1	cytosol	3-hydroxybutyrate DH
HSDL2	SDR13C	peroxisomes	putative role in FA metabolism

Whereas concerning the peroxisomal β -oxidation pathway the key role plays human HSD17B4 also referred to as multifunctional enzyme 2 (MEF2) or D-bifunctional protein (DBP) with D-3-hydroxyacyl-CoA dehydrogenase and enoyl-CoA-hydratase activities thus it catalysis the formation of 3-ketoacyl-CoA intermediates from both straight and 2-methyl-branched chain fatty acids and additionally catalysis the 2-enoyl-acyl-CoA hydratase reaction. Another human SDR enzyme acting in peroxisomal fatty acid metabolism represents DECR2 (2,4-dienoyl-CoA-reducatsse 2) which participates in β -oxidation of unsaturated fatty acids catalyzing the reduction of enoyl-CoA esters like 2,4-dienoyl-CoA into trans 3-enoyl-CoA. Mitochondrial functional analog of this enzyme is DECR1 (2,4-dienoyl-CoA-reducatsse 1). Among human SDR enzymes fulfilling an auxiliary role to the mainstream saturated fatty acid metabolism pathway is mitochondrial BDH1 and its probably cytosolic analog BDH2 (DHRS6). BDH1 has been identified as D- β -hydroxybutyrate dehydrogenase and catalysis the inter-conversion of acetoacetate and (R)-3-hydroxybutyrate. Both substrates are

Introduction

the main ketone bodies produced during fatty acid catabolism and can be initial substrates for lipid synthesis.

1.3.6 Orphan SDR proteins reminding hydroxysteroid dehydrogenases

Due to progress of genomics and proteomics researching the several hundreds of thousands of amino acid sequences have been identified. Usually, the next step in trials to find the function of new identified sequence is searching for the homolog in other organisms. The term 'orphan gene' means then a new discovered amino acid (or DNA) sequence without clear homology to any of known DNA or amino acid sequences in genomes of other organisms. By use of bioinformatics tools the identification of new sequences sharing the domains of SDRs is available and therefore putative new enzymes have been annotated which need to be functionally characterized. In this way sequences reminding structurally the SDR or hydroxysteroid dehydrogenases enzymes were found [79] but their enzymatic activity remains unknown so they are termed temporarily also as 'orphan' till the substrate is found. However, it is worth of note that the concept of the 'orphan enzyme' primary used to mean rather the identified enzymatic activity with assigned an Enzyme Commission (EC) number but without assigned protein or gene sequences. Among hydroxysteroid dehydrogenases reminding amino acid sequences two proteins were identified such as HSDL1 (SDR12C3) [80, 81] and HSDL2 (SDR13C1) where the last one will be here the object of researching.

1.4 Medical implications of SDRs

SDRs are important metabolic regulators of many key biochemical pathways and thereby dysfunction in activity of several of them has been reported to be involved with some severe metabolic diseases [Table 8]. The importance of SDR enzymes has been many times showed in studies using (KO) knockout animal models for given SDR enzyme with/or transgenic (TG) ones abundantly over-expressing the studied SDR enzyme which could rescue the impaired phenotype or manifested some disorders caused by abnormally increased activity of the enzyme, respectively

Introduction

[82]. In other example in knockout animal model for the enzyme 11 β -HSD11 protected from metabolic abnormalities like obese or insulin resistance followed by excessive glucocorticoid exposure [83]. Notable, for some of SDRs, especially involved in crucial for survival metabolisms, (for instance participating in cholesterol biosynthesis like 17 β -HSD4, 17 β -HSD7 etc.) animal knockout phenotypes has been often appearing to be lethal or at least difficult to generate due to severe developmental malfunctions yet in the embryonic phase [84, 85].

Table 8 Examples of diseases associated with impaired activity of SDR enzymes.

Enzyme (Gene)	SDR nomenclature	Disease relevance
UDP-galactose-4'epimerase (GALE)	SDR1E1	galactosemia type III [86, 11]
Quinoid dihydropteridine reductase (QDPR)	SDR33C1	tetrahydrobiopterin deficiency [17]
3 β -HSD2(HSD3B2)	SDR11E2	congenital adrenal hyperplasia [87]
11 β -HSD2 (HSD11B2)	SDR9C3	apparent mineralocorticoid excess syndrome [88]
17 β -HSD3 (HSD17B3)	SDR12C2	male pseudohermaphroditism [89, 90, 91]
17 β -HSD4 (HSD17B4)	SDR8C1	D-bifunctional protein deficiency (DBPD), Perrault syndrome [92], Zellweger syndrom [93].
17 β -HSD6 or RODH (HSD17B6)	SDR9C6	Polimorfism implicated in etiology of polycystic ovary syndrome (POCS) [94]
17 β -HSD7 (HSD17B7)	SDR37C1	Zellweger syndrom [20]
RDH5 (RDH5 or HSD17B9)	SDR9C5	Retinitis pigmentosa, blindness [95]
17 β -HSD10 (HSD17B10)	SDR5C1	Alzheimer disease, 2-methyl-3-hydroxybutyryl-CoA dehydrogenase deficiency (MHBD) [65]
NSDHL	SDR31E1	NSDHL [96]
Sepiapterine reductase (SPR)	SDR38C1	dopa-responsive dystonia [97]

1.4.1 SDR/HSDs as potent targets for inhibitor development in treatment of hormone-related disease

Potent inhibitors of SDR enzymes with a special emphasis on the enzymes acting as hydroxysteroid dehydrogenases since few decades constitute a special and interesting field of biomedical research. Steroid hormones have a wide range of physiological roles in humans thereby any abnormalities in activity of enzymes which primary regulate their metabolism can often lead to multi-factorial disorders including cancers or neuronal diseases. The pathogenesis process is then propagated by abnormal level of steroid hormones and can be implicated with both increased enzyme's activity or it's lost. Naturally then, in the case when a gene expression of given HSD enzyme in some tissue is up-regulated the local application of a specific enzyme's inhibitor could potentially overcome the pathologic effect caused by it's over activity.

On example of glucocorticoids as well modulating their activity 11β -HSD type 1 and 2 (HSD11B1 and HSD11B2) have been reported pathogenic role in development of obesity and metabolic syndrome what can subsequently follow diabetic and cardiovascular diseases [13]. Potent inhibitors of 11β -HSD1 which could thus block activation of cortisol were suggested in therapy of obesity and metabolic syndrome [83]. Several 11β -HSD1 inhibitors are explored and some of them are tested in clinical trials as therapeutics in non-insulin therapies for type 2 diabetes [98, 99]. Another example is 17β -HSD10 shown to interact with β -amyloid peptide in animal model for Alzheimer diseases and which was noticed to be up-regulated in affected brain tissues. In this case it was suggested that the pathologic effect might be involved with high levels of the enzyme thus potentially disrupting steroid hormone homeostasis in synapses and contributing to synapse loss in the hippocampus of the mouse model of Alzheimer's disease [100]. Thereby potent inhibitors of 17β -HSD10 was suggested that could selectively inhibit steroid metabolism in target tissues thus giving therapeutic effects in synapse functioning.

1.4.2 17β -HSDs as drug targets in treatment of hormone cancers

Among hydroxysteroid dehydrogenases 17β -HSDs are a special target group for potent inhibitor development for pharmaceutical companies due to their role in pathogenesis of androgenic and estrogenic sensitive illnesses like breast and prostate cancers. Among other illnesses and ailments

Introduction

connected with abnormal level of sex steroid hormones is testosterone sensitive acne, alopecia or involved with estrogen metabolism osteoporosis. Concerning the latter one transgenic mice over-expressing HSD17B2 gene were shown to develop osteoporosis apart of other dysfunction [101]. Potent 17 β -HSD2 inhibitor potentially can be used in osteoporosis therapy [102].

1.4.2.1 Pathogenesis of hormone –related cancers

Since estrogens and androgens regulate cell proliferation and apoptosis they play a key role in carcinogenesis of various types of cancers being generated especially in hormone-sensitive tissue including breast, ovary, endometrium, prostate, but also colon, skin etc. The main input of estrogens and androgens on hormone –related carcinogenesis process relies then on stimulated by hormones cell proliferation which generally increases the number of cell divisions and thus the opportunity for random genetic errors. Estrogens and androgens can also have the influence on other nonmalignant diseases such as benign prostate hyperplasia, endometriosis, obesity, type 2 diabetic. However, the mentioned diseases are associated with a high risk for some malignancies. Estrogen has a crucial role in supporting the growth of hormone dependent breast cancer in post-menopausal women. Increased level of E2 drives the proliferation of the tumor tissue *via* ER [103].

1.4.2.2 Short overview of sex hormone metabolism. Role of 17 β -HSDs.

Apart of adrenal glands and gonads, the main sex hormone producers in human, many tissues have the ability to convert circulating pre-hormones into active hormones due to local expression of steroidogenic enzymes. Estrogens and androgens are usually exerted into blood in their not active sulfated form such as: Estrone sulfate (E1S), 5 Δ -androstenediol-sulfate (Adiol-S), and dehydroepiandrosterone-sulfate (DHEA-S). In target tissues, they are taken up into cells by organic anion transporting polypeptides or other transporters (from the SLC-family) where are first activated by removal of sulfate in the reaction catalyzed by steroid sulfatase. Inside the cell estrone, 5 Δ -androstenediol and dehydroepiandrosterone are further converted by steroidogenic enzymes like hydroxysteroid dehydrogenases, aromatase, reductases etc.

Among reductive 17 β -hydroxysteroid dehydrogenases which reduce estrone (E1) to the biological most active estradiol (E2) are 17 β -HSD1 with the highest affinity, 17 β -HSD5, 17 β -HSD7 and also 17 β -HSD11 and 17 β -HSD12. *Vice versa*, among oxidative 17 -HSDs which inactivate estradiol

Introduction

converting it into estrone apart of 17 β -HSD2 are 17 β -HSD4, 17 β -HSD8, 17 β -HSD10 and 17 β -HSD14 [49].

17 β -HSDs control the activation of estrogen receptor in both “sulfatase pathway” where estrone is derived in the cell from circulation as estrone-3-sulfate (E1S) as well in so called “aromatase pathway”. In the latter one estrone and estradiol are derived due to activity of aromatase (CYP19) which convert them in the unidirectional aromatization reaction from 4 Δ -androstenedione and testosterone, respectively [104][Figure 18].

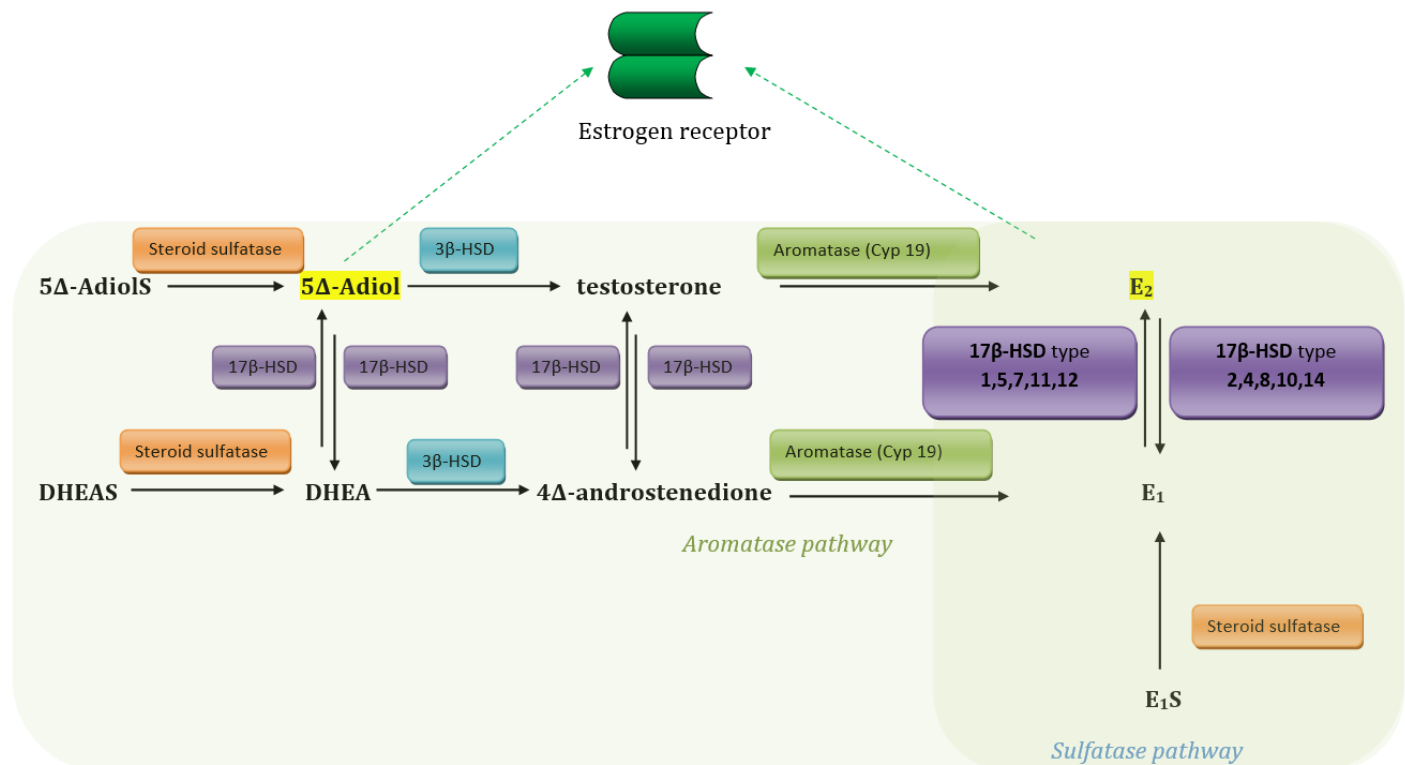


Figure 18 Sulfatase and aromatase pathways of estrogen receptor activation. On yellow marked ligands of ER receptor.

The ‘aromatase pathway’ is the main source of estrogen production in postmenopausal women and usually takes a place in adipose cells. 17 β -HSDs control also the inter-conversion reactions between 4 Δ -androstenedione and testosterone as well between DHEA and 5 Δ -androstenediol of this pathway. Although, structurally 5 Δ -androstenediol is an androgen it can also activate the estrogen receptor however with lower potency as estradiol [105].

Introduction

1.4.2.3 Role of 17 β -HSD enzymes in androgen metabolism

The strongest physiological ligand of androgen receptors are 5 α -dihydrotestosterone (DHT) and testosterone (T), the metabolite of DHT. This both hormones play a crucial role in malignant and benign overgrowth of prostate. Other androgens such as 5 Δ -androstenediol or androstenedione etc. are weak androgens since they trigger admittedly androgen receptor and gene expression, however with much lower potency than DHT or T [106].

Derived from local steroidogenesis or circulation DHEA and 5 Δ -Adiol are inter-converted by at least few types of 17 β -HSDs (type 1 and 5, reduction and 17 β -HSD2 and 17 β -HSD4, oxidation). Both androgens are further converted in a unidirectional action by 3 β -DH/ Δ 5- Δ 4 isomerases to Δ 4-androstenedione and testosterone, respectively. 17 β -HSDs mediate inter-conversion reactions between Δ 4-androstenedione and biologically potent testosterone. The most important enzyme for testosterone production from Δ 4-androstenedione is 17 β -HSD3, primarily expressed in testis. Another enzyme reducing Δ 4-androstenedione at 17 β position at steroid backbone is 17 β -HSD5 responsible for peripheral testosterone production. 17 β -HSD2 and 17 β -HSD8 where notices to oxidize the testosterone backwards to less potent Δ 4-androstenedione. Testosterone is reduced at position 5 by 5 α -reducases (belonging to AKR protein family) to more potent androgen DHT (5 α -dihydrotestosterone). This is the important pathway of DHT peripheral biosynthesis from DHEA involving 3 β -DH/ Δ 5- Δ 4 isomerase and 17 β -HSD5. 17 β -HSD2 can mediate the 3 β -DH/ Δ 5- Δ 4 isomerase reaction [107].

DHT may be further converted to less potent androgens such as 5 α -androstane-3 α ,17 β -diol (3 α -androstenediol), androstenedione or estrogen: 3 β ,17 β -androstenediol (3 β -androstenediol) which is the high-affinity full agonist of estrogen receptor ER β [108]. Several 17 β -HSDs mediate in these reactions thus lowering the potency of DHT for androgen receptor. 17 β -HSD7 and 17 β -HSD6 [109] were found to convert DHT into 3 β -androstenediol whereas 17 β -HSD5, 17 β -HSD7 and 17 β -HSD10 were shown to have 3 α -HSD activity in conversion of DHT into 3 α -androstenediol. This weak androgen has been reported as a weak ligand of estradiol receptor β . 3 α -Androstenediol can be further converted to androsterone in the reaction mediated by 17 β -HSD2, 17 β -HSD5 and 17 β -HSD11. Another pathway of DHT deactivation by oxidation at position 17 to androstenedione is performed by 17 β -HSD2, 17 β -HSD5, 17 β -HSD8 and 17 β -HSD10. In turns, further oxidation of androstenedione to androsterone is catalyzed by 17 β -HSD5 [106][Figure 19]. Mentioned above weak androgens due to 3 α -HSD activity of 17 β -HSD6 (as well few other SDR enzymes with dual activity towards retinoids and hydroxysteroids) can be converted back into DHT: directly from 3 α -androstenediol as substrate or through androsterone and androstenedione. These alternative

Introduction

pathways of DHT biosynthesis and thus AR transactivation has been observed in benign prostate and prostate cancer cells [110, 111].

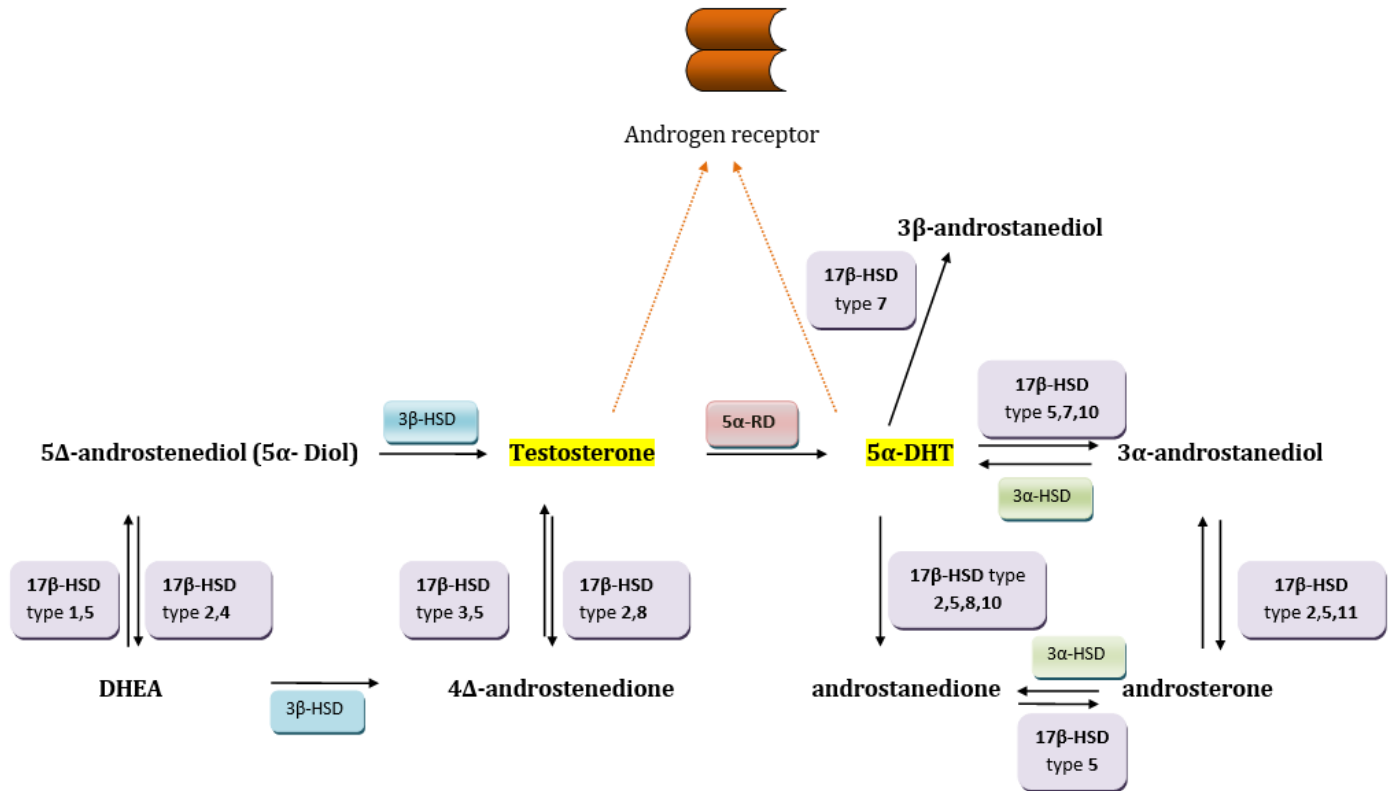


Figure 19 Main metabolic pathway of androgens leading to activation of AR receptor. On yellow marked the most potent ligands of AR receptor.

1.4.2.4 Changes in 17 β -HSD expression in hormone related cancers

Up-regulated expression of some 17 β -HSD is being noticed in many cases of hormone dependent cancers and their pathologic over-expression in some cases is even used as prognostic markers in various types of cancers [Table 9]. What is more, one could notice that usually up-regulation of estrogen/androgen activating (reductive) enzymes may be additionally implicated with down-regulation of hormone deactivating (oxidative) enzymes. For instance in estrogen dependent breast cancer or endometriosis the increased ratio of 17 β -HSD1 to 17 β -HSD2 expression is reported [112]. In other example it was noticed a correlation in polymorphism of oxidative 17 β -HSD4 and 17 β -HSD2 enzyme and risk of endometrial cancer [113]. In the bracket below [Table 9] are shown various 17 β -HSDs and involved with their over-expression pathologies thus potent targets for specific inhibitors development.

Introduction

Table 9 Cancers and other disorders involved with up-regulated expression of 17-HSDs.

Name of the gene for types of 17 β -HSDs	Locally up-regulated or used as marker in case of cancer	Other potent targets In therapy of	references
HSD17B1	breast cancer		[114], [112]
HSD17B2	intestinal cancer, epithelial cancers,	osteoporosis	[113], [101]
HSD17B3	prostate cancer		[115]
HSD17B4	prostate cancer		[116]
AKR1C3	prostate cancer, breast cancer	allopelia, acne, obesity inflammations, hyperandrogenism, asthma	[117, 118, 119, 120]
HSD17B6	prostate cancer		[110,111]
HSD17B7	breast cancer, ductal carcinoma		[121]
HSD17B10	seen in primary prostate cancer cell cultures	Alzheimer disease	[65]
HSD17B11	Cutaneous T-cell lymphoma. Prostate cancer		[122]
HSD17B14	prognostic marker		[123]

1.4.2.5 Role of 17 β -HSD3 and 17 β -HSD5 as inhibitor targets in prostate cancer (PCa) therapy

Among 17 β -HSD enzymes type 3 and 5 both catalyzing the reduction of androstenedione to testosterone are considered as important targets for inhibitor development in therapies of prostate cancer whose carcinogenesis is strictly involved with androgen metabolism and activation of AR receptors. Apart of increased expression of HSD17B3 and HSD17B5 also a differential change in the expression of other reductive and oxidative enzyme pairs favoring the conversion of inactive diones to active androgens have been observed in primary prostate tumors what results from a specific

Introduction

shift on tumor metabolism in prostate cells [124, 125]. Thereby androgen deprivation therapy known also as hormonal therapy remains still the primary treatment method for metastatic prostate cancer.

One of the therapeutic methods aimed to lower the activity of active androgens applied in patients suffering from prostate cancer has been castration. However, clinical practice showed that it not eliminates definitely androgens from prostate tumor in spite of some positive therapeutic effect at the beginning but often follows the recurrence of a more aggressive metastatic disease known as castrate resistant prostate cancer. For observed occurrence are responsible alternative pathways of AR activation as well peripheral actions of some androgenic enzymes like 17 β -HSD5.

17 β -HSD5 due to its pleiotropic activity focus much interest as potent anti-cancer drug target not only for application as supplementation therapy in individuals who have undergone castration for treatment of prostate cancer. Clue is its role in prostaglandins metabolism and proinflammatory effects thus activation of PPAR γ receptor. There are reports showing that long term inflammation of prostate is correlated with higher risk of prostate cancer [126]. Additionally, metabolized by 17 β -HSD5 prostaglandins are believed to have a special role in angiogenesis and neoplasticity of tumor cells observed also in other cancer types like breast cancer [127].

Specific and effective inhibitors blocking the activity of both 17 β -HSD3 (testicle tissue) and 17 β -HSD5 (peripheral) enzymes could allow lowering the amounts of active androgens in affected tumor tissue, lower the risk of malignant development as well avoid the castration as therapeutic method. Thereby it is highly interesting to search potent inhibitors indicating selectivity towards 17 β -HSD3 and 17 β -HSD5 as well concomitant impact on both enzymes.

At least several group of compounds exhibiting effective (in low micromolar or nanomolar concentrations) inhibitory activity towards 17 β -HSD3 or 17 β -HSD5 *in vitro* or *in vivo* has been identified at the time of beginning the work on this project for e.g.[23, 128-137]. Among them are natural occurring environmental chemicals, synthetic substances such as derivatives of steroids as well non-steroidal compounds. The latter group of compounds are especially interesting since they are expected to have low impact on undesirable direct activation of steroid hormone receptors. Until recently, the number of newly identified highly effective inhibitors towards 17 β -HSD3 [138, 139] and 17 β -HSD5 (AKR1c3) [140, 141, 142] is still growing. However, selectivity of newly identified inhibitors among other isoforms, for example towards AKR1C isozymes in case of 17 β -HSD5 often is a challenge in order to be further developed as potent therapeutic agent.

Introduction

1.4.3 Naturally occurring inhibitors of steroidogenesis.

The selective control of chosen steps in process of steroidogenesis since long is an attractive aim for potent inhibitors searching which could be further developed as drug agents utilized in therapies of hormone-dependent diseases. In efforts undertaken for exploring steroidogenesis blockers one can distinguish two strategies such as searching for hormone receptor antagonist or searching for inhibitors of steroidogenic enzyme like COX enzymes, aromatase, sulfatase, 3 β -HSD/isomerase and 17 β -HSDs etc.

Considering the first strategy many naturally occurring substances such as plant derived phytoestrogens like flavone, flavonone, coumestrol, isoflavones etc. as well other industrial chemicals has been reported to interact with estrogen or androgen receptors acting as antagonists or agonists of endogenous hormones. They are named as endocrine-disrupting chemicals (EDC) and usually show close structural similarity to androgen/estrogen hormones.

Some of phytoestrogens apart of interacting with hormone's receptor have been also shown to inhibit the activity of particular steroidogenic enzymes. The example can be some reports showing inhibition of 3 β -HSD type 1 in conversion of pregnenolone to progesterone by isoflavones (genisteine and daidzenin IC₅₀ between 2,9 and 10 μ M) [134] or inhibition of 17 β -HSD1 in conversion of estrone to estradiol (genisteine IC₅₀ 1,2 μ M) [143] as well inhibition of 17 β -HSD5 by biochanin A in both its oxidative and reductive actions [144]. Apart of mentioned enzymes isoflavones were reported also to inhibit sulphotransferases, sulphases and were shown as weak inhibitors of aromatase [134].

Considering the second searching strategy for steroidogenesis blockers 17 β -HSDs are attractive inhibitor development target for potential using in therapies of hormone-dependent cancers since they acting as molecular switchers between biologically active and not active form of estrogens and androgens thus changing directly their affinity to ER or AR receptor.

Among other examples of naturally occurring phytoestrogens which show relatively potent inhibitory activity towards 17 β -HSDs are flavones and flavonones such as apigenine inhibiting 17 β -HSD1, quercitine showing inhibitory activity against HSD17B5 or coumestrol which significantly inhibited 17 β -HSD1, 17 β -HSD5 and aromatase [134]. Against activity of 17 β -HSD5 was also identified belonging to mycotoxines zearalenone as potent inhibitor in both reductive and oxidative activity [144].

Introduction

However mentioned examples of natural environmental substances can inhibit the activation of hormone receptor many studies demonstrate the effect on other target molecules and signaling pathways through which they can exert diverse actions like anti-oxidant action, inhibitions of cell cycle and cell differentiation, modulation of angiogenesis and modulation of the activity or expression of steroidogenic enzymes etc. As an example of unpredictable effects of tested substances on steroid metabolism can serve published lately studies on some synthesized steroid derivatives as 17 β -HSD1 inhibitors where one of them unsuspectedly appeared to be the activator of 17 β -HSD12 causing up to 3-fold increase of endogenous conversion the estradione into estradiol [145, 146].

1.5 Aims of the study

The leading aspect of this PhD project is the identification and initial biological evaluation of new potent inhibitors towards enzymes of the SDR protein family, whose activity may be crucial for human health with a special emphasis on enzymes showing the hydroxysteroid dehydrogenase activity. Nowadays, due to progress in bioinformatics together with computational and graphical methods thousands of potent inhibitory substances may be designed *in silico* based on studies with pharmacophore models which profit from the knowledge about 3D structures of enzymes and/or enzyme/inhibitor complexes. On the other hand not all recently identified SDRs have been analyzed in detail yet and few of them will be here further explored. Therefore, the here presented work is divided into two parts comprising two main aims of the study:

- **Development of selective inhibitors for 17 β -HSD3 (SDR12C2) and 17 β -HSD5 (AKR1C3)**

This part of the study was realized in the frame of a collaboration between the company BioNetWorks, the group of Daniela Schuster in the University of Innsbruck and the group of Jerzy Adamski in the Helmholtz Zentrum München, supported by the Bayerische Forschungsförderung (BSF). In this project the partners were searching for new non-steroidal inhibitors that could significantly decrease the enzymatic activity of human enzymes playing the key role in controlling the testosterone biosynthesis from androstenedione as 17 β -HSD3 and 17 β -HSD5. Both 17 β -hydroxysteroid dehydrogenases type 3 and 5 constitute important therapeutic target for androgen-related diseases such as prostate cancer. In this aim the company BioNetWorks together with the research group of Daniela Schuster in the University of Innsbruck developed some pharmacophore models for the identification of steroidal and non-steroidal 17 β -HSD type 3 and 5 inhibitors and validated the models by *in silico* screening of commercial databases. Subsequently, the most interesting virtual hits, a set of structurally diverse chemical compounds, was intended to be further screened in this work using biological enzymatic efficacy tests and the most promising inhibitory substances evaluated.

- **Further characterization of barely annotated human SDR candidates 17 β -HSD8 (SDR30C1), SDR-O (SDR9C7), and HSDL2 (SDR13C1)**

Two rudimental annotated human SDR candidates such as orphan SDR-O and hydroxysteroid dehydrogenase like 2 (HSDL2) as well human 17 β -HSD8 reported as estradiol metabolizing enzyme

Introduction

were intended to be further characterized in the work here. For this, the amino acid sequence of the first two proteins should be analyzed with regard to cofactor preference and specific SDR motifs. All three enzymes should undergo subcellular localization studies and a screening for their natural substrates including steroid hormones and retinoids.

2 Results

2.1 Inhibitor studies

In vitro screening assays testing the activity of human 17 β -HSD3 and 17 β -HSD5 enzymes at conversion of androstenedione into testosterone were developed and applied for searching the potent inhibitory compounds among virtually selected chemicals. The best inhibitory substances should be then sorted out for further more laborious biological evaluations that could emerge the most promising leading drug agent.

2.1.1 Expression of human 17 β -HSD3

For *in vitro* screening the potent inhibitory compounds against human 17 β -HSD3 there was applied an enzymatic assay with the enzyme derived from mammalian expression system since the recombinant form of 17 β -HSD3 expressed in bacteria was not available. Especially for inhibitor studies the stable transfected HEK293 cells over-expressing human HSD17B3 were generated. Stable transfected cells were obtained in the frame of the bachelor project by Fabian Ströhle at IEG, HMGU.

2.1.1.1 Establishing the 17 β -HSD3 enzymatic activity

Few of frozen human HEK293 clones expressing HSD17B3 were revitalized and checked out for enzymatic activity in conversion of androstenedione to testosterone. All clones of stable transfected cell pellets revealed high enzymatic activity at contents of containing only 300 000 cells in the pellet. However, the activity between some of them was slightly different and seemed to be dependent from number of passage and antibiotic (G418) concentration in selection medium. One of the clones (named as K2) was then used for inhibitor screening experiments.

2.1.2 Expression of human 17 β -HSD5 (AKR1C3)

The enzymatic activity of human 17 β -HSD5 at reduction of androstenedione to testosterone in transiently expressed HEK293 cells had been previously described to be highly labile upon

Results

homogenization in comparison to the activity in intact cells [147]. In respect to this evidence as well for better throughput in planned *in vitro* inhibitor screening it was decided to use assays with human recombinant 17 β -HSD5 produced by bacteria expressing system which was available and well established in the laboratory. Human HSD17B5 gene was then efficiently over-expressed in BL21DE3 *Codon Plus* RP optimized bacteria from pGex2T vector as N' terminally GST-tagged fusion protein. Furthermore, the recombinant protein was found to be well soluble in supernatants (14000 x rpm) from harvested and lysated bacteria pellets thereby allowing further purifications steps crucial for *in vitro* detailed kinetic enzymatic studies performed by use of spectrophotometric methods [Figure 20; Figure 21].

2.1.2.1 Human 17 β -HSD5 purification and *in vitro* assay optimization

Expressed in bacteria as GST-fusion recombinant enzyme was then harvested and subjected to purification protocol by use of the glutathion-sepharose affinity matrix in order to achieve pure 17 β -HSD5 protein [Figure 20; Figure 21]. Next, the potent loss of enzymatic activity during homogenization and purification procedure was tested and assays were optimized for the best yield. Aliquots (10 μ l) of recombinant enzyme suspension from subsequent purification steps were assayed with radio-labelled Δ^4 -androstene-3,17-dione. Samples were normalized by taking the same part (1:250) of the bacteria/enzyme suspension in the final volume. The most efficient conversion to testosterone for 100ml of over-night induced bacteria culture was observed with homogenate bacteria lysates [Figure 20; Figure 21]. Overall, optimization studies showed that the best yield in 17 β -HSD5 activity was achieved when bacteria walls were disrupted and the enzyme released into suspension during subsequent homogenization steps. Further purification process significantly decreased the activity of the enzyme even up to 10% in comparison to bacteria lysate. The observed fact was probably due to the partial loss of the active enzyme molecules which seems to be unavoidable during this procedure (bounded sepharose after elution still showed some activity; results not shown). Presence of N'GST fusion tag had no influence on tested activity of the enzyme [Figure 21; aliquots marked as E and F]. Storage of samples at -20 $^{\circ}$ C was also checked out and it did not influence significantly the enzymatic properties (results not shown). Regarding the optimization results above the supernatants from homogenated bacteria lysates (14000 x rpm) were used for the following *in vitro* inhibitor screening with human 17 β -HSD5.

Results

Control of purification quality for recombinant human 17 β -HSD5.

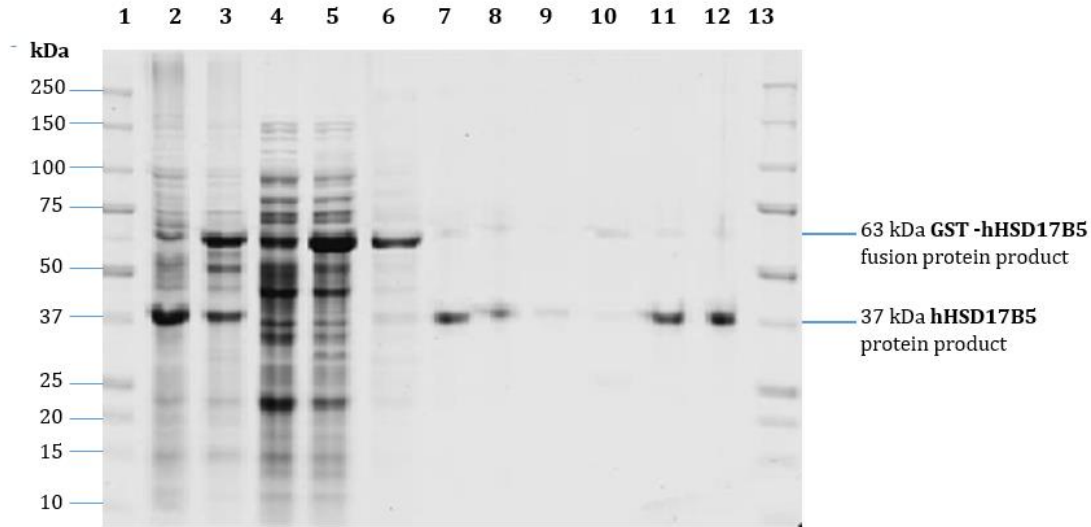


Figure 20 SDS-PAGE showing the homogenated bacteria lysate fractions from purification process of BL21DE3 bacteria expressing human HSD17B5_GST fusion gene product. 1- protein marker; 2- not induced bacteria pellet; 3- IPTG induced bacteria pellet; 4- not induced bacteria supernatant; 5- IPTG induced bacteria supernatant; 6- aliquot from suspension after incubation the with GT-sepharose (after 3x washing with PBS : 500rpm, 5min) ; 7- first elution of cleaved from GST enzyme (after incubation with thrombin); 8- second elution; 9- third elution; 10- forth elution; 11- concentrated from all elutes human 17 β -HSD5; 12- filtered human 17 β -HSD5; 13- molecular mass

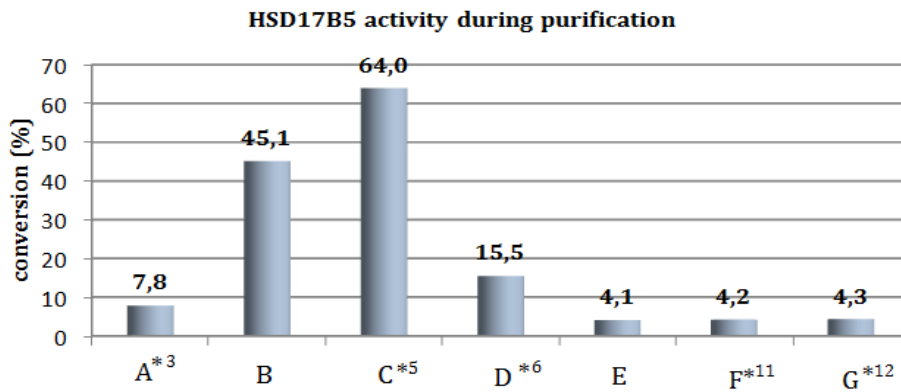


Figure 21 The letters are corresponding to the following aliquots (asterix and the appropriate number is the reference to the SDS-PAGE above): A)- Intact bacteria suspension in PBS; B) – supernatant after bacteria lysis and centrifugation 4500rpm, 15min; C) - supernatant after lysis and subsequent centrifugation at 14000rpm, 30min; D) - suspension after incubation supernatant with GT-sepharose; E) - filtered eluat after GT-elution; F) - filtered eluat after incubation with thrombine; G) - aliquot of purified h17 β -HSD5 (after incubation with thrombine). Samples for given purification fraction were normalized by having the same part (1:250) of the first bacteria suspension in each final volume.

2.1.3 Inhibitor screening results on 17 β -HSD3 and 17 β -HSD5

Potent inhibitory substances were selected by the company BioNetWorks and a group of Daniela Schuster in the University of Innsbruck from commercial compound vendor databases based on their own results of previous virtual studies where finally two ligand- and four structure-based pharmacophore models were applied. Initially, a ligand-based model which profited from knowledge of molecular characteristics of highly active steroidal 17 β -HSD3 inhibitors was generated and optimized for *in silico* compound screening. In this way the first set of 15 chemicals numbered from **1-1** to **1-15** presenting the best fitting score at virtual screening was selected and subjected to biological verification as putative inhibitors of human 17 β -HSD3 and human 17 β -HSD5 as a selectivity control. The fixed final concentration of tested substances was 2 μ M in assays testing the reduction of androstenedione to testosterone at the presence of NADPH as cofactor. Chemical structures of used compounds are to see in the appendix.

2.1.3.1 1st round of inhibitor screening

Results of the first biological screening for 17 β -HSD3 and 17 β -HSD5 inhibitors with 15 selected compounds are presented in the **Figure 22** and **Table 10** below. All 15 tested potent inhibitors displayed some bioactivity towards 17 β -HSD3 which was estimated as slight or medium (5-50% of inhibition).

Results

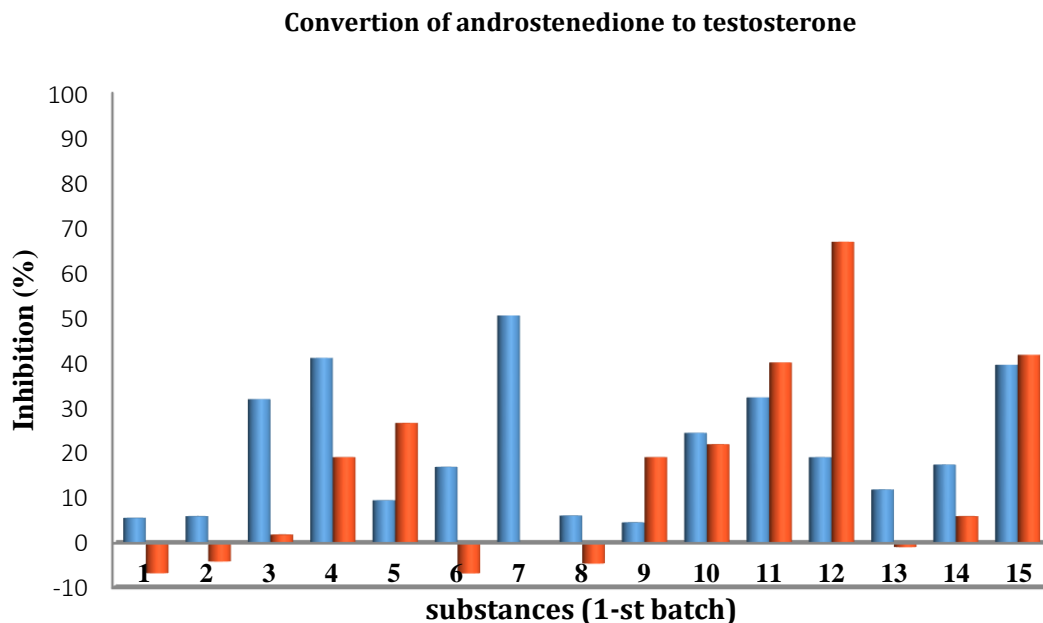


Figure 22 *In vitro* screening results of inhibitory effect of 15 tested substances (2 μ M) on human 17 β -HSD3 (blue) and 17 β -HSD5 (red) in reduction the androstene-3,14-dione to testosterone. In the graphics the inhibition is expressed as a percent (%) of enzymatic activity in the control assay without inhibitor (1%DMSO).

Among them two inhibitor candidates namely **1-4** and **1-7** were able to lower the catalytic activity of HSD17B3 to an appreciable extent by 41.3 and 50.8%, respectively. Additionally, the compound **1-7** demonstrated good preferences to 17 β -HSD3 over 17 β -HSD5. Good selectivity to 17 β -HSD3 showed at least few other compounds like 1-3 or 1-6 but with weak inhibition effect below 33%.

Table 10 Values of inhibitions results (%) for the first batch of compounds tested *in vitro* as potent inhibitors against reductive activity of 17 β -HSD3 and 17 β -HSD5. Values marked on yellow indicates compounds with inhibition over 40%

Number of substance	hHSD17B3 inhibition (%)	hHSD17B5 inhibition (%)
1-1	5.5	-4.6
1-2	5.9	-0.9
1-3	32.1	-0.9
1-4	41.3	20.6
1-5	9.4	27.8
1-6	17.0	-4.8
1-7	50.8	-2.5

Results

1-8	6.0	-2.5
1-9	4.5	2.8
1-10	24.6	25.6
1-11	32.5	40.3
1-12	19.1	67.1
1-13	11.9	-1.0
1-14	17.5	5.9
1-15	39.8	42.6

2.1.3.2 2nd round of inhibitor screening

It was assumed in this project that selected at 2 μ M of working concentration inhibitory compound should selectively inhibit target enzymes at least 70-80% in order to become a candidate worth of further more laborious biological evaluation. Therefore, efforts aimed at improving the efficacy of virtual pharmacophore models were taken. What is more, observed at first screening round conspicuous bioactivity towards 17 β -HSD5 as well availability of its 3D-crystal structure in complexes with chosen ligands at public PDB database has encouraged researchers engaged in BioNetWorks project to actualize a first pharmacophore model by this information. For this purpose BioNetWorks developed and employed four new structure-based pharmacophore models for virtual substance screening. They were basing on the knowledge about ligand-protein interactions from X-ray crystal structure of human 17 β -HSD5 with co-crystalized ligands such as indomethacin, flufenamic acid, EM1404 or rutin. All of analysed structures were previously annotated in the literature as highly active 17 β -HSD5 inhibitors. Next improved model for 17 β -HSD3 inhibitor search was employed.

For biological visualization were selected compounds which were positively screened against more than two models and next against validated ligand-based pharmacophore model for 17 β -HSD3. The new validated model was completed also by information about new reported in literature non-steroidal 17 β -HSD3 inhibitors and regarded the dates from the first screening round. Finally, virtual screening studies followed to selection of subsequent putative inhibitors in the batch of twenty chemicals (named from **2-1** to **2-20**) for visualization in enzymatic assays with 17 β -HSD5 or 17 β -HSD3. Results of the second screening round are presented in the **Figure 23** and **Table 11** below.

Results

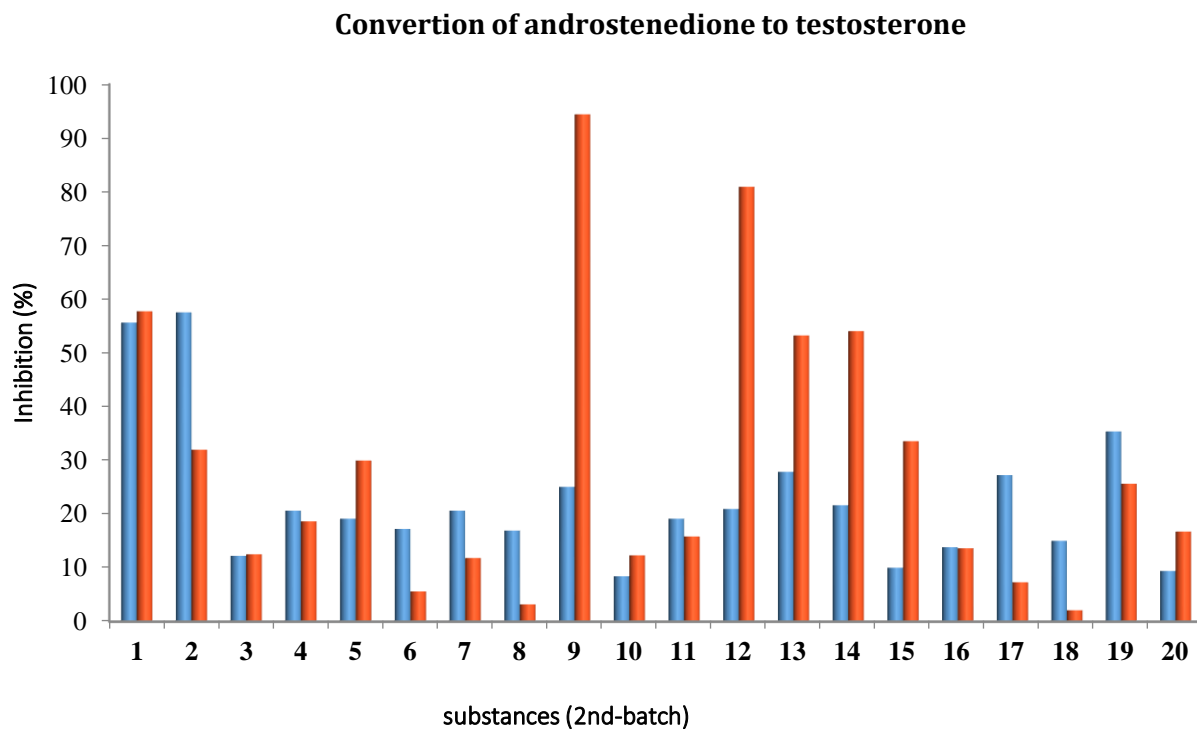


Figure 23 In vitro screening results of inhibitory effect of 20 tested substances from the second batch (2 μ M) on human 17 β -HSD3 and 17 β -HSD5 in reduction the androstene-3,14-dione to testosterone. In the graphics the inhibition is expressed as a percent (%) of enzymatic activity in the control assay without inhibitor (1%DMSO). The source of enzyme in assays for 17 β -HSD3 was stable transfected HEK293 cell pellets, while in case of 17 β -HSD5 homogenated bacteria lysates.

Table 11 Second round of BNW compounds numbered from 2-1 to 2-20 screening their potential inhibitory activity towards 17 β -HSD3 and 17 β -HSD5 in reduction of androstenedione to testosterone. Values marked on yellow indicate compounds with inhibition over 50%.

Number of substance	HSD17B3 inhibition (%)	HSD17B5 inhibition (%)
2-1	55.6	57.7
2-2	57.5	31.9
2-3	12.2	12.5
2-4	20.6	18.6
2-5	19.1	29.9
2-6	17.2	5.6
2-7	20.6	11.8
2-8	16.9	3.2
2-9	25	94.4
2-10	8.4	12.3
2-11	19.1	15.8

Results

2-12	20.9	80.9
2-13	27.8	53.2
2-14	21.6	54
2-15	10	33.5
2-16	13.8	13.6
2-17	27.2	7.3
2-18	15	2.1
2-19	35.3	25.6
2-20	9.4	16.7

Generally, in the second round of biological screening the observed inhibition towards 17 β -HSD3 and 17 β -HSD5 was more efficient in comparison to the first screening experiment. Surprisingly, two substances named as **2-9** (94.4 %) and **2-12** (80.9 %) showed high inhibitory effect on HSD17B5 with relatively low impact (4-5 times) on 17 β -HSD3 activity. Other candidates **2-1**, **2-13**, and **2-14** inhibited testosterone conversion by 17 β -HSD5 over 50 %. Concerning the impact on 17 β -HSD3 catalytic activity at least two compounds **2-1** and **2-2** were able to inhibit this enzyme by more than 50%. Among them **2-1** was only one with dual bioactivity towards 17 β -HSD3 and 17 β -HSD5.

2.1.4 Further biological tests with identified inhibitors

Chemicals which in both *in vitro* screening rounds showed more than 40% of inhibition were initially identified as 17 β -HSD3 or 17 β -HSD5 inhibitors. Most of them reveal diverse chemical structures and nature what can be an interesting starting point for further analysis of molecular ligand-enzyme interactions and useful for improving the pharmacophore models in future. In the frame of the BioNetWorks project all initially selected putative inhibitors were next subjected to specificity assays testing the inhibition effect on catalysis of other non-targeted 17 β - or 11 β -HSDs subtypes. Anyhow, it was decided that at this subproject being the part of the PhD work further biological evaluations will be focused on only few substances showing the strongest inhibitory effect against human 17 β -HSD5. Further biological evaluations means in this case IC₅₀ and K_i estimation, determination the type of inhibition mechanism and ex-vivo tests with living cell cultures.

Results

2.1.4.1 IC₅₀ evaluation and selection of the best inhibitor

Because the highest inhibitory effect among tested substance was found against 17 β -HSD5 the strongest of them were selected for verification as inhibitors. The IC₅₀ value was then determined for the best inhibiting chemicals like **1-12** from the first screening round and compounds **2-1**, **2-9**, **2-12** from the second one [Figure 24]. The lowest IC₅₀ value of 0.26 μ M (0.29 μ M in replied experiment) was presented by the compound **2-9** which was at once the strongest inhibitory compound identified in the performed screening. Thereby the compound **2-9** was further evaluated as potent non-steroidal inhibitor of 17 β -HSD5 in this work and subjected to more detailed kinetic analysis.

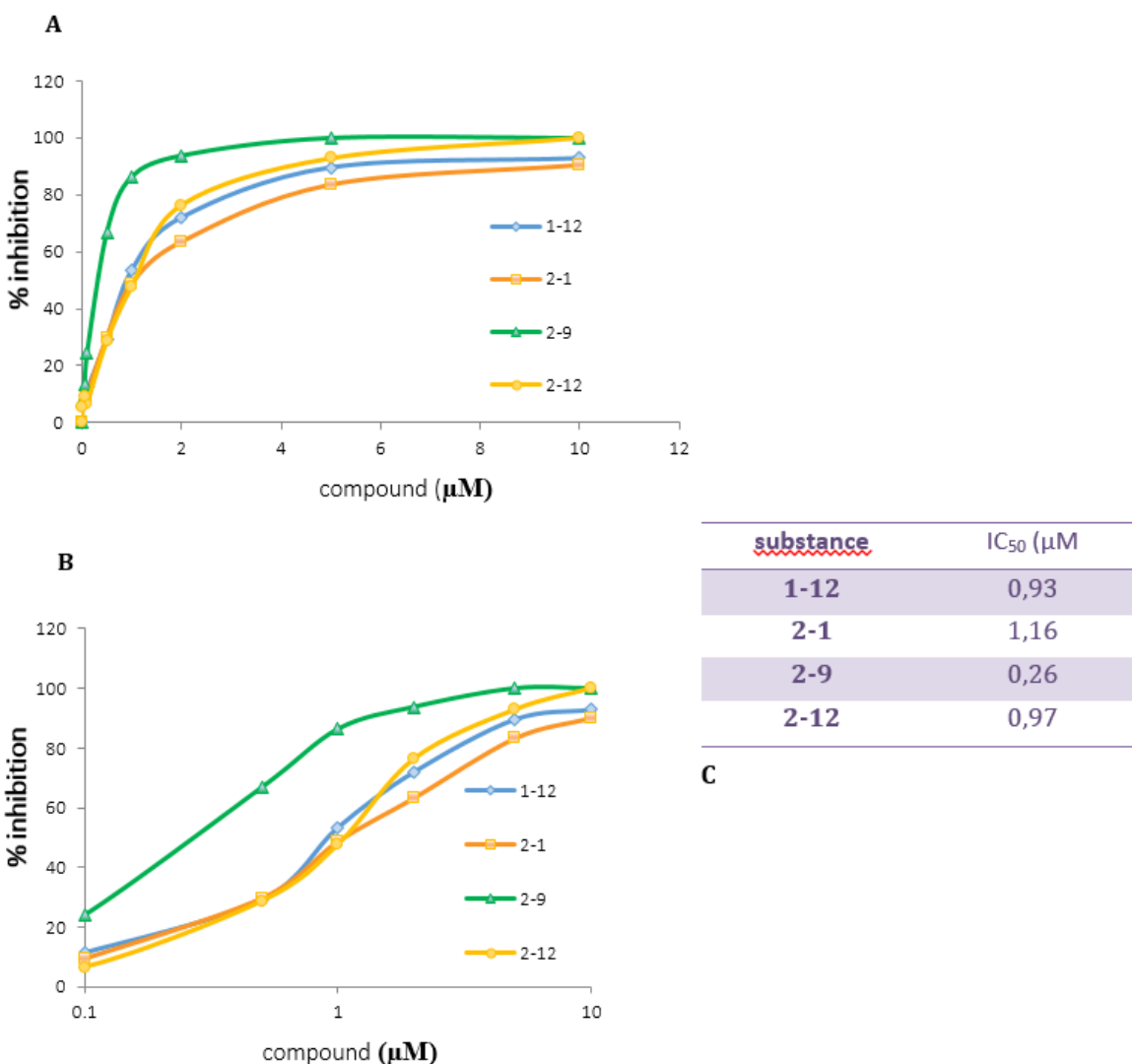


Figure 24 Estimation of IC₅₀ values for the strongest 17 β -HSD5 inhibitors selected from performed screenings. Curves on plots were fitted by use Sigma-Plot 'One site saturation' module. A) Compound concentration dependent inhibitory effect (%) on conversion of androstenedione to testosterone by 17 β -HSD5. B) The plot as above demonstrated in logarithmic scale. C) Calculated IC₅₀ values for selected 17 β -HSD5 inhibitors (Sigma plot program).

Results

2.1.4.2 Specificity assay among other 17 β -HSDs for selected inhibitor

Concerning the performed in the frame of BioNetWorks project specificity assays with all selected from two screening rounds compounds it is remarkable that the strongest 17 β -HSD5 inhibitor **2-9** showed also good selectivity among other 17 β -HSD subtypes. **2-9** revealed slight inhibition (3-4 times lower) towards 17 β -HSD3 in reduction of androstenedione to testosterone and 17 β -HSD1 in conversion of estrone to estradiol. The tested compound seems to have no impact on catalysis of estradiol oxidation by 17 β -HSD2 and 17 β -HSD4 as well on reduction of estrone to estradiol by 17 β -HSD75.

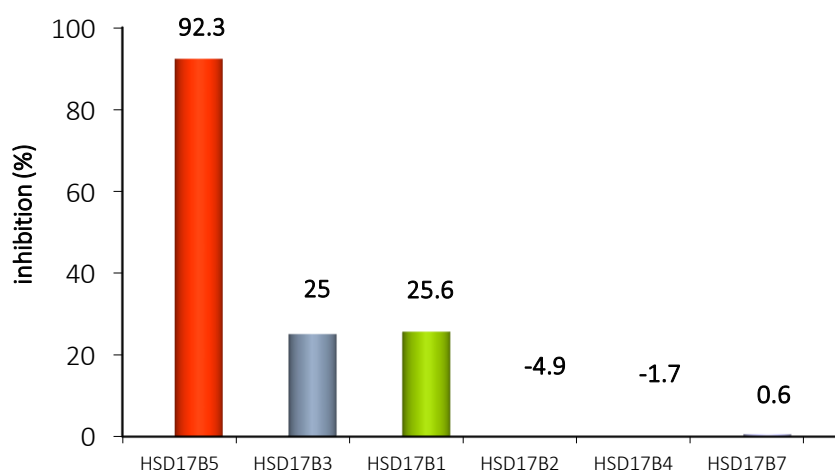


Figure 25 Selectivity of 2-9 inhibitor among chosen 17--HSDs types. There was checked the inhibitory activity of 17 β -HSD3 and 17 β -HSD5 in conversion of androstenedione to testosterone, 17 β -HSD1 and 17 β -HSD7 in reduction of estradiol to estrone and in the case of 17 β -HSD2 and 17 β -HSD4 of estrone to estradiol.

2.1.5 Optimization of *in vitro* enzymatic assay by use of 96-well plates

Inhibitor screening results presented above were performed by use of high sensitive enzymatic assays with radio-labelled steroids and it allowed to select few potent inhibitors against human 17 β -HSD5 reductive activity. Nevertheless, for more detailed kinetic analysis these assay turn out to be quite slow and material consuming. Thereby to provide the higher throughput and lower use of assayed materials the tests utilizing 96-well plates were applied for development of an alternative non-radioactive enzymatic assay based on UV-Vis, fluorescence detection. Because among screened inhibitory substances the highest effect has been found against catalytic activity of

Results

17 β -HSD5 the assays with this enzyme were chosen as a model in optimization tests with application of 96-well plates.

2.1.5.1 Development of assays based on UV-Vis or fluorescent detection method

Since 17 β -HSDs use NAD(P)H/NAD(P)⁺ as cofactor the monitoring of changes in NADH or NADPH is available by use of spectrophotometric detection methods. The processed enzymatic catalysis can be monitored by measuring the changes in amount of reduced cofactor either as changes in absorbation (OD₃₄₀) or as changes in fluorescence intensity (RFU) at λ_{em} =450nm and λ_{exc} = 340nm. Depending on direction of the reaction: reduction or oxidation, depletion or increasing of the reduced cofactor is observed, respectively. However both methods have some advantages and limits which face unavoidably during optimization experiments. Experimentally checked sensitivity for absorbation is around 1 μ M while for fluorescence it is around ten times higher and the minimal differences in changes of cofactor can be detected from around 100 nM [Figure 26]. Nevertheless a disadvantage of fluorescence monitoring is its upper limit where the concentration dependent curve is parabolic with the acceptable linearity ($R^2 > 0.995$) bellow 100 μ M. In case of absorbance the concentration dependent curve is more linear even over 500 μ M of the cofactor.

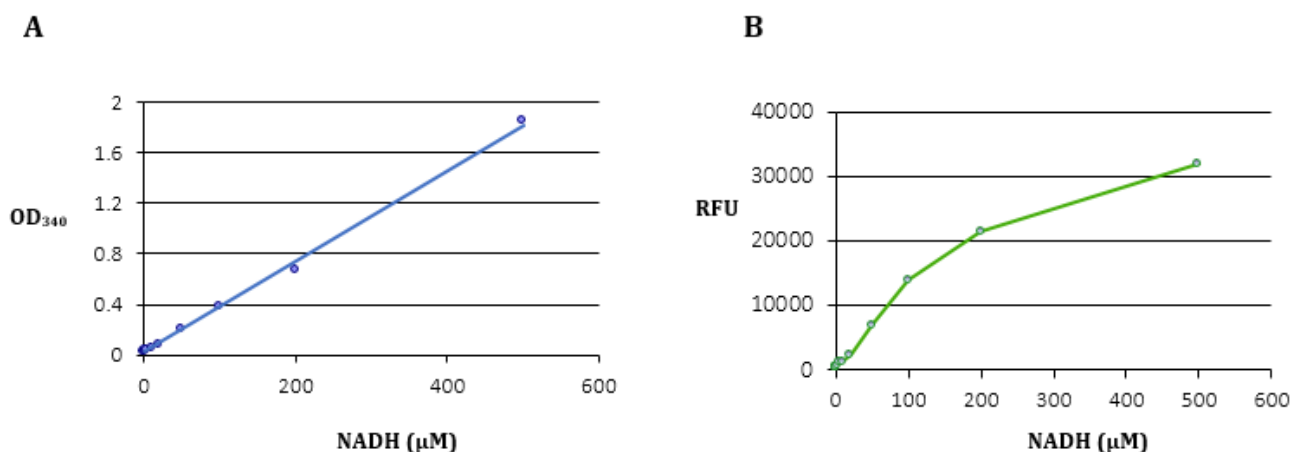


Figure 26 A: Changes in absorbation (OD₃₄₀) at growing NADH concentrations create a linear curve. B: Changes in fluorescence intensity (RFU) at growing NADH concentrations create a parabolic line.

Results of experimental assay optimization revealed that NAD(P)H is not stable in water solution over time due to spontaneous oxidation what means that short time of incubation is needed. At the

Results

temperature 37°C a signal decreased of 4-10% during 1h monitoring of the fluorescence signal [Figure 28]. The effect was dependent from cofactor concentration and localization on the 96-well plate probable because of higher evaporation in wells on the edges of the plate. So the shorter time of incubation as well the care for equal humidity over the plate has to be considered in assay with enzyme.

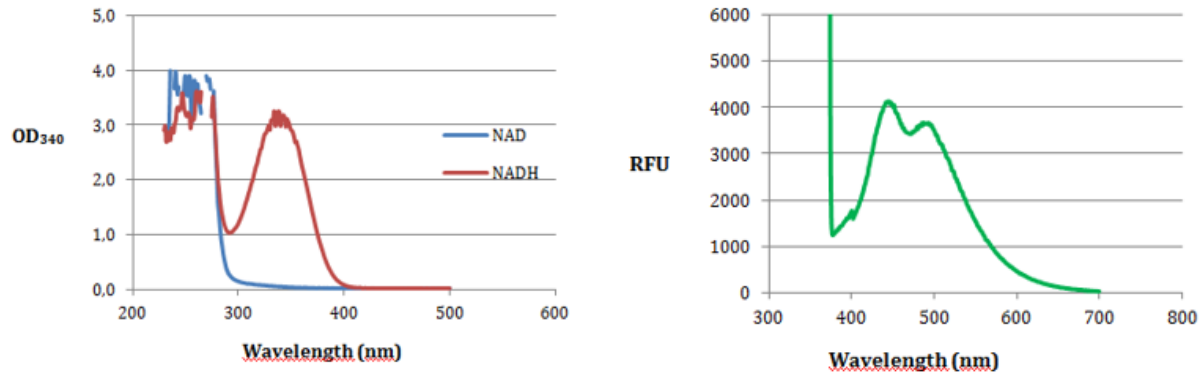


Figure 27 Spectrum of NADH/NAD UV-Vis light absorption (left). NADH fluorescence emission spectrum at $\lambda_{exc}340nm$ (right).

Results

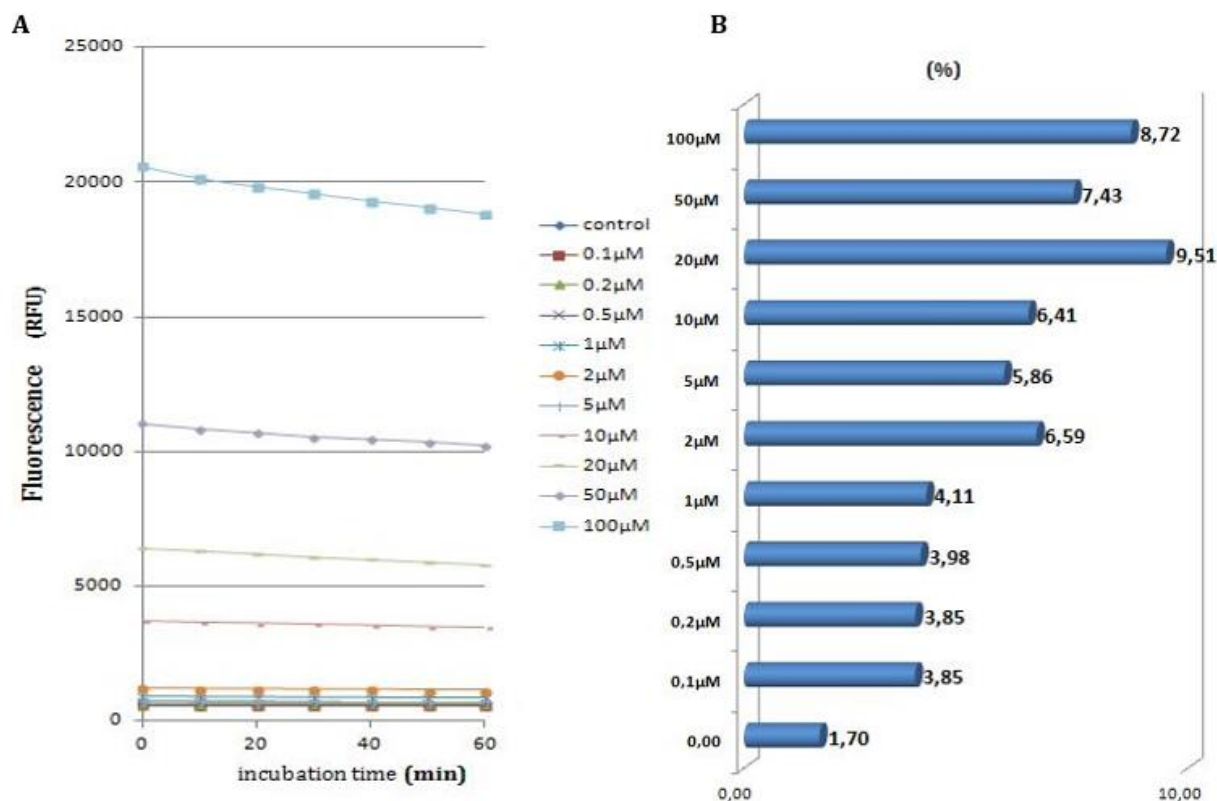


Figure 28 Spontaneous oxidation of NADH during 1h incubation in water solution at 37°C monitored as fluorescence signal depletion ($\lambda_{exc}= 340\text{nm}$, $\lambda_{em}=450\text{nm}$). A) Time progress plot for various NADH concentrations. B) Calculated loss of fluorescence intensity in % during incubation for various NADH concentrations.

2.1.5.2 Enzymatic assays based on NADH/NADPH detection. Time progress curves

Next important step in assay optimization was the determination of proper enzyme amount and cofactor concentrations as well determination the time of incubation in order to observe differences in initial velocities at various substrate concentrations. The tested parameters were namely: the amount of enzyme, the optimal range of substrate and the optimal amount of cofactor. As a model for assay optimization experiments it was chosen the reaction of oxidation the androstanediol to androsterone with purified human 17β -HSD5 enzyme at the presence of NADP+ as cofactor where the signal is increasing in the course of reaction. The velocity of being optimized model reaction even with available maximal amount of 17β -HSD5 enzyme per sample appeared to be slow thereby the more sensitive fluorescence monitoring was next considered in further optimization tests rather than absorbance [Figure 29].

Results

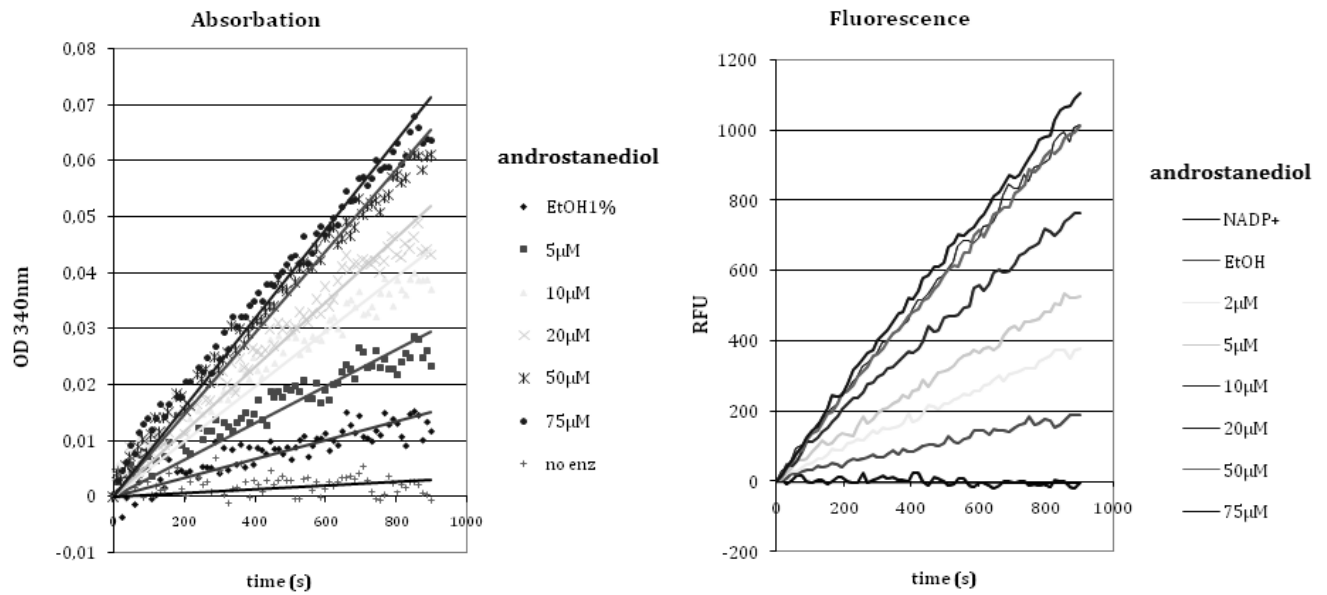


Figure 29 Time progress curves during the oxidation of androstanediol to androsterone at the presence of NADP+ as cofactor by purified form of human 17 β -HSD5. A: Detection of NADPH growing absorbance at 340nm; B: Detection of the fluorescence intensity ($\lambda_{exc340nm}/\lambda_{em450nm}$) is corresponding to the growing NADPH

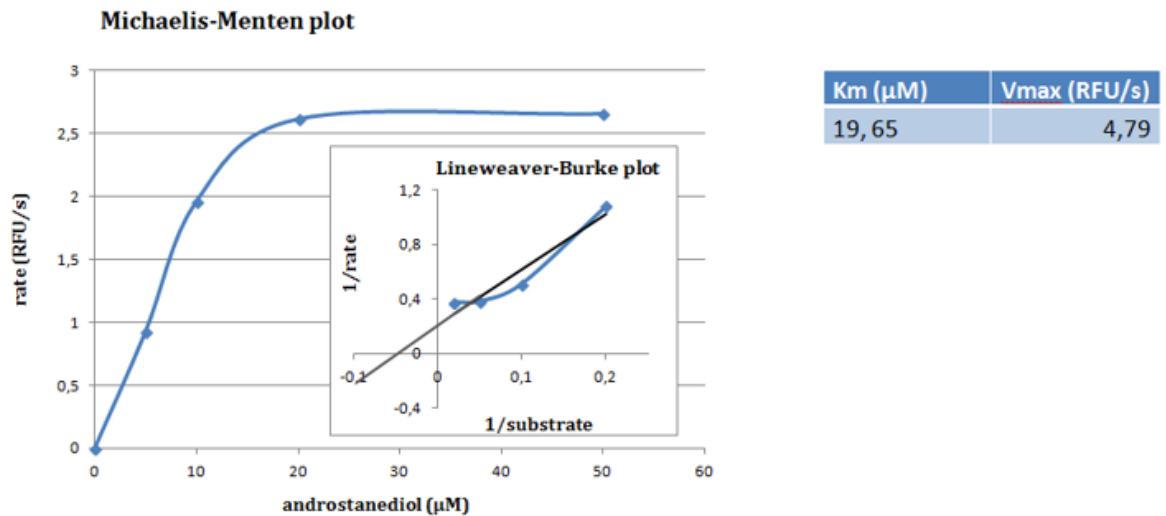


Figure 30 Michealis-Menten substrate saturation plot for oxidation the androstanediol to androsterone by purified human recombinant 17 β -HSD5 (55 μ g per sample). Km and Vmax values were calculated here manually by use Lineweaver-Burke plot. Initial velocities were calculated from linear time progress curves of 15min incubation

Results

Trying to increase the velocity of being optimized assays homogenated bacteria lysates as a source of 17 β -HSD5 enzyme were also checked and they showed higher velocity of proceeded reaction when compared with purified enzyme. Unfortunately, also higher unspecific reduction of NADP⁺ to NADPH was observed in control samples without substrate (instead: 1% ethanol used as a solvent for steroid substrates)

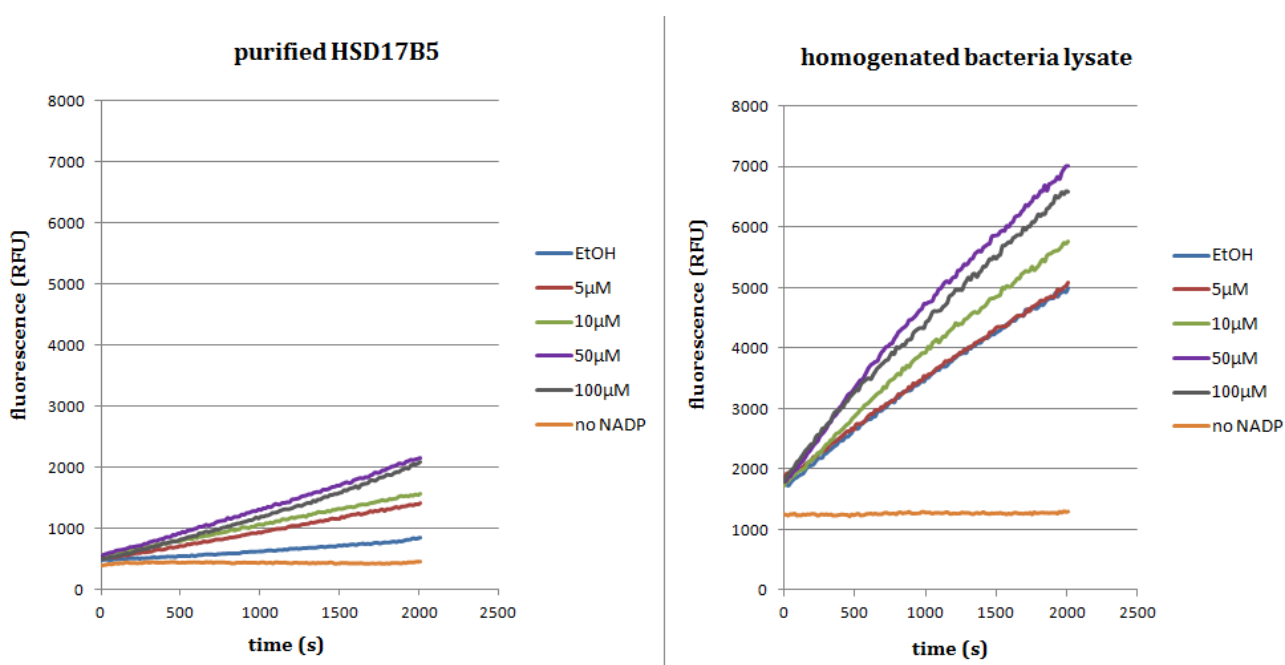


Figure 31 Time progress plots for various concentrations of substrate (5-100 μ M) in oxidation of androstenediol to androsterone t the presence of NADP⁺ as cofactor (200 μ M) by purified form of 17 β -HSD5 (8,25 μ g) and homogenated lysate from IPTG induced bacteria expressing 17 β -HSD5 enzyme.

2.1.5.3 Optimization of *in vitro* test on 96-well plates with use of artificial fluorescent substrate for 17 β -HSD5

Due to low efficiency of being optimized previously assays the use of a fluorochrom based method was next considered as alternative method for monitoring the 17 β -HSD5 activity. Enzymatic assays with specific for this enzyme commercially available artificial substrate were optimized since

Results

unsuccessful trials also with monitoring the reductive 17 β -HSD5 activity based on NADPH detection. The utilized fluorogenic synthetic substrate chemically was a 8-acetyl-2,3,5,6-tetrahydro-1*H*,4*H*-11-oxa-3*a*-aza-benzo[*de*]anthracen-10-one described and published by Yee *et al.* [148]. At optimization tests it was observed that more linear and comprehensive time progress curves were achieved when a purified form of the enzyme was used in the assay rather the bacteria homogenate lysate though the better velocity of reaction. Reaction was processing fast and enabled to determine the K_m .

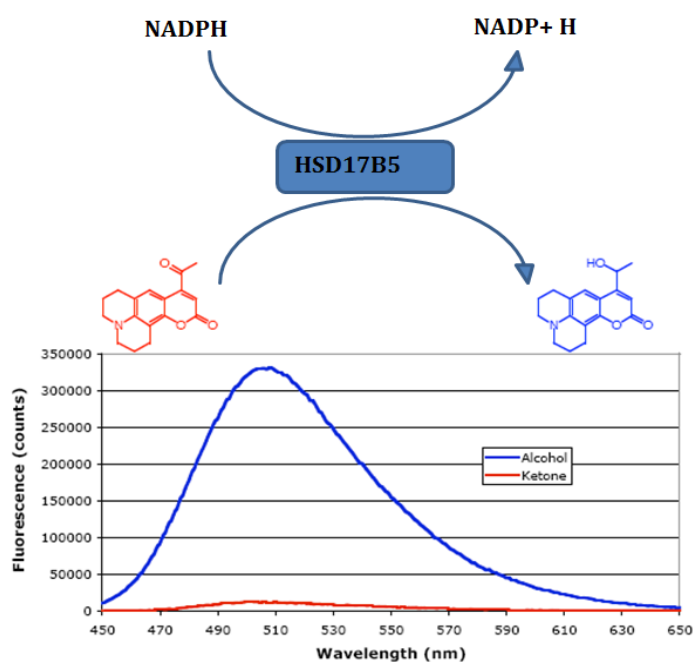


Figure 32 IC₅₀ estimated for assay with artificial substrate for HSD17B5. Picture adopted from [148]

2.1.5.4 In vitro IC₅₀ estimation for assays with artificial substrate

Next, assay with selected 17 β -HSD5 inhibitor was performed for checking the IC₅₀ value to compare it IC₅₀ achieved with assay with bacteria lysate and radio-labelled substrates. IC₅₀ (0.14 μ M) in assays with artificial 17 β -HSD5 substrate and purified enzyme protein was even lower but apparent to IC₅₀ (0.26 μ M) obtained from assays with homogenated bacteria lysates and androstene-3,17-

Results

dione (1,2,6,7-³H) as substrate (see the results above). It confirms that the results with this method can be considered as reliable.

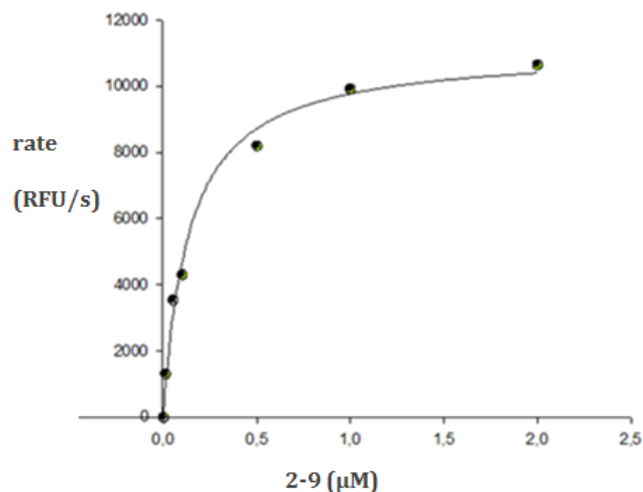


Figure 33 IC50 estimated for assay with artificial substrate for HSD17B5

2.1.6 Determination of K_i and inhibition mechanism of 2-9 compound

The next step was the determination of K_i value and estimation of the mechanism of inhibition for chosen inhibitory compounds. The emission spectrum at $\lambda_{exc}=450\text{nm}$ of tested inhibitory BNW compound 2-9 did not interfere with detection of the fluorescing product in contrary to other BNW inhibitor 2-12 which appeared to be optically active and thus not applicable for this method of measurement. Further, studies on potential mechanism of inhibition suggest that the tested inhibitory compound compete for active site of $17\beta\text{-HSD5}$ with a fluorescent substrate in a classical competitive mechanism. Calculated inhibition constancy (K_i) for this model is $0.23\mu\text{M}$ ($0.18\mu\text{M}$ in the replied experiment) while the best correlation was found for the competitive model of inhibition.

Results

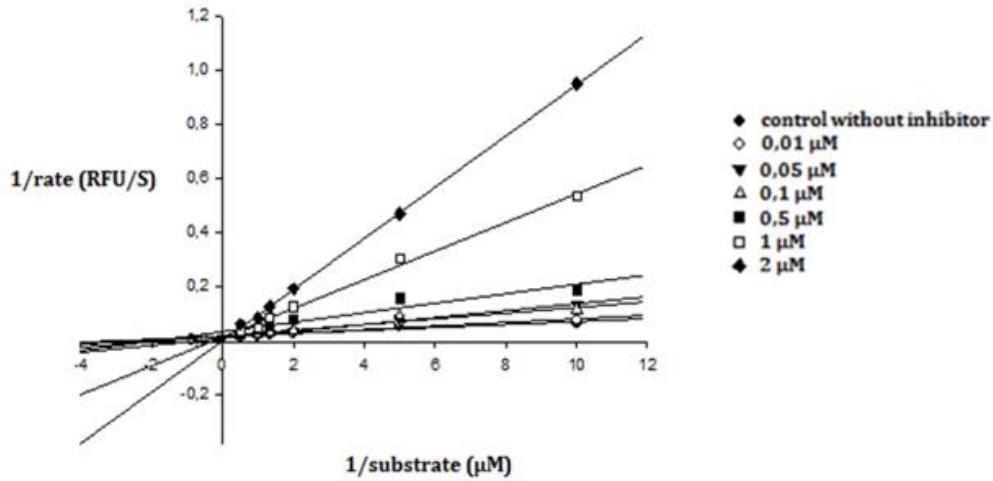


Figure 34 Lineveaver-Burk-plot for the evaluation of K_i . Conversion of 8-acetyl-2,3,5,6-tetrahydro-1H, 4H-11-oxa-3a-aza-benzo[de]anthracen-10-one to fluorescent product catalysed by purified recombinant human 17 β HSD5 was monitored in the presence of inhibitory substance 2-9. Data were fitted by Sigma-Plot Kinetics module.

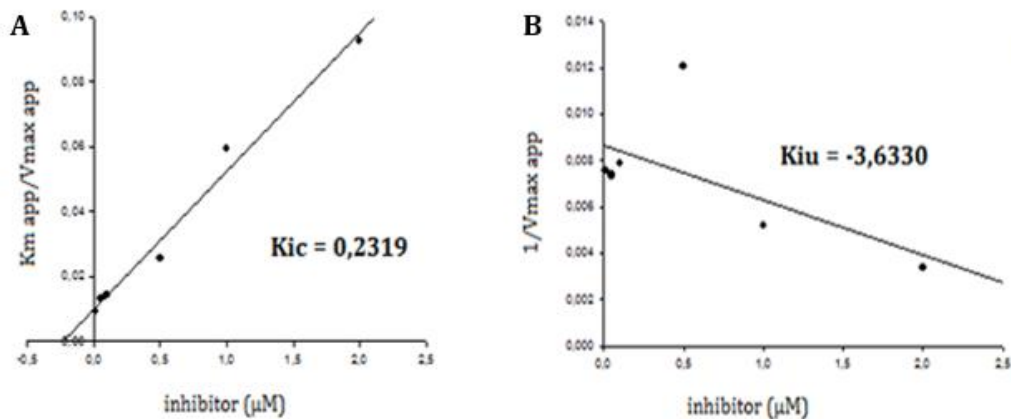


Figure 35 The best fit for competitive model of inhibition. **A:** competitive model; **B:** uncompetitive model of inhibition. Sigma Plot calculations utilizing the one site saturation plots mechanism of inhibition determination.

2.1.7 *Ex vivo* inhibitor studies

Efficiency of the best inhibitor **2-9** was next checked *ex vivo* in human cell cultures in order to compare and verify observed *in vitro* inhibitory effect against 17 β -HSD5 in the conditions of living cells. For this purpose comparison of IC₅₀ values in various enzymatic assays with 17 β -HSD5 converting androstenedione into testosterone as well observation of potent inhibitor's cytotoxic effects were planned.

2.1.7.1 Searching for the best cell line model effectively converting androstenedione by HSD17B5

Human HEK293 cells show no endogenous expression of HSD17B5 that could be detected with Western blot methods. This cell line was primary chosen in order to have comparison with HEK293 stable expressing HSD17B3 used in previous experiments with potent inhibitors. In order to achieve over-expression of investigated enzyme the cDNA coding human HSD17B5 was cloned into pcDNA3 mammalian expression vector and transfected transiently into HEK293 cells. Expression of the transfected enzyme was well visible on Western blot [**Figure 36**]. Subsequently, pelleted cells were assayed *in vitro* with radio-labeled androstenedione and NADPH cofactor and checked for activity of the over-expressed enzyme.

Results

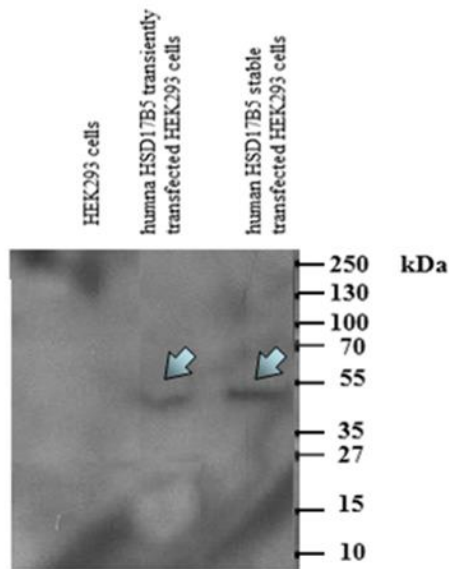


Figure 36 Western blot confirming the overexpression of human HSD17B5 in used for assay stable or transiently transfected HEK293 cell and no detectable endogenous expression.

Unfortunately, 2 mio of tranciently transfected with HSD17B5 HEK293 cells per sample incubated 1h *in vitro* with radio-labeled androstenedione gave no detectable conversion to testosterone. The activity tests were next repeated changing the conditions of the previous assay: with double amount of cells, with stable transfected HEK293 cells and with another alternative cell line MCF7 stable expressing human HSD17B5 enzyme. Only pellets containing doubled amount (4mio) of stable transfected HEK293 cells yielded around 4% of conversion when incubated *in vitro* for 1h with radio-labeled androstenedione and cofactor. The same amount (4mio) of stable transfected MCF7 cells gave around 10% of conversion what was giving more than twice better efficacy of conversion than stable transfected HEK293 cells [**Figure 37**].

Results

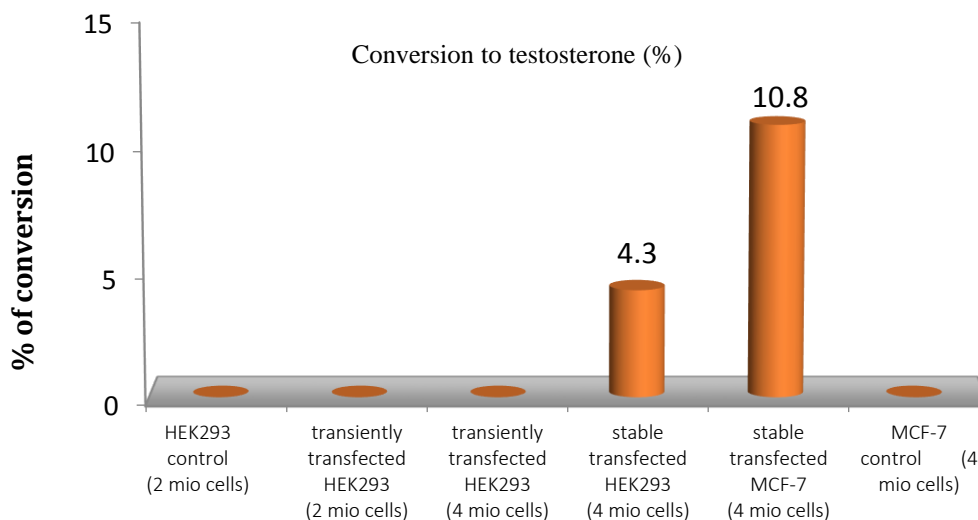


Figure 37 *In vitro* conversion of radio-labeled androstenedione to testosterone during 1h of incubation at 37°C at the presence of NADPH as cofactor and for used various cell pellets of different cell lines types expressing human HSD17B5.

2.1.7.2 Optimization of *in vivo* assays testing the conversion of androstenedione to testosterone by HSD17B5

Optimization of *in vivo* assay effectively converting androstenedione to testosterone was important for planned inhibitor screening. Cells stable over-expressing human HSD17B5 of both cells lines were seeded on plates and incubated with radio-labelled androstenedione substrate in humid conditions (5% CO₂, 37°C). After defined period of time radio-labelled steroids were isolated from incubation medium and separated on HPLC to check the conversion to testosterone. 1mio of stable transfected MCF7_HSD17B5 cells seeded pro well on the plate gave around 30% of conversion after 24h of incubation with androstenedione [Figure 38] whereas in order to achieve the same level of conversion with stable transfected HEK293_HSD17B5 1.5 mio cells had to be seeded.

Results

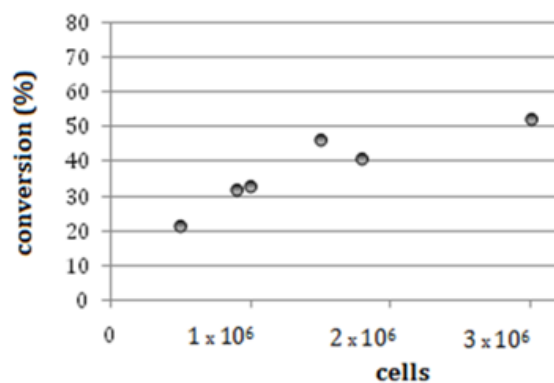


Figure 38 Optimization the amount of cells (HSD17B5 stable transfected MCF7) for 30% conversion *in vivo* during 24h incubation with radio-labeled androstenedione.

HPLC chromatograms were also analyzed to estimate the purity of substrate/product separation. Probes from both cell lines exhibited the presence of some by-products which could be more oxidized products generated from radio-labeled androstenedione substrate probable spontaneous or by endogenous enzymes of cells during incubation. Presence of the additional peak around the 2 minute seemed to be dependent from used amount of cells and time of incubation and did not interfere much with observed conversion to testosterone.

Results

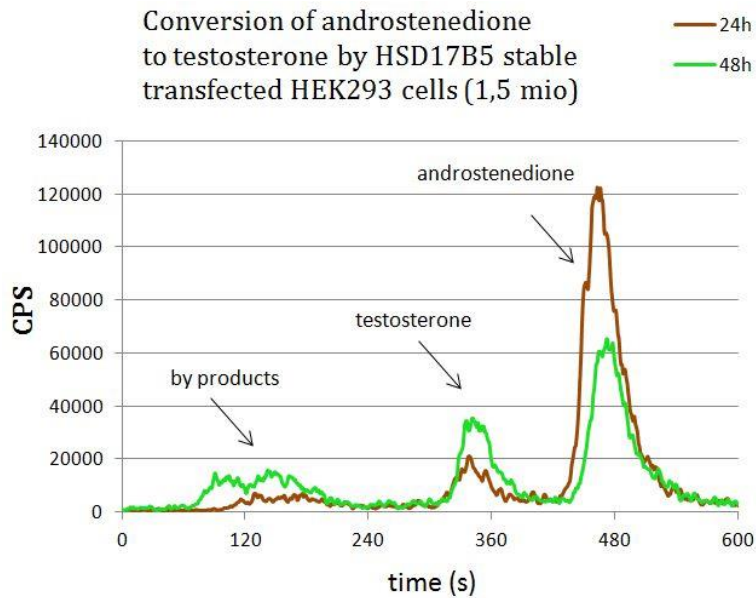


Figure 39 HPLC chromatogram of radio-labeled substrate/product extracted from enzymatic assay with HSD17B5 stable transfected HEK293 cell lines converting androstenedione to testosterone.

Not transfected MCF7 cells used here as a control showed no endogenous conversion of androstenedione to testosterone. However the probable activity of some endogenous enzymes metabolizing the radio-labeled substrate was detectable as additional peak shortly before the second minute of chromatogram development [Figure 40].

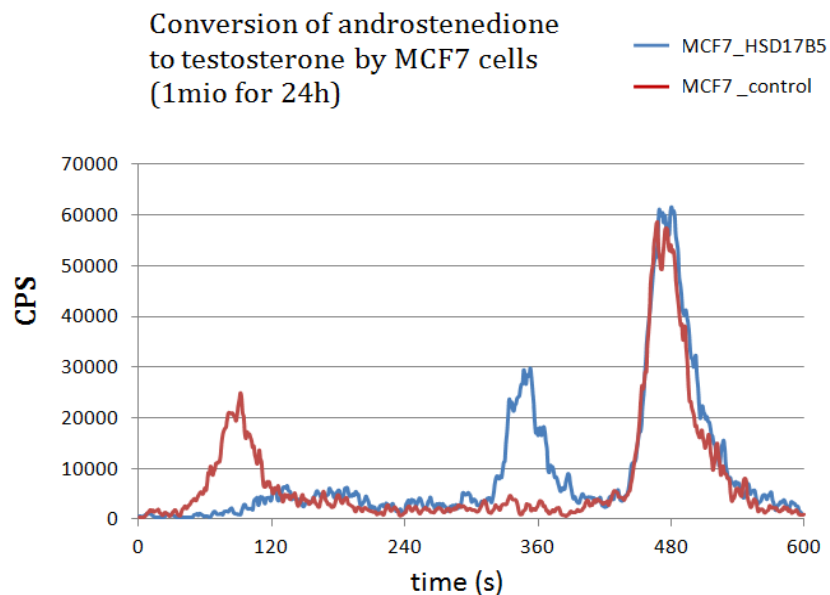


Figure 40 HPLC chromatogram of radio-labeled substrate/product extracted from enzymatic assay with HSD17B5 stable transfected MCF7 cell lines converting androstenedione to testosterone.

Results

Because of unknown reasons HSD17B5 expressing stable transfected MCF-7 cells showed better efficiency in conversion of androstene-3,17-dione than stable transfected HEK293 in preliminary *in vitro* assays and therefore they were selected as first choice for *in vivo* inhibitor studies. However, to eliminate the probable cell line dependent effects on inhibitory activity stable transfected HEK293 cells were also used in experimental work flow just to compare the screening results.

2.1.7.3 *Ex vivo* IC₅₀ determination

In the course of initial optimization assays with living cells it has turned out that presence of full serum in the culture media can significantly decrease the inhibitory effect of tested compound on conversion of androstene-3,17-dione (1,2,6,7-³H) to testosterone *in vivo* by 17 β -HSD5 expressed in human cells. To eliminate the effects of unspecific binding by serum ingredients, incubation with inhibitors was performed in the media with removed serum. The cell viability during the incubation was monitored by eye on optic microscope. Incubation without serum up to 24h was not harmful for cells. The IC₅₀ results appeared to be similar to IC₅₀ obtained in *in vitro* assays with homogenated bacteria lysates expressing HSD17B5 or purified enzyme.

Table 12 IC₅₀ values for different cell line assays with or without serum.

IC ₅₀ (μ M)	Full culture media	Culture media without FBS
HSD17B5 stable transfected MCF-7	1.35	0.33
HSD17B5 stable transfected HEK293		0.20

2.1.7.4 Cell viability tests

Tested inhibitory compound did not exhibited significant cytotoxic effect in both transfected with HSD17B5 or not HEK293 and MCF-7 in the tested concentration range (2 μ M). However, some lost in the viability up to 70-80% could be observed in the inhibitor concentration around 100 μ M suggesting that from higher concentration the compound may become cytotoxic for cells. Cell viability was compared for controls containing DMSO (1%) estimated as 100% [Figure 41; Figure 42].

Results

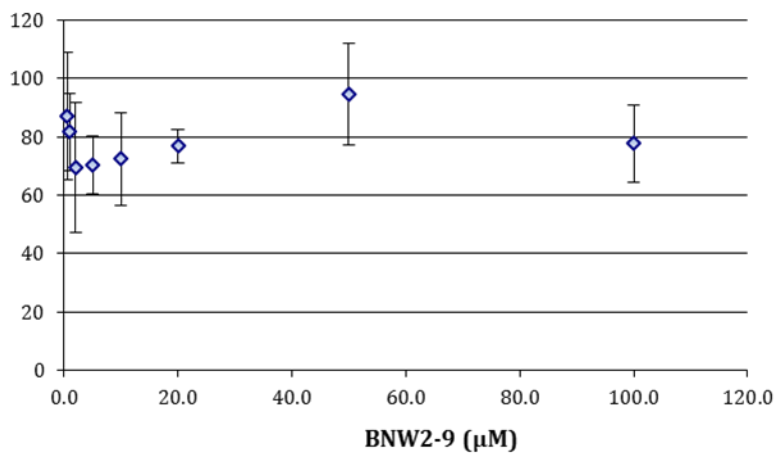


Figure 41 Cell Titer-Glow 24h viability test with not transfected HEK293 cell.

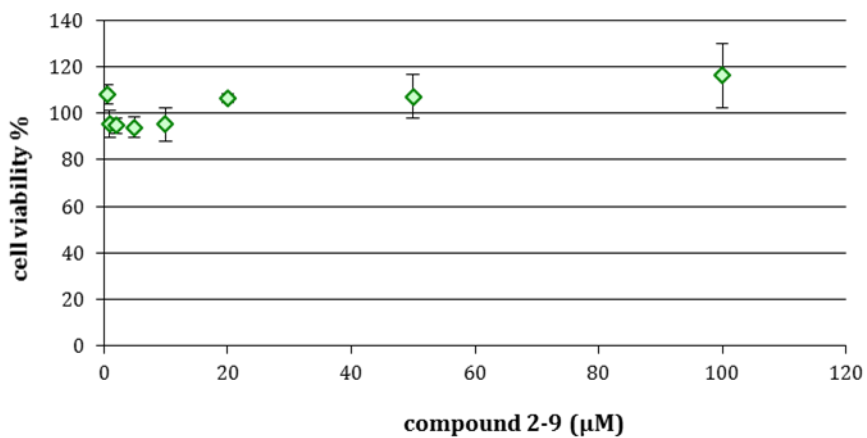


Figure 42 MTT 48h test with stable transfected HEK293 cells.

2.2 Studies on partly characterized new SDR candidates

The following human SDR gene candidates: HSD17B8, SDR-O and HSDL2 were chosen for further investigations in this study. In contrast to human HSD17B8 the two latter up to now have not had characterized substrate specificity that could confirm their any enzymatic activity. In further steps, high yield expression in bacteria as recombinant proteins and eventual purification for potent enzymatic assay development was planned. In case of human 17 β -HSD8 the activity in oxidation of estradiol to estrone at the presence of NAD⁺ as cofactor was well demonstrated in the literature [60]. However, more and more evidences from the literature are suggesting that the enzyme can possess quite other substrate specificity even far different from steroid hormones. The aim would be standardization of the enzymatic assay for other substrate search and potential inhibitor screening. In this purpose the achievement of their expression in mammalian or bacteria expression system for potent substrate screening and in further plans inhibitor screening.

2.2.1 Cloning and expression of human SDR candidates

2.2.1.1 Human HSD17B8 expression

Human recombinant HSD17B8 was expressed from pGex vector as GST fusion protein. Unfortunately, *in vitro* activity assays with estradiol and cofactors revealed bacteria suspension to have no enzymatic activity. The reason of loss the activity in this clone remains unclear. Furthermore, expressed in bacteria human HSD17B8 seemed to be insoluble and retained in bacteria pellet after trials to isolate it in the applied purification method [chapter 3.3.5]. Therefore the attempts for achieving the expression of enzymatic active HSD17B8 in mammalian expression system became the first choice in this study. For this aim HEK 293 cell line was chosen as a host for human HSD17B8 expression. The full coding cDNA was cleaved from pGex vector with restriction enzymes and cloned into pcDNA3 vector. After transfection cell pellets were taken for enzymatic activity tests in oxidation the estradiol to estrone at the presence of NAD⁺ which was also the control of transfection.

Results

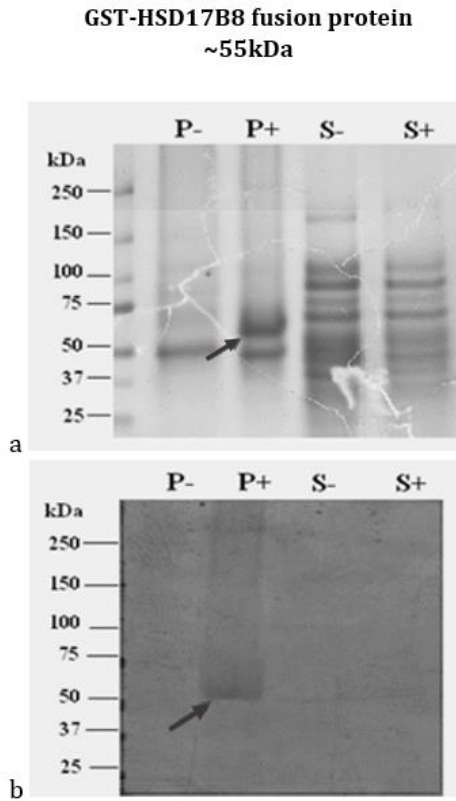


Figure 43 Recombinant human HSD17B8 expressed in BL21DE (3) bacteria as GST-fusion protein. a) SDS-PAGE, b) Western blot. Arrows show human GST-HSD17B8 fusion protein. P+ bacteria pellet induced, P- bacteria pellet not induced, S+ supernatant induced, S- supernatant not induced. Human HSD17B8 appear to be insoluble in a supernatant from lysed bacteria in the where the most of recombinant protein remains in the pellet after centrifugation.

2.2.1.2 Human SDR-O expression

Human SDR-O was cloned from commercially ordered vector carrying the SDR-O sequence. In order to be comparable with existing end described in literature human SDR-O clones there was performed a mutagenesis to repair two point mutations. Finally the achieved cDNA sequence was corresponding to the NCBI data bank: (NM_148897.1) Full coding SDR-O cDNA sequence was next successfully cloned into pGex and pDNA3 vectors and expressed in both bacteria and mammalian expression systems. Molecular mass of the SDR-O is around 38 kDa while together with GST fusion protein comes to 61 kDa. Human recombinant SDR-O over-expressed in bacteria from pGex vector as GST fusion protein has appeared to be rather insoluble in trials for its isolation and purification. Furthermore, the most of the protein has retained in the BL21DE3 bacteria pellet after cell wall

Results

lysis and centrifugation. Eventual purification of human SDR-O needs more efforts and adjustment of the purification method. For substrate screening studies there were used transiently transfected HEK293 cells and transformed induced bacteria pellets. Control of transfection into HEK293 cells were performed by checking the mRNA expression.

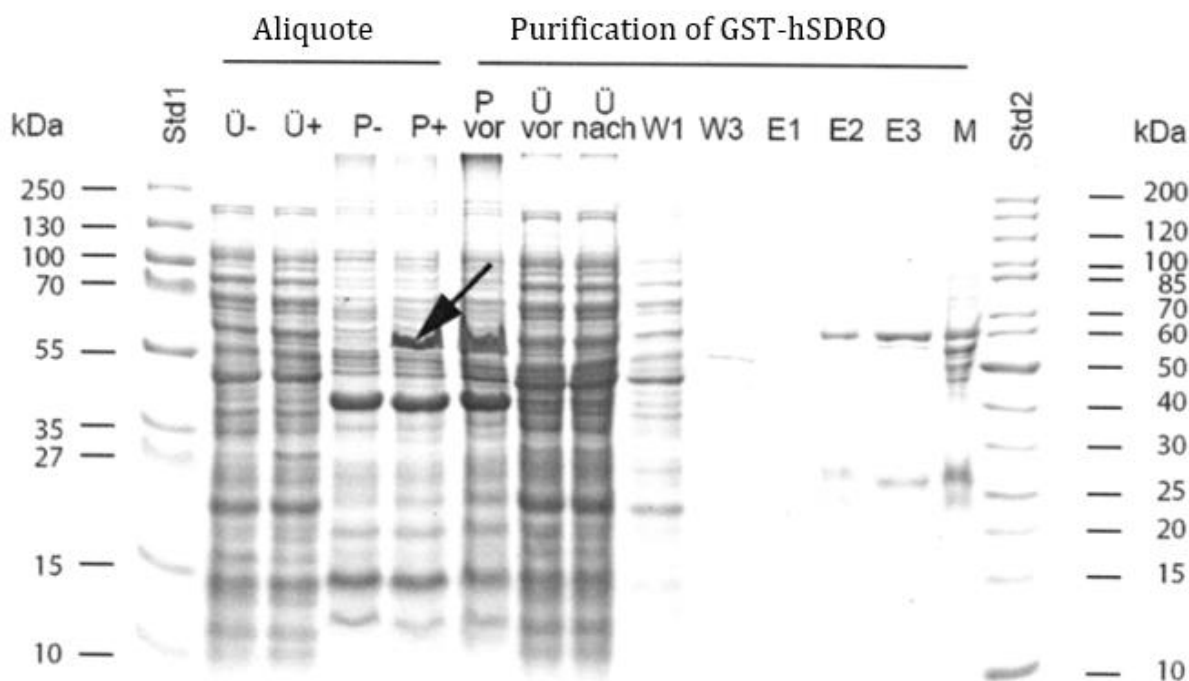


Figure 44 Protein expression in Rossetta2Lys, isolation and purification. Coomassie-stained PAGE. Arrow shows the recombinant SDR-O_GST fusion protein.

2.2.1.3 Human HSDL2 expression

Human HSDL2 was retrieved by use RT-PCR method from HepG2 cell RNA. cDNA full coding of HSDL2 was successfully cloned into pGex and pDNA3 vectors and expressed in both bacteria and mammalian expression systems. Human HSDL2 has a molecular mass around 50kDa and expressed as GST fusion protein appropriately 75 kDa.

Results

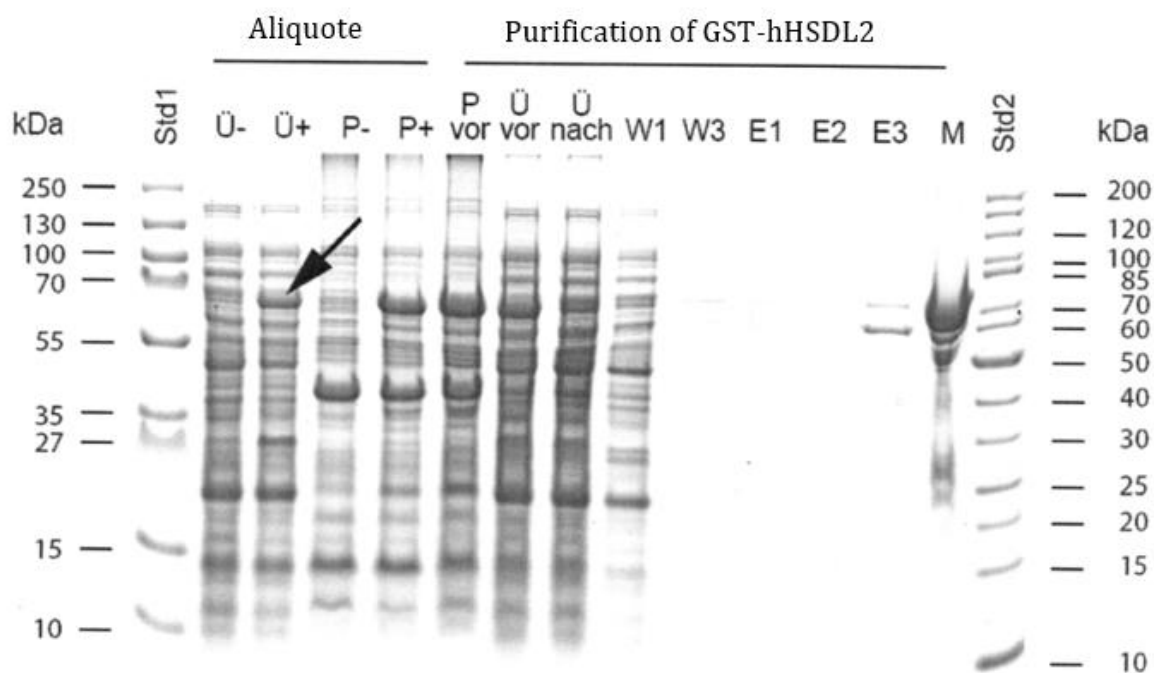


Figure 45 Protein expression in Rossetta2Lys, isolation and purification. Commassie-stained PAGE. Arrow shows the recombinant HSDL2_GST fusion protein.

2.2.2 Characterization and function prediction by use of bioinformatics tools basing on primary amino acid sequence

Nowadays, by use of publicly available on-line numerous bio-informatics computational programs one can predict the key characteristics of an unknown protein basing only on primer amino acid sequence. Among them the crucial is a classification to a proper protein family subgroup (phylogenetic analysis) and identification of specific functional domains and sequence motifs what can hint for putative function. Further, bio-informatics allows predicting with different probability various properties and characteristics such as protein mass, conformation (secondary structure), sub-cellular localization, trans-membrane regions, signaling sequences etc. Undoubtedly, utilization of these tools may be very helpful at designing 'mock' laboratory experiments in search of protein functions. In this study all three SDR candidates has been analyzed for SDR specific motifs in their structural context. Next, cofactor preferences for SDR-O and HSDL2 have been predicted. Further, by use of on-line publicly available protein databases they were analyzed for sequence homology

Results

with other functionally identified potent homolog proteins. There was not performed a thorough phylogenetic analysis because of the fact that for all candidates it has been done yet earlier and published. However, the knowledge about the nearest relatives will be used for comparison by use of pair-wise alignments.

2.2.2.1 Secondary structure and SDR motives of HSD17B8, SDR-O and HSDL2

Contrary to HSD17B8 human SDR-O and HSDL2 had not had recognized experimentally 3D-structure at the time of performing this PhD study. In order to identify the sequences specific for SDR protein family in the context of characteristic α/β folding as well for prediction of cofactor preferences the secondary structure for SDR-O and HSDL2 was initially deduced from primary amino acid sequence by use of on-line publicly available programs and was supported with multiple alignments analysis (not shown) with other functionally defined SDRs. However, presented here below secondary structure in case of HSDL2 is now updated with results of recognized lately 3D-cristal structure of HSDL2 SDR domain which in reality differs slightly in the region of catalytic center from previously deduced one.

Human HSD17B8

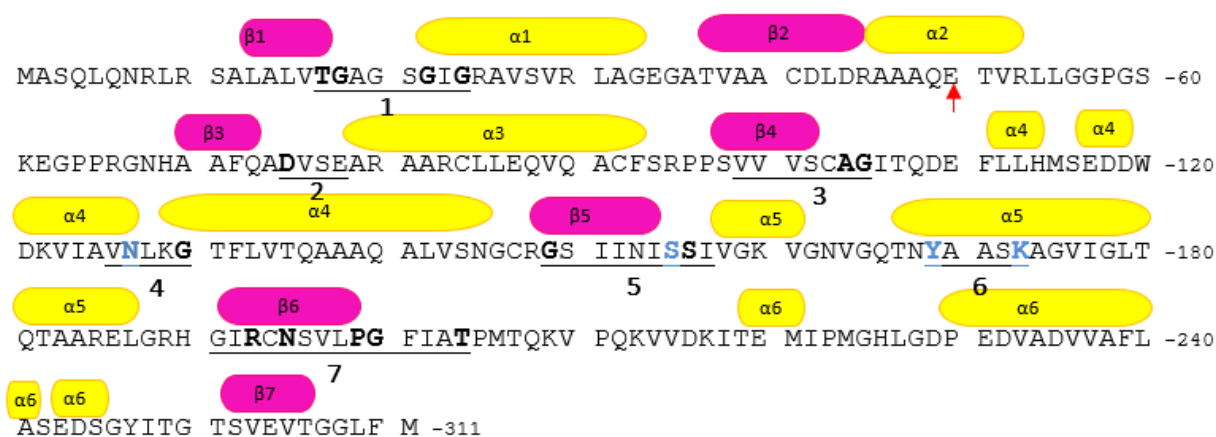


Figure 46 Amino acid sequences of human HSD17B8 with marked SDR specific motifs in the context of recognized secondary structure (available at PDB, SGC; entry code: 2PD6).

Results

Human SDR-O

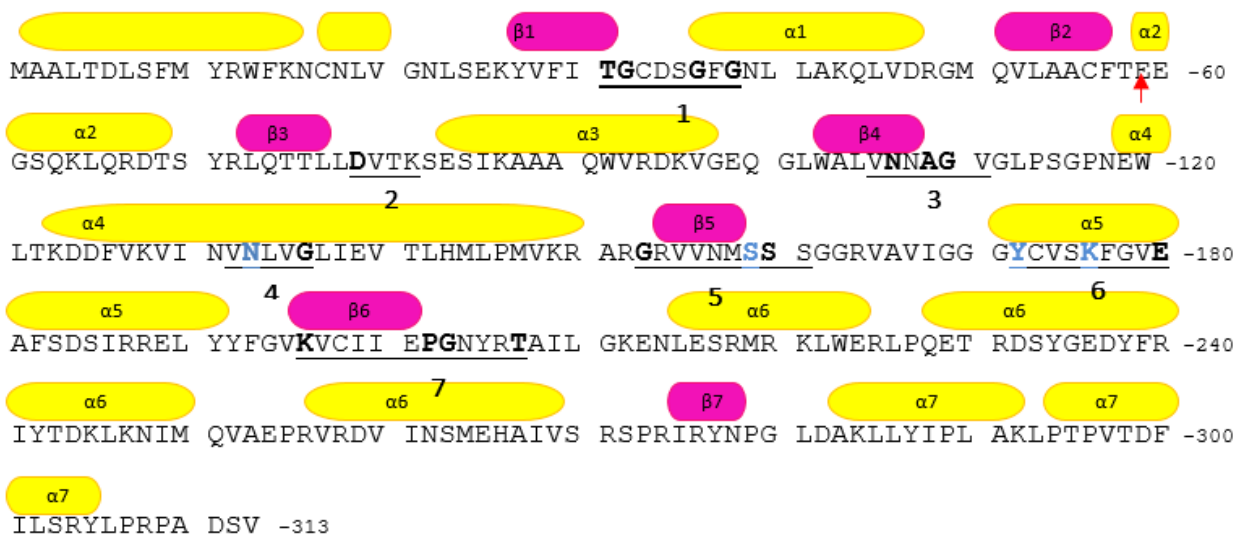


Figure 47 Amino acid sequences of human SDR-O with marked SDR specific motifs in a context of recognized secondary structure deduced from primary amino acid sequence by use of Psiprep program <http://bioinf.cs.ucl.ac.uk/psipred/>

Human HSDL2

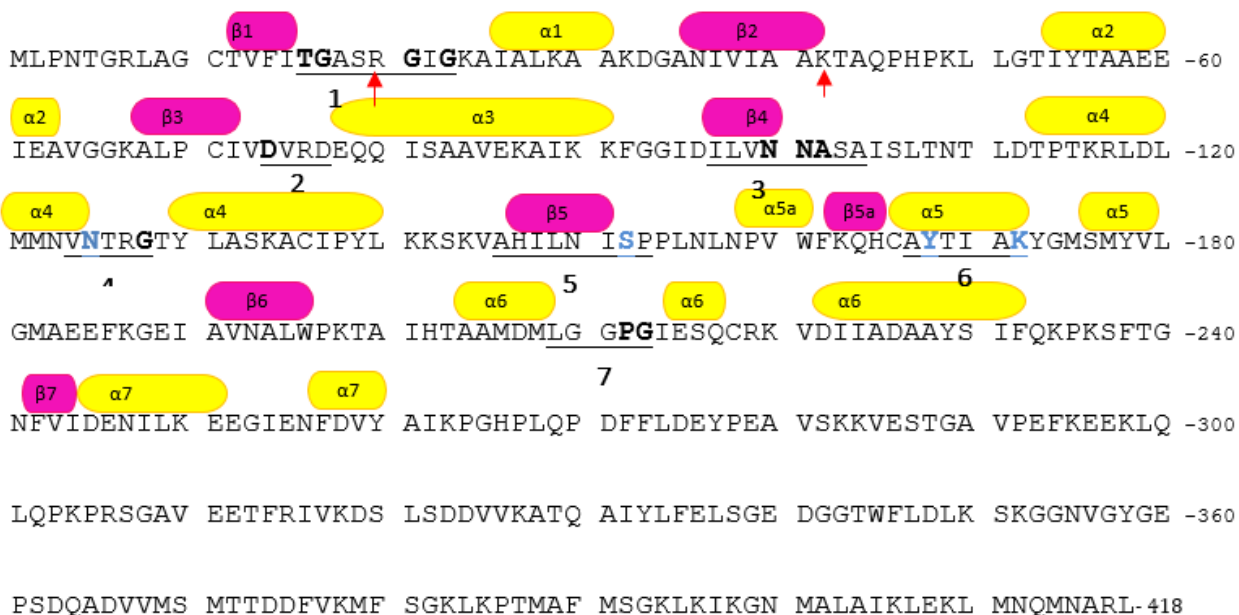



Figure 48 Amino acid sequences of human HSDL2 with marked SDR specific motifs in a context of recognized secondary structure for SDR domain of the protein (available at PDB, SGC; entry code: 3KVO). Legend see table below.

Results

Table 13 Listed SDR characteristic motifs according to *Persson et al. 2003* [9]

Recognized SDR motifs:

symbol	2 nd struct.region	corresponding SDR motives	function
1	($\beta 1 + \alpha 1$)	TGxxxGhG (classical)	cofactor binding
2	($\beta 3 + \alpha 3$)	Dhx[cp] (classical)	cofactor binding (adenine ring of coenzyme)
2a	($\beta 3 + \alpha 3$)	DhxD (extended)	cofactor binding (adenine ring of coenzyme)
3	$\beta 4$	GxDhHHNNAGh (classical)	stabilization of central β -sheet
4	$\alpha 4$	hNhxG (classical)	part of active center
5	$\beta 5$	GxhhxhSSh (classical)	part of active center
6	$\alpha 5$	Yx[AS][ST]K (classical)	part of active center
6a	$\alpha 5$	PYxx[AS]Kxxh[DE] (extended)	part of active center
7	$\beta 6$	xhxPGxxxT motif (classical)	reaction direction
	cofactor binding region	key amino acids [RK]/[DE]	cofactor preferences
S-Y-K	($\beta 5 + \alpha 5$)	S_{xn}YxxxK	catalytic triad
N-S-Y-K	($\alpha 4 + \beta 5 + \alpha 5$)	N_{xn}S_{xn}YxxxK	catalytic tetrad

Human HSD17B8 protein contains all of the most characteristic for SDR fragments which overlap appropriately with expected α/β -folding [Figure 46] Among them the most conserved are tree glycine motif: **TGxxxGxG** (1) and being a part of active center **YxxxK** sequence (6) usually preceded by 10-15 amino acids backward by serine (5) and further back with asparagine (4) which together create a characteristic catalytic tetrad **N_{xn}-S_{xn}-YxxxK**. Analyzing the HSD17B8 amino acid sequence one exception seems to be localized on $\beta 4$ fold motif known as **NNAG**(3) usually consisting of two asparagine residues in classical SDRs which here are not present. Instead, it contains **AG** only. This fragment is believed to play a role in stabilization of β -sheet structure and positioning towards

Results

active center. Moreover, human HSD17B8 has been reported to have activity towards estradiol at the presence of NAD⁺ as cofactor and has been classified as classical SDR.

Similarly, human SDR-O also possess all expected SDR motifs such as **TGxxxGxG(1)**, **NNAG(3)** or **YxxxK(6)** [Figure 48]. However, the last part of active center (6) resemble of extended SDRs where the catalytic lysine is preceded directly by alanine or serine and four amino acid forward the motif is closed by acidic residue such as glutamic acid (**Yxx[AS]KxxxE**). In spite of this SDR-O has been also classified as typical classical SDR member.

Among analyzed here SDR candidates HSDL2 seems to be less conservative concerning the specific SDR sequences [Figure 49]. One of them is localized in the cofactor binding region **DhxD(2)** more characteristic for extended SDRs and the **PG(7)** motif which has appeared to be difficult for unambiguous identifying. The containing aspartic acid **DhxD(2)** is responsible for binding the adenine ring of the coenzyme while originally localized in the region of β 6-strand **PG(7)** is believed to play a structural role and probable have an influence on reaction direction. Another example are **NNASA** instead of typical **NNAG(3)** motif in the region of β 4-strand and some crucial changes in the middle part of active center (5). The potent catalytic serine (S152) of the catalytic triad **S-Y-K** is here unusually distanced from **YxxxK** motif up to 16 residues while it is commonly localized 10-15 amino acids from catalytic tyrosine in the most of SDRs. Additionally, the serine is here not followed by another serine residue nor preceded by glycine 6 amino acids backwards in comparison to other classical SDRs. What is more, the lately experimentally solved 3D structure of HSDL2 SDR fragment in the complex with NADPH is revealing that between serine (S152) and **YxxxK** exist additional α -helix and β -strand (marked here as α 5a and β 5a). However, the serine is localized appropriately at the end of β 5-strand and **YxxxK** falls exactly on α helix what ensure a correct orientation of lysine and tyrosine for putative catalytic activity. It is worth of note that these observed sequence differences in comparison to other classical SDRs changes seems to be conserved in the all phylogenetic clade of HSDL2 homologue proteins from insects to mammals and probable it play some role in catalytic functions. HSDL2 has been classified as classical SDR.

Results

2.2.2.2 Cofactor preference prediction (SDR-O, HSDL2)

Not much is known about the substrate specificities and cofactor preferences of these both enzymes. However lately recognized 3D-cristal structure of HSDL2 in complex with NADPH or high throughput substrate screening approaches seem to confirm preferential to NADP(H) over NAD(H) and thus its potent reductase activity rather than oxidase[149]. Performed previously confirmed experimentally investigations on multiple SDR amino acid sequences allowed to elucidate key amino acid residues in the region of first $\beta\alpha\beta$ -folds which decide the NAD(H)/NADP(H) cofactor preference[9]. While NAD(H) preferring SDR enzymes contain an acidic residue [DE] in position at the end the second β -strand, typical NADP(H) utilizing enzymes instead have usually two basic residues[RK] where first of them precedes directly the second glycine in three glycine (TGxxxGxG) motif. In this way the primary amino acid sequences of SDR-O and HSDL2 was analyzed in a context of secondary structure and key residues. SDR-O possess an acidic amino acid (E59) in key position not far away from the cofactor binding region localized at the end of the second β -strand. It suggests strongly a preference for NAD(H) over NADP(H). The multiple alignments with similar known NAD/NADH utilizing SDRs confirm the key position of this acidic residue [Figure 49].

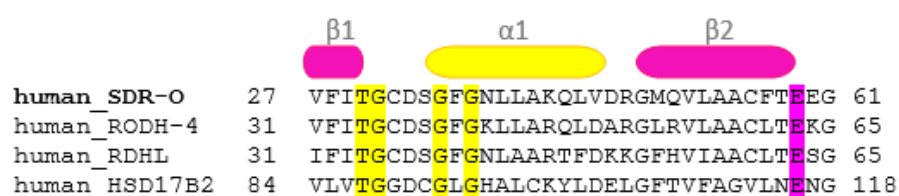


Figure 49 Fragment of multiple alignment. The secondary structure is corresponding to deduced one of SDR-O. Marked on lila: acidic key residues.

On the contrary HSDL2 has two key basic amino acids (R20) and (K42): one localized just inside of the characteristic for cofactor binding region three glycine motifs (TGxxxGxG) and the second one in the corresponding to the key position of [ED] for NAD(H) preferring enzymes, respectively [Figure 50]. Thus HSDL2 is similar for other known NADP(H) preferentially binding SDRs what can be confirmed by primary amino sequences comparison in multiple alignment.

Results

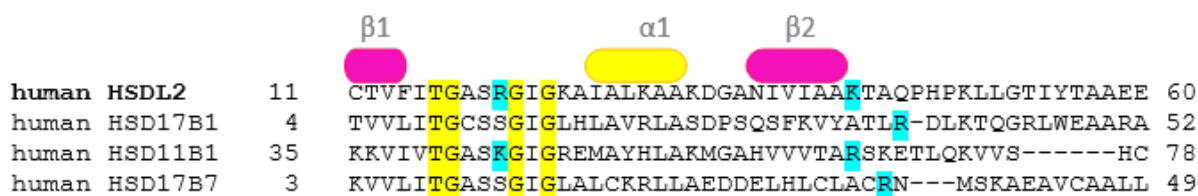


Figure 50 Fragment of multiple alignment. The secondary structure is corresponding to HSDL2. Marked on blue: basic key residues.

2.2.2.3 Amino acid sequence analysis in the context of earlier phylogenetic studies and the sequence homology search (ProDom)

Basing on published knowledge and phylogenetic studies amino acid sequences of studied proteins were compared to their potent chosen homologues in direct pair-wise alignment in order to estimate the sequence similarity/identity (ClustalW). Next, particular sequence regions of the protein were compared by use of ProDom programm which identify common domains with other functionally described protein.

Studied here potent SDR enzymes have been earlier partially characterized and the phylogenetic analysis has been performed. Among them the best studied is up to now human HSD17B8. According to the published results human HSD17B8 shows closer phylogenetic relationship with β -Ketoacyl-[ACP] reductases than with other hydroxysteroid dehydrogenases [60]. The next studied here protein human SDR-O shows sequence similarity to SDR enzymes with dual activity towards retinoids and steroids [53]. HSDL2 is one of the five human proteins possessing fused SCP2 domain at C' terminus. There were published results of phylogenetic analysis of these unusual group of proteins concerning putative fusion and fission processes of SCP2 domain in the course of evolution [150]. However, little is known about potent close HSDL2 homologs with experimentally evidenced enzymatic functionality. Therefore I focused on this gene/protein my searching for amino acid sequence homologs.

- **HSDL2 amino acid sequence multiple alignment results**

Performed numerous multiple alignment of human HSDL2 showed that the HSDL2 gene is well conservative in metazoa group from cnidaria to chordate and form a separate phylogenetic clade distinct from other SDRs [151]. Human HSDL2 shares 89%, 88.3 % and 74.9% sequence identity with its putative ortholog genes in cow, dog and mouse, respectively [151,152]. In fungi (N.crassa)

Results

and more primitive eukaryots such as ciliate (*T. thermophila*) or slime mode (*D.dicoideum*) HSDL2 homolog gene is present as unfused with SCP-2 domain.

Table 14 Blastp selected sequences, ClustalW2 alignment for homology and similarity search, multiple alignment.

Chosen HSDL2 orthologs	NCBI entry	identity and similarity (%)
(Bos Taurus)	Cow XP_613868.3	89.0/95.0
(Canis Familiaris)	Dog XP_867643.1	88.3/94.5
(Mus Musculus)	Mouse NP_077217.2	74.9/81.2
(Xenopus Laevis)	Frog BC059996	73.4/85.4
(Danio Rerio)	Zebrafish BC062838.1	69.9/81.8
(Caenorhabditis elegans)	NP_505812.1	61.7/71.3
(Drosophila melanogaster)	NP_651578.1	56.4/71.1

Similarly, high amino acid sequence similarities to only SDR domain of HSDL2 can be also found among bacteria. The example is an identified gene (YP_001612214) from *Sorangium cellulosum* exhibiting approximately 60% similarity to human HSDL2. Among other selected bacteria putative homolog proteins which show over 40% similarity to SDR domain of HSDL2 most of them has only predicted activity which has not been experimentally proven yet. Some of them are initially named as 3-oxo-ACP reductases [Table 15].

Table 15 Blastp selected sequences, ClustalW2 alignment for homology and similarity search, multiple alignment.

Chosen HSDL2 homologs (of its SDR domain)		identity and similarity (%)
Gamma protobacterium SDR (uncharacterized)	ZP_04958216.1	60.1/75.5
(Rhodococcus sp.) (uncharacterized)	AY394000.1	57.5/74.1
(Nocardia farcinica) (uncharacterized)	NC_006361.1	53.5/70.9
cis-2,3-dihydrobiphenyl-2,3-diol	DH ZP_06066110	51.8/68.0
Sorangium Cellulosum (uncharacterized)	YP_001612214	38.2/58.7 (41.9/62.0)
(Neurospora crassa)	XP_322391.1	29.4/45.9
3-ketoacyl-ACP_reductase	YP_001197355	28.7/43.8
Bacillus 3-ketoacyl-ACP_reductase	YP_001421464	27.2/41.7
3-hydroxybutyrate DH		

J.Dai *et al* [152] who isolated cDNA for human HSDL2 from fetal brain library and characterized this sequence as SDR protein named it as hydroxysteroid like (HSDL2) protein due to partial similarity to 3β -HSD enzymes using blastp program. Next, searching for homology the nearest from hydroxysteroid dehydrogenases related with HSDL2 were shown HSD17B14 (retSDR3, DHR10) and HSD17B4. Basing on this knowledge I compared the amino acid sequence of HSDL2 SDR

Results

domain (1-293aa) to other known human hydroxysteroid dehydrogenases or other functionally recognized proteins exhibiting around 40% similarity to human HSDL2 from previous Blastp search [Table16].

Table 16 Amino acid sequence similarity and identity of chosen SDR proteins compared to full amino acid sequence of HSDL2 (red) and to SDR domain of HSDL2 (1-293aa)solely (black). [http:// www.ebi.ac.uk](http://www.ebi.ac.uk), EMBOSS Pairwise alignment algorithms (matrix: Blosum62, open gap penalty: 10.0, gap extension penalty: 0.2, algorithm: 'water') Few sequences were additionally proven in 'needle' algorithm (Needleman-Wunsch algorithm).

protein	NCBI entry	Similarity (%)	Identity (%)
hHSD17B4	NP_000405	28.2/33.6	18.2/20.6
hHSD17B4(1-280aa)	NP_000405	33.1/33.1/39.7needle	20.7/23.3/20.7 needle
hHSD17B8	NP_055049	30.1/35.6/29.7needle	18.1/21.3/16.4needle
hHSD17B10	NP_004484	26.1/33.7	16.8/20.1
hHSD17B14	NP_057330	30.4/32.6	21.2/22.0
hDEC2	NP_065715	34.7/41.7/36.5needle	24.0/28.1/23.5needle
hHSD17B7	NP_057455	29.9/26.4	17.2/16.3
hHSD17B2	NP_002144	30.0/30.5	18.0/19.7
hHSD17B1	NP_000404	33.2/37.1	21.6/23.0
hHSD17B11	NP_057329	35.7/35.7	20.1/20.1
hHSD17B3	NP_000188	27.1/38.1	16.9/22.8
hHSD17B12	NP_057226	26.7/32.4	17.1/18.5
hHSD11B1	NM_11755.1	34.3/34.3	19.9/19.9
hHSD11B2	NM_000196.3	27.9/29.1	17.6/18.2
hHSD3B1	NM_000862.2	28.5/27.9	17.1/17.0
hHSD3B2	NM_000198.3	25.6/25.0	15.4/15.3
7 α -HSD_E.coli	NP_753906	30.8/43.6	20.4/29.5
Cis-Toulen dihydrodiol DH <i>Pseudomonas putida</i>	ABA10813	35.7/42.4	22.8/24.4
3-oxoacyl-(ACP)-reductase <i>Sorangium cellulosum</i>	YP_001612214	62.0/62.0	41.9/41.9

Results

Average similarity between other humans HSDs and HSDL2 is around 15-30% the same as for other SDRs from other subfamilies. However, among human hydroxysteroid dehydrogenases with well documented functions the most similar seems to be HSD17B4 which consists of SCP-2 apart of SDR (D-3-hydroxyacyl-CoA dehydrogenase) and enoyl-CoA hydratase domain. The similarity between their SDR domains is approximately 40% depending from the used pair-wise align algorithm. ('Needle' alignment which uses a Needleman-Wunsch algorithm is a global alignment of the entire length of compared sequences-39.7% similarity. 'Water' which uses Smith Waterman algorithm allowing to calculate the local alignment show 33.1% similarity). Similar to HSD17B4 SDR domain high sequence similarity has another human peroxisomal protein identified as DECR2 belonging to the SDR subfamily of 2,4-dienoyl-CoA reductases. Further, among human hydroxysteroid dehydrogenases significant similarities showed HSD17B11 and HSD17B8. Among them the lowest similarity as well identity I found for HSD3B1 and HSD3B2 using both algorithms. It is interesting that high similarity was found for bacterial proteins identified as 7 α -HSD from E.coli (~60%), cis-toulen dihydrodiol dehydrogenase and 3-oxoacyl-[ACP]-reductase from *Sorangia cellulorum* showing ~60% sequence similarity and identity ~40%.

- **Sequence homology search. ProDom identified domains**

Particular amino acid sequence regions of studied here SDR candidate proteins were compared by use of ProDom program which identify common domains with other functionally described proteins [Table 17].

Table 17 Identified domains by ProDom program

HSD17B8	SDR-O	HSDL2
PD003795 222 127-171	PD002736 485 223-313	PD003287 450 324-410
PDA1E740 220 56-96	PD738852 273 26-75	PD021573 370 125-193 ADH short
PD885428 203 172-210	PDA1F3U3 239 78-126	PD648223 314 239-298
PD255695 187 16-55	PD467396 211 132-173	PD126102 252 75-124
PD000197 184 223-258	PD885428 190 175-209	PDA1G3V9 249 194-238
PDA0T3J1 158 149-259	PDA1G1L4 239 78-125	PDA0C649 113-265
PD062132 158 97-124	PD277623 26-56	PD744007 183 39-74
PD313173 9-200	PDA2W5I8 142 1-25	PDA76652 163-193
PD915078 75-124		PD929258 126 299-323
PDA8T780 112-258		

Results

Human HSD17B8

MASQLQNRLR SALALV**TGAG SGIGRA**AVSVR LAGEGATVAA CDLDRAAAQE TVRLL**GGPGS**-60
KEGPPRGNHA AFQADVSEAR AARCLLEQVQ ACFSRP**PSVV VSCAGITQDE** FLLHMS**EDDW**-120
DKVIAV**NLKG TFLVTQAAAQ** ALVSN**GCRGS IINISSIVGK** VGNV**GQTNYA ASKAGVIGLT**-180
QTAARELGRH GIRCNSVLEG FIATPMTQKV PQ**KVVDKITE MIPMGHLGDP** EDVAD**VVAF**L-240
ASEDSGYITG TSVEVTGGLF M -311

Human SDR-O

MAALTDLSEFM YRWFKNCNLV **GNLSE**KYVFI **TG**CDS**GFGNL** LAKQLVDRGM QVLAACFTEE-60
GSQKLQRDTS YRLQTTLL**LDV TKSESIKAAA QWVRDKVGEQ** GLWAL**VNNAG** VGLP**SGPNEW**-120
LTKDDFVKVI NVNLVGLIEV TLHMLPMVKR ARGRVV**NMSS** SGRVAVIGG **G**YCV**SKFGVE**-180
AFSDSIRREL YFGVKVCII EPGNYRTAIL GKEN**NLESRMR KLWERLPQET** RDSYGEDYFR-240
IYTDKLNIM QVAEPRVRDV INSM**EHAIVS RSPRIRYNPG** L**DAKLLYIPL AKLPTPVTDE**-300
ILSRYLPRPA DSV-313

Human HSDL2

MLPNTGRLAG CTVFITGASR GIGKAIALKA AKDGANIVIA AKTAQPHPKL LGTIYTAAEE -60
IEAVGGKALP CIVD**VRDEQQ ISAAVEKAIK KFGGIDILVN** NASAI**SLTNT LDTPTKRLDL** -120
MMNVNTRGTY LASKACIPYL KSKVAHILN **ISPPLN**LN**PV WFKQHCA**YTI **AKYGMSMYVL** -180
GMAEEFKGEI AVNAL**WPKTA IHTAAMDMLG** GPG**IESQCRK** VD**IIADAAYS IFQKPKS**FTG -240
NFVIDENILK EEGIENFDVY AIKPGHPLQP DFFLDEYPEA VSKKVESTGA VPEFKEEKLQ -30
LQPKPRSGAV EETFRIVKDS **LSDDVVKATQ** AIYLFELSGE DGGTWFLDLK SKGGNVGYGE -360
PSDQADVMS MTTDDFVKMF SGK**LKPTMAF** MSGK**LKIKGN MALAIKLEKL MNQM**NAR- 418

Figure 51 Amino acid sequences with identified chosen domain by Pro Dom program.

Results

Human HSD17B8 apart of domains containing characteristic SDR motives (beginning from PDA or others). The highest score was identified for **PD003795** domain comprising the catalytic center of the enzyme characteristic. The similar amino acid sequence also share FABG (33), ADHR (8) and FOX2(6) enzymes with reported 3-oxoacyl-[ACP]-reductase activity. Whereas the localized more at C'terminal domain **PD000197** has been also reported by the program as characteristic for enzymes with 3-oxo-[ACP] reductase activity. The most frequent protein names containing this domain are FABI (14), DHRS4 (7) and PECR (5). Another identified domain **PD062132** comprising the AG motif of SDR instead of typical NNAG has been occurred common for other fatty acid biosynthesizing enzymes such as DHB8 (4) and) FABG (4) enzymes with acetoacetyl-CoA or 3-oxoacyl-[ACP]-reductase activity.

Concerning SDR-O excepting the domains containing typical for SDR motifs identified by the program the highest score belong to **PD002736** domain localized at the C' end of the protein. This domain is also identified in other enzymes with NAD⁺ dependent 3 α /17 β -HSD activity. For example this domain possess also human mitochondrial D- β -hydroxybutyrate dehydrogenase or human RDH1. The domain **PD885428** beginning at the end of putative catalytic center of the protein has been identified for few proteins such as FABG (32) BUTA (8) and DHRS4 (7).

HSDL2 is a modular protein consisting of two domains: N' terminal SDR domain and C' terminal SCP2 domain which is identified by Prodom program as PD003287 (amino acid letter symbols marked on grey). Searching for the sequence homology in the region from catalytic centre to the C'terminus of the SDR domain was in the special interest of my research in case of HSDL2 protein. The program has identified two domains in the joining region between SDR and SCP2 domains: PD929258 (299-323aa), and PD648223 (239-298aa). However, they both seem to be characteristic only for HSDL2 similar proteins probably its homologues in other species. Among other domains characteristic sequence homologies for other SDR proteins were identified such as PD021573 (125-193aa), **PDA3G3V9** (194-238aa), **PD126102** (75-124aa), PD744007 (39-74aa). All of them contain characteristic for SDR motifs and are predicted to function as oxidoreductase dehydrogenase/reductase short-chain SDR dehydrogenase. Worth of notice is the domain **PD126102** containing NNASA sequence (instead of typical for classical SDRs NNAG) which also share SDRs bacterial SDRs biosynthesizing antibiotics (15-hydroxyprostaglandin activity). Another interesting domain is **PDA3G3V9** found as characteristic for SDR enzymes localized at inner lipid.

Results

2.2.3 Subcellular localization studies

Determination of the target organelle where the studied protein is transported after translation and modifications can provide valuable hints to a metabolic pathway in which the putative enzyme may be involved. Therefore studies on intracellular distribution of HSD17B8, SDR-O and HSDL2 were performed. In this purpose coding cDNA sequences of chosen SDR candidates were subcloned into pcDNA3_Flag and pcDNA4_MycHisB modified vectors enabling their expression in mammalian cells as tag fusion proteins. Expressed in this way recombinant proteins were subsequently recognized by specific, conjugated with fluorescent label antibodies against Myc or Flag epitopes and revealed by use of fluorescence microscope. Visualized in this way recombinant proteins were initially counterstained with organelles such as ER, nucleus or mitochondria.

2.2.3.1 Preparation of tagged version of studied proteins. Negative control

Concerning a potent masking of targeting signals sequences it was decided to prepare N' and C' terminally tagged alternative constructs for each of the SDR protein candidates with both Myc and Flag fusion tags. Next, verified by DNA sequencing plasmids carrying the gene of studied proteins with appropriately N' or C' fused tags were transfected into HeLa or alternatively into HEK293 cells for expressing and subsequent visualisation. In order to exclude the influence of some unspecific fluorescence signals or false positive results the distribution of unaccompanied tag epitopes expressed from pcDNA3 or pcDNA4 vectors was first checked. Negative controls with pcDNA3_FLAG or pcDNA4_MycHisB transfected into cells without inserts showed a diffused cytoplasmatic distribution of expressed tags [Figure 52].

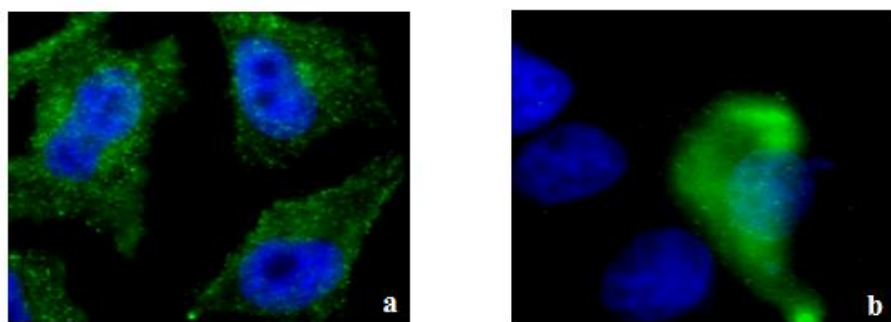


Figure 52 Cytoplasmatic distribution of pcDNA4_C'MycHis (a) and pcDNA3_C'Flag (b) control vectors without insert (Green). Nuclear DNA was stained with Hoechst 3433 (blue). Subcellular localization was revealed with anti-Myc (monoclonal) and anti-Flag antibodies (polyclonal), respectively and subsequently with Alexa Fluor 488 secondary antibodies.

Results

A fashion of the cytoplasmatic distribution was usually visible as covering the whole cell homogenous, speckled and more or less granular, most probably due to the level of expression and time-dependent accumulation of inclusion bodies with over-expressed proteins. Cells were immobilized and subjected to the procedures enabling the visualization 18-24h after transfection.

2.2.3.2 Subcellular localization studies on human HSD17B8

Transient expression of human HSD17B8 fused with Myc-epitope at its C-terminus revealed clear mitochondrial localization [Figure 53; C] Contrary to that, N-terminal fusion of Flag-epitope and 17 β -HSD8 has shown several aggregate spots and cytoplasmic localization most probably due to masking of signal for mitochondrial import since mitochondria targeting signal is localized at the beginning of translated polypeptide [Figure 54; C].

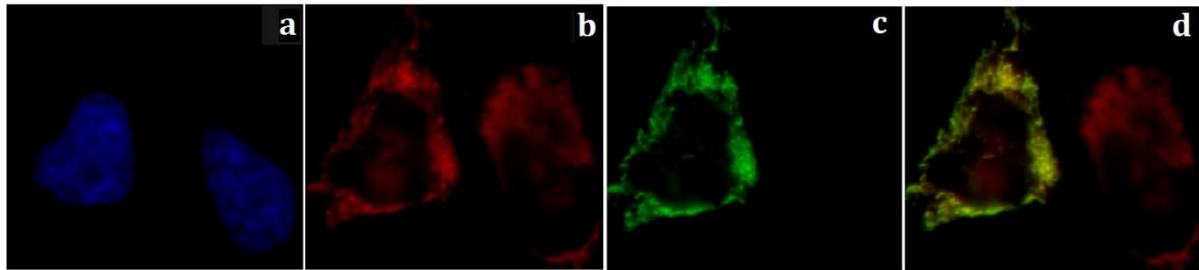


Figure 53 Intracellular localization of HSD17B8_C'myc tagged fusion protein. a) nucleus, b) stained mitochondria, c) mitochondria co-localization of HSD17B8_C'myc, d) overlay of pictures b) and c).

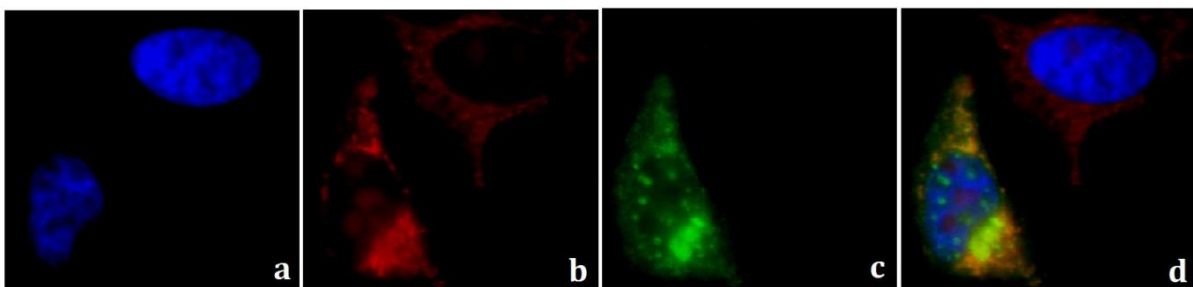


Figure 54 Intracellular localization of HSD17B8_N'flag tagged fusion protein. a) nucleus, b) stained mitochondria, c) delocalized in the cytoplasm HSD17B8_N'flag tagged fusion protein, d) overlay of pictures b) and c).

Observed results are consistent with computational *in silico* prediction by use of Mito Prot and TargetP 1.1 bioinformatic programs. High probability (>0.87) for transport into mitochondria is predicted for HSD17B8 alone as well for C'MycHis tagged versions.

Results

2.2.3.3 Subcellular localization studies on human SDR-O

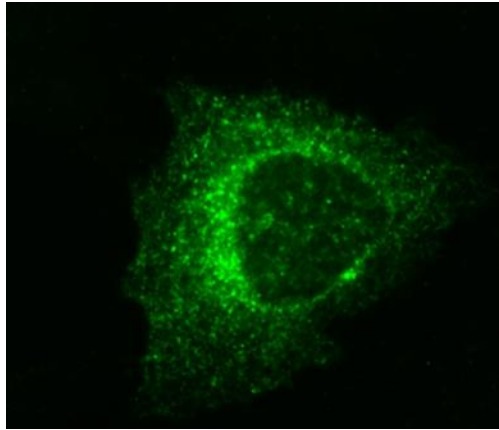


Figure 55 Representative subcellular localization of SDR-O expressed as N- or C- tagged protein in HeLa cells.

Studies on numerous images which visualize a distribution of human SDR-O inside HeLa cells revealed that both N' and C' (Myc or Flag) terminally tagged versions of the protein show a certain common pattern. Namely, it is a granular structure spread out over the cell also into the most fringe areas but with some density at perinuclear region as shown at the picture **[Figure 55]**.

Counterstaining experiments excluded its unambiguous co-localization with endoplasmatic reticulum (ER) as well with early endosomes although some vicinity to microsomes and membrane ruffles seems to be observed. As shown on a pictures below which represent counterstaining with ER markers the granular-net structure of tagged human SDR-O is very different and it is not overlaying the pattern of endoplasmatic reticulum **[Figure 56]**.

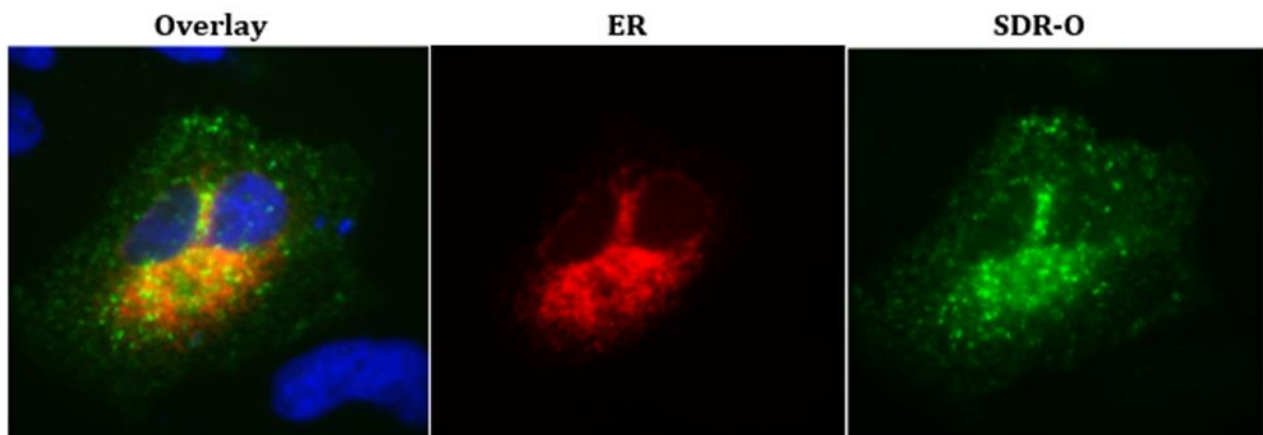


Figure 56 Counterstaining with the endoplasmatic reticulum (red) human N'Flag_SDR-O (green).

Results

Similarly, counterstaining with early endosome marker does not exhibit clear co-localization with partially granular structure of SDR-O. In most pictures early endosomes (visible as green vesicles) seem to be suspended independently on the net-granular structure of SDR-O (red marker) sometimes resembling ER. Merely few of numerous depictions captured as if partial co-localization of granulate form of SDR with early endosomes vesicles visible as yellow overlaying [**Figure 57**].

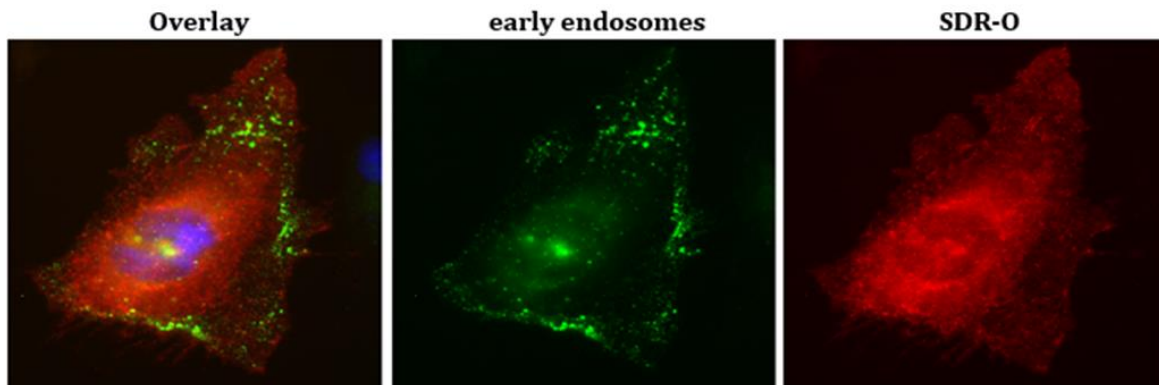


Figure 57 Counterstaining with early endosome markers (green); human SDR-O_N'Myc (red).

Further counterstaining also definitely pointed out that human SDR-O also did not match with markers for mitochondria [**Figure 59**], peroxisomes [**Figure 58**] and cytoplasm (not shown) thus it makes the precise determination of subcellular localization by use of applied methods difficult.

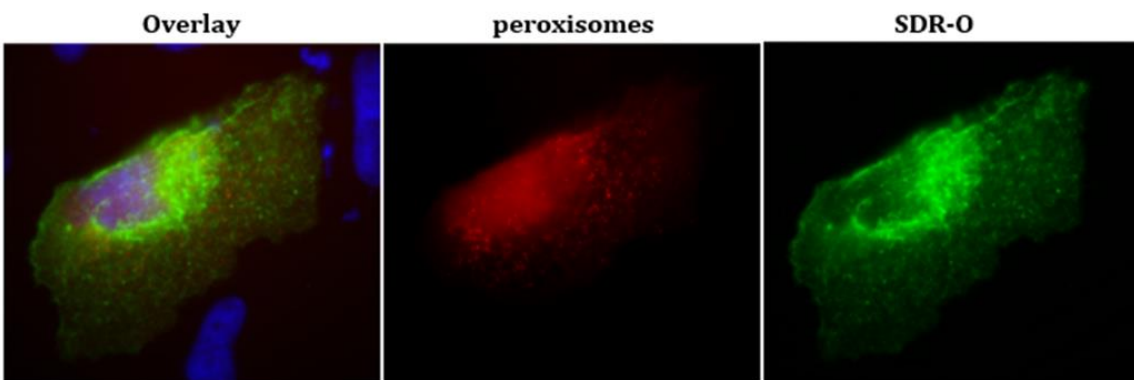


Figure 58 Counterstaining with peroxisomes markers (red); human SDR-O_N'Myc (green).

Results

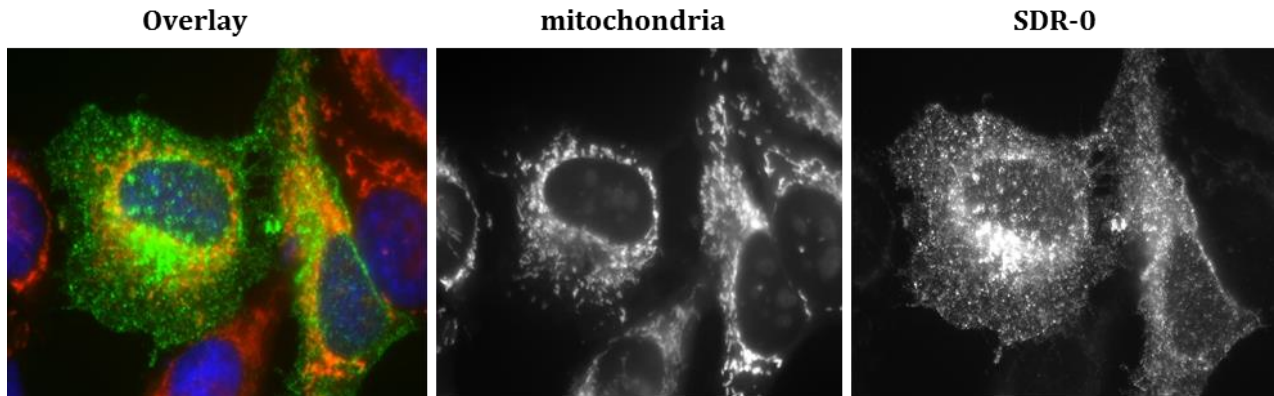


Figure 59 Counterstaining with mitochondria: N' Flag_SDR-0.

2.2.3.4 Subcellular localization studies on human HSDL2

Human HSDL2 due to peroxisomes targeting signal (AKL) on its C' terminus of the SCP2 domain is expected to be found in peroxisomes. *In vivo* experiments in really showed that N'terminally tagged fusion protein is transported to peroxisomes. Images visualizing intracellular distribution of human HSDL2_N'Myc show clear co-localization with used peroxisome markers [**Figure 60**].

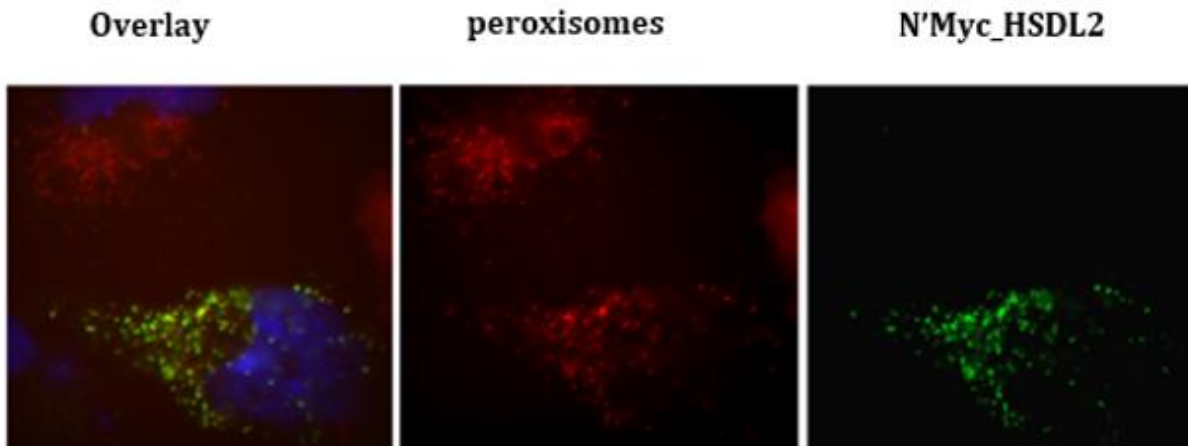


Figure 60 Subcellular localization of human HSDL2 recombinant protein in HeLa cells: co-localization of human recombinant N'tagged HSDL2 with human HSD17B4 in peroxisomes. Red -HSD17B4 (in peroxisomes), green - N'myc-HSDL2.

Results

Remarkable is the fact that N-terminal tagged recombinant HSDL2 was transported into peroxisomes, but the masking of the peroxisomal targeting signal at the C' terminus caused transport into mitochondria. All HSDL2 tagged at C' terminus was found in mitochondria as shown in representative [Figure 61].

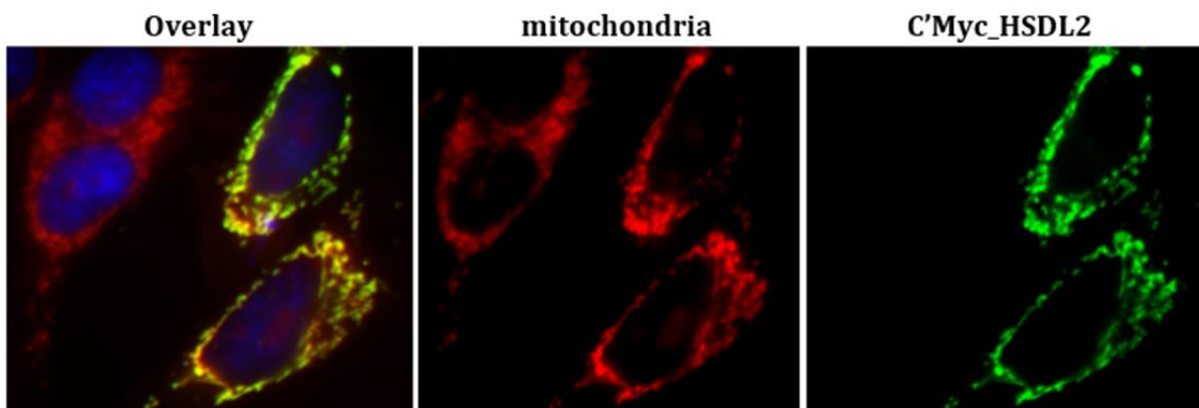


Figure 61 Counterstaining with mitochondria: red-mitochondria; green – C'Myc-HSDL2.

2.2.4 In search for enzymatic activity

2.2.4.1 Control of transfection procedure

The cDNA coding human SDR proteins: HSD17B8, SDR-O or HSDL2 was cloned into mammalian pcDNA3 expression vectors and expressed in HEK293 cells in order to check its potential enzymatic activity for several steroid and retinoid substrates. Especially for substrate screening assays recombinant proteins were expressed without tags for minimizing any impact on their potent enzymatic activity. While for HSD17B8 the success of transfection procedure into HEK293 cells and its further expression can be easily tested in followed activity assays with estradiol and NAD⁺ as cofactor, in case of SDR-O and HSDL2 whose substrate specificity is still unknown the control of transfection was important to verify the potent negative results of substrate screening. Because direct gene expression controlling methods with use specific antibodies or serum against SDR-O or HSDL2 were not available at the time of studies the transfection efficacy had been checked indirectly. By RT-PCR method there was controlled the expression on RNA level, while parallel HEK293 transfections with Flag and Myc tagged DNA for subcellular localization studies showed that recombinant targeted proteins were really present in cells transfected with the same

Results

procedure. Mock transfected HEK293 cells has not detectable by RT-PCR endogenous expression of SDR-O or HSDL2 [Figure 62].

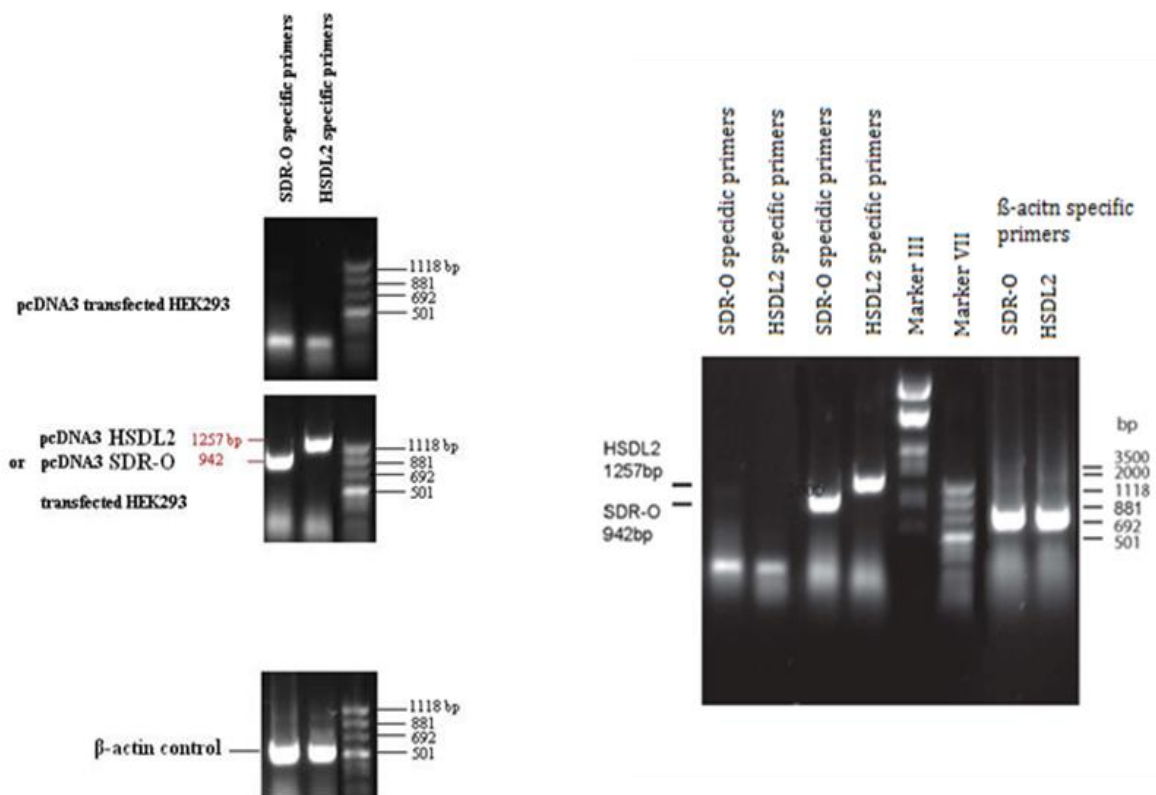


Figure 62 cDNA synthesis from mRNA expression control in pcDNA3_SDR-O or pcDNA3_HSDL2 transiently transfected HEK293 cells.

2.2.4.2 Steroid substrate screening

Transfected cell pellets containing over-expressed SDR proteins: HSD17B8, SDR-O or HSDL2 were subjected to enzymatic assays for screening the potential activity towards steroid substrates. Substrates and products were next analyzed by use the sensitive HPLC method. Tested steroids with results are listed in the table [Table 18] below:

Results

Table 18 The list of ^3H radio-labeled steroid substrates used in assays for activity screening studies of human HSDL2, SDR-O and HSD17B8. The last three columns show screening results for three enzymes.

Substrate	cofactor	expected product	Tested activity	Conversion		
				HSD17B8	SDR-O	HSDL2
Progesterone	NADH/NADPH	17 α -progesterone	17 α - reduction	no	no	no
Progesterone	NADH/NADPH	20 α -progesterone	20 α - reduction	no	no	no
20α-progesterone	NAD/NADP	progesterone	20 α - oxidation	no	no	no
Hydrocortisone	NAD/NADP	Cortisone	11 β - oxidation	no	no	no
Corticosterone	NADH/NADPH	Cortisone	11 β - reduction	no	no	no
Cortisone	NADH/NADPH	Hydrocortisone	11 β - reduction	no	no	no
Estrone	NADH/NADPH	Estradiol	17 β - reduction	no	no	no
Estradiol	NAD/NADP	Estrone	17 β - oxidation	Yes (4-10%)	no	no
Androstenedione	NADH/NADPH	Testosterone	17 β -reduction	no	no	no
Androstanediol	NAD/NADP	Androsterone	17 β - oxidation	no	no	no
Androstanediol	NAD/NADP	Dihydrotestosterone	3 α - oxidation	no	no	no
Androsterone	NADH/NADPH	Androstanediol	17 β -reduction	no	no	no
DHT	NAD/NADP	Testosterone	5 α - oxidation	no	no	no
DHT	NADH/NADPH	Androstandiol	3 α - reduction	no	no	no
Testosterone	NAD/NADP	Androstenedione	17 β - oxidation	no	no	no
Testosterone	NADH/NADPH	Androstanediol	3 α - reduction	no	no	no

Screening studies showed that human HSDL2 and SDR-O have no significant activity with any of tested steroid substrates in which the expected product would be higher from endogenous level in the control with mock transfected HEK293 cells. Only low activity was seen in the case of HSD17B8 transfected cells towards estradiol with NAD⁺ as cofactor (4-10% of conversion during 1h of incubation) what just can confirm the successful transfection and some expression of this protein in HEK293 cells. It is notable that in case of HSD17B8 also activity towards DHT and androstenediol was also not detectable in this assay.

Results

2.2.4.3 Retinoid substrate screening

The same HEK293 cell pellets were next tested for enzymatic activity with retinoid substrates. There was tested activity towards all-trans-retinal or all-trans-retinol at the presence of NADH/NADPH and NAD/NADP as cofactor, respectively.

Table 19 Retinoid substrates tested in assays with HEK293 cell pellets over-expressing human HSD17B8, SDR-O, and HSDL2. Results signed with a yellow star were repeated in assays with suspension of bacteria pellet.

substrate	cofactor	expected product	Results HSD17B8	Results SDR-O	Results HSDL2
All-trans- Retinal	NADH/NADPH	All-trans-Retinol	no	no	no
All-trans-Retinol	NAD/NADP	All-trans-Retinol	no	no	no

None of tested SDR proteins in cell pellets showed the substantial activity in oxidation of all-trans-retinol or reduction the all-trans retinal with NAD⁺/NADP⁺ or NADH/NADPH as cofactor, respectively. High endogenous conversion of retinoids observed in all control samples with mock transfected HEK293 cells caused the performing of extra optimization assays aimed to minimize the background effect by shortening the time of incubation. Numerous repeats of this enzymatic assays and detailed analysis revealed some weak tendency (but at the level of standard deviation around 1-1.5% of netto conversion) for higher reduction of retinal to retinol in case of pellets with SDR-O in comparison to control samples [**Figure 63; blue bars**]. It prompted me to repeat this reaction with an alternative enzymatic assay where SDR-O was expressed as GST fusion in bacteria lysate.

Results

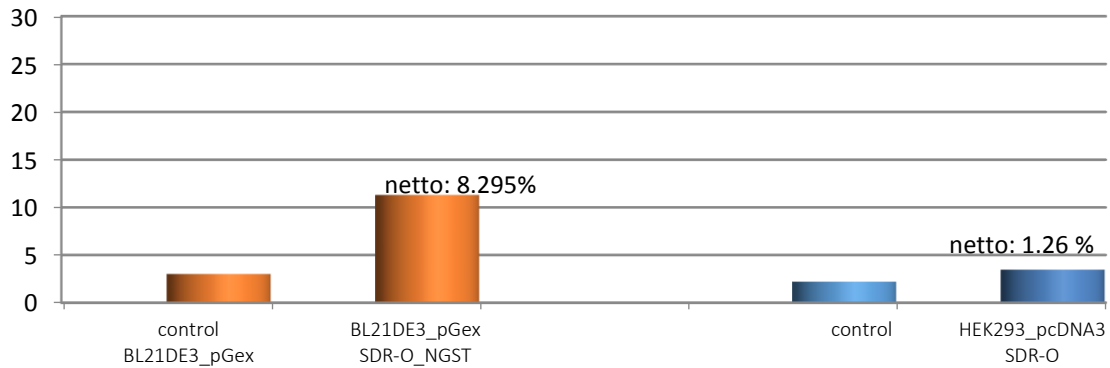


Figure 63 Comparison of all-trans-retinal conversion into all-trans-retinol at the presence of NADH by SDR-O in bacteria cell lysate and transfected HEK293 cells.

Surprisingly, results showed that only when SDR-O was expressed in the bacterial system the reduction of retinal was detectable well above background conversion [**Figure 63; orange bars**]. Further detailed experiments (F. Haller, IEG, HMGU) confirmed the predicted activity. Observed rate was then 16pmol/min/mg total protein in assay [**Figure 64**].

Results

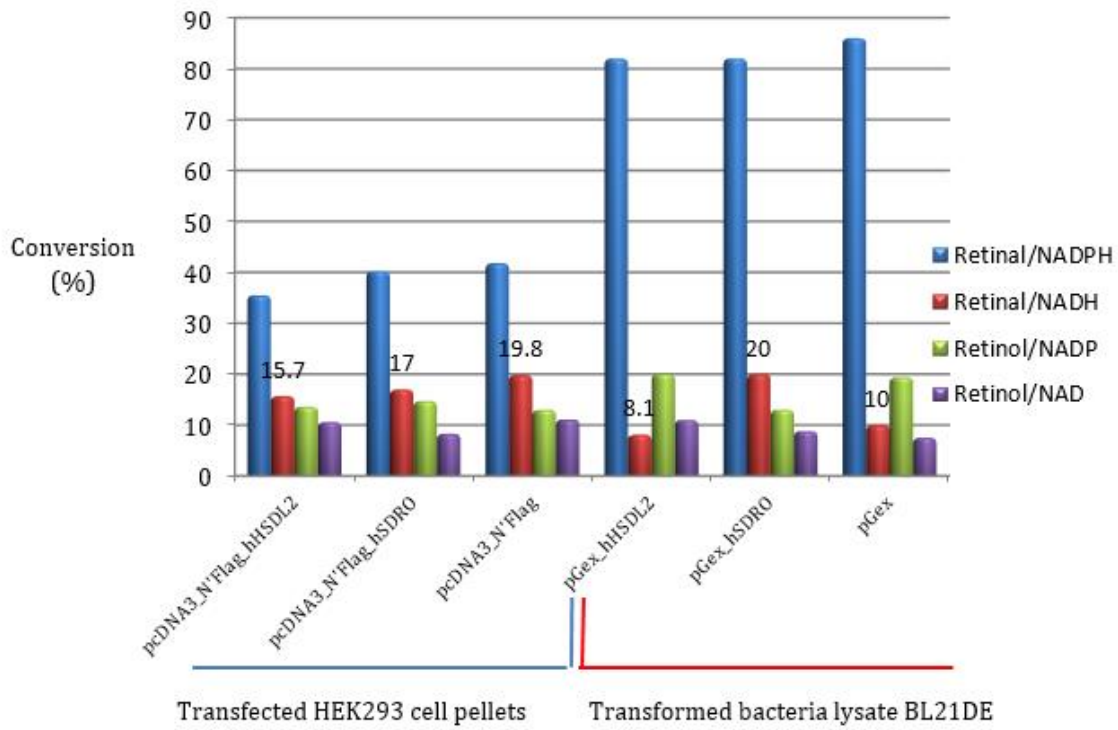


Figure 64 Results of conversion of all-trans-retinal to all-trans-retinol by transfected HEK293 cells or bacteria in the presence of NADH/NADPH or NAD/NADP, respectively (F. Haller, HMMG, IEG).

3 Methods

3.1 Bacteria techniques

3.1.1 Media for bacteria cultures

All used in this work *E.coli* strains were cultivated in two forms of LB (Lysate Broth) bacteria culture media: the liquid one or stable form containing agar.

- LB-Medium (Luria-Bertani-Medium)

1 % *Bacto- tryptone (digested by trypsin caseine),*

0,5% *Bacto- yeast extract,*

1 % *NaCl with NaOH up to pH 7,0*

All ingredients tittered thoroughly in bidest water

Autoclaved

- LB-Agar

LB-Medium (as above),

15 g/l Difco-Agar,

Autoclaved

The sterilized LB 0,5L flasks with liquid media or solidified LB-agar were storage at 4°C until use.

3.1.2 Preparation the antibiotic selection media

Selection media allow growing only *E.coli* strains carrying plasmid with the resistance to antibiotic. To prepare the selection media the antibiotic was added to the flask before inoculation. In case of solid agar LB, the flask was first melted by heating in microwave, cooled to 50°C and then antibiotic was added and poured into Petri's plates to solidify. The dishes were then turn upside down and storage at 4°C until use. If some water droplets were collected on the lid, just before use, agar plates were dried around 1h upside down in incubator at 37°C. Depending on vectors used ampicilin, chloramphenicol or kanamycyn were used for selection.

Methods

The working concentrations of

- Ampicilin 100µg/mL
- Choramphenicol 25µg/mL
- Kanamycin 50µg/mL

All antibiotics were first sterilized before adding to LB media.

3.1.3 Bacteria inoculation

Bacteria were inoculated from glycerol stocks by use of sterilized in flame inoculation loop and transferred into flask or 13ml Falcon tubes with LB media or plated out on agar plates in surface covering manner. For cloning purpose and selection the bacteria clones were grown in 96 well- 1ml plates or Eppendorfs in LB medium (see cloning) incubated usually overnight. For other purposes the bacteria were grown up to achieve appropriate OD₆₀₀.

3.1.4 Bacteria cultivation and harvesting

Bacteria were cultivated in flasks at 37°C under vigorous shaking (≥ 200 rpm). Depending on purpose overnight culture was usually transferred to biggest flask in 1:100 dilution and were grown up to achieve the appropriate OD₆₀₀. Bacteria were harvested by centrifugation for 15 min and 4500 rpm at 4°C usually in 50 ml or 13 ml Falcon tubes. The supernatant was discarded and bacteria pellets washed with equal amount of PBS buffer. After another centrifugation (15', 4500 rpm at 4°C) and discarding the supernatant cell pellets were stored at -20 or -80 °C (for long term) until used or directly subjected to further experimental procedures.

3.1.5 Bacteria growth control

Growth of bacteria was controlled spectrophotometrically by measure the light absorbance at $\lambda_{600\text{nm}}$ (OD₆₀₀). In this purpose 1ml of diluted bacteria culture was placed in cuvees and then measured for checking the bacteria density. The OD₆₀₀ value measured for pure incubation LB-media without

bacteria was used as reference. When by measuring the OD₆₀₀ value was higher than 2 (corresponding to beginning of saturation phase at the absorbance curve) bacteria probe had to be more diluted in order to achieve more reliable measurement.

Measurements of OD₆₀₀ were utilized in this study for calculations the amount of bacteria by normalizing the probes used in enzymatic assays and for estimation the phase of bacteria growth. For example in aim of protein induction bacteria were grown up to OD₆₀₀ around 0.6-1.0 before adding the inductor which corresponds to mid to late log phase of bacteria growth. At this density bacteria cells does not compete for metabolites in cultivation media and can express proteins more effectively than if they were under starvation stress. Otherwise for protein harvesting from induced bacteria cultures where the efficiency of yield is connected to amount of bacteria cells the OD₆₀₀ was usually higher corresponding to the stationary phase of bacteria growth.

3.1.6 Glycerol stock preparation

For long term storage the 800µl of overnight bacteria culture were mixed with 800µl of 80% sterilized glycerol in cryotubes. Glycerol stocks were stored at -80°C.

3.1.7 Induction of fusion-protein expression by bacteria.

All enzyme proteins designed for purification or further enzymatic analysis used in this studies were expressed as N-terminally tagged GST fusion proteins from pGex 2T vector (Leenders et al.; 1996). Constructs were transformed into E.coli BL21DE3 Codon Plus RP bacteria strain and stored as glycerol stocks after previous verification of correct cloning by sequencing. In other aims for example obtaining of specifically tagged construct for subcellular localization studies in cell lines were used pcDNA vectors and DH5α bacteria strains (see cloning strategies). In order to induce protein expression 5 ml overnight pre-culture of transformed with appropriate expression vector bacteria strains were transferred to flasks containing 100-200ml fresh LB media with corresponding antibiotic and incubated at 37°C until OD₆₀₀ reached 0.6-1.0. The culture was then split evenly and bacteria in one of two aliquots were induced with 0,25mM isopropyl-β-D-

thiogalactopyranoside (IPTG) and both aliquots followed further incubation. Around 3.5-4h later after OD₆₀₀ measurement bacteria were harvested and pellets stored at -20°C until use or directly subjected to experimental procedures. In this study induced for protein expression bacteria were utilized for enzymatic assays or further protein purification protocols [chapter 3.3.5]. Protein expression was controlled by SDS-PAGE and Western Blots [chapters 3.3.3-3.3.4]. Not induced with IPTG aliquot was then separated for inducing control.

3.1.8 Bacteria transformation with plasmid DNA.

100µl commercially obtained chemocompetent *E.coli* strains: DH5α or BL21(DE3) without antibiotic resistance were thawed from -80°C and incubated on ice. Next, 8-10µl of ligate solutions was added very carefully on surface of bacteria and incubated on ice for 20min. Transformation of plasmid DNA to bacteria was performed by placing the Eppendorfs tube to water bath or heat block set on 42°C for 45 sec followed by immediately placing back on the ice. Fresh transformed bacteria were supplemented with 150µl of LB medium without antibiotics and incubated at 37°C for 45min. with continuously shaking. Next 100 or 150µl of transformed bacteria was inoculated on agar plate containing the appropriate antibiotic.

3.1.9 Bacteria clones analysis.

For transformation control and further selection of transformed with DNA plasmid bacteria grew up plated on selective agar. The single colonies were picked up by use of sterilized wooden sticks into 96-well plates or Eppendorf tubes with 250µl of LB media with antibiotics and incubated at 37 °C up to 2 hours. Bacteria suspension aliquots were next used directly for PCR analysis as a template.

3.1.10 Preparation of bacteria pellets and homogenated bacteria lysates for enzymatic assays.

For checking the enzymatic activity of transformed bacteria there were used for assays just pelleted bacteria cells (harvesting as described in 3.1.4) re-suspended in appropriate reaction buffers or homogenated bacteria lysates in case of BL21(DE3) Codon Plus RP expressing recombinant

Methods

HSD17B5. In this purpose bacteria pellets were re-suspended and lysed by lysozyme in the 50mM Tris/HCl, 500mM NaCl, 1mM EDTA, (pH=7.8) buffer containing proteinase inhibitors and next subjected to vigorous vortexing. In order to disrupt the bacteria walls and release into solution the wanted enzyme protein the sample with lysed bacteria pellet was alternately frozen and thawed few times in liquid nitrogen. Next, after adding the endonuclease in 100mM MgCl₂ buffer the mixture was subjected to cetrifugation (15', 4500 rpm at 4°C). Finally, the supernatant containing the demand soluble enzyme was gained after centrifugation (30', 14000 rpm at 4 °C), aliquoted and stored at -20°C until use.

3.2 Cell culture techniques

3.2.1 Cell culture media

Cell culture media were bought originally from PAA and usually contained L-glutamine. Fetal bovine serum (Invitrogen) as well the antibiotics (Invitrogen) were added extra just before use.

Medium: **DMEM** (High Glucose Dulbecco's Modified Eagle Medium)

(containing glucose 450mg/L, GlutaMAX and puryvate)

+10% FBS

+, 100 µg/µl streptomycin

+ 100 U/ml penicillin

+/- 250µg/ml (final conc.) G418 (for HSD17B5 stable transfected cell line)

+/- 300µg/ml (final conc.) G418 (for HSD17B3 stable transfected cell line)

Medium: **M-MEM** (Modified Eagle Medium)

(containing L-glutamine)

+10% FBS

+, 100 µg/µl streptomycin

+ 100 U/ml penicillin

Medium: **RPMI-1640**

(containing L-glutamine)

+10% FBS

+, 100 µg/µl streptomycin

+ 100 U/ml penicillin +/- 250µg/ml (final conc.) G418 (for HSD17B5 stable transfected cell line)

3.2.2 Cell cultivation

All used in this work human cell lines were grown adhesively in monolayer in T-75 flask designed for cell culture. However primarily cells were maintained in T-75 flasks for experimental purposes cells were transformed to other formats as T-25 flasks, 6-well, 12-well or 96-well plates according to the needs. Details of seeding in different formats will be presented below in the course of this chapter describing the corresponding methods and experimental. To maintain cells in good conditions they had to be diluted with fresh medium and transferred to another flask before achieved the 100% confluence. For experimental purposes the cells were transferred into 6-well, or 96-well plates. All manipulations were performed in sterile conditions under laminar flow. Flasks with cells were incubated in humidified conditions, at 37°C and 5% CO₂.

3.2.2.1 Cell splitting

In order to remove the cells from the flask for different purposes the old medium was sucked off. The cells were next washed with 2mL of sterilized PBS. 1.5mL of trypsin solution with EDTA was then added to cells and incubated for few minutes at 37°C in incubator till the cells came off the dish bottom. Detaching of cells was checked visually on inverted microscope: during the trypsinization cells were cramping into small round ones. Then 4.5µl of fresh media was added and appropriate amount of cell suspension was transferred to new flask with freshly prepared media. In serum are present natural inhibitors of trypsin.

3.2.2.2 Cell Counting

After trypsinization and cell collecting into tubes the aliquot of 30µl was taken for counting in cell counting camera (Rosenthal or Neubauer). Cells were counted in squares by eye under inverse microscope.

3.2.2.3 Cell freezing

For storage purposes there were prepared sterilized 1.8mL cryo-tubes with 180 μ L of DMSO. Cells were collected minimum 3 x10⁶ cells. (In case of smaller amount cells were centrifuged 5min 500-1500 rpm.) Cell solution was into the tubes fulfilling up to 1.8mL (final concentration of DMSO 10%). Cell so prepared tubes were quickly placed in box with isopropanol and subsequently transferred into at -80°C. Presence of isopropanol prevented from rapid lowering the temperature and DMSO before spontaneous creating the crystal and thereby cell damage. In -80°C cells could be storage for few months. For longer time they were move to liquid nitrogen at -196°C.

3.2.2.4 Cell thawing

Cells were thawed quickly in water bath with a temperature set on 37°C. The cells were centrifuged (2-3min, 500-1800 rpm, the supernatant containing DMSO discarded, cells.

3.2.2.5 Cell pelleting

Cell pellets were used in this work for transfection analysis, and enzymatic activity tests. For pelleting cells were first trypsinized, diluted with PBS, counted and aliquoted into 2.2mL or 1.5mL Eppendorf's tubes (2x10⁶ or 4x10⁶ cells each). Tubes were centrifuged 5min at 1800 rpm and 4°C, supernatant discarded. For enzymatic assay cell pellets were usually washed ones with PBS to remove the rests of media. Cell pellets were stored at -80°C until use.

3.2.3 Cell viability tests

Adding of different substances such as enzyme inhibitors can be harmful for the cells. Cell viability in the easiest way was controlled by eye under microscope. The aliquot of cell solution designed for counting was mixed in the same volume with trypan blue and incubated at room temperature for few minutes. The cells were counted dark blue cells which could not actively rid off the stain meant

Methods

dead cells and the percentage of them was calculated. However, for more precise results the cell viability studies were additionally supported with commercially available kits:

MTT –cell viability test

Cell Titer Glow- cell viability test

Caspase Glow- apoptosis test

3.2.4 Cell transfection

For transfection purposes were used cells in culture in appropriate dishes at least 18h. Transfection was performed at confluency in the range 40-70% depending from future applications. For transfection the cells with plasmid DNA carrying the genes for expression of recombinant proteins lipoplectamine were used.

Table 20 List of used Flask for cell transfection

Dish	Media volume (ml)	DNA (μg)	FuGene6 (μl)
T-75 flasks	12-15	8	800
T-25 flasks	7-10	2	400
6-well plates	2	1	100

Fugene6 transfection reagent was added to medium and incubated at room temperature for 5 minutes avoiding the direct contact with plastic walls of the tube. Next, DNA was carefully added and incubated 20min. After this time the transfection solution with DNA was carefully added to cells in drop manner way.

3.2.5 Stable transfected cell line

In this work for enzymatic activity assays were used three stable transfected cell lines: human 17 β -HSD5 stable transfected HEK293 and MCF7 cells and stable transfected with human 17 β -HSD3 HEK293 cells. The two first were received by courtesy of Trevor Penning from University of Pensilvania. The last one was generated in frames of BioNetWorks project and was performed by a Bechelors' degree student Fabian Ströhle as a part of his work.

3.3 Methods with proteins

3.3.1 Isolation of protein fraction from bacteria pellets

For further recombinant protein analysis such as control of protein expression bacteria pellets were re-suspended in lysis buffer and lysed by 3-5 freeze/thaw cycles using liquid nitrogen and warm water. The genomic DNA was digested by addition of 1U endonuclease (Benzonase, Sigma) and Mg_2Cl_2 (5 mM final concentration). Samples were centrifuged to separate soluble and insoluble proteins (14 000 rpm, 30', 4°C). The supernatant was transferred to a fresh tube and the pellet fraction re-suspended in an equal amount of PBS. Gained in this way aliquots could be further subjected to SDS-PAGE procedure.

Lysis buffer:

PBS: 10mM sodium-phosphate buffer
 150mM NaCl
 pH 7.4

+ 0,1 mg/ml Lysozyme

+ protease inhibitor mix (1000x): 20mg/ml Antipain
 0.2mg/ml Aprotinin
 0.2mg/ml Leupeptin

3.3.2 Isolation of protein fraction from mammalian cells

For control the protein expression in transfected mammalian cells the protein fraction was isolated using the M-MEM (Pierce) Kit. Cells directly harvested from the cell culture or pellets stored at -80C before were lysed with the buffer appropriately and centrifuged 14 000 rpm, 10 min at room

temperature. Amounts of buffer were depending from cell type and amount of cells in the pellet, according to the manufacturer's protocol. Gained in this way supernatants were directly subjected for SDS-PAGE procedure.

3.3.3 SDS-Polyacrylamide Gel Electrophoresis (SDS-PAGE)

Protein from fractions gained by isolation procedures from bacteria or mammalian cells were separated under denaturing conditions by SDS-PAGE using minigels (8.6 x 6.8cm) and subsequently visualized by Coomassie staining.

- **Preparation of protein fraction**

10 μ l of each fraction was added to 10 μ l 5x Laemmli buffer containing SDS adding the negative charge, heated for 5-10 minutes at 95°C. After this time the proteins in tubes were denaturated and subsequently loaded on SDS-PAGE or alternatively storage at 4°C until used.

5x Laemmli buffer:

- 50% glycerol
- 4% SDS
- 0.1 % Coomassie blue G250 (filtrate)
- 0.2M Tris-HCl, pH 6.8

- **Separation on SDS-PAGE**

Prepared with Laemmli buffer and denaturated previously protein samples were loaded together with a protein marker on a Tricin-Gel (10% resolving gel, 4% stacking gel) and then separated in a constant electric field. Separation was continued till marker achieved the end edge of the gel.

Anode buffer: 0.2M Tris HCl, pH 8.9

Cathode buffer

- 0.1M Tris
- 0.1 M Tricin
- 0.1 % SDS

Gel buffer:

- 3M Tris-HCl, pH 8.45
- 0.3 % SDS

Methods

Acrylamide solution: acrylamide/bisacrylamide, 30% (30: 0.8)

Resolving gel (10%) 3.3 ml acrylamide solution
 3ml Gel buffer
 1ml H₂O
 2.5ml glycerol (50%)
 20µl TEMED
 50µl APS

Collecting gel (4%) 0.67ml acrylamide solution
 0.67ml gel buffer
 3.67ml H₂O
 10µl TEMED
 40µl APS

- **Staining and drying SDS-polyacrylamids**

For detection of the sampled proteins the gel was immersed in Coomassie staining solution for 30 minutes and de-stained by washing with 10% acetic acid at room temperature overnight. For documentation, gels were equilibrated in H₂O and dried between two sheets of cellophane.

Coomassie staining solution: 200ml methanol
 5ml acetic acid
 295ml H₂O
 500mg Coomassie blue G250 (filtrate)

3.3.4 Western-blot

To visualize the fusion proteins via monoclonal antibodies against their specific tags, the separated protein fractions from SDS-PAGE gels were transferred onto a PVDF-membrane by semi-dry blotting. The gel was equilibrated in blotting buffer for 10 minutes, the membrane pre-wet with methanol and then immersed in blotting buffer; filter paper was soaked with blotting buffer. The blot was set up in the sequence 'anode-2x filter paper-membrane-gel-2x filter paper-cathode' and the proteins were transferred onto PVDF in 30 minutes at 20 V. After blotting in order to control

Methods

the complete transfer of the sample on the membrane or to visualize all separated previously on SDS-PAGE proteins from the sample the membrane was soaked for 1minut in the Ponceau S solution and next destained with H₂O. This is a rapid and reversible staining method for loading protein bands on Western blot. In some cases, stained membrane was scanned and documented. Washing with H₂O thoroughly destained the membrane from Ponceau S solution, completely. Next, the membrane was blocked in PBS/5% milk powder at RT for 30 minutes, rinsed with PBS and incubated overnight at 4°C with the primary antibody diluted 1:5000 in PBS/0,5% milk powder. Alternatively, incubated at RT for 2h at gentle continuously shaking. The membrane was rinsed three times for 5 minutes each in PBS and incubated for 2 hours at room temperature with the secondary antibody conjugated with peroxidase diluted 1:2000 in PBS/0.5% milk powder. After rinsing the membrane three times for 5 minutes each in PBS, 25 ml freshly prepared developing solution was added. Color development was stopped by removal of developing solution and rinsing the membrane with H₂O.

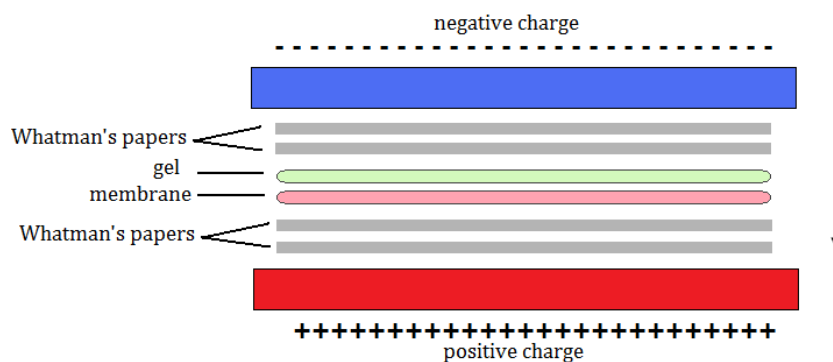


Figure 65 Western-blot layer composition.

Alternatively, rinsed with PBS membrane was soaked with a solution containing substrate for luminescention (PerkinElmer, Western blot chemiluminescence Reagent) after enzymatic reaction performed by horseradish peroxidase (HRP). HRP catalyzes light emission from the oxidation of luminal. The light was captured on Kodak Film. The procedure was performed according the manufacturer protocol. Rinsed with the solution membrane was exposed to the film (Kodak) in the darkness. Film was developed in the darkness. This method yields fast, permanent, hardcopy results on Kodak X-Omat Blue Autoradiography Film.

Methods

The membrane was incubated in the Chemiluminescence Reagent for 1minute at RT. Next, the membrane was placed between the covers of a polypropylene sheet protectors. The membrane (after smoothing out any air bubbles) was placed protein side up in the film cassette. In the darkness the film was placed on the top of the membrane, exposed for 1minute and developed. The film exposure was next repeated, varying the time as needed for optimal detection.

5x developing buffer (pH 7.5) 0.225g NaH_2PO_4
 1.59g Na_2HPO_4
 11g NaCl
 8.5g Imidazol
 625 μl Tween -20

 + 250 ml with H_2O

Blotting buffer: 48mM Tris
 33mM Tricin
 1.3 mM SDS (10%)
 20% methanol

Developing solution: 1x Developing buffer
 100 μl CoCl_2 (10mg/ml)
 1mg Diaminobenzidine (DAB) Sigma
 10 μl H_2O_2
 + 25ml with H_2O

PBS 10mM sodium-phosphate buffer, pH 7.4
 150mM NaCl

Ponceau S Staining Solution: (0.1% (w/v) Ponceau S in 5% (v/v) acetic acid)
 1g Ponceau S
 50ml acetic acid

 + 1L with bidest H_2O

3.3.5 Purification of GST-fusion protein

Purified HSD17B5 enzyme was applied in this work for enzymatic assays performed on 96-well format. This purification protocol was also used in tries to purify GST fused SDR-O and HSDL2 proteins. The following procedure was applied for pellets from 100ml of IPTG induced bacteria cultures [as described in chapter 3.1.7].

- **Bacteria cells lysis and homogenization**

Bacteria pellets were re-suspended in 5ml of ice-cold PBS. After centrifugation (4500 rpm, 15', 4°C) pellets were re-suspended again in 5ml of lysis buffer [prescription at the end of this chapter] containing added extra lysozym and protease inhibitor and incubated for 5 minutes at room temperature. Next, bacteria cell walls were further disrupted and homogenized by few cycles of freezing in liquid nitrogen and thawing in warm water bath, alternately, till viscid suspension was visible. Viscosity caused by released genomic DNA has disappeared after 5 minutes incubation at room temperature with 300µl of endonuclease solution in MgCl₂ [endonuclease solution as prescription in the chapter 3.1.10]. Next, the sample was further homogenized in two centrifugation steps:

- 1st centrifugation (4500rpm/15min/4°C)
- 2nd centrifugation of supernatant from the step 1 (14000rpm/30min/4°C)

Two step centrifugation allowed separating insoluble part of the sample from soluble one which contained most of the recombinant protein. Supernatants from this step were used in enzymatic assays for two rounds of screening with BNW chemicals testing the inhibitory activity towards human HSD17B5 in converting the androstenedione to testosterone.

5ml of Lysis buffer:

50mM Tris
500mM NaCl
1mM EDTA
pH 7.4

+10µl of lysozym (see chapter above)
+ 5µl of protease inhibitor mix (1000x)

Methods

- **Binding to the GT-sepharose**

100µl of glutation-spharose, previously washed 3 times in 1ml of ice cold PBS (500rpm, 1', RT) was mixed with the supernatant containing recombinant protein and incubated for 2h at 4° by gently shaking or rotation. Alternatively, binding of the GST-fusion protein to the glutation sepharose was performed by incubation overnight. Next, after centrifugation (500rpm, 5', 4°C) the supernatant was carefully discarded from matrix with bound GST-fusion proteins. The sample was subsequently washed 3 times with the same volume of ice cold PBS (500rpm, 5', 4°C) every time carefully discarding the supernatant with unbound proteins. To the quality control the equal aliquots of discarded supernatants were collected.

- **Thrombine cleavage**

To release the recombinant protein from the matrix and to cut the N'GST fragment of the fusion protein the sample was mixed carefully with 100µl of trombine solution and incubated overnight at 4°C and gently shaking or rotation. Next, the liquid part of the solution with the demand protein was separated from the matrix (500 rpm, 5', 4°C). Matrix was 3 times washed with 100µl PBS (500 rpm, 5', 4°C). All eluats were mixed together and in order to separate from parts of matrixwere shortly centrifuged (10000 rpm, 30'', RT). The supernatant was next filtred by PVDF, large of pore, 0,45 µm). Protein solution was aliquoted and storage at -20°C until use. One aliquot was taken for protein concentration measurement and for quality control on SDS-PAGE.

- **GT elution**

In order to elude the whole fusion protein from GT-sepharose, matrix was mixed with 100µl of glutation elution buffer and incubated overnight at 4°C and gently shaking or rotation. Next steps are corresponding to the elution with thrombine.

To control the efficacy of purification there were taken appropriate aliquots from each step, induction, homogenization, binding, washing and elution and subjected to SDS-PAGE.

3.4 DNA –based methods

3.4.1 DNA gel agar electrophoresis

This method was performed for qualitative measurement of DNA or for subsequent DNA isolation. Agar gel was prepared in 1x TBE buffer, mixed thoroughly and heated in micro-well for dissolving. Next, the liquid agar was poured into chambers with EtBr to solidify. DNA probes subjected for analysis were previously mixed with Loading Dye buffer and then applied on to the solidified agar gel. DNA was mobilized in voltage from 80-160V depending on the size of the gel. For determination of DNA fragments size there were added DNA control markers from fermentsas III and VIII containing fragments of λ -phage. For analysis of most dsDNA fragments (size 0,5-4 kb) used in this work application of 1% agar was sufficient and extra optimization of agar percentage was not needed. 1% agar is usually the best optimized for dsDNA fragments of the size ~2-5 kb. In really the percentage was usually a little bit more than 1% probably due to TBE buffer evaporation during heating and it explains observed good resolution for shorter dsDNA fragments. DNA bands were monitored and photographed with UV transillumination ($\lambda=254\text{nm}$) on a BioVison gel documentation system (PeqLab). For further isolation DNA fragments were excised from the gel and purified [chapter 3.4.3].

- **10x TBE**

108g Tris

55g boric acid

9.3 g EDTA

- **1% agar gel**

150 μ l 1xTBE

1.5g agar (Amersham)

15-18 μ l EtBr (0,5 μ g/ml)

- **6x Loading Dye**

15% Ficoll 400 (Pharmacia)

0.25% bromophenol blue

0.25% xylene cyanol FF

Alternatively, there was used the loading dye purchased as ready-to-use solution from Fermentas.

3.4.2 Plasmid DNA isolation from E.coli

Depending on experimental purposes and needs plasmid DNA was isolated in this work in two scales: mini preparation from 3-5ml of overnight culture by use NucleoSpin Plasmid Kit (Macherey & Nagel) and midi preparation- for amount of bacteria up to 30ml of overnight culture – NucleoBond PC 100 Kit (Macherey & Nagel). Usually, freshly harvested bacteria from overnight culture (centrifugation at 4°C, 15min, 4500 rpm) were subjected for plasmid DNA isolation. Alternatively, frozen bacteria pellets storage at -20°C was used. Bacteria pellets were re-suspended in the appropriate buffers from the kit. Next, all isolation steps were carried out according to the manufacturer's protocol with a difference at the end where the DNA was eluted with Ampuwa water instead of TE or AE buffers provided with the Kit. Eluted DNA was subjected next for quality control and concentrations measurements. DNA yield of mini-prep was usually in the range of 20-400 ng/μl for 35-50μl of elute, while for midi-preps concentration of precipitated DNA was usually in the range of 0.2-8μg/μl for 100-200μl of solution.

3.4.3 Purification of dsDNA fragments from agar gel or from reaction assays.

Chosen DNA fragment visualized in EtBr stained agarose gel under UV light were cut from gel using a sharp scalpel. The DNA containing slice was transferred to reaction tubes and subjected to further purification processes by use of Gel Extraction Kit (Qiagen) as described in the manufacturer's protocol. In case of DNA purification from other aqueous solutions containing enzymes, dNTP, salts from buffers etc. there was used the PCR Clean-Up System Kit (Promega). All purification steps were performed according to manufacturer's protocol. In both cases the final elution of the DNA was carried out with 35μM Ampuwa water.

3.4.4 Quality and quantity measurements of nucleic acids by optical density (OD)

For quality and concentration estimation DNA (or RNA) was measured spectrophotometrically by light absorbance at 260nm and 280nm. For this purposes DNA (or RNA) probes were diluted in the H_2O_{dist} and 100 μ l of the solution was added into cuvette for the measurements. The concentration of the nucleic acid solutions was calculated according to the following formula:

For dsDNA: $OD_{260} \times \text{dilution factor} \times 50\text{ng}/\mu\text{l} = c \text{ (ng}/\mu\text{l)}$

For RNA: $OD_{260} \times \text{dilution factor} \times 40\text{ng}/\mu\text{l} = c \text{ (ng}/\mu\text{l)}$

The quality was assessed by the ratio value R (OD_{260}/OD_{280}) where R = 1.8 for dsDNA is an optimum case. The OD measurements were conducted using the Beckman DU 530 Life Sciences UV/Via Spectrophotometer.

Alternative quick method was NanoDrop spectrophotometry. It needed only 1 μ l of DNA solution and gives precise calculated results as final concentrations.

3.4.5 DNA amplification (PCR method)

Polymerase Chain Reaction (PCR) was applied for amplification the site –specific DNA fragments. Reaction was performed in 20 μ l or 50 μ l format containing:

- 0.2 mM dNTP-mix,
- 1 μ M mixture of forward and reverse primers (0.5 μ M each),
- 0.5-2.5 U polymerase in 1xPCR buffer *.
- DNA template

***10x PCR buffer:**

100mM Tris-HCl pH 9.0

500 mM KCl

15mM MgCl₂

Usually, lab-made Taq-polymerase was used. For some experiments which required more reliable proof-reading polymerase: Pfu Turbo DNA polymerase (Stratagene) or KOD HIFI DNA polymerase (Novagen) was used instead of Taq. DNA template included: genomic DNA, cDNA, plasmid DNA,

Methods

linear dsDNA or bacterial culture. The standard program on Robo-Cycler PCR machine (Stratagene) implied an initial denaturing for 5 min at 95°C followed by at least 35 cycles with 30 sec at 95°C, 35 sec at annealing temperature (T_a), 1min per 1kb at 72°C, where T_a is the melting temperature $T_m - 5^\circ\text{C}$ specific for the applied primer pair. Usually the cyclic reaction was followed by a 10 min final elongation step at 72°C. For bacteria culture as PCR template initial denaturing was prolonged to 10 min.

Standart PCR program:

95°C	5'	<i>initial denaturing</i>
95°C	30"	} x 35 cycles
T_a °C	35"	
72°C	1'/1kb	
72°C	10'	<i>final elongation</i>

3.4.6 Mutagenesis method

It is the PCR-based method. The method allows generating mutations in demand location and requires the use of specially designed DNA sequences as primers and in this work it was applied for changing two SDR-O point mutation (T141A and F177L) from commercially ordered version of the gene from RZPD to achieve the sequence consistence with NCBI data bank (database entries: NM_148897 and five different SDRO ESTs). Previously designed appropriate primers were ordered and used in PCR reaction by use of Quikchange mutagenese kit method (Stratagene). For this procedure a pair of complementary specific primers were designed containing the repaired point mutation in their core region and flanking it to both sides ~15-20bp (synthesized by Metabion). Back- mutagenesis was performed here in two steps. The 20µl PCR reaction with 2,5 U Pfu Turbo DNA polymerase (Stratagene) containing template plasmid (pReceiver-M09-SDR-O), 0,2 mM dNTP-mix and 10µM of each mutagenesis primer in 1x Pfu Buffer. After 3' denaturing at 95°C and 16 cycles with 30"95°C, 1' 55°C and 68 °C (about 1' per 1000bp), template DNA was digested by addition of 1µl DpnI (10U/µl, NEB) to the PCR reaction and incubation at 37 °C for 1hour. 3µl of this mixture were subjected to transformation into DH5α chemocompetent cells and checked for correct mutagenesis.

3.4.7 DNA sequencing

To identify or verify DNA sequences, DNA was sequenced on the ABI3730 (Applied Biosystems) by the method of controlled termination of replication (Sanger dideoxy method) according to the manufacturer's protocol. Amplified DNA was purified from PCR mixture with the millipore kit in a 96-well format for higher throughput analysis. (purification steps according to the manufacturer's protocol) or for single probes on Qiagen purification kit.

PCR sequencing mix:

5x sequencing buffer	1 μ l
Dye 3.1 dNTP	1 μ l
DNA template (~90ng/ μ l)	1 μ l
H ₂ O seq	1 μ l
Primer (10mM)	1 μ l

Alternatively, plasmids or DNA fragments were sent to SequiServa Company.

3.4.8 Restriction analysis

Restriction analysis is an alternative method for screening the clones by use of enzymes. The same DNA probes were digested with different restriction enzymes. After incubation with digest enzymes and DNA gel electrophoresis DNA was analyzed visually for expected DNA fragments.

3.5 RNA –based methods

3.5.1 Total RNA isolation from cell

In this work two ways of RNA isolation were utilized: the large scale total RNA isolation from HepG2 cells in searching of transcripts of chosen SDR candidates by use of RNasy midi kit (Qiagen) and the mini scale total RNA isolation using the RNasy mini kit (Qiagen) for controlling the transcription in transfected HEK293 cells. All RNA extraction steps were performed according to manufacturer's protocols. Isolated total RNA was stored at -80°C.

3.5.2 mRNA isolation and cDNA synthesis

One microgram total RNA previously isolated from 2 million transfected HEK293 cells using the RNasy mini kit (Quiagen) was reverse transcribed into cDNA using the Revert Aid™ First Strand cDNA Synthesis Kit (Fermentsas) and oligo (dT)₁₈ primers. The following program was used for PCR with sequence specific primers 1cycle 3'95°C, 35 cycles 45''95°C, 30''50°C, 1'30'' 72°C.

3.6 Cloning strategies

In order to clone a chosen gene there were designed primers with flanking regions start and end with appropriate restriction sites for cleaving enzymes. PCR was performed with DNA or primary carrying vector. DNA was purified, amount and quality measured. Next DNA as well the predestinated vector incubated with the same type restriction enzymes. After purification and DNA measurement the linearized vector and DNA insert were ligated. Ligate was than transformed into bacteria. Bacteria were then screened for the right with PCR method with specific for insert primers or in combination reverse insert forward vector and in turn. Further verification by restriction analysis and finally sequencing.

3.6.1 TOPO-TA cloning

For direct cloning of DNA fragments from PCR reactions without prior cleanup, the TOPO-TA cloning Kit (Invitrogen) was used. In this method, A-overhangs produced in the elongation step of the PCR by the Taq-polymerase are ligated to T-overhangs in the respective vector (TA-cloning). The yield of ligation products is enhanced by topoisomerase, attached to the vector's cloning sites (TOPO-cloning). Following amplification of the DNA by PCR 4µl of the reaction mixture were subjected to the ligation procedure into vector pCRII or pCR2.1 and transformed into chemocompetent TOP 10 cells as recommended by the manufacturer. In this work the method was used as a step for cloning of human hsd12 gene.

3.6.2 Cloning *via* restriction sites

Methods

Insert DNA had usually modified ends. Alternatively, DNA fragments were also inserted into vectors *via* restriction sites. Digestion of DNA fragments and vector with restriction enzymes yields complementary DNA ends which can then be used for ligation. Utilization of two different restriction sites additionally allows for a site-directed insertion.

Restriction digestion:

DNA fragments (inserts) and vectors were digested with the particular restriction enzymes. 1-10 μ g DNA were digested in 20-50 μ l reaction volume containing appropriate concentrations of buffers, BSA (for NEB enzymes) and enzyme for 2 hours up to overnight at the optimum temperature for the enzyme's activity as reported by manufacturer. The adequate amount of enzyme was calculated according to the assumption that 1U of enzyme digest 1 μ g DNA in 1 hour under optimum conditions. Following restriction reaction was stopped by heat inactivation of the enzyme and was removed by DNA purification using the PCR Purification Kit (Qiagen).

Ligation:

Inserts were cloned into vector via restriction sites by T4-DNA Ligase (NEB or MBI) activity. The 10 μ l reaction mixture contained 100-200 ng vector and 5-10 times more moles of insert than vector in 1X T4-DNA-Ligase buffer. Ligation was carried out at room temperature for 2 hours up to overnight.

Transformation:

So prepared plasmid were subsequently transformed into chemocompetent bacteria strains (as described in 3.1.8) and checked for proper cloning.

3.6.3 Control of proper cloning

In order to check the proper cloning suspensions of bacteria colonies (as described) were used as template for PCR with specific primers. PCR-products were next screened and visualized on EtBr agar electrophoresis. DNA from bacteria colonies showing the demand length of searched DNA fragment was further subjected to restriction analysis and ultimately DNA sequencing.

3.7 Immunochemistry methods

3.7.1 Immunocytochemical and immunofluorescent methods for intracellular localization studies:

For visualization the intracellular structures and distribution of the expressed proteins the immunofluorescence and immunocytochemical methods were applied. Studied organelles were stained with specific dyes or visualized by expressing specific organelle targeted markers fused with fluorescent dyes. For counterstaining with studied proteins, there were constructed vectors carrying the protein of interested with fused tags: MYC or FLAG, alternatively on C' or N' ends. Both tags were recognized by specific antibodies and next with secondary antibodies conjugated with specific fluorochrom.

Constructs

All C'Myc tagged proteins were expressed from pcDNA4_MycHisB vector. N'myc fusion proteins were first cloned and then expressed from modified pcDNA3_NMyc. While FLAG fusion proteins were expressed from pcDNA3 NFLAG or pcDNA3_CFLAG were the tag was localized appropriately upstream or downstream from Multi Cloning Site (MCS) of the vector. All used in these studies constructs are given in the **Table 21** below. [Details of cloning procedures are to see in the chapter 3.6.2 and details of primers and used restrictions enzymes in the **[Table 27]**.

Table 21 Vector constructs for intracellular localization analysis of chosen SDR proteins

HSD17B8	pcDNA3_N'Flag_HSD17B8
	pcDNA3_N'Myc_HSD17B8
	pcDNA3_C'Flag_HSD17B8
	pcDNA4_C'MycHisB_HSD17B8
SDR-0	pcDNA3_N'Flag_SDR-0
	pcDNA3_N'Myc_SDR-0
	pcDNA3_C'Flag_SDR-0
	pcDNA4_C'MycHisB_SDR-0
HSDL2	pcDNA3_N'Flag_HSDL2
	pcDNA3_N'Myc_HSDL2
	pcDNA4_C'MycHisB_HSDL2

Methods

Organelle structure visualization:

Mitochondria were stained with 300nM MitoTracker Orange that gives red coloured mitochondria in the fluorescence microscope. For ER counterstaining there was applied co-transfection with pcDsRed2_ER commercially ordered vector that after transfection expresses fused with red fluorescent protein ER targeting sequence of calreticulin. Peroxisomes were counterstained alternatively with co-transfection with pcDsRed2_peroxi vector expressing red fluorescence protein containing the peroxisomal targeting signal (PTS1) with tripeptide SKL or alternatively cells were co-transfected with pcDNA3 vector carrying the human HSD17B4 also targeted to peroxisomes. For human HSD17B4 were available specific rat monoclonal antibodies (generated by E. Kremmer, Helmholtz Zentrum München). Golgi apparatus were counterstained with pAcGFP1-Golgi lighting on green.

For endosomes counterstaining there was applied Organelle lights Endosomes-GFP (Invitrogen) based on very effective baculovirus transfection system introducing the DNA and expressing fused with GFP Rab5a protein targeted to early endosomes. Transfection in this case was performed according to the manufacturer's protocol.

Table 22 Summary of organelle counterstaining

Organelle/protein	method	vector	fluorescent dye	light spectrum
Mitochondria	Staining		MitoTracker (Orange)	red
Nucleus	Staining		Hoechst 33342	blue
ER	Co-transfection	pDsRed2_ER	RFP	red
Golgi	Co-transfection	pAcGFP1-Golgi	GFP	green
Peroxisomes	Co-transfection/ immunohybridization	pDsRed2_peroxi, pcDNA3_hHSD17B4	RFP Cy3_2 nd antibodies	red red

Methods

Transfection

HEK293 or HeLa cells (obtained from DSMZ, Braunschweig, Germany) were seeded on 6-well plates containing glass coverslips and incubated at 37°C and 5% CO₂ in DMEM or MEM medium supplemented with 10% FBS, 1% penicillin and streptomycin, respectively. When the cells reached 40-60% confluency, transient transfection was performed with 1µg of DNA in 3µl of FuGENE6 Transfection Reagent according to the previously described protocol in chapter 3.2.4. When cells were co-transfected with both different DNA vectors (for example DNA of the protein of interest and DNA of specific organelle marker) total amount of DNA did not exceed 1µg and ratio of both vectors was usually 1:1.

Mitochondria staining

24h after transfection HEK293 or HeLa cells designed for mitochondria visualization were incubated for 30min with a fresh staining medium (DMEM or MEM supplemented as above, respectively) with with 300nM MitoTracker Orange (Molecular Probes, Invitrogen, Eugene, Oregon, USA). Subsequently the cells were washed twice with PBS and fixed with 3,7% formaldehyde for 10min at 37°C. Usually all cells in this studies were submitted for nucleus staining which was performed on the end of the protocol.

Visualisation with antibodies:

Next following steps were performed to enable the binding of specific antibodies: permeabilization of fixed cells in 0,5% Triton for 5min at RT, blocking with 3% BSA in PBS for 30min at RT, incubation in solution (200µl, 1:1000 in 3% BSA/PBS) of primary antibodies: anti-Flag (rabbit polyclonal IgG, Sigma) or anti-Myc (mouse monoclonal, Cell Signaling Technology) and finally, incubation (200µl, 1:2000 in 3% BSA/PBS) with secondary antibody coupled with a fluorescent marker (goat anti-mouse or anti-rabbit IgG [H+L] AlexaFluor 488 green, Invitrogen). Each of the last steps was preceded with washing twice the cells in PBS.

Table 23 Antibodies used for visualisation

1 st - antibodies	2 nd - antibodies
anti-Flag (rabbit, polyclonal)	goat anti-rabbit-Alexa Fluor 488
anti-Flag (mouse, mnclonal)	goat anti-mouse-Alexa Fluor 568
anti-Myc (mouse, monoclonal)	goat anti-mouse-Alexa Fluor 488
	goat anti-mouse-Alexa Fluor 568
anti-HSD17B4 (rat; monoclonal)	mouse anti-rat Cy3

Nucleus staining:

Nuclei were stained with (1:5000) solution of Hoechst 33342 (Molecular Probes Invitrogen, Eugene, Oregon, USA) for 2min at RT as the last step. After twice washing with PBS the coverslips with cells were fixed on glass slides on a drop of Vectashield medium (VectorLabs, Grünberg, Germany) and studied on Axiophot Epifluorescence Microscope (Zeiss, Jena, Germany).

3.8 Enzyme activity measurements

3.8.1 *In vitro* radio-labeled steroid assays for HPLC analysis

Reactions were performed in glass tubes in a final volume 0,5mL of the following assays showed below. All reactions were started with adding the cofactor as the last component and placing the reaction tube in water bath at 37°C. Reactions were stopped by adding 100µl stop solution* and by keeping the sample at room temperature.

*Stop solution: 0.21M ascorbic acid in 1% methanol in acetic acid

Assay for activity of HSD17B3 and HSD17B5:

Reduction of androstenedione to testosterone

sodium phosphate, pH=6,6, 100mM

androstene-3,17-dione (1,2,6,7-³H), 25nM (final concentration)

enzyme: 10µl of bacteria lysate containing recombinant hHSD17B5-GST fusion protein or 300 000 transformed HEK-293 cells over expressing hHSD17B3, clone K2),

DMSO 1% (+/- putative inhibitor 2µM)

NADPH (5mg/ml) prepared freshly

Incubation: at 37°C , time adjusted for 30% conversion in the control sample

Assay for activity of HSD17B1 and HSD17B7:

Methods

Reduction of estrone to estradiol :

sodium phosphate, pH=7,4 , 100mM

estrone (2,4,6,7-³H), 25nM (final concentration)

enzyme (cell pellets),

DMSO 1% (+/- putative inhibitor 2μM),

NADPH 5mg/ml prepared freshly.

Incubation: at 37°C , time adjusted for 30% conversion in the control sample

*Assay for activity of **HSD17B2** and **HSD17B4***

Oxidation of estradiol to estrone

100mM sodium phosphate, pH=7.7

estradiol (6,7-³H), 25nM (final concentration)

enzyme (bacteria cell pellets),

DMSO 1% (+/- putative inhibitor 2μM),

NAD⁺ 5mg/ml prepared freshly.

Incubation: at 37°C time adjusted for 30% conversion in the control sample

3.8.2 *In vitro* substrate specificity screening assays for chosen SDR enzymes:

3.8.2.1 Enzymatic assays with ³H labeled steroid substrates

androstenedione, androstenediol, androsterone, cortisone, corticosterone, cortisol, dihydrotestosterone, dehydroepiandrosterone, estradiol, estrone, hydroxyprogesterone, progesterone, testosterone

100mM sodium phosphate, pH=7,0

25nM of given radio-labeled steroid substrate:

Enzyme: 4 mio of transiently transfected with pcDNA3 HEK293 pelleted cells (control)

4 mio of transiently transfected with pcDNA3_**HSD17B8** HEK293 pelleted cells

4 mio of transiently transfected with pcDNA3_**SDR-O** HEK293 pelleted cells

4 mio of transiently transfected with pcDNA3_**HSDL2** HEK293 pelleted cells

5mg/ml of NAD(P)⁺ or NAD(P)H for oxidation or reduction, respectively, prepared freshly

Incubation: 90min at 37°C

3.8.2.2 Enzymatic assays with retinoid substrates

All-trans-retinal, all-trans-retinol

100mM sodium phosphate, pH=7.4, 1mM EDTA

5µl of retinol or retinal (10µM final conc., dissolved in DMF, Sigma)

Enzyme: 4 mio /6 mio of transiently transfected with pcDNA3 HEK293 pelleted cells (control)

4 mio of transiently transfected with pcDNA3_**HSD17B8** HEK293 pelleted cells

4 mio/6mio of transiently transfected with pcDNA3_**SDR-O** HEK293 pelleted cells

4 mio of transiently transfected with pcDNA3_**HSDL2** HEK293 pelleted cells

Bacteria cell pellets (BL21DE3 pGex) control sample

Bacteria cell pellets (BL21DE3 pGex_SDR-O)

5mg/ml of NAD(P)⁺ or NAD(P)H for oxidation or reduction, respectively, prepared freshly

Incubation: at 37°C, time 15min

Dilution of bacteria cell pellets and time of incubation was adjusted to the lowest background conversion at the control sample. Tested bacteria sample were normalized to the OD₆₀₀ of the control. All procedures were performed with taking care for darkness because of sensitivity to light. After reaction 500µl of H₂O was added, reaction mixture moved into Eppendorfs and centrifuges 10min, 14000 rpm at 4°C.

3.8.3 Extraction of radio-labeled steroids from enzymatic assay for HPLC analysis

After performed reaction the mixture of ³H -labelled steroids was extracted from the assays by use of solid-phase extraction (SPE) columns C18-E (Phenomenex). Mobility of the liquid phase through the solid-phase was induced by vacuum. Columns were previous conditioned with 2x 1ml methanol followed by washing 2x 1ml H₂O. The samples were next applied on columns and in case of in vitro assays followed with 0.5ml of water. Finally, steroids were eluted 2x with 200µl methanol directly into designed for HPLC 1ml vials. So prepared purified samples were directly analysed on HPLC or alternatively, stored at -20°C until use.

3.8.4 Extraction of retinoids from enzymatic assays for HPLC analysis

Retinoids were extracted from reaction assays analogically to steroids on SPE columns (C18-E, Phenomenex) but because of higher hydrophobicity than classical steroids the procedure of extraction was modified:

Conditioning: 1x1ml acetonitrile
 2x 1ml acetonitrile: water (60:40)
 Sample loading: the supernatants from reaction assays
 Washing: 2x 1ml acetonitrile: water (60:40)
 Elution: 2x 200µl acetonitrile: methanol (95:5)

3.8.5 HPLC measurement

³H -labelled steroid substrate and products were separated by use the Reverse Phase High Performance Liquid Chromatography (RP-HPLC). As for reverse phase HPLC the column LUNA 5µm C18 column (Phenomenex) was packed with a polar substance containing C18 carbons in chain and was running by the moderately polar mobile isocratic (H₂O: acetonitrile) phase with a flowrate 1ml/min. In the RP-HPLC more hydrophobic analytes are more attracted to the hydrophobic bounded phase, spend more time associated with bonded phase and are eluted last. For expected highly hydrophobic analytes the retention time was adjusted by regulation the polarity of the mobile phase where higher percentage of acetonitrile or methanol (less polar than water) in water mixture decreased retention time. The parameters of mobile phase for different substrate-product analytes are shown in the **Table 24** below.

Table 24 HPLC parameters of mobile phase for utilized substrate-product analytes

Substrate	Components of the mobile phase	Percentage
Androstenedione	Acetonitrile : water	43:57
Androstanediol	Acetonitrile : water	43:57
Androsterone	Acetonitrile : water	43:57
Corticosterone	Acetonitrile : water	43:57
Cortisol	Acetonitrile : water	43:57

Methods

Cortisone	Acetonitrile : water	43:57
Dihydrotestosterone	Acetonitrile : water	43:57
Dihydroepiandrosterone	Acetonitrile : water	43:57
Estradiol	Acetonitrile : water	43:57
Estrone	Acetonitrile : water	43:57
Hydroxyprogesterone	Acetonitrile : water	43:57
Progesterone	Acetonitrile : water	43:57
Retinol (all-trans)	Acetonitrile : water	92:8
Retinal (all-trans)	Acetonitrile : water	92:8
Testosterone	Acetonitrile : water	43:57

Injection volume was 20µl. The HPLC apparatus was conjugated with scintillation and UV detector. Evaluation and analysis of substrate and product were analysed in chromatogram after integration the peaks controlled by 32Karat software (Beckmann). For radiolabeled analytes detection was proceeded with an on-line liquid scintillate after mixing with scintillator solution (Berhold) (1:1).

Samples containing retinoid substrate/products were analyzed by HPLC (Beckman-Coulter) using a Synergi 4µ Fusion RP18, 150mm x 4.6 mm column (Phenomenex). Retinoids were detected by absorbtion at 345nm and were handled in the dark, to prevent isomerization.

3.8.6 *Ex vivo* inhibitor activity measurements

Human HSD17B5 stable transfected MCF-7 or HEK293 were seeded (1×10^6 or 1.5×10^6 , respectively) on 6-well plates (Falcon) and were cultivated in 2ml of appropriate culture media under humilified conditions. At the confluence 90% just before adding the ^3H -labelled androstene-3,17-dione (6,25 nM) and DMSO(0,1%) +/- inhibitor (2µM) the cells were washed in PBS and the culture medium was changed for one without fetal bovine serum. After 24h incubation with assay ingredients supernatants were collected, radio-labelled substrate and products extracted by use SPE columns and analyzed on HPLC as described above in the procedure for radio-labeled steroid substrates/products.

3.8.7 *In vitro* enzymatic assays based on UV-Vis, fluorescence spectrophotometry.

3.8.7.1 Assay monitoring the oxidative HSD17B5 activity by measuring the changes in NAD(P)H/ NADH absorption or fluorescence:

All assays were developed in 96-well format and measured on reader Safire² at 37°C by use of spectrophotometric plate: transparent or with black walls (Greiner) in case of absorbance or fluorescence, respectively. The final volume was 250µl and contained:

Buffer: 100mM Tris-HCl, pH= 9.0

Enzyme: 2.5 µl of purified 17β-HSD5 (various final concentrations up to 55 µg/per assay)

Cofactor: 200µM NADP⁺

Substrate: various concentrations (5-100µM) of androstanediol in EtOH (1% final concentration)

Substrate control sample with EtOH 1%

Reaction was started with adding enzyme as the last component with multichannel pipette.

Increase in absorbance or fluorescence was observed on-line. Detection was interrupted after the curves reached the saturation.

3.8.7.2 Assays with application of fluorogenic substrate (8-acetyl-2,3,5,6-tetrahydro-1H, 4H-11-oxa-3a-aza-benzo[de]anthracen-10-one) for HSD17B5

Assays were performed on one 96 well plate designed for fluorescence measurements (black walls, transparent bottom, Greiner) in a final volume of 250µl per well and contained:

- 100mM NaPi, pH=6.6
- various concentrations of fluorogenic substrate in EtOH (1%),
- 1% DMSO (+/- putative inhibitor 2µM),
- NADPH prepared freshly (200µM),
- 2.5µl of enzyme (1.25µg/µl purified HSD17B5)

Reaction was started with adding enzyme. The changes in the fluorescence emission $\lambda_{em}=510\text{nm}$ ($\lambda_{exc}=450\text{nm}$) were detected in real-time till the saturation was achieved by use spectrophotometric plate reader (Safire², Tecan).

3.8.8 Enzyme kinetic and inhibition analysis

Conversion of steroid or retinoid substrates into appropriate products measured by use of HPLC method was here expressed in percentage (%) for given enzyme (it's appropriate amount) and time of incubation. All assays were run in duplicate, the mean was reported and further worked out.

3.8.8.1 Calculation of inhibition percentage

Inhibition value was expressed in percentage and it was calculated as a difference between conversion in a control sample with a solvent only instead of inhibitor (set to 100% conversion or 0% inhibition) and a sample with tested inhibitor according to the algorithm:

$$\text{Inhibition (\%)} = 100 - [I]/[C] \times 100$$

[C] mean of conversion in the control sample

[I] mean of conversion in the inhibitor sample

3.8.8.2 Determination of IC₅₀ value for selected inhibitory compounds

IC₅₀ value is such a concentration of inhibitor causing the 50% inhibition of enzyme's activity. In this aim enzymatic assays with various inhibitor concentrations varied between 0.005 and 5μM were performed. Since obtaining of IC₅₀ value requires extrapolation calculations, in this work it was determined by help of "one site saturation" model of the SigmaPlot kinetics module.

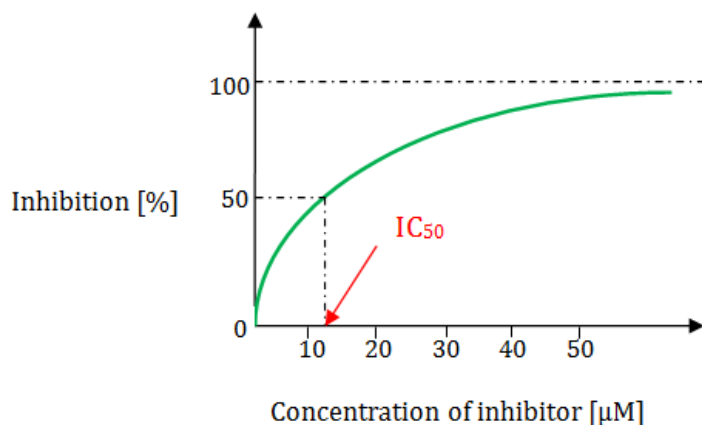


Figure 66 Graphical visualization of IC₅₀ determination.

3.8.8.3 Determination of Michaelis-Menten constants and maximum velocity of substrate conversion.

Michaelis-Menten constants as well maximum velocities of substrate conversion were estimated in this studies in case of being optimized enzymatic assays for purified recombinant HSD17B5 activity with androstanediol or fluorogenic artificial substrate performed in 96-well format. The K_m value allow to show the affinity of the enzyme to the substrate. In practical aspect it allowed to estimate the potent partial loss of enzyme's activity from various aliquots for example after long or not proper storage. In this aim assays of various substrate concentrations ranging usually between 0.2 and 5 magnitude of expected K_m value were set. Similarly to previous IC₅₀ estimation studies the substrate concentration saturation curves were adjusted by help of "one site saturation" model of the SigmaPlot kinetics module.

3.8.8.4 Determination of K_i value and mechanism of inhibition (by use of fluorescence detecting methods)

For determination the K_i as well mechanism of inhibition the set of experiment assays were performed at 37°C in a final volume of 250 µl in one 96 well plate designed for fluorescence measurements (black walls, transparent bottoms, Greiner) and contained: Various concentration (0.01-2 µM in 1% EtOH, final conc.) of the fluorogenic substrate: 8-acetyl-2,3,5,6-tetrahydro-1H, 4H-11-oxa-3a-aza-benzo[de]anthracen-10-one, DMSO with and without inhibitory compound **2-9** in

Methods

increasing concentrations (0.02-2 μ M, 1% DMSO, final conc), freshly prepared NADPH (200 μ M final) and 3.125 μ M of purified recombinant human HSD17B5 in 100mM NaPi buffer, pH=6.6. Reaction was started by simultaneous addition of enzyme. The increase in fluorescence emission at $\lambda_{em}=510\text{nm}$ ($\lambda_{exc}=450\text{nm}$) was detected in real-time until saturation was achieved by use of Safari II plate reader (Tecan). Initial velocities were obtained from linear time curves (at 200-300s of incubation). K_i value were determined using the Sigma Plot "Single Substrate, Single Inhibitor" Kinetics model.

4 Materials

4.1 Used bacteria strains

- JM107 *E.coli* (Stratagene)
- DH5 α *E.coli* (Life Technologies)
- Epicurian Coli $\text{\textcircled{R}}$ BL21DE3-CodonPlus (RP) TM (Stratagene)
- Top 10F One Shot TM (Invitrogen)
- *E.coli* strain provided by RZPD library as host of ordered cDNA (Gene Copoeia, #Ex-T7021-M09)

4.2 Used cell lines

HEK293 , adherent, maintained in DMEM

HeLa, adherent, maintained in MEM

HepG2, adherent, maintained in DMEM

MCF7, adherent, maintained in RPMI

} distributed by DSMZ

MCF7, as well MCF7 and HEK293 cells stable transfected with the human HSD17B5 gene, were kindly provided by Prof. T. Penning , University of Pennsylvania

4.3 Used plasmid vectors

- | | |
|--------------------------------------|-----------------------------|
| pcDNA3 | Invitrogen |
| pGex (2T Δ BamHI) | Amersham and Pharmacia |
| pReceiver-M09 vector (SDR-O) | GeneCopoeia, #Ex-T7021-M09) |
| pCR R 2.1 | Invitrogen |
| pRep10 | Invitrogen |

Vectors used for subcellular localization studies:

- | | |
|-----------------|---|
| pcDsRed2_peroxi | Clontech |
| pcDsRed2_ER | Clontech |
| pcDNA3_CFLAG | pcDNA3 vektor modified by Rebekka Mindnich/Ferdinand Haller |

Materials

pcDNA3_NFLAG	pcDNA3 vektor modified by Rebekka Mindnich/Ferdinand Haller
pcDNA4myc-His Version B	Invitrogen
pAcGFP1-Golgi lighting	Invitrogen

4.4 List of utilized antibodies

Table 25 List of utilized primary antibodies.

<i>Primary antibodies</i>	
Anti-GST	Zymed
Monoclonal mouse anti-Myc	NEB
Polyclonal rabbit IgG anti FLAG	Sigma
monoclonal mouse anti-human HSD17B5	Kind gift of Prof. Trevor Penning, USA
Monoclonal rat anti-human HSD17B4 (SCP2 domain)	E. Kremmer, Helmholtz Zentrum München

Table 26 List of utilized secondary antibodies.

<i>Secondary antibodies</i>	
Goat anti mouse IgG, AlexaFluor488 coupled	Invitrogen
Goat anti mouse IgG, AlexaFluor568 coupled	Invitrogen
Goat anti mouse IgG, HRP coupled	Dianova
Goat anti rabbit IgG, AlexaFluor488 coupled	Invitrogen
Goat anti rat IgG, HRP coupled	Dianova
Goat anti rat IgG, Cy3 coupled	Dianova

4.5 List of used primers (sequences) for PCR methods

Table 27 List of used primers

Name	Sequence 5' - 3'
pGEX <i>for</i>	TCCAGCAAGTATATAGCATGG C
pGex153 <i>rev</i>	GGTTCTGGCAAATATTCT G
pGEX <i>for</i>	GCTGGCAAGCCACGTTTGGTG
pGEX <i>rev</i>	CCGGGAGCTGCATGTGTCAG
pcDNA3 <i>for</i> GCG	GCGGTAGGCGTGTACGGTGGG
pcDNA3 <i>for</i> AGA	AGAGAACCCACTGCTTACTGGCTTAT
pcDNA3 <i>for</i> GTA	GTAACAACTCCGCCCATTTGAC
pcDNA3 <i>rev</i> GGG	GGGCAAACAACAGATGGCTGG C
pcDNA3 <i>rev</i> CTA	CTAGAAGGCACAGTCGAGGCTGAT
h17 β -HSD5 <i>for</i> ATG	ATGGATTCCAAACAGCAGTGTGTAAG
h17 β -HSD5 <i>rev</i> TAA	TTAATATTCATCTGAATATGGATAATTAGG GTG
h17 β -HSD8 <i>for</i>	TTTTGAATTCATGGCGTCTCAGCTCCAGAACCG
h17 β -HSD8 <i>rev</i>	TTTTCTCGAGTTACATGAAAAGACCTCCAGTGA CTCC
h17 β -HSD5 <i>kpn</i>	TTTGGTACCTTAATATTCATCTGAATATGGATAATTAGGGTG
M13 <i>for</i>	GTAAAACGACGGCCAG
M13 <i>rev</i>	CAGGAAACAGCTATGAC
T7 <i>for</i>	AATACGACTCACTATAGGG
T7 <i>rev</i>	AGCTATTTAGGTGACACTATAG
β -actin <i>for</i>	GGATTCCTATGTGGGCGACGAGG
β -actin <i>rev</i>	CACGGAGTACTTGCCTCAGGAGG

Materials

Primers with modified ends for restriction sites* for cloning		Restrict. Enz.
pcDNA3_HSDL2 for	TTTGGATCCATGTTACCCAACACCGGGAG	BamHI
pcDNA3_HSDL2 rev	TTTCTCGAGTCACAGTCTGGCATTTCATCTGATTCAT	XhoI
pGex_N'GST_HSDL2 for	TTTGGATCCTTACCCAACACCGGGAGGCTG	BamHI
pGex_N'GST_HSDL2 rev	TTTCTCGAGTCACAGTCTGGCATTTCATCTGATTCAT	XhoI
pcDNA3_SDR-0 for	TTTGAATTCATGGCGGCCCTCACAGACCTC	EcoRI
pcDNA3_SDR-0 rev	TTTCTCGAGTTAGACTGTCCGCTGGCCT	XhoI
pcDNA3_N'Flag_SDR-0 for	TTTGAATTCCTGGCGGCCCTCACAGACCTCTCATTTA	EcoRI
pcDNA3_N'Flag_SDR-0 rev	TTTCTCGAGTTAGACTGTCCGCTGGCCT	XhoI
pcDNA3_N'Myc_SDR-0 for	TTTGAATTCGCGGCCCTCACAGACCTCTCATTTAT	EcoRI
pcDNA3_N'Myc_SDR-0 rev	TTTCTCGAGTTAGACTGTCCGCTGGCCTTGA	XhoI
pcDNA3_C'Flag_SDR-0 for	TTTGAATTCATGGCGGCCCTCACAGACCTC	EcoRI
pcDNA3_C'Flag_SDR-0 rev	TTTCTCGAGGACTGTCCGCTGGCCTTGG	XhoI
pcDNA4_C'MycHis_SDR-0 for	TTTGAATTCATGGCGGCCCTCACAGACCTC	EcoRI
pcDNA4_C'MycHis_SDR-0 rev	TTCCGCGGACACTGTCCGCTGGC	SacII
pcDNA3_N'Flag_HSDL2 for	TTTGGATCCTTACCCAACACCGGGAGGCTG	BamHI
pcDNA3_N'Flag_HSDL2 rev	TTTCTCGAGTCACAGTCTGGCATTTCATCTGATTCAT-	XhoI
pcDNA3_N'Myc_HSDL2 for	TTTGGCGCGCAATTACCCAACACCGG-3'	NotI
pcDNA3_N'Myc_HSDL2 rev	TTTCTCGAGTCACAGTCTGGCATTTCATCTGATTCATTAGC	XhoI
pcDNA4_C'MycHis_HSDL2 for	TTTGGATCCATGTTACCCAACACCGGGAG	BamHI
pcDNA4_C'MycHis_HSDL2 rev	TTTCCGCGGCAGTCTGGCATTTCATCTG	SacII
pcDNA4_C'MycHis_HSD17B8	TTTCCGCGGCATGAAAAGACCTCCAGTGAC	SacII

Materials

pcDNA3_N'Flag_HSD17B8	TTT GAATT CTGGCGTCTCAGCTCCAGAACC	EcoRI
pcDNA3_C'Flag_HSD17B8	TTT CTGAG CATGAAAAGACCTCCAGTGA CTTC	XhoI

4.6 List of used ³H-labeled substances

Androst-4-ene-3,17-dione (1, 2, 6, 7-³H (N))

Estrone (2, 4, 6, 7-³H (N))

Estradiol (6, 7-³H (N))

Testosterone (1, 2-³H (N))

Corticosterone (1,2-³H)

Cortisol (1,2,6,7-³H)

Androsterone (9,11-³H)

Dihydrotestosterone (1,2,4,5,6,7-³H)

Progesterone (1,2,6,7-³H)

20_hydroxy progesterone (1,2-³H)

NEN Life Science Products

4.7 List of utilized enzymes

Endonuclease (Benzonase)

Lysozyme

Herkulase Horstart Polymerase

KOD HiFi DNA Polymerase

Pfu Turbo DNA polimerase

Restriction endonucleases

Taq-DNA Polimerase

T4-DNA Ligase

Trypsin

Sigma Aldrich GmbH

Merck

Stratagene

Novagen

Stratagene

MBI Fermentas or NEB

MBI Fermentas

MBI Fermentas

Gibco

4.8 Kits

DyeEx or DyeEX96

MicroSpin™ S-200 HR columns

QIAGEN

GE Healthcare

Materials

Nucleobond PC 100 Kit	MACHERY & NAGEL
NucleoSpin Plasmid Kit	MACHERY & NAGEL
QuikChange	Stratagene
QIAquick Gel Extraction Kit	QIAGEN
QIAquick PCR Purification Kit	QIAGEN
TOPO TA Cloning Kit	Invitrogen
RNasy Midi Kit	QIAGEN
RNasy Mini Kit	QIAGEN
RevertAid™ First Strand cDNA Synthesis Kit	Fermentas
Strata C18-E columns	Phenomenex
SV Total RNA Isolation Kit	Promega
Wizard SV Gel and PCR Clean-Up System	Promega
Organelle lights Endosomes-GFP	Invitrogen
MTT	Roche
Caspase Glo™ 3/7 Assay	Promega
CellTiter-Glo™ Luminescent Cell Viability Assay	Promega

4.9 Solutions for cell staining

DAPI	Invitrogen
ER-Tracker Blue-White DPX	Invitrogen
Hoechst33342	Invitrogen
MitotrackerOrange	Invitrogen
AlexaFluor350 or 568	Invitrogen
Vectashield	Vectalabs

4.10 Chemicals, supplements, media

Acrylamide/Bisacrylamide (30%/0.8%)	Roth
Agarose	Biozym
Ammonium peroxodisulphate (APS)	Biozym
Ampicillin	Fluka
Ampuwa water	Frasenius
Androstanediol	Sigma

Materials

Androstenedione,	Sigma
Androsterone	Sigma
Bacto - Agar	Difco
Bacto-Tryptone	Difco
BSA (Bovine Serum albumin)	NEB
Chloramphenicol	Sigma
Coomassie blue G250	Biomol
Diaminobenzidine (DAB)	Biomol
Dimethylsulfoxide (DMSO)	Sigma
DMEM	Invitrogen
dNTPs	Fermentas
Ethanol	Merck
Ethidium bromide	Sigma
Ethylendiamintetraacetate (EDTA)	Biomol
FBS	Biochrom
FluoroTrans W Membrane (PVDF)	Pall
Formaldehyde, 37%	Roth
FuGene6	Roche
Glucose	Merck
L-Glutamine	Invitrogen
Imidazol	Sigma
Isopropylthiogalaktosid (IPTG)	Fermentas
Kanamycin	Sigma
Markers 3 and 8	Fermentas
6x Loading Dye	Fermentas
Mangan chloride (tetrahydrate)	Sigma
Magnesium hexahydrate	Merck
MEM	Invitrogen
NAD, NADP, NADH, NADPH	Fluka
Parafilm	American National Can
Penicillin/Streptomycin	Invitrogen
Potassium chloride	Merck
Potassium hydrogen phosphate	Merck

Materials

Potassium acetate	Merck
2-Propanol	Merck
Ready Flow III	Beckman
Retinal	Sigma
Retinol	Sigma
Reverse phase LUNA 5u C18 (2) column	Phenomenex
RPMI	PAA
Sodiumacetat	Merck
Sodium chloride	Merck
Sodium dodecylsulfat (SDS)	Serva
Sodium hydrogenphosphate monohydrate	Merck
Sodium hydroxide	Merck
TEMED	Sigma
Tris base	Merck
Triton-X100	Merck
TRIzol	Invitrogen
Trypsin/EDTA	Invitrogen
Tween-20	Merck
Yeast extract	Difco

4.11 Bioinformatic tools, software

Sequencing Analysis Software 5.1	Applied Biosystems
Sigma Plot (version 2002, Windows 8.02)	Systat Software GmbH
Vector NTI	Invitrogen
BLAST –programms: blastp, psi-blast	http://ncbi.nlm.nih.gov/BLAST
ClustalW	http://www.ebi.ac.uk/Tools/msa/clustalw2
ProDom	http://prodom.prabi.fr/
VisionCapt	Vilber Lourmat
XFluor4	Tecan
Secondary structure analysis	http://zeus.es.nl

4.12 Laboratory equipment

Materials

Axiophot	Zeiss
Cell counting camera	Rosental or Neubauer
Centrifuge Avanti J-20	Beckman
Hettih Universal 32R, 3730 DNA-Analyzer	Eppendorf 5415
BioVision gel documentation	Applied Biosystems
HPLC system assembly "32Karat Gold"	PeqLab
Robo-Cycler 96	Beckman
Mini-PROTEAN II - vertical electrophoresis cell	Stratagene
Trans-Blot SD - Semidry Transfer Cell	BioRad
HPLC radioactivity monitor LB 506D	BioRad
pH Meter 766 calimetric	Berthold
Thermomixer comfort	Knick
Trans-Blot SD - Semidry Transfer Cell	Eppendorf
Vortexer	BIO-RAD
Micropipettes , multichannel micropipettes	Scientific Industries Vortex Genie
GENios Pro	Gilson
Safire ² Microplate Reader	Tecan
Incubators	Tecan
Incubation shaker Innova 4230	Haereus Instruments
NoanoDrop ND-1000 Spectrophotometer	New Brunswick Scientific
Life Science UV/Vis Spectrophotometer	NanoDrop Technologies
	Beckman

5 Discussion

5.1 Inhibitor studies

In this part of my PhD study I was working experimentally with selected chemicals previously identified in theoretical studies as potent inhibitors of human 17β -HSD enzymes type 3 and 5. For this purpose the chosen substances were purchased from commercial chemical laboratories. Next, the potent inhibitors were subjected to enzymatic assays in order to screen their inhibitory activity against studied enzymes. The initial screening assays contained human recombinant 17β -HSD3 or 17β -HSD5, respectively and they catalyzed the reduction of androstenedione to testosterone in the presence of NADPH as cofactor. Finally, two screening rounds with two batches of compounds allowed identification new inhibitors and selection the most effective ones for further biological analyses. 11 of 35 screened substances initially identified as 17β -HSD3 or 17β -HSD5 inhibitors were further checked for selectivity among other hydroxysteroid dehydrogenases and the IC_{50} values were estimated for four of them (**2-9**, **2-12**, **1-12**, and **2-1**) exhibiting the highest inhibitory activity. For the strongest one: the substance **2-9** the K_i value and the mechanism of inhibition was estimated. Next, its inhibitory potency expressed as IC_{50} value and potential toxicity were further validated *ex vivo* in living human cells.

5.1.1.1 Composition of the enzymatic assay for new inhibitor screening.

- *In vitro enzymatic assays as priority*

For initial inhibitor screening as well for further kinetic evaluations with chosen inhibitory compounds *in vitro* enzymatic assays were employed. The use of *in vitro* tests at early steps of new inhibitors as potent drugs development has some obvious rationales and usually precedes efficacy and toxicity studies with more complex systems such as living cells or organisms. Comparing to *in vivo* tests the main advantage of *in vitro* assays apart of lower costs and very often experiment duration is the facilitated ability to control the assay variable such as enzyme, substrates or inhibitor concentrations what is crucial at preliminary efficacy and kinetic studies. Besides, they enable to research the essential enzymatic reaction of the interest with reduced influences from other cellular components and potent unpredictable side effects are minimized.

Discussion

- *The form of applied enzyme in assay.*

Depending on the assay purposes the enzyme can be added to the probe in various forms for example as cell pellets, extracts or homogenates from living cells containing the over-expressed protein and also as purified enzyme molecules dissolved in water solution. The use of more simple in components assay as well more pure form of the enzyme logically may significantly minimize undesirable impacts on the catalyzed reaction and sometimes may be crucial by using some measurement methods of enzymatic activity such as UV-Vis or fluorescence spectrometry. Therefore, one of the aspirations was the achievement of all studied here targeted for inhibitor studies recombinant enzymes in the purified form.

Relatively cheap and high yield of recombinant protein production suited for further purification are provided by commercially available bacteria expression systems. In this way all planned to use in the project enzymes were alternatively cloned into pGex vector and expressed after induction with IPTG in *E.coli* BL21DE3 bacteria strain as GST fusion proteins enabling the quick isolation from lysed bacteria cells by use of glutation sepharose. Nevertheless, it should be taken into account that using the purified enzyme can be charged with the risk of the loss of enzymatic activity during the purification process. Additionally, the production of mammalian enzyme proteins in prokaryotic expression system sometimes has a negative influence on the expected enzymatic activity due to absence of post-translational events specific for eukaryotic cells. Concerning only the purification process sometimes the necessity to challenge the low solubility of the protein for better harvest can occur.

- *Form of applied enzyme at inhibitor screening assay*

Trials with cloning human HSD17B3 gene into bacteria expression vector as fusion with GST tag for eventual purification resulted in production of inactive enzyme in bacteria. Thereby 17 β -HSD3 was expressed in HEK293 cells from mammalian expression pcDNA3 vector which in turn showed high enzymatic activity by conversion of androstenedione to testosterone at assays with cell pellets. Stable transfected cells were in this purpose generated and the clones exhibiting the highest activity towards androstenedione selected. Finally, *in vitro* assays checking out the influence of screened potent inhibitory compounds on activity of 17 β -HSD3 contained stable transfected HEK293 cell pellets at the amount of only 300 000 cells per probe. Reason for production of inactive 17 β -HSD3 enzyme by bacteria remains unknown but one can suppose that it may be caused by improper folding and lack of some post-translational modifications usually required for mammalian proteins.

Discussion

Instead, for inhibitor screen towards HSD17B5 the functionally active forms of enzyme from either bacteria or mammalian expression systems were available. Preliminary activity tests revealed that the best yield of conversion to testosterone (assays with androstenedione and NADPH as substrates) was observed in case of homogenized bacteria lysates containing recombinant HSD17B5 with GST fusion tag. Nevertheless, further purification steps resulted in gradual loss of the activity. What is more, later enzymatic tests with assays which contained cell pellets of both transiently or stable transfected HEK293 and MCF7 cell lines producing human HSD17B5 showed very low activity incomparable to that of HSD17B3 stable expressing HEK293 cells. Therefore bacteria homogenate were used for initial inhibitor tests with HSD17B5 since the criterion of conversion efficacy had a priority.

- *Inhibitor concentration in screening assay*

Usually at high throughput inhibitor screening assays the conventional one or few concentrations of tested compounds is established. In the present inhibitor screening assay the working concentration of 2 μ M for each of tested compounds dissolved in DMSO (1% final concentration) was set up. Basing on the literature at the first part of the study for theoretical validation of pharmacophore models all utilized for research and described in literature 17 β -HSD3 and 17 β -HSD5 inhibitors were grouped into activity classes. Whereas inhibitors showing IC₅₀ or K_i values no more as >10 μ M were regarded as active inhibitors, 10 μ M >50 μ M as medium active, >50 μ M was not active [153]. Although the most demanded and usually considered as highly active inhibitors are substances able to inhibit the enzyme in the Nano molar range. Chemicals showing at least 50% of inhibition at 2 μ M fixed concentration according to the evaluations above would be then a good inhibitor and so set in concentration assures relatively random selection.

5.1.1.2 Choice of the method for measurement the enzymatic activity.

The screening of potent inhibitors as well many further enzymatic tests were performed here by use of assays with radio-labeled substrates followed by separation techniques suited for radioactivity detection. The measurement of enzymatic activity in this method is based on analysis of so called 'end-point' assays (or discontinuous assay) where the reaction is stopped during catalysis in the determined period of time. In case of inhibitor screening assay the time of incubation was optimized for approximately 30% of conversion and was 10 min. Finally, after

Discussion

isolation from reaction mixture by use of reverse phase columns, separation by HPLC and scintillation detection the amount of radioactively signed substrate/product was calculated.

One of the premises that facilitated the choice of exactly this method was the fact that laboratory where the project was realized offers well established protocols for enzymatic assays using radio-labeled steroids as well techniques for their separation and detection optimized especially for measuring the activity of steroid metabolizing enzymes such as hydroxysteroid dehydrogenases. Therefore, for initial inhibitory screening against human 17β -HSD3 and 17β -HSD5 this measurement method was chosen as the first choice.

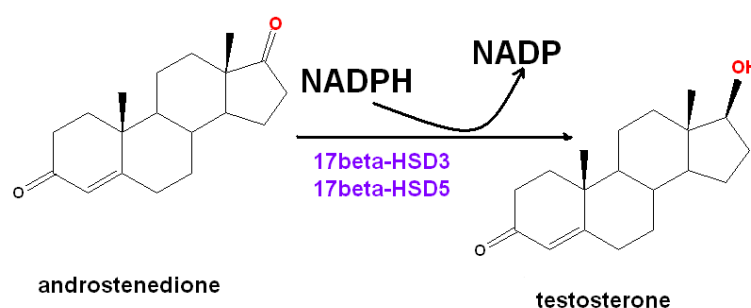


Figure 67 Reduction of androstendione to testosterone by human 17β -HSD3 and 17β -HSD5.

Generally, assays with radio-labeled components are often used in laboratories due to their some unbeatable advantages which are: high sensitivity, precision of the measurement, freedom from environmental influences on detected probe like temperature, pH and ion strength etc. as well no background effect from reagents or not analyzed ingredients of the assay. Concerning the application in enzymatic studies the use of radioactively signed substrates is attractive due to its high sensitivity and possibility for direct detection the labeled product of reaction. This method can be useful in studies where the criterion of sensitivity has a priority for instance in qualitative tests with enzymes of not quite determined activity. In this way the radioactive assays were applied for initial steroid substrate screening with newly identified SDR proteins in the second part of this PhD project. Further, in order to compare how sensitive is this method it can serve as example the problem which arose during optimization the assay with purified 17β -HSD5 for spectroscopic detection of changes in cofactor's concentration. Whereas by radioactive assays the weak activity of the enzyme was well detected at oxidation of androstanediol to androsterone even at the presence

Discussion

of NAD⁺ as cofactor (over 30% conversion after 1h incubation), by spectroscopic (fluorescence) measurement which detected the changes in amounts of the cofactor there was difficult to estimate any enzymatic activity although the similar condition of reaction were provided even if cofactor was then NADP⁺ for which the enzyme have more affinity (chapter 5.1.1.3, **Figure 71**). Therefore all new aliquots of enzymes used in this study were previously subjected to the activity test using this well-established method.

However, in spite of all merits the obvious disadvantage of assays with radiolabeled substrates is the use of radioactive material itself. Because the work with radioactive isotopes is inevitable associated with health hazard it entails special handling and disposal that is not indifferent to the time and costs of planned experiment and thus the throughputs is limited. Among other alternative methods performed in our laboratory for measuring the enzymatic activity in assays with steroid substrates that avoid the use of radioactive material are GC-MS and TLC. But, they are rather tedious in preparation and do not possess a throughput similar to the HPLC method which allowed analyze in one experiment around 30-40 probes. However, in order to challenge the better throughput of the assay additional efforts for development of assays basing on UV-Vis or fluorescence spectroscopy were further made.

5.1.1.3 In search for alternative, high throughput and non-radioactive enzymatic assay for inhibitor studies. Development of assays based on UV-Vis, fluorescence detection.

UV-Vis or fluorescence spectroscopy which utilizes the physicochemical properties of substances when interacted with monochromatic rays of ultraviolet-visible light spectrum is commonly employed as a tool for measuring the enzymatic activity. Present advanced instrumental concepts of spectrometric techniques enable among others the quantitative measurements of the assayed probe during incubation at low time intervals what enables performing of continuous assays. Additionally, by use of specialized microplate reader system the detection may be performed on multi-well plates (Safire², Tecan). Sampling on 96-well plates provides many practical advantages such as lower use of material and ability to simultaneous measurement of many probes or their repeats at the same environmental conditions what has a pivotal meaning for the value and reliability of the experiment. Additionally, performing of enzymatic assays in 96-well format can be automated when combined with specialized devices for sample preparation (liquid handling

Discussion

robots) what increases the throughput and minimizes the error of precision by pipetting that can appear when assay components are dosed manually. The proper (meniscus effect) and equal volume of assay dosing onto wells is especially important by spectrometric OD measurements since the light path is vertical. By searching for higher throughput of measuring the enzymatic activity in planned more detailed kinetic studies with inhibitors mentioned above practical aspects prompted the concern about development of assays based on UV-Vis, fluorescence detection. The choice of this method seems to be rational especially since SDR/17 β -HSD enzymes are NAD(P)/NAD(P)H dependent and by use of absorbance or fluorescence spectroscopy the changes in NAD(P)H during reaction can be directly monitored. Theoretically, in further perspective the effort could be also concerned on development of a universal enzymatic assay that would be quickly optimized and applied also for more SDR/HSD enzymes which utilize steroids as substrate.

UV-Vis or fluorescence detection of changes in cofactor concentrations.

By employing this method the measurement is based on properties of NAD(P)H which absorbs the light at $\lambda = 340\text{nm}$ or emits the fluorescence ($\lambda_{\text{em}}=450\text{nm}$ at $\lambda_{\text{exc}}= 340\text{nm}$) while the oxidized form NAD(P)⁺ does not. Concerning the stoichiometry of catalyzed by SDR enzymes reaction the mole ratio of substrate and utilized cofactor is 1:1. Therefore depending from reaction direction directly tracked changes in amount of NAD(P)H in the course of enzymatic process can be read as substrate depletion or increase of catalysis product, respectively.

In the frame of inhibitor studies the efforts to develop the alternative non-radioactive enzymatic assay with recombinant human 17 β -HSD5 were next made since the purified form of this enzyme was available. Additionally, few effective inhibitory compounds with selective inhibitory activity against 17 β -HSD5 over 17 β -HSD3 were selected and ready for further analysis.

First assay optimization trials with use of 96-well plates were performed on example of oxidative activity of the enzyme at androstenediol conversion into testosterone where the growing cofactor concentration (NADPH) during catalysis is directly monitored [**Fig. 71**].

Discussion

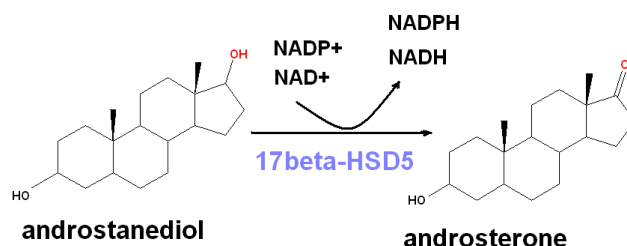


Figure 68 Catalyzed by human 17 β -HSD5 oxidation of 3 α -androstenediol to androsterone. NADP(H) is more preferable cofactor than NAD(H) for 17 β -HSD5. However by use of sensitive measurement methods the conversion by use of NAD(H) may be also detected.

Due to relatively low velocity of catalyzed reaction more sensitive detection of fluorescence was preferred to absorption (OD_{340}) measurement since the obtained in this way substrate concentration dependent time progress curves were more coherent and linear. Unfortunately, up to now being optimized assays appeared to have too low velocity and too high K_m in order to be effectively utilized by UV-Vis or fluorescence spectrometry methods of cofactor detection at available concentrations of the purified enzyme. Assay enabling estimation of Michealis-Menten parameters such as K_m or V_{max} was performed by as much as 55 μ g of the enzyme in probe. Similarly, low velocity of catalyzed reaction that forces longer time of incubation in order to observe a sufficient linear signal at time progress plots as well restricted amounts of available to use enzyme aliquots made it also difficult to optimize the reductive activity of HSD17B5 by conversion of androstenedione to testosterone. Additionally, the effect of spontaneous oxidation of the cofactor interfered with observed depletion of cofactor in probes with various concentration of substrate. In case of 17 β -HSD5 as well as in many other steroid hormones metabolizing enzymes the effect of inhibition by product of catalysis can have also an influence. Therefore next efforts were focused on searching for alternative and fast enzymatic assay utilizing fluorimetric methods which directly detect the product of catalysis.

Summarizing, the spectrophotometric methods utilized and tested in this study are rather restricted to high active enzymes (low K_m /high V_{max}) in order to be applied for high throughput kinetic measurements with studied enzymes. But even in the case of reactions with lower rate of catalysis the assay can be optimized for efficient measurement by increasing the amount of the enzyme in the probe that of course raises the costs in use of material. The problem can be partially challenged by improvement of purification efficacy or use of extra techniques increasing the

Discussion

enzyme concentration. However, in this way the use of fluorescence method in case of 17 β -HSD5 would be a certain compromise between better throughput and costs.

- **Fluorimetric measurements**

A novel substrate: 8-acetyl-2,3,5,6-tetrahydro-1H,4H-11-oxa-3a-aza-benzo[de]anthracen-10-one (the commercial name: B10720841) specific for human 17 β -HSD5 that on reduction becomes a fluorescing product was published by Dominic J. Yee *et al.* [148] [Figure 69]. The structure of this specific fluorogenic substrate is based on so called “push pull” structural feature wherein the electron-donating and electron-withdrawing groups are electronically connected via an extended π -conjugated system. The ketone carbonyl group is a part of this system. Reduction of the carbonyl group to an alcohol convert an electron withdrawing group, resulting in a profound electronic change of the system, which in turn lead to a change in the emission profile. Enzymatic reductive activity can be followed by increase of fluorescence at 510 nm at excitation of 450 nm.

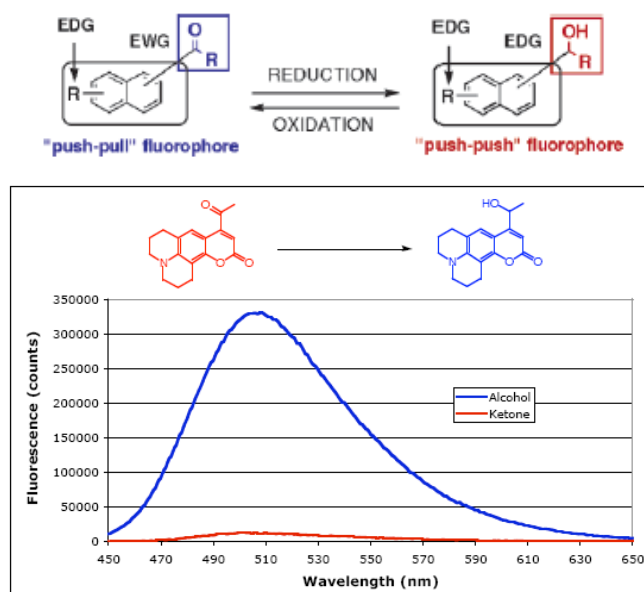


Figure 69 The keto-form of the substrate **8-acetyl-2,3,5,6-tetrahydro-1H,4H-11-oxa-3a-aza-benzo[de]anthracen-10-one** is effectively reduced by 17 β -HSD5 in the presence of NADPH as cofactor to its hydroxy-form that gives a fluorescence signal with a maximum at $\lambda=510\text{nm}$ when excited at $\lambda=450\text{nm}$ (Figure adapted from [148]).

The reaction depends on NADPH as cofactor and is very fast and efficient. It allow for using smaller amount of substrate and enzyme (even less than 1 μg /per assay) in comparison to the oxidative assays for fluorescent measurements with androstanediol. Therefore it was the first choice of a fast

Discussion

enzymatic assay for testing the reductive activity of 17 β -HSD5. Moreover the mentioned fluorogenic substrate theoretically can be applied in either *in vitro* and *in situ* assays with living cells. However the latter need to work out the problem of sterility during the measuring and optimization of cell medium (without Phenol red) compatible with fluorescence measurement.

General remarks for optimization of spectrophotometric detection methods:

- purified form of target enzyme should be the first choice in high throughput enzymatic assays with inhibitors by use of spectrophotometric detection methods
- spectrum of assay ingredients may not interfere with NAD(P)H or other monitored product. Therefore the method cannot be applied for big scale screening of unknown compounds screening as potent inhibitors or requires previous control measurements excluding the potent interferences. However the method can be used for further detailed kinetic analysis with previously checked chosen inhibitors
- product of reaction should not inhibit reaction, especially in case of low efficient assays

5.1.1.4 IC₅₀ and K_i as values describing the inhibitor potency.

The both values are frequently reported in the literature and serve to assess inhibitor's potency against target enzyme or to compare it among others. IC₅₀ is defined as such a concentration of an inhibitor that causes 50% of inhibitory effect *in vitro*. Thus in order to determine this value conversion of inhibition magnitude into percentage was performed. In the present study the observed inhibitory effect on enzymatic activity was normalized from 0% to 100% of inhibition where 0% stands for blank control probes without inhibitors and 100% means observed no enzymatic activity due to inhibition. IC₅₀ can be then derived (by support of curve fitting programs) from dose dependent plots for given inhibitor at constant concentration of the substrate. In the frame of the present project IC₅₀ was determined for four the strongest inhibitors against HSD17B5 selected from two screening rounds. Further, by comparing IC₅₀ values the selectivity among other hydroxysteroid dehydrogenase was estimated.

Discussion

Table 28 List of selected the best inhibitory compounds against activity of 17 β -HSD5 from two screening rounds (results from repeated experiments).

compound	IC ₅₀ (μ M)
BNW 1-12	1.04 \pm 0.12
BNW 2-1	1.21 \pm 0.05
BNW 2-9	0.29 \pm 0.03
BNW 2-12	1.26 \pm 0.18

Nevertheless, although IC₅₀ allow quick assessment and comparing of inhibitor's potency among tested chemicals it should be taken into account that it is not an absolute value characterizing the inhibitor and depends strictly from assay conditions in which the experiment was conducted. For example the factors affecting the magnitude of IC₅₀ are concentration of the substrate and enzyme or incubation time along many other experimental conditions. Thus, reported in the literature IC₅₀ values for given enzyme's inhibitor may slightly vary. Discrepancies of observed IC₅₀ depending from kind of the applied assay will be discussed later. Another routinely determined at inhibitor studies entity is inhibition constant K_i. Contrary to IC₅₀, K_i is more intrinsic value characterizing the inhibitors potency and it is defined as dissociation constant between inhibitor and enzyme-inhibitor complex. Because K_i is a constant value thus independent from assay conditions and it depends on properties of studied enzyme and inhibitor only. However, in order to derive reliable K_i the knowledge about mechanism of inhibition is required. It follows a need to perform more complex experiment such as dose-response analysis of inhibitor's activity in assays for growing concentrations of substrate. Regarding this K_i was estimated in this study only for one of the best selected inhibitor by use of optimized assays with artificial fluorogenic substrate monitoring the reductive activity of 17 β -HSD5. Determined mechanism of inhibition in the case of compound **2-9** indicated competitive pattern of action therefore the relationship between IC₅₀ and K_i may be expressed by use of Cheng Prusoff equation. The equation allows derive K_i from IC₅₀ value and can be applied only for competitive inhibitors:

$$K_i = \frac{IC_{50}}{\frac{[S]}{1 + K_m}}$$

if $[S] = K_m$, $K_i = IC_{50}/2$

if $[S] \gg K_m$, $K_i \ll IC_{50}$

if $[S] \ll K_m$, $K_i \sim IC_{50}$

(Cheng Y, Prusoff W.H., *Biochem Pharmacol.* 22: 3099-3108, 1973) [154]

Additionally, it demonstrates that depending from concentration of the substrate at which the IC_{50} is estimated the value of K_i can respectively vary from IC_{50} in regards how far from K_m it is set up. Calculated K_i value for the compound **2-9** came to $0.18\mu\text{M}$. In the same assay determined the Michaelis-Menten constant K_m for fluorogenic substrate was $1.1\mu\text{M}$.

5.1.1.5 Inhibition mechanism for compound 2-9. Can the use of an artificial fluorescence substrate affect the results?

As was mentioned above kinetic analysis aimed at K_i estimation was performed by use of assay utilizing the fluorescent substrate and purified 17β -HSD5 enzyme. Kinetic experiments with artificial substrate showed that compound 2-9 was able to inhibit the reductive activity of 17β -HSD5 in the classical competitive way and the K_i value has been determined. Human 17β -HSD5 is a multi-specific enzyme acting as aldo-keto reductase able to metabolize wide spectrum of substrates. Regarding the present inhibitor studies in the context of unusual multispecificity of the target enzyme few questions should be raised. Is the tested inhibitory compound metabolized by the enzyme for instance as competitive substrate and how does it implicate the efficacy of inhibitor's activity or its future utilization as a potent drug? Further, how does application of 17β -HSD5 enzymatic assay with various substrates affect the results of inhibitor studies like mechanism of inhibition? Or, is it possible that performing of inhibitor analysis by use of artificial substrate give distinct results from assays with physiological substrates? If tested inhibitory candidate should be used in future as a drug the two former questions have substantiation and can be verified by use of

Discussion

ex vivo/in vivo efficacy or toxicological tests. In turns, two latter seem to be worth of interest in respect of reported studies on crystal structure of HSD17B5 and its mechanism of catalysis.

Byrns *et al* 2007 [135] studying the inhibitory potency of indomethacin analogs towards human 17 β -HSD5 noticed that the pattern of inhibition (competitive or uncompetitive) as well K_i value can be various even for the same analyzed inhibitor depending from what kind of substrate was tested. In cited example the enzymatic assays testing the reduction of Δ^4 -androstane-3,17-dione with indomethacin as well its analogs inhibited the reductive activity of 17 β -HSD5 in competitive way while reductive assays with more catalytically efficient substrate such as 9,10-Phenanthrenequinone (PQ) exhibited uncompetitive mode of action. Next, basing on the analysis of enzyme- ligand interactions of few available 3D -crystal structures of human 17 β -HSD5 as well on observed kinetic with various substrates they have deduced the ordered bi bi mechanism of catalysis by 17 β -HSD5 [Figure 70]. In the proposed model the cofactor is binding first to the enzyme prior the substrate and after catalysis the product is expelled followed by cofactor release as the last. This prediction of the catalytic mechanism were supported by the analysis of 3D-crystal structure with cofactor (NAD⁺) and Δ^4 -androstane-3,17-dione or testosterone as ligands. The authors revealed also that the ligand binding pocket, where the active center of the enzyme is located, has a shape of elliptic cavity formed by hydrophobic amino acid residues with a narrow entry. The cofactor binding site is located deep inside the enzyme in the bottom of this cavity, while the substrate binding pocket is much closer to the protein surface. Additionally, there was observed that the cavity together with its entry may change its shape and volume after the catalysis and can flexibly accommodate to different ligand structures. These facts may elucidate the sequence of cofactor and substrate/product binding and release as well the multi-specificity of the enzyme. Additionally, assuming that the given inhibitor is binding to the ligand binding pocket the model predict a possibility of various affinity of inhibitory compound to either the complex of enzyme with oxidized or reduced cofactor and thus implications in observed mode of inhibition mechanism.

Discussion

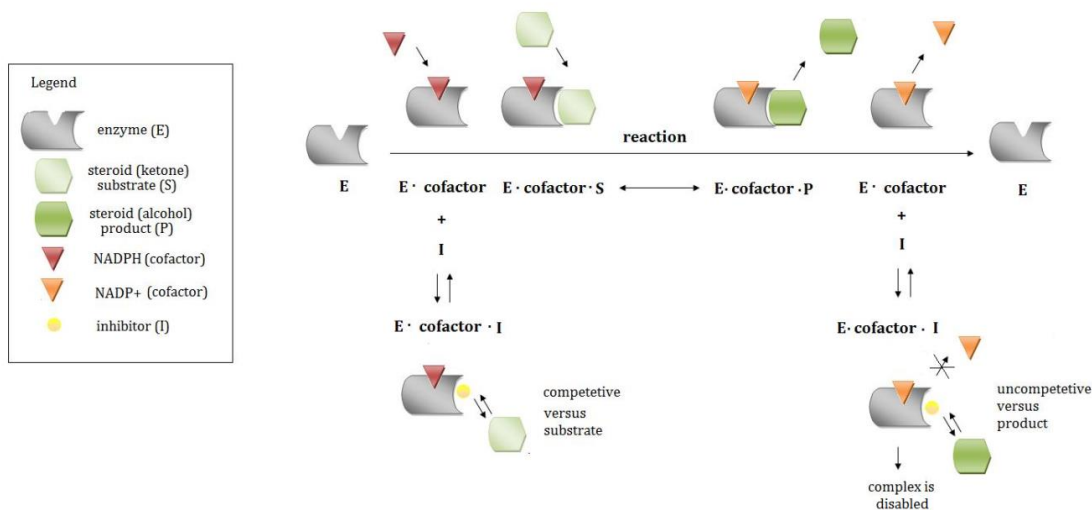


Figure 70 Mechanism of catalysis by 17 β -HSD5. Picture modified on base of the scheme *Byrns et al* [135].

Returning back to the cited example with indomethacin as inhibitor the deduced order of ligand binding to HSD17B5 during catalysis elucidates the observed differences in inhibition mode in the reductive reaction with use of substrates of different catalytic efficiency such as relatively weak Δ^4 -androstane-3,17-dione and strong 9,10-phenanthrenequinone [Table 29]. Because indomethacin probably exhibits more affinity to the complex of enzyme with oxidized cofactor NADP⁺ than with NADPH in assays where the reduction of 9,10-phenanthrenequinone was catalyzed the releasing of inhibitor from NADP⁺ complex was likely a rate limiting step resulting in uncompetitive mode of inhibition while in reductive assays with less efficient Δ^4 -androstane-3,17-dione this step did not affect the rate of catalysis and thus competitive mechanism of inhibition was observed.

Simultaneously, the competitive inhibition by indomethacin was reported in oxidative reaction catalyzed by 17 β -HSD5 with testosterone as a substrate and it supports the deduced sequence model.

Table 29 Physiological and artificial human 17 β -HSD5 substrates of various affinity to the enzyme

Substrate	direction	type of activity	Product	K _m (μ M)	Ref
PGH ₂	reduction	PG 11-ketoreductase	PGF _{2α}		
PGD ₂	reduction	PG 11-ketoreductase	PGF _{2α}	0.6	
9,10-Phenanthrenequinone (PQ)	reduction			1.5	[155]

Discussion

1-acenaphthenol	oxidation				
5 α -dihydrotestosterone (5 α -DHT)	reduction	3 α -HSD activity	5 α -androstane-3 α , 17 β -diol	19.8; 26.2	[136] [156]
Δ^4 -androstane-3,17-dione	reduction	17 β -HSD activity	testosterone	8.96	[136]
5 α -androstane-3,17-dione	reduction	17 β -HSD activity	5 α -dihydrotestosterone (5 α -DHT)		
progesterone	reduction	20 α -HSD activity	20 α -hydroxyprogesterone		
estrone	reduction	17 β -HSD activity	17 β -estradiol		
5 α -androstane-3,17-dione	oxidation	3 α -HSD activity	androsterone		
3 α -androstanediol	oxidation			19.1	[156]
5 α -androstane-3 α , 17 β -diol	oxidation		Δ^4 -androstane-3,17-dione	27.2	[136]
Solvay substrate	reduction				
NADH				0.0071	
NADPH					

Regarding the conclusions above in context of the present results of kinetic analysis with selected inhibitory candidate it can be supposed that the compound **2-9** competes with a fluorescent substrate in a classical way for a ligand binding site of the enzyme rather than for a cofactor binding region. Similarly, the compound **2-9** as an inhibitor probably exhibits more affinity to the enzyme complex with NADPH than with NADP⁺, since the reductive activity of 17 β -HSD5 exhibiting competitive mode if inhibition was tested. However in order to confirm and verify the latter postulation the inhibitor studies with reverse reaction for example such an oxidation of androstanediol to androsterone at the presence of NADP⁺ should be performed or determination and further comparing of K_i achieved by use of assays with Δ^4 -androstane-3,17-dione since the applied in this study fluorescent substrate was reported as 10 times more efficient than more likely physiological substrates of 17 β -HSD5 such as 5 α -DHT.

5.1.1.6 Evaluation of inhibitor potency in living cells cultures. Comparison of IC₅₀ values depending on kind of enzymatic assay.

The inhibitory potency of the most active compound BNW 2-9 was further checked in assay with living cells. Two different human cell lines MCF7 and HEK293 stably expressing human HSD17B5

Discussion

were employed for *ex vivo* studies with inhibitor. Primarily HEK293 cell line was chosen as a model for verifying the inhibitory potency against 17 β -HSD5 at *ex vivo* conditions since stable transfected with human HSD17B3 gene HEK293 cells produced high yield of androstenedione conversion into testosterone and thus the assays for both target in this study enzymes: 17 β -HSD5 and 17 β -HSD3 would be comparative. But, because of unknown reasons by use of either transiently or stably transfected with human HSD17B5 gene HEK293 cells I could not achieve the similar level of androstenedione conversion as in case of 17 β -HSD3 assays. Stable transfected with human HSD17B5 MCF7 cells appeared to be 2,5 time more efficient. Therefore they were further chosen apart of HEK293 cell lines for studies with inhibitor. Application of two different cell lines has also another advantage because allow observing potent cell dependent inhibitory effect.

In order to further evaluate the potency of chosen inhibitor MCF7 and HEK293 cells stably expressing human HSD17B5 were incubated with radioactively labeled substrate androstenedione in the presence of increasing concentrations of compound BNW 2-9. IC₅₀ values were estimated and compared. To eliminate the effect of serum steroids as well unspecific binding incubation with inhibitor was performed in serum-depleted medium. Up to 24h there was not noticeable differences in cell viability in comparison with cells incubated with full medium. Additionally, to exclude that observed catalytic inhibition could be caused by potent cytotoxic effect of tested inhibitor the cell viability tests with MTT were performed which showed that at least up to concentration of 100 μ M of the tested inhibitor was not harmful significantly to the cells.

- **Comparison of observed IC₅₀ in various enzymatic assays.**

As mentioned above IC₅₀ value is very useful for initial estimations of studied inhibitor effect especially at high throughput inhibitor characterizations. However, it depends from many factors such as: concentrations of the enzyme, the kind of inhibitor and substrate along other experimental conditions. Thereby observed IC₅₀ may slightly differ depending from applied enzymatic assay. In this study IC₅₀ value for the best inhibitor: compound **2-9** was determined in few different assay types: from the most “pure” with purified form of the enzyme and artificial substrate to assays with living cell cultures *ex vivo*. Because the probability of collision of two molecules for example such as inhibitor and enzyme can be different in *in vitro* and *ex vivo* assays according to the expectations the more complex assay the lower inhibition effect was observed which manifested slightly higher IC₅₀ value in comparison to the assays with purified form of enzyme [**Table 30**].

Discussion

Table 30 IC₅₀ values for the same compound in various types of enzymatic assay

Enzymatic assay:	IC ₅₀ (μM) at constant substrate concentration	
<i>In vitro</i> purified enzyme	0.14	fluorescent substrate (750 nM)
Homogenated bacteria lysate	0.26	androstenedione (6.25 nM)
<i>Ex vivo</i> in stable transfected MCF7 cells	0.33	androstenedione (6.25 nM)
<i>Ex vivo</i> in stable transfected HEK293 cells	0.20	androstenedione (6.25 nM)

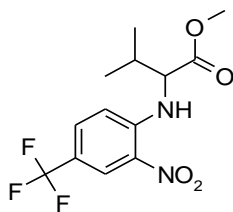
Nevertheless, in spite of all observed not significant differences in various types of enzymatic assays with 17βHSD5 the IC₅₀ values seem to be comparative between all of them. Comparable IC₅₀ can also suggest that in more complicated system such as living cell environment the inhibitor is not metabolized or inactivated. However to make a reliable statement on that theme a prior normalization of substrate concentration in relation to K_m in all compared assays should be made

5.1.1.7 Chances of selected 2-9 compound for further development as 17β-HSD5 inhibitor

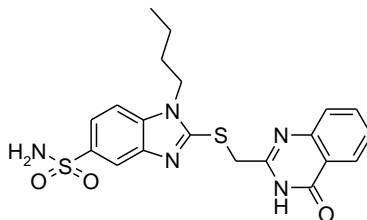
- **2-9 among other known potent HSD17B5 inhibitors**

There was shown that two compounds temporally named **2-9** and **2-12** effectively inhibited reductive activity of human 17β-HSD5. Depending from the kind of enzymatic assay IC₅₀ for **2-9** substance came to 0.14-0.33 μM. K_i for this compound is 0.23 (0.18) μM calculated from assays with purified form of the enzyme and enzyme specific artificial fluorogenic substrate. Additionally, studies on mechanism of inhibition suggest the most desired activity competitive mechanism of inhibition. These all above mentioned facts make it an attractive candidate to be in the interest of further development. Since, the crystal structure in complex with few inhibitors and the mechanism of substrate binding was known, Byrns *et al* [135], proposed competitive and uncompetitive mechanism as desired. First known 17β-HSD5 inhibitors were so called suicide-inhibitors which bounded irreversibly to the enzyme leading to its elimination.

Discussion



2-12



2-9

The strongest known in literature 17β -HSD5 inhibitor at the time of performing this thesis was EM1404 with K_i value 6.9nM described by Wei Qiu *et al.*, [157], which is a polyethylene glycol steroid derivative. Steroid derivatives can trans-activate nuclear steroidal receptors thus trigger undesirable reactions. EM1404 inhibits in competitive way. Lately, a novel inhibitor of 17β -HSD5 showing only 11nM of IC_{50} value and over 100-fold selectivity over isoform AKR1C2 has been researched in preclinical studies [141].

Table 31 Examples of 17β -HSD5 inhibitors.

Inhibitor type	name	K_i (μ M)	IC_{50} (μ M)	substrate	Ref.nr
Phytoestrogens	zymosterol, quercitine, coumosterol, biochanin A		2-14	A-dione, 3α -diol (reduction,oxidation)	45
Trans-cinnamic acid derivatives	α -methylycinnamic acid		6.4		155
Benzodiazepines	Cloxazolam		2.5		157
Spirolactones	EM1404	0,0069	0.0032	A-dione (reduction)	157
NSAIDs	Flufenamic acid	3,1 0,14		A-one (reduction) 3α -diol (Oxidation)	158
NSAIDs	Indomethacine	2,1 0,27	8.5	A-one (reduction) 3α -diol (Oxidation)	137 158
NSAIDs	N-phenylanthranilic acid analogs	0,3-5,2	0.39-10.8	1-acenaphtenol (oxidation)	159
N-sulphonylindole derivatives:	Ex 144 Patent: WO		< 0.1		Astellas Pharma, Tokyo

Discussion

Brazilian propolis derived cinnamic acid derivatives	Baccharine	0.056	30		160
	Baccharine analogs		0.44		161
			0,1		
NSAIDs	N-(4-chlorobenzoyl)-melatonin		11.4	A-dione (reduction)	162
Non steroidal 2,3-Diarylpropenoic acids			4.9-139.2	1-acenaphtenol (oxidation)	163
Morpholyureas	morpholino(phenylpiperazin-1-yl)methanones		0,1		140
ASP9521	(4-(2-hydroxy-2-methylpropyl)piperidin-1-yl)(5-methoxy-1H-indol-2-yl)methanone		0.011	A-dione (reduction)	141

Chemical structure of the substance **2-12** reminds reported earlier another non-steroidal drug with known inhibitory potency towards 17β -HSD5 utilized in this project for structure-based modeling: it is a flufenamic acid. Flufenamic acid was a potent inhibitor in oxidative reactions, but less potent and exhibiting the mixed type of inhibition when reductive direction was tested in conversion of androstenedione to testosterone [**158**].

- **Selectivity of 2-9**

Selectivity studies among other 17β -HSD isozymes as 17β -HSD1, 17β -HSD2, 17β -HSD3, 17β -HSD4 and 17β -HSD7 showed quite good specificity. However to full image of the compound selectivity among other AKR1C isoenzymes should be tested also in future experiments since 17β -HSD5 belongs to AKR superfamily. Considering the potent development and application as a drug in anti-cancer therapy the good selectivity for 17β -HSD5 seems to be an important issue since AKR1C isoforms play distinct roles in metabolism of steroidal hormones.

5.1.2 Summary of inhibitor screening studies

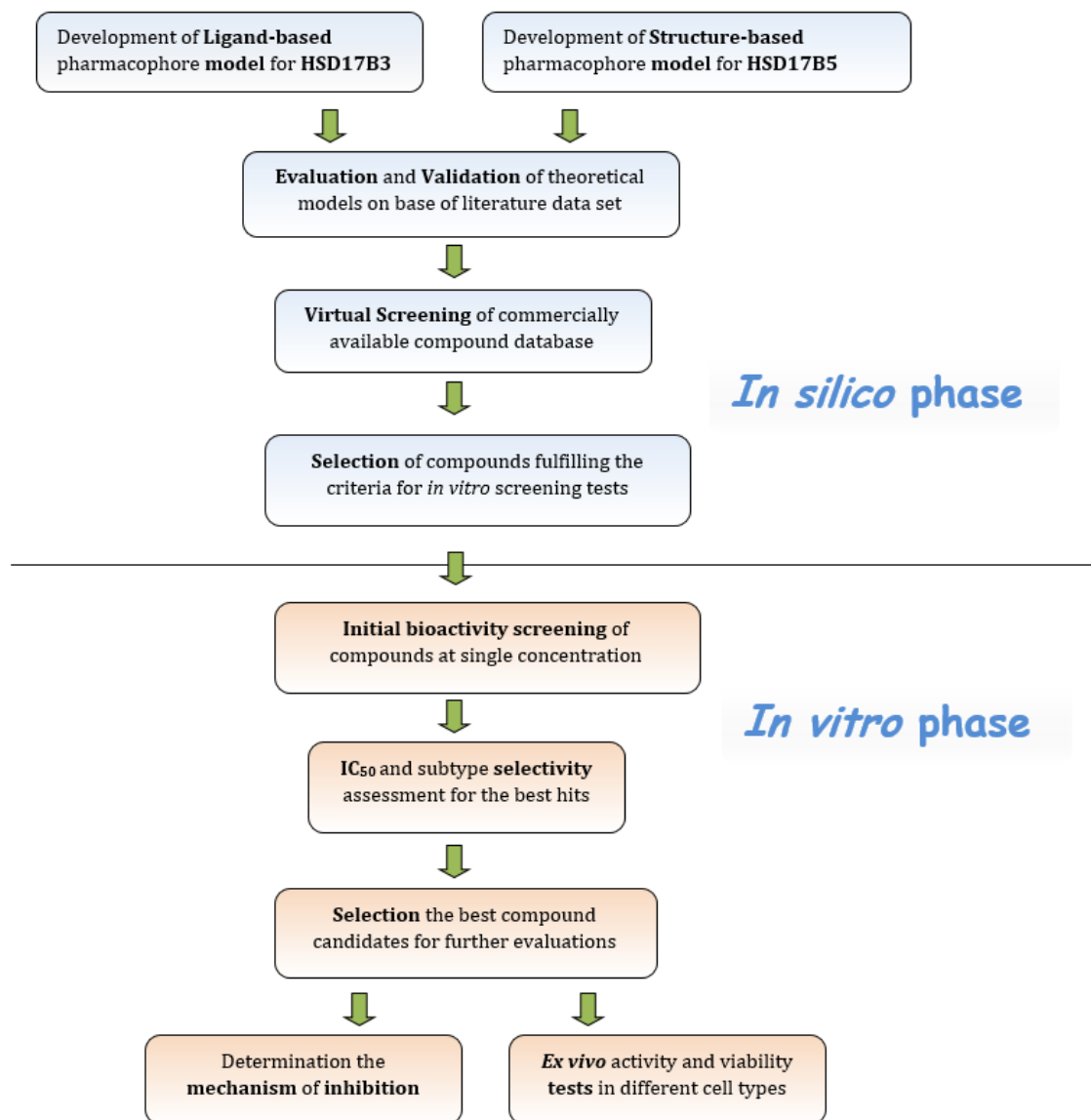


Figure 71 Workflow of the BioNetWorks inhibitor project. Picture modified after [153].

The presented here workflow [Figure 72] consisting of two-phase approach can be an example of systematic and rational new inhibitor development for selected group of enzymes like SDR/AKRs.

The performed in this PhD project *in vitro* phase comprised initial biological evaluations of

previously selected substances in enzymatic bioactivity screening at a single inhibitory compound concentration and further for the best hits IC_{50} , selectivity assessment, *ex vivo* activity in different human cells as well more detailed kinetic studies such as determination mode of actions. However, to improve the throughput of *in vitro* initial compound screening for example by use of UV-Vis, fluorescence detection methods the previous optimization of enzymatic assay to the low K_m /high V_{max} may be very important. Selected in this study potent 17β -HSD5 inhibitor can be a promising candidate for further *in vivo* evaluation or used as a tool for new pharmacophore models designing.

5.2 Characterization of new SDR candidates

5.2.1 Further characterization of human HSD17B8 gene

HSD17B8 was first identified as Ke6 gene involved in polycystic kidney disease (PKD) in mouse. The gene was found to be down-regulated in kidney in few congenital PKD (Polycystic Kidney Disease) mouse models (Cpk, Pcy and Jck) whereas in liver its expression was without change [164]. There was also observed that the gene was down-regulated together with HSD11B gene. Therefore it was suggested that abnormal regulation of sex steroid may have an influence on steroid metabolic defect in PKD model and thus the role in development of disease. Experiments with antisense RNA arresting the Ke6 gene transcription showed no expression of HSD11B1 gene and the down-regulation of Ke6 gene was suggested as potential causative factor of PKD development [165, 166]. In further investigations the coded by Ke6 gene enzyme was classified and named as 17β -HSD type 8 due to its homology to 17β -HSD4 [60]. In the same studies it was found that in mice 17β -HSD8 selectively oxidized estradiol into estrone and testosterone into androstenedione. 17β -HSD8 may also catalyze the reduction of estrone to estradiol and oxidation of 5α -dihydrotestosterone at low levels [60]. Apart of abundant expression in kidney and liver [164] the expression of hsd17b8 gene was found in ovaries and testis [60] and other tissues [167]. Similarly, studies on the role of 17β -HSDs in moscullscs showed that indentified in scollop *C.farreri* as Cf- 17β -HSD8 due to homology to other 17β -HSD8 homologues, could effectively convert

Discussion

estradiol to estrone and weakly testosterone to androstenedione in the presence of NAD⁺ as cofactor when expressed in bacteria *E. coli* [168]. The same studies suggest the role of this enzyme in gametogenesis through modulating estradiol levels in gonads of these animals.

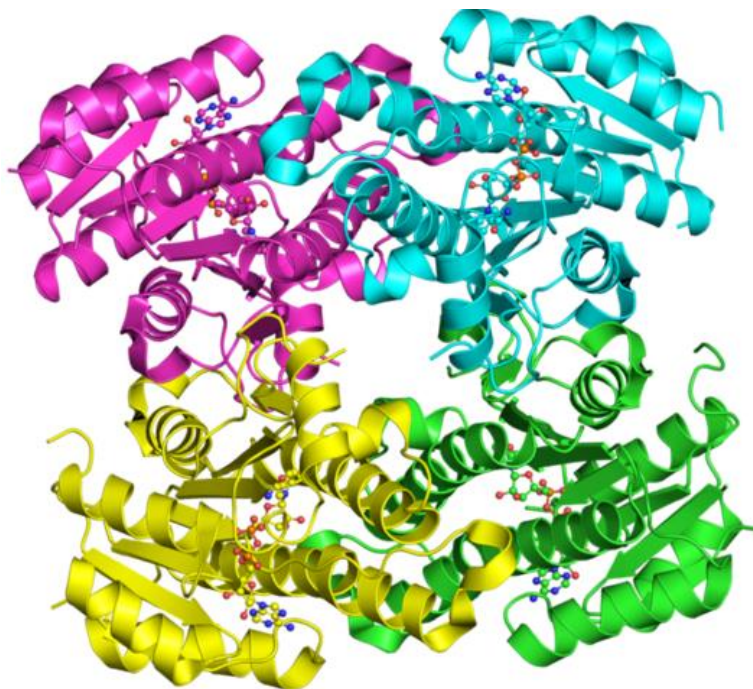


Figure 72 Structure of human 17β-HSD8. Picture adapted from PDB database (PDB: 2pd6)

Another confirmation of the potential role of HSD17B8 in sex steroid metabolism comes from studies on human HSD17B8 gene promoter. Villar *et al.* [169] showed that in liver cell line HepG2 expression of human HSD17B8 was regulated by promoter for C/EBPβ, which is trans-activated by estrogen and ER receptor. Transcription factors from C/EBP family are usually associated with expression of genes implicated with immune system and proliferation. Therefore there were strong experimental argues that HSD17B8 gene may be involved in the control of intracellular levels of active steroids in some tissues.

In spite of established activity of 17β-HSD8 towards steroids (evidences also from tissues distribution as well enzymatic tests) [61], phylogenetic analysis gave an interesting insight into possible other potent 17β-HSD8 substrates. Because the 17β-HSD8 enzyme shows homology to bacteria β-ketoacyl-ACP-reductases and BKR substrates and also to several other bacterial or mammalian dehydrogenase/ oxidoreductases putative involvement in fatty acid metabolisms was suggested [60].

The presumption that human 17β-HSD8 can be more likely involved in fatty acid metabolism confirm modeling studies performed by Pletnev and Duax who showed the better fitting of the β-

Discussion

ketoacyl-CoA substrate into the substrate-binding pocket of the enzyme compared to the steroid. It strongly suggests a role of the enzyme in fatty acid metabolism rather in steroid metabolism which is probably only a secondary function [170].

5.2.1.1 Comparison of the results with the present state of knowledge

The role of 17 β -HSD8 in humans is not clear yet. In searching the enzymatic function subcellular localization as well enzymatic assays testing the activity towards chosen available in the laboratory steroid and retinoid substrates were performed. In this aim human HSD17B8 was cloned into pcDNA3 vector and subjected into transfection to human HEK293 cells for performing substrate screening assays since retrieved 17 β -HSD8 in bacteria expression system turned out to be not active. Assays containing human HSD17B8 transfected HEK293 cell pellets were able to convert estradiol to estrone at the presence of NAD⁺ as cofactor. But, efficacy of the conversion was not high that means up to 10% of conversion during 1h of incubation in used assays containing as much as 4-mio cells in a probe. Unfortunately, oxidation of testosterone or reduction as reported in the literature was not observed. Probable the lack of noticeable conversion could be caused by low efficacy of applied assay and low affinity of these substrates to the studied enzyme at all. Similarly, no conversion was observed with all-trans retinal or all-trans- retinol.

5.2.1.2 Meaning of mitochondrial localization of HSD17B8 in context of putative role in steroid or fatty acid metabolism.

In this study was experimentally shown that the human 17 β -HSD8 is localized in mitochondria. Such a result supports and hence the hypothesis of a role in fatty acid metabolism. From other hand mitochondria are also very important place for steroid hormone biosynthesis from cholesterol where the first reaction converting cholesterol to (C₁₈, C₁₉ and C₂₁ steroids) pregnenolone is catalyzed by enzymes from P450 cytochrom complex and is rate limiting step in steroid hormone biosynthesis. Presence of 17 β -HSD8 in mitochondria together with its NAD⁺/NADH dependent oxido-reductive activity toward sex steroids may suggest that it is not the main activity of the enzyme.

Reported phylogenetic analysis indicates the strong homology of mice and human 17 β -HSD8 to prokaryotic BKR reductase enzyme [60]. Concerning the mammalian proteins, recent structure-based phylogenetic analysis place HSD17B8 in a group with 17 β -HSD4 and 17 β -HSD10 and 17 β -

Discussion

HSD14 enzymes [1, 171]. The two first mentioned 17 β -HSD enzymes apart of activity towards steroids can catalyze the conversion of fatty acyl-CoA substrates and exhibit 3-hydroxyacyl-CoA dehydrogenase activity [172]. 17 β -HSD10, known also as mitochondrial human 3-hydroxyacyl-CoA dehydrogenase type II catalyzing the NADH dependent reduction of S-acetoacetyl-CoA exhibit homology (~30%) to HSD17B8 and it is expressed at high levels in Alzheimers disease.

However, Fomitcheva *et al.* [60] showed closer homology to prokaryotic *E. coli* acyl-carrier protein reductases (FabG) than to human 17 β -HSD4 and 17 β -HSD10. Although, BKR and 17 β -HSDs belong to the same SDR family constitute two different subfamilies. Phylogenetic and structural similarity to prokaryotic reductases seems to be unusual since HSD17B8 was earlier shown to prefer NAD⁺/NADH as cofactor. Due to the cellular NAD/NADH and NADP⁺/NADPH ratios there is believed that NAD⁺/NADH utilizing enzymes act as dehydrogenases while NADP⁺/NADPH dependent enzymes are reductases rather *in vivo* [149]. Meanwhile up to now well characterized NADP-dependent BKR enzymes catalyzes the reversible reduction of 3-oxoacyl-ACP to the D- β -hydroxyacyl-ACP isomer in the multistep biochemical pathway of fatty acid synthesis. Additionally, determined subcellular localization of 17 β -HSD8 in mitochondria may complicate the previous suggestion of the role as β -ketoacyl-CoA reductase. Fatty acid synthesis (FAS) is a multistep reaction performed by multifunctional homodimeric fatty acid synthase which in mammalian occurs in cytosol in contrast to catabolic oxidative reactions catalyzed by mono-functional enzymes in mitochondria and peroxisomes. 17 β -HSD4 and 17 β -HSD10 mentioned above as partially similar to 17 β -HSD8 are both involved in fatty acid metabolism as 3-hydroxyacyl-CoA dehydrogenases and are localized in peroxisomes and mitochondria, respectively. Regarding the inconsistencies by trying to compare the potent 17 β -HSD8 activity to known schemes of fatty acid metabolism the searching for alternative mitochondrial metabolic pathways in context of potent substrate would be worth of interest

- **Human 17 β -HSD8 implicated in mitochondrial fatty acid synthesis**

Recent studies show that mitochondria in yeast and human are able to fatty acid biosynthesis in malonylo-CoA manner similar to bacterial FASII [173]. However the role of mitochondrial fatty acid synthesis is still enigmatic and is a subject of intensive studies. The mentioned pathway is responsible for generation of octanoyl groups required for further synthesis of lipoic acid and is linked to mitochondrial RNA metabolism. Mitochondrial fatty acid *de novo* synthesis is alternative for cytosolic pathway. While writing this thesis the publication representing results confirming the role of human 17 β -HSD8 in mitochondrial FAS synthesis has been appeared. Zhijun Chen *et al.*

[174] reported that human 17 β -HSD8 and human carbonyl reductase type 4 form a heterotetramer of long sought KAR complex (β -ketoacyl thioester reductase). Both proteins display a stable physical interaction and form an active hetero-tetramer. Further studies demonstrated that both proteins together expressed could rescue the respiratory deficiency and restore the lipoic acid content in yeast *oar1* Δ cells. The same authors indicate 17 β -HSD8 mitochondrial targeting thus confirm the role in mitochondrial FAS synthesis. It is notable that KAR acts as reductase utilizing NADH as cofactor while reductases participating in fatty acid synthesis are usually NADP⁺ dependent. However the enzymatic assay demonstrating *in vitro* the use of β -ketoacyl as substrate has not been yet developed, since 17 β -HSD8 probable act in this reaction in complex with other enzyme.

5.2.1.3 Human 17 β -HSD8 as potent inhibitor development target.

Crystal structure of the 17 β -HSD8 has been dissolved and it is available on PDB database [Figure 72]. Knowledge of the molecular structure is a basis for rational designing and development the potent specific inhibitor. The latest studies show that the 17 β -HSD8 is present in mitochondria as heterotetramer with CBR4 enzyme and functions as NADH-dependent 3-ketoacyl carrier protein reductase [174]. The heterotetrame contains two molecules of 17 β -HSD8 and CBR4. The activity of this complex is clue in mitochondrial fatty acid synthesis process (FASII). Correct functioning of this synthesis pathway seems to be essential for mammalian cell survival as shows the experiment with down-regulation of some components participating in the mitochondrial FAS process resulting in cell apoptosis [175]. According to my knowledge up to now there is no report of any disease that would be correlated with over-expression of this enzyme. Rather down-regulation of HSD17B8 gene seems to be more likely associated with development of some disorders. Up to now 17 β -HSD8 was suggested as a causative gene of disease only in case of kidney syndrome in mouse where it is down-regulated. Aziz *et al.* [165, 166] indicated that down-regulation of Ke6 is correlated with parallel down-regulation of HSD11B1 enzyme responsible for glucocorticoids metabolism. In turns, glucocorticoids were proven to induce cysts development in kidney elucidating in this way mechanism of pathogenesis of the disease.

Searching the publicly available electronic expression profiles one can notice that HSD17B8 is rather down-regulated in many tumor tissues for example such as breast cancers. For example there is a report showing its down-regulation in neck and head squamous cancers [176]. Significant lower RNA expression of this gene was observed in tumour tissues of oral cavity patients without

lymph node metastasis compared to its surrounding healthy tissues. Since it was proven that human 17 β -HSD8 acts as oxidase performing reactions leading to rather inactivation of estrogen and androgen it seems that its down regulation may be only one of many factors causing the estradiol dependent carcinogenesis.

However in the context of recent discoveries of mitochondrial fatty acid synthesis metabolism in humans a development of specific 17 β -HSD8 inhibitors could be helpful in research aimed at understanding the physiological role of the enzyme when applied in *in vitro* or *in vivo* experiment. In further plans, concerning the potent essential role in cell survival, it would be worth to test experimentally the specific 17 β -HSD8 inhibitors as tissue targeted pro-apoptotic agents in tumor affected cells.

5.2.2 In search of function of human SDR-O (SDR9C7)

In 2002 Chen *et al.* [177] as the first reported and cloned cDNA that encoded a novel short-chain dehydrogenase/reductase conserved in mouse human and rat assigned primary as orphan (SDR-O). The same authors mapped the localization of human SDR-O gene on chromosome 12 in the neighbourhood of other genes coding enzymes involved with retinol metabolism, such as RDH5 or RoDH. In the same report performed enzymatic tests did not indicated any activity of SDR-O towards retinol, 3 α -, 11 β - or 17 β -hydroxysteroids. Concerning the phylogenetic analysis SDR-O seems to have its orthologs only in mammals. The nearest human SDR-O homologs: 11-cis-RDH, RoDH4, RoDH-like 3 α -HSD (RL-HSD) and RDHL/DHRS9 are all NAD⁺ dependent retinoid active enzymes acting as oxidases [53].

In order to further characterize this little annotated potent enzyme human SDR-O cDNA was cloned into mammalian or prokaryotic expression systems for performing enzymatic assays with retinoid and steroid substrates as well in aim to estimate its subcellular localization.

5.2.2.1 Subcellular localization of human SDR-O

- **SDR-O expected to be present in ER**

Phylogenetic and genomic analyses of human SDR-O show close connections to retinol/steroid metabolizing SDRs usually identified as microsomal enzymes thus the localization of SDR-O in ER

Discussion

would be expected [53]. All of four the nearest for human SDR-O homologs such as RoDH4, 11-cis-RDH, RDHL and RDHL-3 α HSD are found in microsomal fractions. This fact allows presuming that SDR-O would be also transported to endoplasmatic reticulum similarly to the majority of catalytically active enzymes from this subfamily. Belyaeva, *et al.* [53] suggests that some C' terminal motif of common for SDR-O and these enzymes PD002736 domain may be involved in protein interaction with intracellular membranes and thus responsible for such a frequently observed subcellular localization in this protein group. In support of these presumptions the authors indicate studies on rat RODH-1 where was shown that hydrophobic fragment of amino acid sequence (289-311) being a part of mentioned above domain directly improved protein associations with microsomal membranes. Within the domain there is a conserved block of 4 amino acids (CMEH) that seems to be characteristic for all RODH-like SDRs. In case of SDR-O the cysteine in this sequence is replaced by serine (SMEH). The role of these highly conserved sequences is yet not completely understood.

- **SDR-O subcellular localization still an open issue.**

In this study the intracellular localization of transiently transfected in HeLa cells human SDR-O was assessed by use of confocal microscopy for matching with various markers of cellular components such as ER, mitochondria, nucleus, peroxisomes and additionally with early endosomes markers. Unfortunately, obtained images did not confirm unambiguously any of checked intracellular co-localizations and thus do not provide a satisfactory answer to SDR-O target localization in cell. At first glance the displayed by the protein intracellular pattern appeared to be associated with endoplasmatic reticulum or some plasmatic vesicular due to more or less granular net structure spread out through the cell. In contrary to many of cytosolic proteins it does not exhibit a typical homogenous mode of distribution. Sometimes the distribution of human SDR-O protein even has appeared to mimic the pattern of endoplasmatic reticulum by more concentrated granulate at areas overlaying with ER for example at its perinuclear regions where endoplasmatic membranes are usually more dense. Nevertheless, counterstaining with ER marker often revealed two independent, not completely overlaying and different from each other structures as shown in **Figure 57** or below **[Figure 73]**.

Discussion

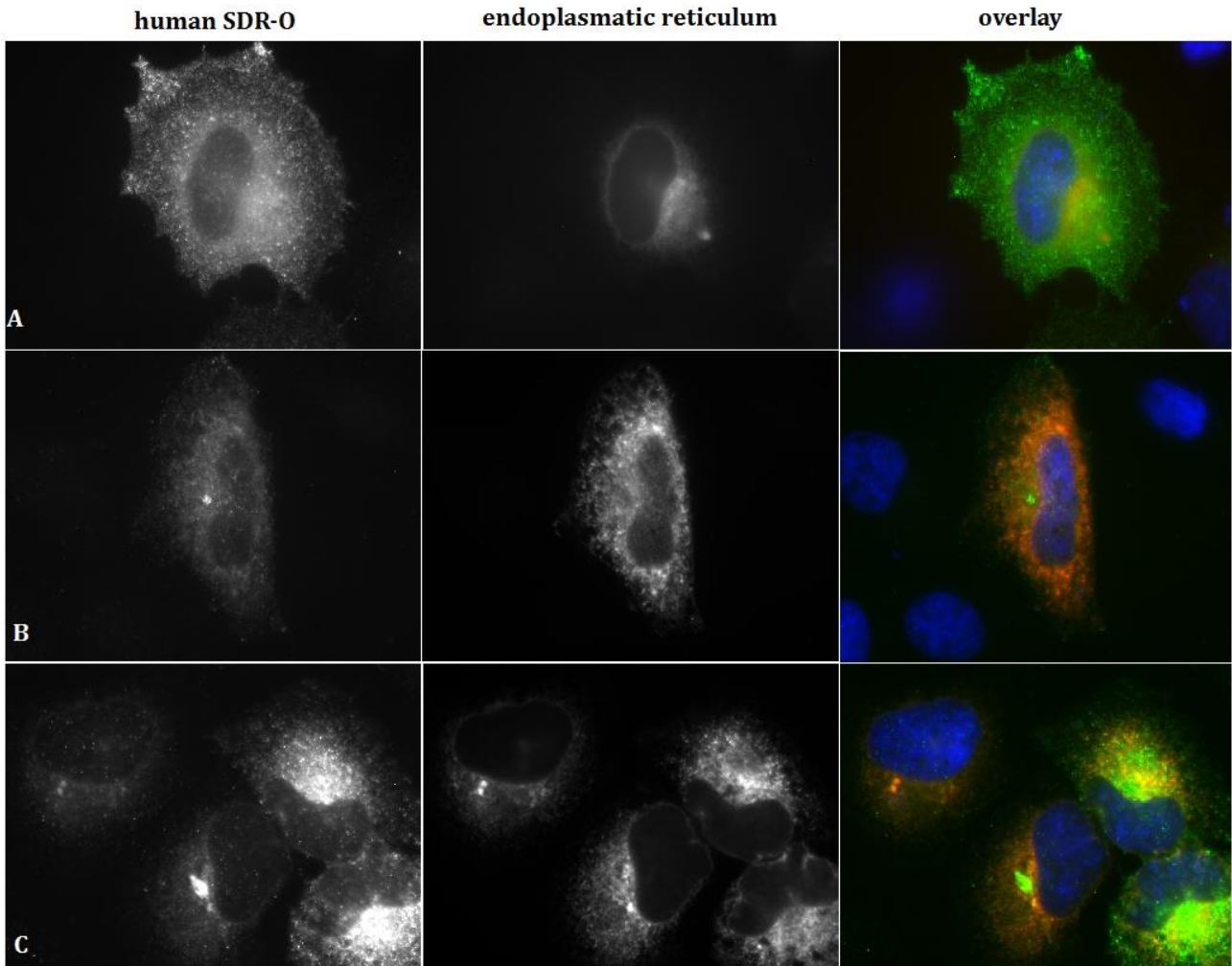


Figure 73 Few examples of numerous captures showing the subcellular pattern of human SDR-O counterstained with ER markers: A: N'Flag-SDR-O, B: Second column depict endoplasmatic reticulum (pDsRed_ER from Clontech which contains a fused with red fluorescent marker ER signaling sequence of carleticulin); Third column shows overlay images of SDR-O (green), ER (red) and nucleus (blue).

On the other hand, it should be also taken into account that displayed by human SDR-O pattern may just result from incorrect localization due to putative not proper folding after translation. However, against this presumption evidence images of negative control which depict a delocalized fluorescent tags expressed from empty vectors (without insert). Noticeable, observed subcellular pattern was the same regardless of C' or N' terminally tagged SDR-O variant was used what can suggest that intracellular distribution may be determined by putative targeting signal localized internally if such exists. Internal targeting signals are conceivable for proteins transported into ER or cytoplasm.

Discussion

- **Comparison with subcellular localization results affiliated to the Human Protein Atlas**

Interesting insight to localization of SDR-O may give data deposited in the Human Protein Atlas Project and coming from systematic studies on subcellular localization of 466 human proteins by use of confocal microscopy [178]. SDR-O among other protein was checked here in three different human cell lines. Evaluated subcellular localization for this enzyme was annotated in the category as cytoplasm+nucleus staining. Into such a category were assigned studied proteins in which the annotator was able to distinguish different staining intensities within in two localization in contrast to unspecific homogenous localization [178].

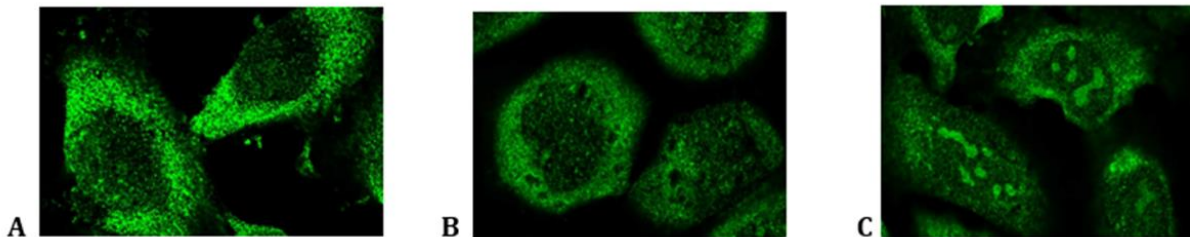


Figure 74 Staining pattern for SDR-O antibodies in three various human cell lines: A) U-251, B) A-431 C) U-2 OS. Pictures adapted from <http://www.proteinatlas.org/ENSG00000170426/subcellular> [178].

The shown above subcellular localization pattern for SDR-O protein [Figure 74] are similar to observed ones in my studies as well the counterstaining pattern with ER and nucleus (not shown in this picture). It is worth of note that in this case were used no tag-fused constructs but specific SDR-O antibodies. The results cited above suggests that SDR-O may be expressed and fulfill some functions in both cytosolic and nucleus compartments of the cell.

- **Murine SDR-O localized in mitochondria**

What may complicate the findings above is previously performed in our laboratory experiment with mouse SDR-O protein which showed mitochondria localization (B.Keller, PhD thesis) [79]. Although it was a 'foreign' mouse protein expressed in human HeLa cells the probability of incorrect localization due to interspecies expression seems to be low since among vertebrates the cellular signaling system of transport into right compartments is rather well conserved. Mouse and human SDR-O share 83% sequence identity and they seem to be right ortholog genes due to their genomic

Discussion

organization although the functionality and substrate specificity is still unknown for both of them. It is commonly observed that RODH-like SDRs into which belongs SDR-O exhibit high redundancy in mice when are compared to human and rats. Putative orthologs genes may show differences in retinoid stereospecificity and may varying in tissue distribution. Maybe this is an example that RODH-like orthologs may differ also in respect of subcellular localization.

SDR members are found in different cellular components as: cytoplasm, mitochondria, nuclei, peroxisomes, ER. However, it is possible that some of SDR enzymes which act on the same endogenous substrates can exhibit different subcellular localization, cofactor specificity, substrate affinity and tissue distribution.

5.2.2.2 Human SDR-O as retinaldehyde reductase? Confrontation with the present state of knowledge.

In this study the substrate specificity with steroids and retinoids of human SDR-O was analyzed. No substantial 3 α -, 17 β -, 20 α - and 11 β -HSD activity was detectable with steroid substrates. On the other hand remarkable is the fact that a weak but significant conversion of all-trans-retinal to all-trans retinol was observed for human SDR-O in the presence of NADH what simultaneously match the predicted NAD(H) preferences. However, it is observed that NAD(H) preferring enzymes rather act as oxidase *in vivo* and NADP(H) preferring enzymes as reductase [149]. Surprisingly, this activity was detectable only when SDR-O was expressed in the bacterial system. In an earlier screen for substrate specificity of murine SDR-O, neither activity towards steroids not towards retinoids was observed [177]. In the same report SDR-O protein was only expressed in mammalian cells but not in bacteria. Activity tests were then performed by use of assays *in vitro* containing homogenated supernatants from transiently transfected CHO cells.

Rational explanation of observed in this study retinal conversion may be the fact that much higher protein concentration can be achieved when induced proteins are expressed in *E.coli* rather than in any mammalian cells. Assays were also performed *in vitro* in harvested and pelleted transiently transfected HEK293 cells.

Concerning the potential activity towards retinoids the specific conditions and cellular environment like presence of cellular retinoid binding proteins (CRBP) for successful reaction should be taken into the account. Human SDRs active towards all-trans retinol may differently recognize the bound or unbound with CRBP form of this substrate in mammalian cells [179]. Assuming, maybe the

Discussion

conditions of expression the human SDR-O in bacteria system could thus somehow expose this observed remnant activity towards retinal which could be hardly observed in physiological environment.

Additionally, the poor catalytic activity of SDR-O in combination with its unusual cofactor preference suggests that the conversion of all-trans-retinal to all-trans retinol is not the main function of the enzyme. Several SDR enzymes are known for their promiscuous activities and the catalysis of retinoid conversion by SDR-O may represent a remnant of its retinol dehydrogenase.

- **Suggestions of SDR-O to have a non catalytic function**

Since experiments with mouse SDR-O showed no activity towards its most likely substrates as retinoids and steroids Chen *et al.* [177] suggested that SDR-O may have no catalytic function but its expression may regulate metabolism by binding potential substrate/products or may act as a regulatory factor. Alternatively, it may catalyse the metabolism of another class of nuclear receptor ligand different from steroid and retinoids. The authors hypothesize of its putative implication in metabolizing/generation of some lipid ligands if an orphan nuclear receptor for them exist. On the other hand, similarly to human HSD17B8 it can be also conceivable that SDR-O can reveal their main function when associated in complex with another enzyme.

Some hints for these presumption may give latest studies on lymph node metastases in patients with poor prognostic esophageal squamous cell carcinoma [180]. SDR-O protein over-expression was found here to be closely correlated with metastasis in the tumor. Down-regulation of SDR-O expression inhibited the metastatic abilities *in vitro* and *in vivo* and repressed the expression of MMP11 protein involved in the breakdown of extracellular matrix known to be active in highly invasive tumor cells. Therefore it was suggested that up-regulation of SDR-O promotes the methastasis partially through regulating MMP11 expression level. However, more detailed studies elucidating the molecular mechanism of this regulation by SDR-O have to be performed.

5.2.2.3 Comments on SDR-O mRNA expression profile

Human SDR-O has been found to be expressed exclusively in liver where the SDR-O gene is intensely transcribed into mRNA [177]. This finding is consistent for enzyme metabolizing fatty acid and retinoids. The same report indicates that human embryonic liver as well the mouse embryo can

express sdr-o mRNA. Whereas in mouse EST database GenBank apart of liver one can find sdr-o corresponding clones originating from skin, pancreas and salivary gland in case of human EST GenBank there are SDR-O encoding clones from esophagus (*DB013559.1*, *DB335393.1*) and skin (*CU452249.1*, *CU449279.1*, *CU445598.1*, *CU449847.1*).

In the context of recent studies on esophageal cancer and evidenced role in propagation of metastatic form of this type of cancer [180] SDR-O emerge to be interesting target for further studies and anti-cancer drugs development.

5.2.3 In search of function of human HSDL2

At the present studies human HSDL2 gene was retrieved by use RT-PCR method from HEPG2 cells and subsequently cloned and expressed in HEK293 cells or bacteria BL21DE3 in aim to perform enzymatic tests towards steroids and to check the subcellular localization.

5.2.3.1 Comparison of the results with the state of knowledge from literature

HSDL2 was first identified by large-scale sequencing analysis of human fetal brain cDNA library by Dai *et al.* [152]. The authors established that the gene is mapped to chromosome 9q32 and is expressed as a modular 418aa protein which consists of short chain dehydrogenase/reductase (SDR) domain on N' terminus and the domain similar to the sterol carrier protein 2 (SCP-2) on its C'terminus where last three amino acids (ARL) are a peroxisomal targeting signal (PTS1) recognized by receptors in these organells. The same authors showed by RT-PCR analysis that the protein is ubiquitously expressed in human tissues but with relatively high expression level in liver, kidney, prostate, pancreas, testis and ovary. Lately, the SDR catalytic domain of HSDL2 has been crystallized and the secondary structure was recognized by the team from SGC (Structural Genomics Consortium of Oxford) and deposited in PDB database [181] [Figure 75].

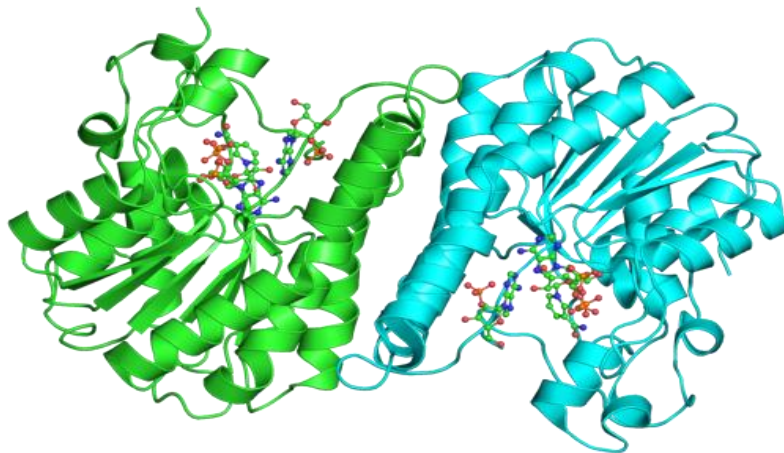


Figure 75 Resolved homodimeric crystal structure of HSDL2 SDR catalytic domain in complex with NADP cofactor. Picture adopted from PDB database. PDB code: 3KVO [155].

- **HSDL2 in the phylogenetic context (based on literature)**

Sequence characterization of HSDL2 showed that human cDNA shares 67, 55 and 51% identity with putative SDR proteins in mouse, fruit fly and in *C.elegans* [152]. SCP-2 is a specific protein domains characterized by α/β -fold with five β -sheet and five α -helices which form a hydrophobic tunnel suitable for binding of lipids. Up to now, apart from HSDL2 only few genes has been reported to possess this domain: HSD17B4, SCPx and STOML1 which exists assembled on their C terminus [150]. In humans there is also a gene C20orf79 which encodes unfused SCP2 protein. HSDL2 together with HSD17B4 and SCPx are conserved and have homologs in all animal world. Edqvist and Blomqvist [150] have performed a thorough philogenetic analysis of SCP2 assembled proteins which gave an interesting insight into molecular evolution of SCP-2 genes in eukaryots. They suggest several fission and fusion events in metazoa group in the course of evolution and hypothesize that a common eukaryotic SCP-2 ancestral was present as a fusion with D-3-hydroxyacyl-CoA dehydrogenase. As a support to this hypothesis is the fact of presence of fused SCP-2 with archat has to be said that proteins with SCP2 domain are present also in bacteria. According to their results human HSDL2 form a separated and rather conserved branch. Orthologs and homologs of HSDL2 are present in all *Metazoa* group from *Cnidaria* to *Chordata*. Authors

Discussion

indicate that domain for HSDL2 share a common origin with homologous and unfused proteins also from bacteria and fungi. However, as fused with SCP-2 domain HSDL2 homologs exist in nematode, insects and asceolate.

Comparing the amino acid sequence of only HSDL2 catalytic domain (without SCP2) by use of alignment blastp program with other available from database amino acid sequences from various species I have found significant similarities to some bacterial enzymes (over 40%) such as 3-oxoacyl-(ACP)-reductase (*Sorangium cellulosum*), 7 α -HSD (*E.coli*) or Cis-Toulen dihydrodiol DH (*Pseudomonas Putida*). Considering the human enzymes the high alignment scoring with catalytic domain of HSDL2 showed belonging to SDR family: DECR2 acting as 2,4-dienoyl-CoA reductases and further to HSD17B4 (SDR domain), HSD17B8, HSD17B11 (similarities between 35-41%).

- **Subcellular localization**

Performed here studies on HSDL2 intracellular distribution revealed both peroxisomal and mitochondrial localization depending on which N' or C' tagged construct was used. Peroxisomal localization was observed in the case of HSDL2 when N-terminally tagged enzyme was transiently expressed in HeLa (or HEK293) cells. It fits to the predictions of peroxisomal targeting due to the presence of PTS1 targeting sequence at its C-terminus. Remarkable is the fact that with C-terminus tagged proteins covering the peroxisomal targeting signal the enzyme was found in mitochondria. Such a construct probably allowed to expose better the putative mitochondrial targeting sequence (MTS) and transport to mitochondria. *Dai et al.* [151] reported that mouse hsd12 N-terminally tagged with GFP localized in the cytoplasm and not in peroxisomes, as would be expected considering its peroxisomal targeting signal (RKL). Comparing amino acid sequences of human and mouse HSDL2, an additional peptide sequence of around 60 amino acids with low complexity (only containing amino acids Q, E, P, L, and K) can be found inside the mouse protein. This peptide stretch is integrated in the SCP2-like protein domain and might have an impact on the subcellular targeting process.

Additionally, interesting complementation (updated) to the observed here results can be assigned lately subcellular localization of human HSDL2 originating from Human Protein Atlas Project [178] (available online: <http://www.proteinatlas.org/ENSG00000119471/subcellular>) which revealed mitochondrial localization in three various human cell lines with use of specific anti-HSDL2 antibodies. For checking the native subcellular localization using of specific antibodies against

Discussion

epitopes on studied protein undoubtedly has the advantage over the experiments with modified tagged constructs which may impact on correct exposing and thus recognizing the targeting signals.

Coming back to my results one could raise a question if observed different localization of N' or C'tagged HSDL2 is just only an experimental artefact caused by selective exposition of specific targeting sequences or does it really reflect the putative dual localization of the studied protein? Moreover, if the predicted mitochondrial (MTS) or peroxisomal (PTS1) targeting sequences play a role in the observed intracellular localization, it would be interesting to check and discuss about how potent they are or compete with each other in the intracellular environment. HSDL2 possess a SCP2 domain which alone was shown to bind with cholesterol or other lipids (in unspecific manner) and supposed to play a role in intracellular trafficking between cell compartments [182 -184]. Apart of preferred peroxisomal localization SCP2 protein has been reported to be found also in other organells like mitochondria, ER or cytosol [185, 186]. However, the physiological functions and the putative role of the SCP2 in cholesterol intracellular transport is still researched [187]. Considering the facts above either peroxisomal or mitochondrial localization of HSDL2 could not be excluded.

5.2.3.2 Enzymatic assay results

Presented here experimental studies revealed that recombinant human HSDL2 showed no catalytic activity towards steroid and retinoid substrates in enzymatic assays originating from both mammalian and bacteria expression systems. Therefore, I was not able to experimentally confirm the predicted preference for NADP(H) over NAD(H) as it can be deduced from the amino acid sequence. However, creating of complexes with NADP(H) evidence the latest crystallization studies on catalytic domain of HSDL2 [181]. It still remains to be clarified if the enzyme is able to support catalysis. In SDR proteins, the amino acids Tyr, Lys, and a Ser located 10-15 amino acids upstream of the Tyr form the catalytic triad in substrate binding site. In HSDL2 proteins, the respective Ser(152) can be found 16 amino acids upstream of Tyr(168). This unusual distance might influence the catalytic activity at least towards steroid substrates. Any mutations in this strictly conservative region are known to be very sensitive on enzymatic activity. As example may serve another HSD-like enzyme, the human HSDL1 protein, which is natively inactive due to fenyloalanine instead of tyrosine in the catalytic region [81]. From the other hand such a distance between serine and tyrosine as well the pattern of

Discussion

amino acid sequence in active site of the studied potent enzyme seems to be conserved in all known hsd12 orthologs of another species.

Different to the catalytic region all other SDR-specific motifs seem to be intact for proper enzymatic function and they are properly located in predicted secondary structure according to the rule. However, the discussed situation is changed when one could consider the alternative splicing isoform2 (described below) missing a fragment (94-166) overlapping the catalytic centre of the protein described below [Figure 76].

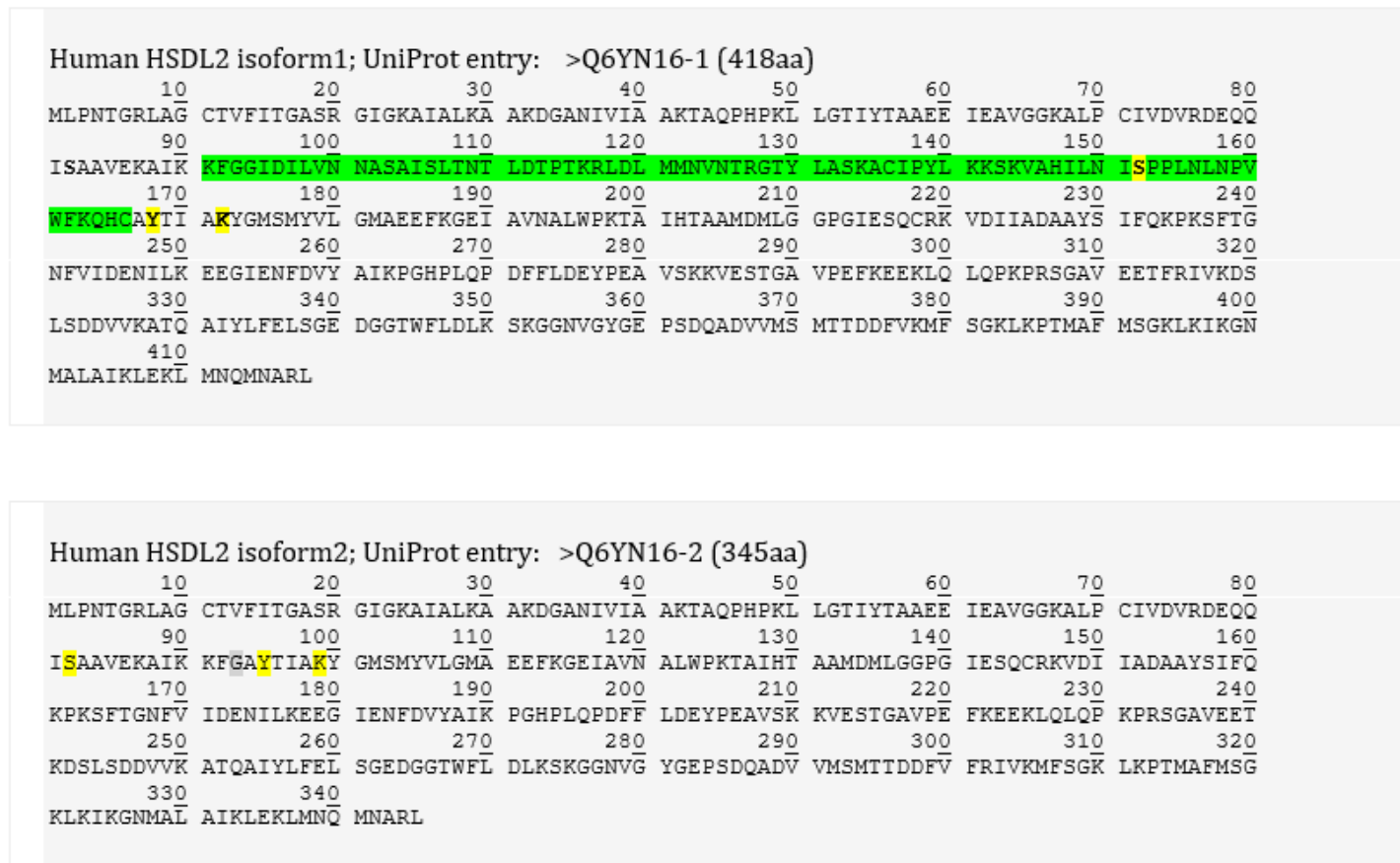


Figure 76 Two reported alternative splicing products of human HSDL2 gene: isoform1 and isoform2 UniProt. *Genome Research "The status, quality, and expansion of the NIH full-length cDNA: the Mammalian Gene Collection (MGC)", The MGC Team Project, 2004.* Fragment of amino acid sequence marked on green is excised in alternative splicing isoform 2. Yellow marked amino acid are putative catalytic triad S-Y-K.

- **Human HSDL2 gene produces at least two alternative splicing isoforms**

Another information hits about human HSDL2 comes from rudimentary performed global project on human and mouse genomes. There were reported two isoforms of human HSDL2 in tissues such as blood vessels and uterus. These reports originate from the Mammalian Gene Collection (MGC) project designed to generate and sequence a publicly accessible cDNA resource containing a complete open reading frame for every human and mouse gene. It is noticeable that human HSDL2 gene is encoded by 11 exons. Putatively, it gives a possibility of 12 different mRNA transcripts resulting from alternative splicing. Among them only 9 could putatively encode good functional protein. Reporting of two isoforms in these tissues may be interesting because of structural differences in putative catalytic center between both isoforms. Excised region at the isoform number two (SDR13C1-2) putatively change the distance of another putative catalytic serine (Ser82) to YxxxK motive from 16aa to 13aa).

New light on structure of active site of the enzyme cast the newest results of 3D-structure analysis achieved by HSDL2 crystallization available on PDB database [181]. In the structure study it was evidenced that the protein is bounding to NADP as cofactor and exist as homodimer. Similarly to other SDRs HSDL2 monomer consists of a central 7-stranded β -sheet core sandwiched between two arrays of parallel helices located on each side of β -sheet. The real secondary structure of the protein has appeared to be slightly but significantly different only in the region of its putative catalytic center in comparison to previously deduced secondary structure by use of bioinformatic programs in my previous studies. Potent catalytic triad of HSDL2 is composed of Ser₁₅₂, Tyr₁₆₈ and Lys₁₇₂ localized on helices α 5 and α 6. These both helices in homodimeric protein complex form a four helix-bundle which are probable the right place of catalysis. It is worth of note that unusually to other SDR-like proteins the potent catalytic serine in one HSDL2 monomer apart of discussed above distanced 16 amino acid residues upstream of conserved tyrosine from YxxxK active site motif (rather than 10-15aa like in most of SDRs) is additionally separated by an extra β -strand (β 5a). In other catalytically active SDR enzymes the catalytic triad S_{X_n(10-15)}YxxxK is usually localized in the region of β 5- α 5 folds where YxxxK falls on α 5 helise. It would be interesting to verify how the existence of extra α/β -folding influence on geometrical orientation of serine towards YxxxK and its potent catalytic activity.

5.2.3.2 HSDL2 may be involved in cholesterol or fatty acid metabolism

Either peroxisomal or mitochondrial localizations of human HSDL2 may suggest involvement in fatty acid metabolism. Support for the hypothesis comes from the modular assembly of the enzyme, which consists of two domains, an SDR and an SCP2-like domain. Other enzymes carrying the SCP2-like domain are known to play a role in fatty acid metabolism, as e.g. 17 β -HSD4 or SCPx. Other human SDR enzymes similar to HSDL2 SDR domain are also localized in mitochondria or peroxisomes and metabolize fatty acids. Additionally, a recent publication reports the involvement of HSDL2 in cholesterol metabolism and homeostasis [188]. HSDL2 has been identified as one of the central cholesterol-responsive atherosclerosis genes regulating cholesterol-ester accumulation. These genes prevents the formation of advanced plaques in artherosclerosis in response to plasma cholesterol-lowering. There are some reports from literature suggesting the role of HSDL2 in cholesterol metabolic processess. Expression of *hmdl2* in mice is induced after cholesterol rich food [151].

It still remains to be clarified if the enzyme is able to support catalysis by searching for new potent ligands among other substrate groups than steroids and retinoids. This evidence together with a presence of sterol carrier protein domain (SCP2 like) at C'-terminal may suggest involvement in cholesterol or lipid metabolism.

5.2.4 Closing remarks on new SDR candiadates characterization studies

Three barely annotated human SDR candidates such as HSD17B8 (SDR30C1), SDR-O (SDR9C7) and HSDL2 (SDR13C1-1) were chosen in this work for further characterization and searching their potent catalytic activities.

Considering the first candidate performed here subcellular localization studies indicated that 17 β -HSD8 is transported into mitochondria and thus it confirms the newest reports indicating its involvement in the second pathway of fatty acid biosynthesis *de novo* in mitochondria.

Development of enzymatic assay checking the activity of 17 β -HSD8 allowing screening of potent inhibitors is still pending as well the more intensive studies about linkage between two activities of the enzyme in either fatty acid and steroid hormone metabolism.

Discussion

For SDR-O a weak conversion of retinal into retinol was detectable in the presence of the cofactor NADH whereas the reverse reaction: oxidation of retinol into retinal at the presence of NAD⁺ was not observed. This unusual cofactor preference together with poor catalytic activity suggest that observed *in vitro* retinal conversion is not the main function of the enzyme *in vivo* and could be exposed by specific assay conditions. Further potent substrate screening studies different from utilized in this study steroid or retinoid substances would be pending. Supposed cytosolic localization of SDR-O protein does not enhance the potent participation in metabolism of fatty acid or derivatives but not excludes. However, in the context of the recent reports suggesting the role of sdr-o gene in pathogenesis of oesophageal cancer SDR-O seems to be worth of further studies as well as a target of rational specific inhibitor or antagonist design if natural ligand is discovered. Different to HSD17B8 and SDR-O studied here HSDL2 showed no catalytic activity with the tested steroid and retinoid substrates. Deduced from amino acid sequence cofactor preference as well the latest crystalization studies indicate rather performing of reductive reactions than oxidations by HSDL2. The presence of SCP2 -like domain on C' terminus and determined here mitochondrial/ peroxisomal subcellular localization support the hypothesis of involvement in fatty acid metabolism. Therefore, further development of enzymatic assays screening the potent catalytic activity of HSDL2 towards new potent substrates such as fatty acids and cholesterol derivatives is still pending.

6 Literature

1. Kallberg Y, Oppermann U, Persson B; Classification of the SDR superfamily of Short-Chain Dehydrogenases/Reductases Using a Hidden Markov Models. FEBS Journal 2010, volume 277, issue 10
2. Jörnvall H., Persson B., Jeffrey J.; Alcohol and polyol dehydrogenases are both divided into two protein types, and structural properties cross-relate the different enzyme activities within each type. Proc Natl Acad Sci USA.
3. Krook, M., Marekov, L., and Jörnvall, H. Purification and structural characterization of placental NAD⁺-linked 15-hydroxyprostaglandin dehydrogenase. The primary structure reveals the enzyme to belong to the short-chain alcohol dehydrogenase family. *Biochemistry* 29, 738-743 (1990).
4. H. Peltoketo, V. Isomaa, O. Mentausta, and R. Vihko. Complete amino acid sequence of human placental 17 β -hydroxysteroid dehydrogenase deduced from cDNA. *FEBS Letters*, 239(1):73-77, 1988.
5. Jörnvall H., Persson B., Krook M., Atrian S., Gonzales Duarte R., Jeffrey J., Ghosh D.; Short-chain dehydrogenases/reductases (SDR); *Biochemistry* 34 (1995) 6003-6013
6. Udo Oppermann, Charlotta Fillings, Malin Hult, Naeem Shafqat, Xiaoqi Wu, Monica Lindh, Jawed Shawqat, Erik Nordling, Yvonne Kallberg, Bengt Persson, Hans Jörnvall.; Short-chain dehydrogenases/reductases (SDR): the 2002 update. *Chemico-Biological Interactions* 143-144 (2003) 247-253
7. Kristan K, Deluca D, Adamski J, Stojan J, Lanišnik Rižner T; Dimerization and enzymatic activity of fungal 17 β -hydroxysteroid dehydrogenase from the short-chain dehydrogenase/reductase superfamily. *BMC Biochemistry*, 6:28, (2005)
8. Charlotta Fillings, Kurt D. Berndt, Jordi Benach, Stefan Knapp, Tim Prozorovski, Erik Nordling, Rudolf Ladenstein, Hans Jörnvall, Udo Oppermann.; Critical Residues for Structure and Catalysis in Short-chain Dehydrogenases/Reductases. *The Journal of Biological Chemistry*, Vol.277, No. 28, Issue of July 12, pp. 25677-25684, 2002
9. Bengt Persson, Yvonne Kallberg, Udo Oppermann, Hans Jörnvall.; Coenzyme-based functional assignment of short-chain dehydrogenases/reductases (SDRs). *Chemico-Biological Interactions* 143-144 (2003) 271-278.
10. Persson B., Bray J.E., Bruford E., Dellaporta S.L., Favia A., Gonzales Duarte R., Jörnvall, Kallberg, Kavangh K. L., Kedishvili N., Kisiela M., Maser E., Mindnich R., Orchard S., Penning T. M., Thornton J.M., Adamski J., Opperman U., The SDR (Short-Chain Dehydrogenase/Reductase and Related Enzymes) Nomenclature Initiative. *Chem Biol Interat.* 2009 March 16; 178(1-3): 94-98
11. Timson DJ "Functional analysis of disease-causing mutations in human UDP-galactose 4- epimerase. (December 2005) *FEBS J.* 272 (23): 6170-7

Literature

12. Moeller G, Adamski J: Integrated view on 17 β -hydroxysteroid dehydrogenases. In: *Mol Cell Endocrinol.* 301, S. 7-19
13. Agarwal AK (2004). "Cortisol metabolism and visceral obesity: role of 11 β -hydroxysteroid dehydrogenase type I enzyme and reduced co-factor NADPH.". *Endocr. Res.* 29 (4): 411-8.
14. Karlsson T, Vahlquist A, Kedishvili N, Törmä H. 13-cis-retinoic acid competitively inhibits 3 α -hydroxysteroid oxidation by retinol dehydrogenase RoDH-4: a mechanism for its anti-androgenic effects in sebaceous glands? *Biochem Biophys Res Commun.* 2003 Mar 28; 303(1):273-8.
15. Clish C.B., Levy B.D., Chiang N., Tai H.-H., Serhan C.N. "Oxidoreductases in lipoxin A4 metabolic inactivation: a novel role for 15-lipoxygenase 13-reductase/leukotriene B4 12-hydroxydehydrogenase in inflammation." *J. Biol. Chem.* 275:25372-25380(2000)
16. Ichinose H, Katoh S, Sueoka T, Titani K, Fujita K, Nagatsu T. Cloning and sequencing of cDNA encoding human sepiapterin reductase--an enzyme involved in tetrahydrobiopterin biosynthesis. *Biochem Biophys Res Commun.* 1991 Aug 30; 179(1):183-9.
17. Dahl HH, Hutchison W, McAdam W, Wake S, Morgan FJ, Cotton RG. Human dihydropteridine reductase: characterisation of a cDNA clone and its use in analysis of patients with dihydropteridine reductase deficiency. *Nucleic Acids Res.* 1987 Mar 11; 15(5):1921-32
18. Alphey M.S., Yu W., Byres E., Li D., Hunter W.N. "Structure and reactivity of human mitochondrial 2,4-dienoyl-CoA reductase: enzyme-ligand interactions in a distinctive short-chain reductase active site." *J. Biol. Chem.* 280:3068-3077(2005)
19. Cheng J.B., Russell D.W. "Mammalian wax biosynthesis: I. Identification of two fatty acyl-coenzyme A reductases with different substrate specificities and tissue distributions." *J. Biol. Chem.* 279:37789-37797(2004)
20. Marijanovic Z, Laubner D, Moller G, et al. (2004). "Closing the gap: identification of human 3-ketosteroid reductase, the last unknown enzyme of mammalian cholesterol biosynthesis.". *Mol. Endocrinol.* 17 (9): 1715-25
21. Rock Breton, Dominique Housset, Catherine Mazza and Juan Carlos Fontecilla-Camps. The structure of a complex of human 17 β -hydroxysteroid dehydrogenase with estradiol and NADP⁺ identifies two principal targets for the design of inhibitors. *Structure.* Volume 4, Issue 8, p905-915, 15 August 1996
22. Tanaka N, Nonaka T, Nakanishi M, Deyashiki Y, Hara A, Mitsui Y. Crystal structure of the ternary complex of mouse lung carbonyl reductase at 1.8 \AA resolution: the structural origin of coenzyme specificity in the short-chain dehydrogenase/reductase family. *Structure.* 1996 Jan 15;4(1):33-45

Literature

23. D. Deluca, G. Moller, A. Rosinus, W. Elger, A. Hillisch, J. Adamski, Inhibitory effects of fluorine-substituted estrogens on the activity of 17beta-hydroxysteroid dehydrogenases, *Mol Cell Endocrinol* 248(1-2) (2006) 218-224.
24. Dominga Deluca, Andreas Fritz, Rebekka Mindnich, Gabriele Möller and Jerzy Adamski.; Biochemical genetics of 17beta-hydroxysteroid dehydrogenases. *Current Topics in Steroid Research* Vol.4, 2004
25. Luigi Di Costanzo, Trevor M. Penning, and David W Christianson. Aldo-Keto Reductases in which the Conserved Catalytic Histidine is Substituted: *Chem Biol Interact* . 2009 March 16; 178(1-3): 127-133. doi:10.1016/j.cbi.2008.10.046
26. D.Hyndman, D.R. Bauman, Vladi V Heredia, T.M. Penning, The aldo-keto reductase superfamily homepage. *Chemico-Biological Interactions* 143-144 (2003) 621-631
27. Penning TM, Drury JE, Human aldo-keto reductases: Function, gene regulation, and single nucleotide polymorphisms. *Arch Biochem Biophys*. 2007 Aug 15; 464(2):241-50.
28. Anil K. Agarwal and Richard J. Auchus.; Minireview: Cellular Redox State Regulates Hydroxysteroid Dehydrogenase Activity and Intracellular Hormone Potency. *Endocrinology* 146(6):2531-2538
29. Anil K. Agarwal and Richard J. Auchus.; Minireview: Cellular Redox State Regulates Hydroxysteroid Dehydrogenase Activity and Intracellular Hormone Potency. *Endocrinology* 146(6):2531-2538
30. Wilson DK, Bohren KM, Gabbay KH, Quijcho FA (July 1992). "An unlikely sugar substrate site in the 1.65 Å structure of the human aldose reductase holoenzyme implicated in diabetic complications". *Science* 257 (5066): 81-4.
31. Tea Lanišnik Rižner and Trevor M. Penning. Role of Aldo-Keto Reductase Family 1 (AKR1) Enzymes in Human Steroid Metabolism. *Steroids*. 2014 January; 79: . doi:10.1016/j.steroids.2013.10.012.
32. Giménez-Dejóz J, Kolář MH, Ruiz FX, Crespo I, Cousido-Siah A, Podjarny A, Barski OA, Fanfrlík J, Parés X, Farrés J, Porté S. Substrate Specificity, Inhibitor Selectivity and Structure-Function Relationships of Aldo-Keto Reductase 1B15: A Novel Human Retinaldehyde Reductase. *PLoS One*. 2015 Jul 29;10(7):e0134506. doi: 10.1371/journal.pone.0134506. eCollection 2015.
33. Weber S, Salabei JK, Möller G, Kremmer E, Bhatnagar A, Adamski J, Barski OA. Aldo-keto Reductase 1B15 (AKR1B15): a mitochondrial human aldo-keto reductase with activity toward steroids and 3-keto-acyl-CoA conjugates. *J Biol Chem*. 2015 Mar 6;290(10):6531-45. doi: 10.1074/jbc.M114.610121
34. Gilbert, Scott F. (2000). "Juxtacrine Signaling". *Developmental biology* (6. ed.). Sunderland, Mass.: Sinauer Assoc.
35. F. Labrie. *Intracrinology*. *Mol Cell Endocrinol*, 78(3):113-118, 1991.

Literature

36. F.Labrie et al. The key role of 17 β -hydroxysteroid dehydrogenases in sex steroid biology. *Journal of Molecular Endocrinology* (2000) 25, 1-16
37. Nuclear Receptors Nomenclature Committee. A unified nomenclature system for the nuclear receptor superfamily. *Cell*. 1999; 97(2):161-3.
38. Novac N, Heinzl T. Nuclear receptors: overview and classification. *Curr Drug Targets Inflamm Allergy*. 2004; 3(4):335-46
39. Anthony W. Norman, Mathew T. Mizwicki and Derek P. G. Norman. Steroid-hormone rapid actions, membrane receptors and a conformational ensemble model. *Nature reviews*. Volume 3. January 2004, page: 27-41
40. Brigitte Boldyreff and Martin Wehling, Non-genomic actions of aldosterone: mechanisms and consequences in kidney cells. *Nephrol. Dial. Transplant.* (2003) Volume 18, Issue 9 Pp. 1693-1695
41. K. Kimura, M. Markowski, C. Bowen, and E.P. Gelmann. Androgen blocks apoptosis of hormone-dependent prostate cancer cells. *Cancer Res*, 61(July 15):5611-5618, 2001.
42. Lambert JJ1, Cooper MA, Simmons RD, Weir CJ, Belelli D. Neurosteroids: endogenous allosteric modulators of GABA(A) receptors. *Psychoneuroendocrinology*. 2009 Dec;34 Suppl 1:S48-58. doi: 10.1016/j.psyneuen.2009.08.009.
43. Lambert JJ, Belelli D, Hill-Venning C, Peters JA. Neurosteroids and GABAA receptor function. *Trends Pharmacol Sci*. 1995;16:295–303.
44. Trevor M. Penning, Michael E. Burczynski, Joseph M. Jez, Chien-Fu Hung, Hseuh-Kung Lin, Haiching Ma, Margaret Moore, Nisha Palackal and Kapila Ratman.; Human 3 α -hydroxysteroid dehydrogenase isoforms (AKR1C1-AKR1C4) of the aldo-keto reductase superfamily: functional plasticity and tissue distribution reveals roles in the inactivation of formation of male and female sex hormones. *Biochem. J.* (2000) 351, 67-77
45. T.M. Penning, Y. Jin, S. Steckelbroeck, T. Lanišnik Rižner, M. Lewis.; Structure-function of human 3 α -hydroxysteroid dehydrogenases: genes and proteins. *Molecular and Cellular Endocrinology* 215 (2004) 63-72.
46. Lachance Y, Luu-The V, Labrie C, Simard J, Dumont M, de Launoit Y, Guérin S, Leblanc G, Labrie F (February 1992). "Characterization of human 3 beta-hydroxysteroid dehydrogenase/delta 5-delta 4-isomerase gene and its expression in mammalian cells". *J. Biol. Chem.* 267 (5): 3551
47. Thomas JL, Boswell EL, Scaccia LA, Pletnev V, Umland TC. Identification of key amino acids responsible for the substantially higher affinities of human type 1 3beta-hydroxysteroid dehydrogenase/isomerase (3beta-HSD1) for substrates, coenzymes, and inhibitors relative to human 3beta-HSD2. *J Biol Chem*. 2005 Jun 3;280(22):21321-8. Epub 2005 Mar 28.

Literature

48. van Uum SH, Hermus AR, Smits P, Thien T, Lenders JW. The role of 11 beta-hydroxysteroid dehydrogenase in the pathogenesis of hypertension. *Cardiovasc Res.* 1998 Apr;38(1):16-24.
49. G. Moeller, J. Adamski, Multifunctionality of human 17beta-hydroxysteroid dehydrogenases, *Mol Cell Endocrinol* 248(1-2) (2006) 47-55
50. Shen Zhongyi, Pia Rantakari, Tarja Lamminen, Jorma Toppari, and Matti Poutanen, Transgenic Male Mice Expressing Human Hydroxysteroid Dehydrogenase 2 Indicate a Role for the Enzyme Independent of Its Action on Sex Steroids, *Endocrinology* 148(8):3827–3836
51. Nabil Moghrabi, Ieuan A. Huges, Andrea Dunaif and Stefan Andersson,; Deleterious Missense Mutations and Silent Polymorphism in the Human 17 β -Hydroxysteroid Dehydrogenase 3 Gene (HSD17B3). *The journal of Clinical endocrinology & metabolism.* Vol 83, No. 8 2855-2860, 1998
52. Adamski, J., Normand, T., Leenders, F., Monte, D., Begue, A., Stehelin, D., Jungblut, P.W. & de Launoit, Y. Molecular cloning of a novel widely expressed human 80 kDa 17 β -hydroxysteroid dehydrogenase. (1995) *Biochem. J.* 311, 437-43.
53. Olga V. Belyaeva, Sergei V. Chetyrkin, Amy L. Clark, Natalia V. Kostereva, Karen S. SantaCruz, Bibie M. Chronwall, and Natalia Y. Kedishvili. Role of Microsomal Retinol/Sterol Dehydrogenase-Like Short-Chain Dehydrogenases/Reductase in the Oxidation and Epimerization of 3 α -Hydroxysteroids in Human Tissues. *Endocrinology*, 2007 May; 148(5):2148-2156
54. Moeller G, Leenders F, van Grunsven EG, Dolez V, Qualmann B, Kessels MM, Markus M, Krazeisen A, Husen B, Wanders RJ, de Launoit Y, Adamski J (1999) Characterization of the HSD17B4 gene: D-specific multifunctional protein 2/17beta-hydroxysteroid dehydrogenase IV. *J Steroid Biochem Mol Biol* 69(1-6):441-446.
55. Michael C. Byrns, Ling Duan, Seon Hwa Lee, Ian A. Blair, and Trevor M. Penning, Aldo-Keto Reductase 1C3 Expression in MCF-7 Cells Reveals Roles in Steroid Hormone and Prostaglandin Metabolism that may Explain its Over-Expression in Breast Cancer. *J Steroid Biochem Mol Biol.* 2010 February 15; 118(3): 177. doi:10.1016/j.jsbmb.2009.12.009
56. Michael C. Byrns, Rebekka Mindnich, Ling Duan, and Trevor M. Penning, Overexpression of Aldo-Keto Reductase 1C3 (AKR1C3) in LNCaP Cells Diverts Androgen Metabolism towards Testosterone Resulting in Resistance to the 5 α -Reductase Inhibitor Finasteride. *J Steroid Biochem Mol Biol.* 2012 May; 130(1-2): 7–15. doi:10.1016/j.jsbmb.2011.12.012.
57. Biswas M.G. and Russell D.W. Expression cloning and characterization of oxidative 17beta- and 3alpha-hydroxysteroid dehydrogenases from rat and human prostate. *J Biol Chem.* 1997 Jun 20;272(25):15959-66.

Literature

58. Huang XF, Luu-The V. Gene structure, chromosomal localization and analysis of 3-ketosteroid reductase activity of the human 3(α - \rightarrow β)-hydroxysteroid epimerase. *Biochim Biophys Acta*. 2001 Aug 30;1520(2):124-30.
59. Krazeisen A, Breitling R, Imai K, Fritz S, Möller G, Adamski J. Determination of cDNA, gene structure and chromosomal localization of the novel human 17 β -hydroxysteroid dehydrogenase type 7(1). *FEBS Lett*. 1999 Oct 29; 460(2):373-9.
60. Julia Fomitcheva, Michael E. Baker, Everett Anderson, Gloria Y. Lee, and Nazneen Aziz. ; Characterization of Ke 6, a New 17 β -Hydroxysteroid Dehydrogenase, and Its Expression in Gonadal Tissue. (1998)
61. Ohno S., Nishikawa K., Honda Y., Nakajin S., Expression in *E. coli* and tissue distribution of the human homologue of the mouse Ke 6 gene, 17 β -hydroxysteroid dehydrogenase type 8. *Mol. Cell. Biochem*. 309:209-215(2008)
62. Rajaram Venkatesan, Shiv K. Sah-Teli, Luqman O. Awoniyi, Guangyu Jiang, Piotr Prus, Alexander J. Kastaniotis, J. Kalervo Hiltunen, Rik K. Wierenga Zhijun Chen, Insights into mitochondrial fatty acid synthesis from the structure of heterotetrameric 3-ketoacyl-ACP reductase/3R-hydroxyacyl-CoA dehydrogenase; *Nature Communications*, 5, Article no. 4805, 2014
63. J Su; M Lin; J L Napoli, Complementary deoxyribonucleic acid cloning and enzymatic characterization of a novel 17 β /3 α -hydroxysteroid/retinoid short chain dehydrogenase/reductase. *Endocrinology* 1999 Vol: 140:5275-5284
64. Napoli JL. 17 β -Hydroxysteroid dehydrogenase type 9 and other short-chain dehydrogenases/reductases that catalyze retinoid, 17 β - and 3 α -hydroxysteroid metabolism. *Mol Cell Endocrinol*. 2001 Jan 22; 171(1-2):103-9.
65. Song-Yu Yang, Xue-Ying He Horst Schulz; Multiple functions of type 10 17 β -hydroxysteroid dehydrogenase; *Trends in Endocrinology & Metabolism*, Volume 16, Issue 4, 167-175, 1 May 2005
66. Brereton P, Suzuki T, et al. Pan1b (17 β HSD11)-enzymatic activity and distribution in the lung. *Mol Cell Endocrinol*. 2001;171(1-2):111-7.
67. Yasuyuki Fujimoto, Hiroyuki Itabe, Jun Sakai, Minoru Makita, Junich Noda, Masahiro Mori, Yusuke Higashi, Shinichi Kojima, Tatsuya Takano, Identification of major proteins in the lipid droplet-enriched fraction isolated from the human hepatocyte cell line HuH7, *Biochimica et Biophysica Acta* 1644 (2004) 47– 59.
68. Moon YA, Horton JD. Identification of two mammalian reductases involved in the two-carbon fatty acyl elongation cascade. *J Biol Chem*. 2003 Feb 28; 278(9):7335-43. Epub 2002 Dec 13.
69. Luu-The, P. Tremblay, F. Labrie, Characterization of type 12 17 β -hydroxysteroid dehydrogenase, an isoform of type 3 17 β -hydroxysteroid dehydrogenase responsible for estradiol formation in women, *Mol Endocrinol* 20(2) (2006) 437-443.

Literature

70. Liu S, Huang C, Li D, Ren W, Zhang H, Qi M, Li X, Yu L. Molecular cloning and expression analysis of a new gene for short-chain dehydrogenase/reductase 9. *Acta Biochim Pol.* 2007;54(1):213-8. Epub 2007 Feb 20.
71. Yuka Horiguchi, Makoto Araki, Kiyoto Motojima, 17 β -Hydroxysteroid dehydrogenase type 13 is a liver-specific lipiddroplet-associated protein. *Biochemical and Biophysical Research Communications* 370 (2008) 235–238
72. Lukacik P, Keller B, Bunkoczi G, Kavanagh KL, Lee WH, Adamski J, Oppermann U.; Structural and biochemical characterization of human orphan DHRS10 reveals a novel cytosolic enzyme with steroid dehydrogenase activity. *Biochem J.* 2007 Mar 15; 402(3):419-27.
73. W. Bollag, E.E.Holdener; Retinoids in cancer prevention and therapy. *Annals of Oncology* 3: 513-526, 1992.
74. Wade Smith, Nabil Saba, *Critical Reviews in Oncology / Hematology* Volume 55, Issue 2 , Pages 143-152, August 2005
75. Chetyrkin SV, Hu J, Gough WH, Dumauual N, Kedishvili NY. Further characterization of human microsomal 3 α -hydroxysteroid dehydrogenase. *Arch Biochem Biophys.* 2001 Feb 1;386(1):1-10.
76. Massengo-Tiassé R.P., and Cronan J.E., 2007, *Vibrio cholerae* fabV defines a new class of enoyl acyl-carrier-protein reductase, *The Journal of Biological Chemistry*, 283(3): 1308-1316 doi:10.1074/jbc.M708171200 PMID:18032386
77. Massengo-Tiassé R.P., and Cronan J.E., 2009, Diversity in enoyl-acyl carrier protein reductases, *Cell Mol. Life Sci.*, 66(9): 1507-1517 doi:10.1007/s00018-009-8704-7 PMID:19151923 PMCID:281991
78. J. Kalervo Hiltunen, Melissa S. Schonauer, Kaija J. Autio, Telsa M. Mittelmeier, Alexander J. Kastaniotis, and Carol L. Dieckmann Mitochondrial Fatty Acid Synthesis Type II: More than Just Fatty Acids. *J Biol Chem.* Apr 3, 2009; 284(14): 9011-9015.
79. Keller B, Search for new steroid hormone metabolizing enzyme: functional genomics of the short-chain dehydrogenase/reductase superfamily, PhD Thesis, 2006
80. Huang Y, Tang R, Dai J, Gu S, Zhao W, Cheng C, Xu M, Zhou Z, Ying K, Xi Y, Mao Y. A novel human hydroxysteroid dehydrogenase like 1 gene (HSDL1) is highly expressed in reproductive tissues *Mol Biol Rep.* 2001; 28(4):185-91.
81. Meier M, Tokarz J, Haller F, Mindnich R, Adamski J. Human and zebrafish hydroxysteroid dehydrogenase like 1 (HSDL1) proteins are inactive enzymes but conserved among species. *Chem Biol Interact.* 2009 Mar 16; 178(1-3):197-205. doi: 10.1016/j.cbi.2008.10.036. Epub 2008 Nov 5
82. Taija Saloniemi, Heli Jokela, Leena Strauss, Pirjo Pakarinen, Matti Poutanen, The diversity of sex steroid action: novel functions of hydroxysteroid (17 β) dehydrogenases

Literature

- as revealed by genetically modified mouse models. *J Endocrinol* January 1, 2012 212 27-40
83. Wake DJ, Walker BR. 11 beta-hydroxysteroid dehydrogenase type 1 in obesity and the metabolic syndrome. *Mol Cell Endocrinol*. 2004 Feb 27; 215(1-2):45-54.
84. Steven Huyghe, Guy P. Mannaerts, Myriam Baes, Paul P. Van Veldhoven. Peroxisomal multifunctional protein-2: The enzyme, the patients and the knockout mouse model. *Biochimica et Biophysica Acta (BBA) - Molecular and Cell Biology of Lipids*. Volume 1761, Issue 9, September 2006, Pages 973-994
85. Shehu A, Mao J, Gibori GB, Halperin J, Le J, Devi YS, Merrill B, Kiyokawa H, Gibori G. Prolactin receptor-associated protein/17beta-hydroxysteroid dehydrogenase type 7 gene (*Hsd17b7*) plays a crucial role in embryonic development and fetal survival. *Mol Endocrinol*. 2008 Oct;22(10):2268-77. doi: 10.1210/me.2008-0165. Epub 2008 Jul 31
86. Wohlers TM, Christacos NC, Harreman MT, Fridovich-Keil JL. Identification and characterization of a mutation, in the human UDP-galactose-4-epimerase gene, associated with generalized epimerase-deficiency galactosemia. *Am. J. Hum. Genet*. 1999 Feb; 64(2):462-70.
87. Jacques Simard, Anne Marie Moisan, Yves More. Congenital Adrenal Hyperplasia due to 3?-Hydroxysteroid Dehydrogenase/ ?5-?4 Isomerase Deficiency. *Semin Reprod Med* 2002; 20(3): 255-276
88. Palermo M, Quinkler M, Stewart PM. Apparent mineralocorticoid excess syndrome: an overview. *Arq Bras Endocrinol Metabol*. 2004 Oct;48(5):687-96. Epub 2005 Mar 7.
89. Annemie L. M. Boehmer, Albert O. Brinkmann, Lodewijk A. Sandukujl, Dicky J. J. Halley, Martinus F. Niermeijer, Stefan Andersson, Frank H. de Jong, Hülya Kayserili, Monique A. de Vroede, Barto J. Otten, Catrienus W. Rouwe, Berenice B. Mendonça, Cidade Rodrigues, Hans H. Bode, Petra E. de Ruiter, Henriette A. Delemarre-van de Waal, and Stenvert L.S. Drop.; 17 β -Hydroxysteroid Dehydrogenase-3 Deficiency: Diagnosis, Phenotypic Variability, Population Genetics, and Worldwide Distribution of Ancient and de Novo Mutations. *The Journal of Clinical Endocrinology & Metabolism*. Vol.84, No. 12, 1999
90. Stefan Andersson, Wayne M. Geissler, Ling Wu, Daphne L. Davis, Melvin M. Grumbach, Maria I. New, Hans P. Schwarz, Sandra L. Blethen, Berenice B. Mendonca, Walter Bloise, Selma F. Witchel, Gordon B. Cutler, Jr.; James E. Griffin, Jean D. Wilson, David W. Russel. Molecular Genetics and Pathophysiology of 17 β -Hydroxysteroid Dehydrogenase 3 Deficiency. *Journal of Clinical Endocrinology and Metabolism* Vol. 81, No. 1, 1996
91. J. Ramón Bilbao, Liliane Loridan, Laura Audí, Encarnación Gonzalo and Luis Castaño.; A novel missense (R80W) mutation in 17- β -hydroxysteroid dehydrogenase type 3 gene associated with male pseudohermaphroditism. *European Journal of Endocrinology* (1998) 139, 330-333
92. Pierce SB, Walsh T, Chisholm KM, Lee MK, Thornton AM, Fiumara A, Opitz JM, Levy-Lahad E, Klevit RE, King MC. Mutations in the DBP-deficiency protein HSD17B4 cause

Literature

- ovarian dysgenesis, hearing loss, and ataxia of Perrault Syndrome. *Am J Hum Genet.* 2010 Aug 13;87(2):282-8.
93. de Launoit, Y., Adamski J : Unique multifunctional HSD17B4 gene product: 17beta-hydroxysteroid dehydrogenase 4 and D-3-hydroxyacyl-coenzyme A dehydrogenase/hydratase involved in Zellweger syndrome. . *J. Mol. Endocrinol.* (1999)
94. Jones MR, Italiano L, Wilson SG, Mullin BH, Mead R, Dudbridge F, Watts GF, Stuckey BG, Polymorphism in HSD17B6 is associated with key features of polycystic ovary syndrome. *Fertil Steril.* 2006 Nov;86(5):1438-46
95. Tom S. Kim, Akiko Maeda, Tadao Maeda, Cynthia Heinlein, Natalia Kedishvili, Krzysztof Palczewski and Peter S. Nelson. Delayed Dark Adaptation in 11-cis-Retinol Dehydrogenase-deficient Mice. A role of rdh11 in visual processes in vivo. *J.Biol.Chem.* 2005, 280:8694-8704.
96. Konig, A., Happle, R., Bornholdt, D., Engel, H., Grzeschik, K.-H. Mutations in the NSDHL gene, encoding a 3-beta-hydroxysteroid dehydrogenase, cause CHILD syndrome. *Am. J. Med. Genet.* 90: 339-346, 2000
97. Clot F, Grabli D, Cazeneuve C, Roze E, Castelnau P, Chabrol B, Landrieu P, Nguyen K, Ponsot G, Abada M, Doummar D, Damier P, Gil R, Thobois S, Ward AJ, Hutchinson M, Toutain A, Picard F, Camuzat A, Fedirko E, Sân C, Bouteiller D, LeGuern E, Durr A, Vidailhet M, Brice A; French Dystonia Network. Exhaustive analysis of BH4 and dopamine biosynthesis genes in patients with Dopa-responsive dystonia. *Brain.* 2009 Jul;132(Pt 7):1753-63
98. Anagnostis P, Athyros VG, Tziomalos K, Karagiannis A, Mikhailidis DP (2009). "Clinical review: The pathogenetic role of cortisol in the metabolic syndrome: a hypothesis". *The Journal of Clinical Endocrinology and Metabolism* 94 (8): 2692–2701
99. Classen-Houben D., Schuster D., Da Cunha T., Odermatt A., Wolber G., Jordis U., Kueenburg B., Selective inhibition of 11beta-hydroxysteroid dehydrogenase 1 by 18alpha-glycyrrhetic acid but not 18beta-glycyrrhetic acid. *The Journal of steroid biochemistry and molecular biology* 03/2009; 113(3-5):248-52
100. He XY, Wen GY, Merz G, Lin D, Yang YZ, Mehta P, Schulz H, Yang SY. Abundant type 10 17 beta-hydroxysteroid dehydrogenase in the hippocampus of mouse Alzheimer's disease model. *Brain Res Mol Brain Res.* 2002 Feb 28; 99(1):46-53.
101. Shen Z, Peng Z, Sun Y, Väänänen HK, Poutanen M., Overexpression of human hydroxysteroid (17beta) dehydrogenase 2 induces disturbance in skeletal development in young male mice. *J Bone Miner Res.* 2008 Aug;23(8):1217-26
102. Wetzell M, Gargano EM, Hinsberger S, Marchais-Oberwinkler S, Hartmann RW. Discovery of a new class of bicyclic substituted hydroxyphenylmethanones as 17β-hydroxysteroid dehydrogenase type 2 (17β-HSD2) inhibitors for the treatment of osteoporosis. *Eur J Med Chem.* 2012 Jan;47(1):1-17

Literature

103. Brian E. Henderson and Heather Spencer Feigelson, Hormonal carcinogenesis. *Carcinogenesis* vol.21 no.3 pp.427–433, 2000
104. Lena Secky, Martin Svoboda, Lukas Klameth, Erika Bajna, Gerhard Hamilton, Robert Zeillinger, Walter Jäger, and Theresia Thalhammer. The Sulfatase Pathway for Estrogen Formation: Targets for the Treatment and Diagnosis of Hormone-Associated Tumors. *Journal of Drug Delivery* Volume 2013, Article ID 957605
105. Fernand Labrie, Richard Poulin, Jacques Simard, Hui Fen Zhao, Claude Labrie, Sophie Dauvois, Martine Dumont, Anne-Catherine Hatton, Donald Poirier and Yves Mérand Interactions between Estrogens, Androgens, Progestins, and Glucocorticoids in ZR-75-1 Human Breast Cancer Cells. *Annals of the New York Academy of Sciences*, Volume 595, pages 130–148, June 1990
106. Padma Marwah, Ashok Marwah, Henry A. Lardy, Hiroshi Miyamoto and Chawnsiang Chang C19-Steroids as androgen receptor modulators: Design, discovery, and structure-activity relationship of new steroidal androgen receptor antagonists; *Bioorganic & Medicinal Chemistry* 14 (2006) 5933–5947
107. Takashi Suzuki, Hironobu Sasano, Stefan Andersson, J. Ian Mason; 3β -Hydroxysteroid Dehydrogenase/ $\Delta 5$ -4-Isomerase Activity Associated with the Human 17β -Hydroxysteroid Dehydrogenase Type 2 Isoform. *The Journal of Clinical Endocrinology & Metabolism*, Vol. 85, No.10
108. André G. Oliveira, Polyanna H. Coelho, Fernanda D. Guedes, Germán A.B. Mahecha, Rex A. Hess, Cleida A. Oliveira. 5α -Androstane- $3\beta,17\beta$ -diol (3β -diol), an estrogenic metabolite of 5α -dihydrotestosterone, is a potent modulator of estrogen receptor ER β expression in the ventral prostate of adult rats. *Steroids*, Volume 72, Issue 14, December 2007, Pages 914–922
109. Selvaraj Muthusamy, Stefan Andersson, Hyun-Jin Kima, Ryan Butlera, Linda Waageb, Ulf Bergerheimb, and Jan-Åke Gustafsson, Estrogen receptor β and 17β -hydroxysteroid dehydrogenase type 6, a growth regulatory pathway that is lost in prostate cancer. *PNAS* December 13, 2011 vol. 108 no. 50, 20090–20094
110. James L. Mohler, Mark A. Titus, Suxia Bai, Brian J. Kennerley, Fred B. Lih, Kenneth B. Tomer, and Elizabeth M. Wilson. Activation of the Androgen Receptor by Intratumoral Bioconversion of Androstanediol to Dihydrotestosterone in Prostate Cancer. *Cancer Res*; 71(4); 1486–96. 2011 AACR.
111. James L. Mohler, Mark A. Titus, and Elizabeth M. Wilson, Potential prostate cancer drug target: Bioactivation of androstanediol by conversion to dihydrotestosterone. *Clin Cancer Res*. 2011 September 15; 17(18): 5844–5849. doi:10.1158/1078-0432.CCR-11-0644.
112. Suzuki T, Moriya T, Ariga N, Kaneko C, Kanazawa M & Sasano H (2000) 17β -Hydroxysteroid dehydrogenase type 1 and type 2 in human breast carcinoma: a correlation to clinicopathological parameters. *British Journal of Cancer* 82 518–523

Literature

113. Karageorgi S, McGrath M, Lee IM, Buring J, Kraft P, De Vivo I. Polymorphisms in genes hydroxysteroid-dehydrogenase-17b type 2 and type 4 and endometrial cancer risk. *Gynecol Oncol.* 2011 Apr; 121(1):54-8.
114. Juliette A Aka, Mouna Zerradi, François Houle, Jacques Huot and Sheng-Xiang Lin 17beta-hydroxysteroid dehydrogenase type 1 modulates breast cancer protein profile and impacts cell migration. *Breast Cancer Research* 2012,14:R92
115. Koh E, Noda T, Kanaya J & Namiki M (2002) Differential expression of 17β-hydroxysteroid dehydrogenase isozyme genes in prostate cancer and noncancer tissues. *Prostate* 53 154–159.
116. Rasiah KK, Gardiner-Garden M, Padilla EJ, Möller G, Kench JG, Alles MC, Eggleton SA, Stricker PD, Adamski J, Sutherland RL, Henshall SM, Hayes VM HSD17B4 overexpression, an independent biomarker of poor patient outcome in prostate cancer. *Mol Cell Endocrinol.* 2009 Mar 25; 301(1-2):89-96167.
117. K-M Fung, E N S Samara, C wong, A Metwalli, R Krlin, B Bane, C Z Liu, J T Yang, J V Pitha, D J Culcin, B P Kropp, T M Penning, Hsueh-Kung Lin.; Increased expression of type 2 3α-hydroxysteroid dehydrogenase (AKR1c3) and its relationship with androgen receptor in prostate carcinoma. 2006
118. Marcus Quinkler, Binayak Sinha, Jeremy W. Tomlinson, Iwona J. Bujalska, Paul M. Steward and Wiebke Artl.; Androgen Generation in Adipose Tissue in Women with Simple Obesity- A Site-Specific Role for 17β-Hydroxysteroid Dehydrogenase Type 5.
119. Julian C. Desmond, Joanne C. Mountford, Mark T. Drayson, Elisabeth A. Walker, Martin Hewison, Jonathan P. Ride, Quang T. Luong, Rachel E. Hayden, Elio F. Vanin, and Christopher M. Bunce.; The Aldo-Keto Reductase AKR1C3 is a Novel Suppressor of Cell Differentiation That Provides a Plausible Target for the Non-Cyclooxygenase-dependent Antineoplastic Actions of Nonsteroidal Anti-Inflammatory Drugs. *Cancer Research* 63, 505-512, January 15, 2003
120. Yuantong Tian, Lijing Zhao, Haitao Zhang, Xichun Liu, Lijuan Zhao, Xuejian Zhao, Yi Li and Jing Li. AKR1C3 overexpression may serve as a promising biomarker for prostate cancer progression. *Diagn Pathol.* 2014; 9: 42. doi: 10.1186/1746-1596-9-42
121. Shehu A, Albarracin C, Devi YS, Luther K, Halperin J, Le J, Mao J, Duan RW, Frasor J, Gibori G. The stimulation of HSD17B7 expression by estradiol provides a powerful feed-forward mechanism for estradiol biosynthesis in breast cancer cells. *Mol Endocrinol.* 2011 May; 25(5):754-66.
122. Mirja Rotinen, Joaquín Villar, Jon Celay, Irantzu Serrano, Vicente Notario, and Ignacio Encío, Transcriptional Regulation of Type 11 17β-Hydroxysteroid Dehydrogenase Expression in Prostate Cancer Cells. *Mol Cell Endocrinol.* Jun 6, 2011; 339(1-2): 45–53.
123. Tove Sivik, Cecilia Gunnarsson, Tommy Fornander, Bo Nordenskjöld, Lambert Skoog, Olle Stål, Agneta Jansson. 17β-Hydroxysteroid dehydrogenase type 14 is a predictive marker for tamoxifen response in oestrogen receptor positive breast cancer. *PLoS One* 2012 6; 7(7):e40568. Epub 2012 Jul 6

Literature

124. Elahe A. Mostaghel. Steroid hormone synthetic pathways in prostate cancer Transl. Androl Urol. Sept 2013; 2(3): 212-227
125. Stanbrough M, Bubley GJ, Ross K, et al. Increased expression of genes converting adrenal androgens to testosterone in androgen-independent prostate cancer. *Cancer Res* 2006;66:2815-25
126. Fung KM, Samara EN, Wong C, et al. Increased expression of type 2 3alpha-hydroxysteroid dehydrogenase/type 5 17beta-hydroxysteroid dehydrogenase (AKR1C3) and its relationship with androgen receptor in prostate carcinoma. *Endocr Relat Cancer* 2006;13: 169-80.
127. Lin HK, Steckelbroeck S, Fung KM, et al. Characterization of a monoclonal antibody for human aldo-keto reductase AKR1C3 (type 2 3a-hydroxysteroid dehydrogenase/type 5 17b-hydroxysteroid dehydrogenase); immunohistochemical detection in breast and prostate. *Steroids* 2004;69:795-801
128. Ohno S, Nakajima Y & Nakajin S 2005 Triphenyltin and tributyltin inhibit pig testicular 17β-hydroxysteroid dehydrogenase activity and suppress testicular testosterone biosynthesis. *Steroids* 70 645–651.
129. Thomas E. Spires, Brian E. Fink, Ellen K. Kick, Dan You, Cheryl A. Rizzo, Ivone Takenaka, R. Michael Lawrence, Zheming Ruan, Mark E. Salvati, Gregory D. Vite, Roberto Weinmann, Ricardo M. Attar, Marco M. Gottardis, and Matthew V. Lorenzi. Identification of Novel Functional Inhibitors of 17b Hydroxysteroid Dehydrogenase Type III (17b-HSD3). *The Prostate* 65:159 170 (2005).
130. Tchédam Ngatcha B, Luu-The V, Labrie F, Poirier D. Androsterone 3alpha-ether-3beta-substituted and androsterone 3beta-substituted derivatives as inhibitors of type 3 17beta-hydroxysteroid dehydrogenase: chemical synthesis and structure-activity relationship. *J Med Chem.* 2005 Aug 11; 48(16):5257-68.
131. Le Lain R, Barrell KJ, Saeed GS, Nicholls PJ, Simons C, Kirby A & Smith HJ 2002 Some coumarins and triphenylethene derivatives as inhibitors of human testes microsomal 17β-hydroxysteroid dehydrogenase (17β-HSD type 3): further studies with tamoxifen on the rat testes microsomal enzyme. *Journal of Enzyme Inhibition and Medicinal Chemistry* 17 93–100.
132. Lorenzi MV, Rizzo CA, You D, et al. In vivo suppression of testosterone biosynthesis with a novel series of non-steroidal 17β-hydroxysteroid dehydrogenase type III (17β-HSD3) inhibitors. *AACR Meeting Abstracts.* 2005;2005(1):605-a
133. Brozic P, Golob B, Gomboc N, et al. Cinnamic acids as new inhibitors of 17beta-hydroxysteroid dehydrogenase type 5 (akr1c3) *Mol Cell Endocrinol.* 2006; 248(1–2):233–235.
134. Le Bail JC, Champavier Y, Chulia AJ, Habrioux G. Effects of phytoestrogens on aromatase, 3beta and 17beta-hydroxysteroid dehydrogenase activities and human breast cancer cells. *Life Sci.* 2000 Feb 25; 66(14):1281-91.

Literature

135. Michael C. , Stephan Steckelbroeck, Trevor M. Penning.; An indomethacin analogue, N-(4-chlorobenzoyl)-melatonin is a selective inhibitor of aldo-keto reductase 1C3 (type2 3 β -HSD, type 5 17 β -HSD, and prostaglandin F synthase), a potential target for the treatment of hormone dependent and hormone independent malignancies. *Biochemical Pharmacology*, 2007
136. Joanna M Day, Helena J. Tutill, Atul Purohit and Michael J Reed. Design and validation of specific inhibitors of 17 β -hydroxysteroid dehydrogenases for therapeutic application in breast and prostate cancer, and in endometriosis. *Endocrine-Related Cancer* (2008) 15 665-692.
137. Donald Poirier; Inhibitors of 17 β -Hydroxysteroid Dehydrogenases. *Current Medical Chemistry*, 2003, 10, 453-477
138. Day JM, Foster PA, Tutill HJ, Schmidlin F, Sharland CM, Hargrave JD, Vicker N, Potter BV, Reed MJ, Purohit A. STX2171, a 17 β -hydroxysteroid dehydrogenase type 3 inhibitor, is efficacious in vivo in a novel hormone-dependent prostate cancer model. *Endocr Relat Cancer*. 2013 Feb 18; 20(1):53-64. doi: 10.1530/ERC-12-0231
139. Roy J, Fournier MA, Maltais R, Kenmogne LC, Poirier D. Reprint of "In vitro and in vivo evaluation of a 3 β -androsterone derivative as inhibitor of 17 β -hydroxysteroid dehydrogenase type 3". *J Steroid Biochem Mol Biol*. 2015 Sep; 153:170-8. doi: 10.1016/j.jsbmb.2015.08.014
140. Flanagan JU, Atwell GJ, Heinrich DM, Brooke DG, Silva S, Rigoreau LJ, Trivier E, Turnbull AP, Raynham T, Jamieson SM, Denny WA. Morpholylureas are a new class of potent and selective inhibitors of the type 5 17- β -hydroxysteroid dehydrogenase (AKR1C3). *Bioorg Med Chem*. 2014 Feb 1; 22(3):967-77. doi: 10.1016/j.bmc.2013.12.050
141. Kikuchi A, Furutani T, Azami H, Watanabe K, Niimi T, Kamiyama Y, Kuromitsu S, Baskin-Bey E, Heeringa M, Ouatas T, Enjo K. In vitro and in vivo characterisation of ASP9521: a novel, selective, orally bioavailable inhibitor of 17 β -hydroxysteroid dehydrogenase type 5 (17 β HSD5; AKR1C3). *Invest New Drugs*. 2014 Oct; 32(5):860-70. doi: 10.1007/s10637-014-0130-5. Epub 2014 Jul 1.
142. Michael C. Byrns, Yi Jin, and Trevor M. Penning, Inhibitors of Type 5 17 β Hydroxysteroid Dehydrogenase (AKR1C3): Overview and Structural Insights. *J Steroid Biochem Mol Biol*. 2011 May; 125(1-2): 95–104. doi:10.1016/j.jsbmb.2010.11.004
143. Mäkelä S, Poutanen M, Lehtimäki J, Kostian ML, Santti R, Vihko R. Estrogen-specific 17 beta-hydroxysteroid oxidoreductase type 1 (E.C. 1.1.1.62) as a possible target for the action of phytoestrogens. *Proc Soc Exp Biol Med*. 1995 Jan; 208(1):51-9.
144. A.Krazeisen, R. Breitling, G. Möller, J. Adamski.; Phytoestrogens inhibit human 17 β -hydroxysteroid dehydrogenase type 5. *Molecular and Cellular Endocrinology* 171 (2001) 151-162

Literature

145. Trottier A, Maltais R, Poirier D. Identification of a first enzymatic activator of a 17 β -hydroxysteroid dehydrogenase. *ACS Chem Biol*. 2014 Aug 15;9(8):1668-73. doi: 10.1021/cb500109e. Epub 2014 Jun 9.
146. René Maltais, Alexandre Trottier, Audrey Delhomme, Xavier Barbeau, Patrick Lagüe, Donald Poirier. Identification of fused 16 β ,17 β -oxazinone-estradiol derivatives as a new family of non-estrogenic 17 β -hydroxysteroid dehydrogenase type 1 inhibitors. *European Journal of Medicinal Chemistry*, Volume 93, 26 March 2015, Pages 470–480
147. Dufort I, Rheault P, Huang X-F, Soucy P & Luu-The V 1999 Characteristics of a highly labile human type 5 17 β - hydroxysteroid dehydrogenase. *Endocrinology* 140 568–574.
148. Dominic J. Yee, Vojtech Balsanek, Dalibor Sames. New tools for molecular imaging of redox metabolism: development of a fluorogenic probe for 3 α -Hydroxysteroid Dehydrogenases. *J.AM.CHEM.SOC*, 2004, 126, 2282-2283
149. Naveed Khan, Kamalesh K. Sharma, Stefan Andersson, and Richard J. Auchus.; Human 17 β -hydroxysteroid dehydrogenases types 1,2 and 3 catalyze bi-directional equilibrium reactions, rather than unidirectional metabolism, in HEK-293 cells. *Archives of Biochemistry and Biophysics* 429 (2004) 50-59.
150. Johan Edquist, Kristina Blomquist, Fusion and Fission, the Evolution of Sterol Carrier Protein-2. *J Mol Evol* (2006) 62:292-306
151. Dai,J. Li,P.,Ji,Ch.Feng,C., Gui,M. Sun,Y.,Zhang,J. Zhu, J.Dou, Sh. Gu,Y. Xie,Y. Mao,Y. Cloning and characterization of a novel mouse short chain dehydrogenase/reductase cDNA mHsd12#, encoding a protein with a SDR domain and a SCP2 domain. *Molekularnaja biologija*, 2005 Moscow, 39, No 5, 799-805
152. Jianfeng Dai, Yi Xie, QihanWu, LiuWang, Gang Yin, Xin Ye,Li Zeng, Jian Xu, Chaoneng Ji, Shaohua Gu, Qingshan Huang,Robert Chunhua Zhao, and Yumin Mao ;Molecular Cloning and Characterization of a Novel Human Hydroxysteroid Dehydrogenase-Like 2 (HSDL2) cDNA from Fetal Brain. *Biochemical Genetics*, 2003. 41 (5): p. 165-17
153. Schuster, D. ; Kowalik, D. ; Kirchmair, J. ; Laggner, C. ; Markt, P. ; Aebischer-Gumy, C.; Ströhle, F. ; Möller, G. ; Wolber, G. ; Wilckens, T. ; Langer, T. ; Odermatt, A. ; Adamski, J. Identification of chemically diverse, novel inhibitors of 17 β -hydroxysteroid dehydrogenase type 3 and 5 by pharmacophore-based virtual screening. *J. Steroid Biochem. Mol. Biol.* 125, 148-161 (2011)
154. Cheng Y, Prusoff WH. Relationship between the inhibition constant (K1) and the concentration of inhibitor which causes 50 per cent inhibition (I50) of an enzymatic reaction. *Biochem Pharmacol*. 1973 Dec 1;22(23):3099-108
155. Trevor M. Penning, Michael C. Byrns.; Steroid Hormone transforming aldo-keto reductases and cancer. *Annals of the New York Academy of Sciences*, (2009) Volume 1155 Issue Steroid Enzymes and Cancer, pages 33-42
156. Stanislav Gobec, Petra Brožic, Tea Rižner.; Nonsteroidal anti-inflammatory drugs and their analogues as inhibitors of aldo-keto reductase AKR1C3: new lead compounds for the

Literature

- development of anticancer agents. *Bioorganic & Medical Chemistry Letters* 15 (2005) 5170-5175
157. Wei Qui, Ming Zhou, Mausumi MAzumdar, Arezki Azzi, Dalila Ghanmi, Van Luu-The, Fernand Labrie, and Sheng-Xiang Lin.; Structure-Based Inhibitor Design for an Enzyme which Binds Different Steroids: a Potent Inhibitor for Human Type 5 17 β -Hydroxysteroid Dehydrogenase. *The Journal of Biological Chemistry* Vol. 282, No. 11, pp. 8368-8379, March 16, 2007.
158. Andrew L. Lovering, Jon P. Ride, Christopher M. Bunce, Julian C. Desmond, Stephen M. Cummings, and Scott A. White.; Crystal Structure of Prostaglandin D2 11-Ketoreductase (AKR1C3) in Complex with the Nonsteroidal Anti-Inflammatory Drugs Flufenamic Acid and Indomethacin. *Cancer Research* 64, 1802-1812, March 1, 2004
159. Trevor M. Penning, Michael E. Burczynski, Joseph M. Jez, Hseuh-Kung Lin, Haiching Ma, Margaret Moore, Kapila Ratnam, Nisha Palackal.; Structure-function aspects and inhibitor design of type 5 17 β -hydroxysteroid dehydrogenase (AKR1C3). *Molecular and Cellular Endocrinology* 171 (2001) 137-149.
160. Endo S, Matsunaga T, Kanamori A, Otsuji Y, Nagai H, Sundaram K, El-Kabbani O, Toyooka N, Ohta S, Hara A. Selective inhibition of human type-5 17 β -hydroxysteroid dehydrogenase (AKR1C3) by baccharin, a component of Brazilian propolis. *J Nat Prod.* 2012 Apr 27;75(4):716-21. doi: 10.1021/np201002x.
161. Zang T, Verma K, Chen M, Jin Y, Trippier PC, Penning TM. Screening baccharin analogs as selective inhibitors against type 5 17 β -hydroxysteroid dehydrogenase (AKR1C3). *Chemico-Biological Interactions* Volume 234, 5 June 2015, Pages 339–348.
162. Lin H-K, Jez JM, Schlegel BP, Peehl DM, Pachter JA & Penning TM.; Expression and characterization of recombinant type 2 3 α -hydroxysteroid dehydrogenase (HSD) from human prostate: demonstration of bifunctional 3 α /17 β -HSD activity and cellular distribution. *Molecular Endocrinology* 11 1971-1984, 1997
163. Gazvoda M, Beranič N, Turk S, Burja B, Kočevar M, Rižner TL, Gobec S, Polanc S. 2,3-Diarylpropenoic acids as selective non-steroidal inhibitors of type-5 17 β -hydroxysteroid dehydrogenase (AKR1C3). *Eur J Med Chem.* 2013 Apr; 62: 89-97. doi: 10.1016/j.ejmech.2012.12.045.
164. Aziz N, Maxwell MM, St Jacques B, Brenner BM Downregulation of Ke6, a Novel Gene Encoded within the Major Histocompatibility Complex, in Murine Polycystic Kidney Disease. (1993) *Mol Cell Biol.* 1993 Mar;13(3):1847-53. Erratum in: *Mol Cell Biol* 1993 Oct;13(10):6614.
165. N. Aziz, M. M. Maxwell and B. M. Brenner.; Coordinate regulation of 11 beta-HSD and Ke 6 genes in cpk mouse: implications for steroid metabolic defect in PKD. (1994) *Am J Physiol.* 1994 Nov;267(5 Pt 2):F791-7.
166. Michele M. Maxwell, Jacqueline Nearing, and Nazneen Aziz; Ke 6 Gene Sequence And Organization And Aberrant Regulation In Murine Polycystic Kidney Disease. (1995) *The Journal of Biological Chemistry* Vol. 270, No. 42, Issue of October 20, pp. 25213–25219

Literature

167. Georges Pelletier, Van Luu-The, Songyun Li, and Fernand Labrie. Localization of Type 8 17 β -hydroxysteroid Dehydrogenase mRNA in Mouse Tissues as Studied by In Situ Hybridization. *Journal of Histochemistry & Cytochemistry*, Volume 53(10): 1257-1271, 2005
168. Jianguo Liu, Zhifeng Zhang, Xiaoshi Ma, Shaoshuai Liang, Dandan Yang. Characteristics of 17 β -hydroxysteroid dehydrogenase 8 and its potential role in gonad of Zhikong scallop *Chlamys farreri*. *The Journal of Steroid Biochemistry and Molecular Biology* Volume 141, May 2014, Pages 77-86
169. J.Villar, J. Celay, M.M. Alonso, Mirja Rotinen, C. de Miguel, M. Migliaccio, I. Encío (2007) Transcriptional regulation of the human type 8 17 β -hydroxysteroid dehydrogenase gene by C/EBP β . *Journal of Steroid Biochemistry & Molecular Biology* 105 (2007) 131-139
170. Vladimir Z. Pletnev, William L. Duax, Rational proteomics IV: modeling the primary function of the mammalian 17 β -hydroxysteroid dehydrogenase type 8. *Journal of Steroid Biochemistry & Molecular Biology* 94 (2005) 327-335
171. Ricard Albalat, Frederic Brunet, Vincent Laudet, and Michael Schubert. Evolution of Retinoid and Steroid Signaling: Vertebrate Diversification from an Amphioxus Perspective. *Genome Biol. Evol.* 3:985-1005.
172. Peltoketo, H., LuuThe, V., Simard, J. and Adamski, J. (1999). 17 β -hydroxysteroid dehydrogenase (HSD)/17-ketosteroid reductase (KSR) family: nomenclature and main characteristics of the 17HSD/KSR enzymes. *Journal of Molecular Endocrinology* 23, 1-11.
173. Hiltunen JK, Autio KJ, Schonauer MS, Kursu VA, Dieckmann CL, Kastaniotis AJ. Mitochondrial fatty acid synthesis and respiration. *Biochim Biophys Acta*. 2010 Jun-Jul;1797(6-7):1195-202.
174. Zhijun Chen, Alexander J. Kastaniotis, Ilkka J. Miinalainen, Venkatesan Rajaram, Rik K. Wierenga, and J. Kalervo Hiltunen. (2009) 17 β -Hydroxysteroid dehydrogenase type 8 and carbonyl reductase type 4 assemble as a ketoacyl reductase of human mitochondrial FAS. *The FASEB Journal* 08/2009; 23(11):3682-91
175. Dejiang Feng, Andrzej Witkowski and Stuart Smith. Down-regulation of Mitochondrial Acyl Carrier Protein in Mammalian Cells Compromises Protein Lipoylation and Respiratory Complex I and Results in Cell Death. *J. Biol. Chem.* (2009) 284:11436-11445
176. J. Reinders, E.H. Rozemuller, P. van der Weide, A. Oka, P.J. Slootweg, H. Inoko, M.G. Tilanus Genes in the HLA region indicative for head and neck squamous cell carcinoma. *Molecular Immunology* 44 (2007) 848-855
177. Chen W, Song MS, Napoli JL. SDR-O: an orphan short-chain dehydrogenase/reductase localized at mouse chromosome 10/human chromosome 12. *Gene*, 2002 Jul 10;294(1-2):141-6
178. Laurent Barbe, Emma Lundberg, Per Oksvold, Anna Stenius, Erland Lewin, Erik Björling, Anna Asplund, Fredrik Pontén, Hjalmar Brismar, Mathias Uhlén, and Helene

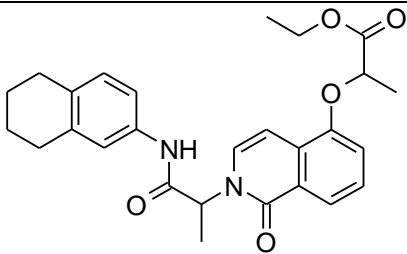
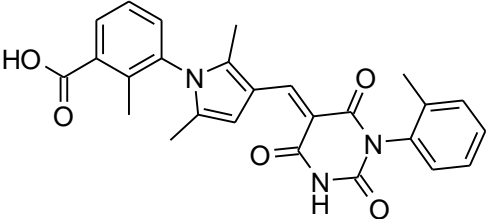
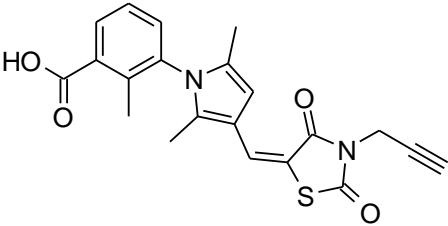
Literature

- Andersson-Svahn. Toward a Confocal Subcellular Atlas of the Human Proteome *Mol Cell Proteomics* March 2008 7: 499-508
179. Elena A. Lapshina, Olga V. Belyaeva, Olga V. Chumakova, Natalia Y Kedishvili. Differential recognition of the free versus bound retinol by human microsomal retinol/sterol dehydrogenases: characterization of the holo-CRBP dehydrogenase activity of RoDH-4. *Biochemistry* 02/2003; 42(3):776-84
180. Shanhong Tang, Liucun Gao, Qian Bi, Guanghui Xu, Simeng Wang, Guohong Zhao, Zheng Chen, Xiushan Zheng, Yanglin Pan, Lina Zhao, Jianqin Kang, Guitao Yang, Yongquan Shi, Kaichun Wu, Taiqian Gong, and Daiming Fan. SDR9C7 Promotes Lymph Node Metastases in Patients with Esophageal Squamous Cell Carcinoma. *PLoS One*. 2013; 8(1): e52184.
181. Ugochukwu E, Bhatia C, Huang J, Pilka E, Muniz JRC, Pike ACW, Krojer T, Von Delft F, Verdin EM, Oppermann U, Kavanagh KL. Crystal structure of the catalytic domain of human hydroxysteroid dehydrogenase like 2 (Hsd12). http://www.thesgc.org/sites/default/files/activeSite/SDHLA_3kvo_v1_372a/SDHLA_3kvo_v1_372a_index.html
182. Pfeifer SM, Furth EE, Ohba T, Chang YJ, Rennert H, Sakuragi N, et al. (1993) Sterol carrier protein 2: a role in steroid hormone synthesis? *J Steroid Biochem* 47: 167–172. doi: 10.1016/0960-0760(93)90071-4
183. Gallegos AM, Atshaves BP, Storey SM, McIntosh AL, Petrescu AD, Schroeder F. (2001) Sterol carrier protein-2 expression alters plasma membrane lipid distribution and cholesterol dynamics. *Biochemistry-US* 40: 6493–6506. doi: 10.1021/bi010217l
184. Puglielli L, Rigotti A, Greco AV, Santos MJ, Nervi F. (1995) Sterol carrier protein-2 is involved in cholesterol transfer from the endoplasmic reticulum to the plasma membrane in human fibroblasts. *J Biol Chem* 270: 18723–18726. pmid:7642518 doi: 10.1074/jbc.270.32.18723
185. Gallegos AM, Atshaves BP, Storey SM, Starodub O, Petrescu AD, Huang H, et al. (2001) Gene structure, intracellular localization, and functional roles of sterol carrier protein-2. *Prog Lipid Res* 40: 498–563. pmid:11591437 doi: 10.1016/s0163-7827(01)00015-7
186. Starodub O, Jolly CA, Atshaves BP, Roths JB, Murphy EJ, Kier AB, et al. (2000) Sterol carrier protein-2 localization in endoplasmic reticulum and role in phospholipid formation. *Am J Physiol-Cell Ph* 279: C1259–C1269.
187. Li NC, Fan J, Papadopoulos V, Sterol Carrier Protein-2, a Nonspecific Lipid-Transfer Protein, in Intracellular Cholesterol Trafficking in Testicular Leydig Cells. *PLoS One*. 2016 Feb 22;11(2):e0149728. doi: 10.1371/journal.pone.0149728. eCollection 2016.
188. J. Skogsberg, J. Lundstrom, A. Kovacs, R. Nilsson, P. Noori, S. Maleki, M. Kohler, A. 448 Hamsten, J. Tegner, J. Bjorkegren, Transcriptional profiling uncovers a network 449 of cholesterol-responsive atherosclerosis target genes, *PLoS Genet*. 4 (3) (2008) 450 e1000036. 451

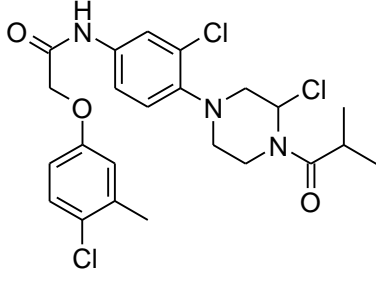
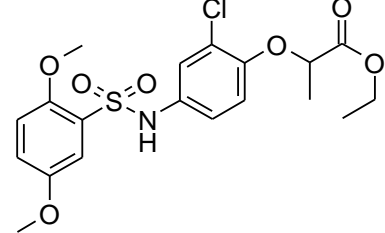
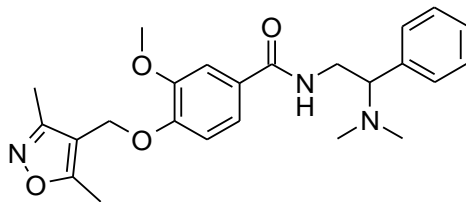
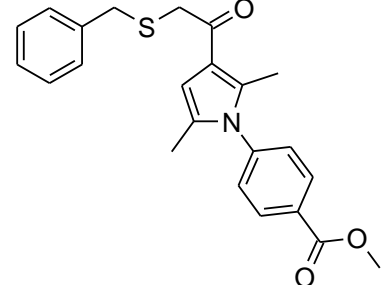
7 Appendix

7.1 Chemical structures of used compounds in screening assays as potent inhibitors of HSD17B3 and HSD17B5

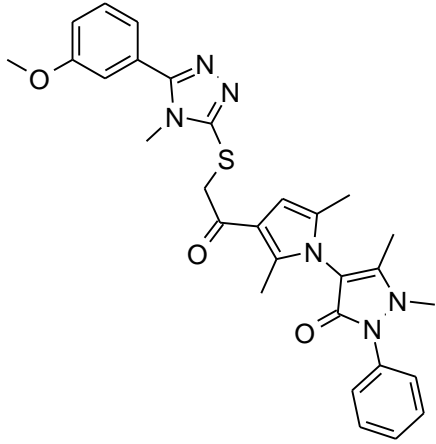
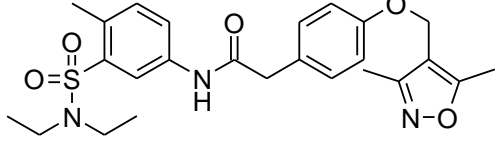
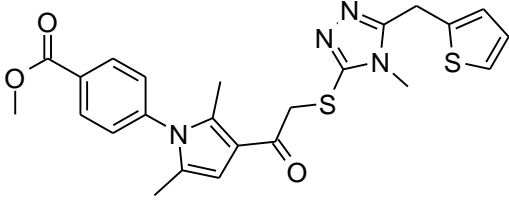
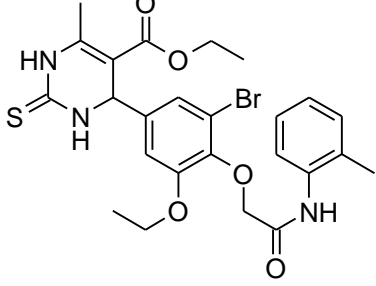
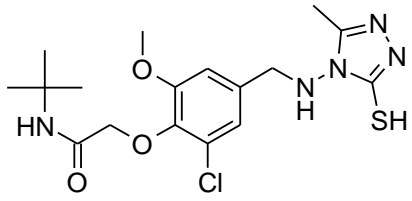
7.1.1 1st screening round

Number	Compound	Molecular Weight	Database/Name
1-1		452.46	IF Labs/ F1808-0160
1-2		457.48	Vitas-M/ STK201183
1-3		408.47	Vitas-M/ STK027936

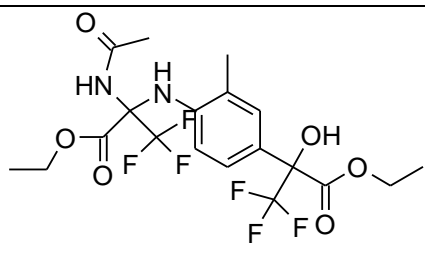
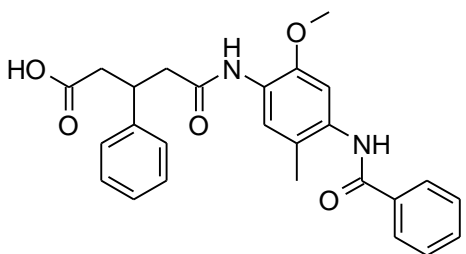
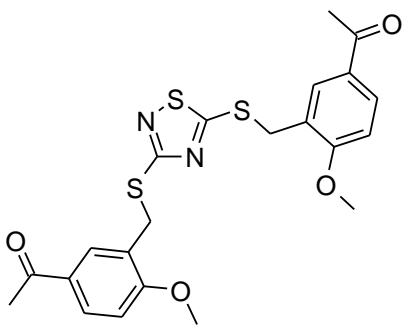
Appendix

Number	Compound	Molecular Weight	Database/Name
1-4		464.39	Vitas-M/ STK141979
1-5		443.90	Maybridge/ RDR 02467
1-6		423.51	Enamine/ T5214638
1-7		393.50	Enamine/ T5253714

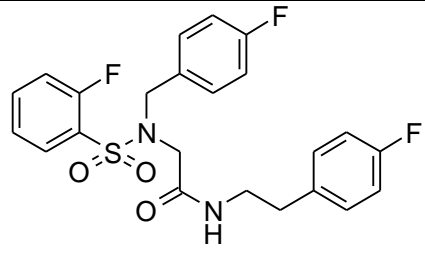
Appendix

Number	Compound	Molecular Weight	Database/Name
1-8		542.65	Enamine/ T5274599
1-9		485.60	Enamine/ T5363562
1-10		480.60	Enamine/ T5367602
1-11		562.48	Chembridge/7596803
1-12		413.92	Chembridge/7734886

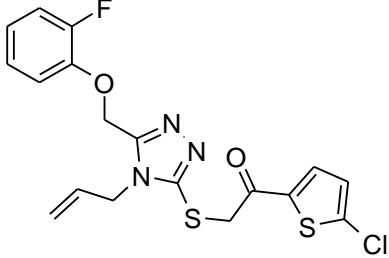
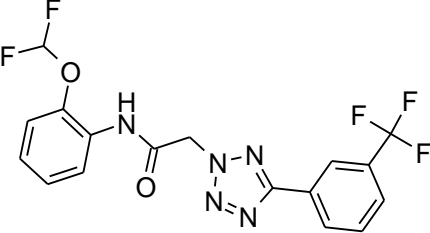
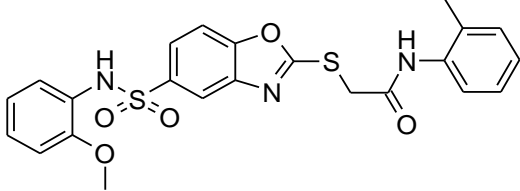
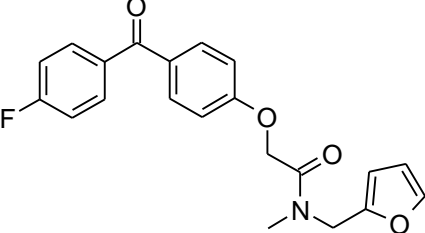
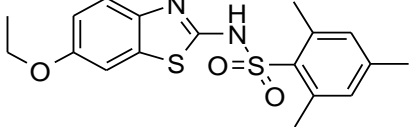
Appendix

Number	Compound	Molecular Weight	Database/Name
1-13		488.38	Maybridge/JFD 02140
1-14		446.50	Maybridge/HTS 06057
1-15		474.61	Maybridge/CD 08345

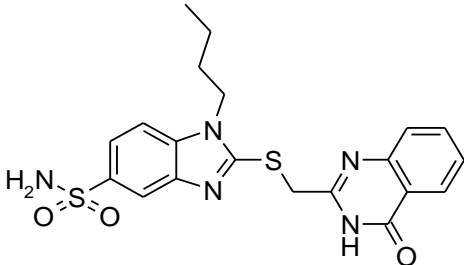
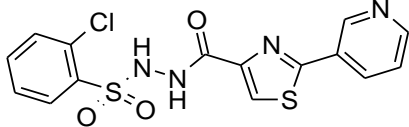
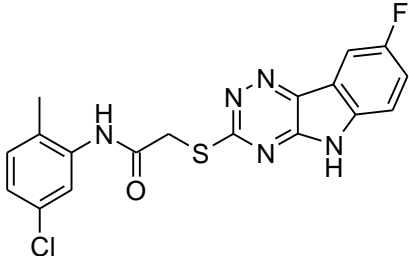
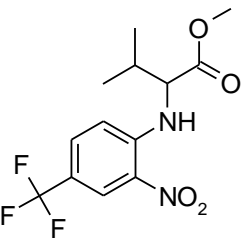
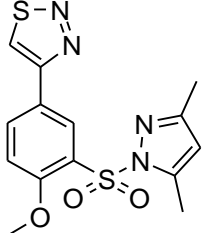
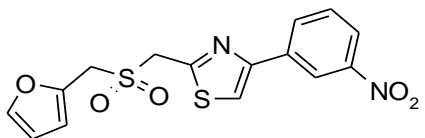
7.1.2 2nd screening round

Number	Compound	Molecular Weight	Database/Name
2-1		462.5	Enamine / T5373557

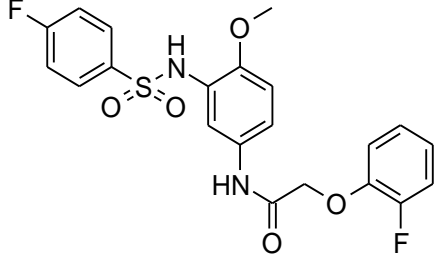
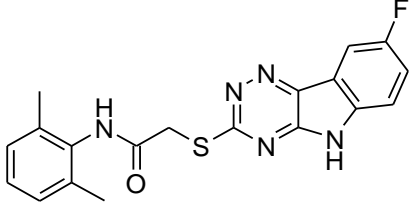
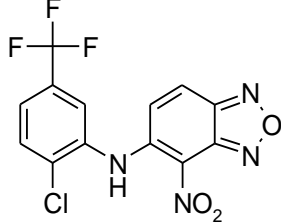
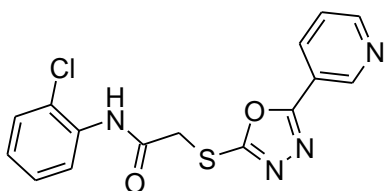
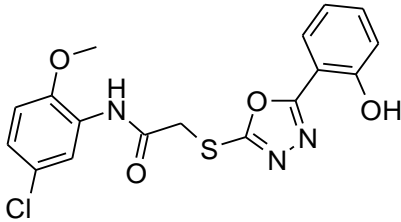
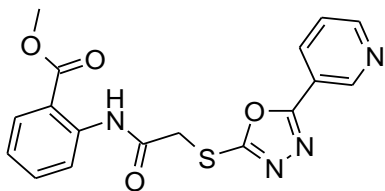
Appendix

Number	Compound	Molecular Weight	Database/Name
2-2		423.9	Enamine / T5278990
2-3		413.3	Enamine / 0514-7788
2-4		483.6	Enamine/ T0510-7338
2-5		367.4	Enamine/ T5363560 /
2-6	Structure not given	299.36	AG-690#13777239
2-7	Structure not given	251.3	AP-501#43179283
2-8		376.5	Specs/ AK-968#41024830

Appendix

Number	Compound	Molecular Weight	Database/Name
2-9		443.5	Enamine / T5223670
2-10		394.9	Maybridge/ MWP 00344
2-11		401.8	AsinexGold / BAS 02070553
2-12		320.3	AsinexGold /BAS 01259763
2-13		350.4	Maybridge/ NRB 00956
2-14		364.4	Maybridge/ KM 03219

Appendix

Number	Compound	Molecular Weight	Database/Name
2-15		448.4	Enamine/ T5261165
2-16		381.4	Specs/ AG-690#40720632
2-17		358.7	AsinexGold/ BAS 01237125 Specs/ AG-690#12618169
2-18		346.8	Specs/ AG-690#40696533
2-19		391.8	Asinex Gold/ BAS 01213203 Specs/ AG-690#13507574
2-20		370.4	AsinexGold/ BAS 01516658 Specs / AG-690#40696647

7.2 List of Figures

Figure 1 Ribbon diagram of human 17 β -Hydroxysteroid dehydrogenase type 1. β -strands (blue) and α -helices (red) compose two Rossmann folds enabling the cofactor NADP(H) (green) binding. The steroid substrate (estrone) is marked in yellow. Picture adapted from pdb, modified by J. Adamski.....	2
Figure 2 Oxido-reduction on example of 17 β -hydroxysteroid dehydrogenase type 1	4
Figure 3 Reaction mechanism for the reduction of estrone to estradiol by human HSD17B1 and the role of S-Y-K residues at catalytic center. Black arrows show hypotesized proton transfer during reaction; red arrow indicates the pro-S-hydrid transfer. Picture modified on base of a scheme at Deluca et al. 2004 [23].....	6
Figure 4 Ribbon diagram of human AKR1C3. Picture adopted from pdb (ID 1XF0).....	9
Figure 5 SDR catalytic amino acids (left) versus catalytic amino acids of AKRs (right) and hydride transfer on example of reduction reaction of carbonyl group. Picture modified on the base of the scheme after [25].....	9
Figure 6 Simplified scheme for mechanisms of hormone action.....	11
Figure 7 Simplified scheme of classical model for cellular mechanism of steroid hormone (A) and retinoid (B) action.....	15
Figure 8 Numbering rule of steroids shown in cholesterol molecule.....	16
Figure 9 Scheme of steroid hormone biosynthesis. The yellow star shows the place of action of the enzymes: 17 β -HSD type 3 and 5, being of interest in the inhibitor project of this PhD.....	20
Figure 10 3 α -hydroxysteroid oxidoreduction.....	21
Figure 11 3 β -hydroxysteroid oxidoreduction.....	22
Figure 12 3 β -hydroxysteroid dehydrogenases in steroidogenesis.....	23
Figure 13 Corticosteroid biosynthesis pathway and 11 β -hydroxysteroid oxidoreduction.....	24
Figure 14 20 α -hydroxysteroid oxidoreduction	24
Figure 15 Physiologically occurring retinoids in humans.....	29
Figure 16 Main activities of SDR enzymes in retinol oxidation pathway.....	30
Figure 17 Simplified scheme of classical chemical reaction involved in cyclic processes of saturated fatty acids β -oxidation and synthesis. Possible catalytic activities of SDR enzymes are marked on yellow. Fab enzymes represented by SDR members.....	32
Figure 18 Sulfatase and aromatase pathways of estrogen receptor activation. On yellow marked ligands of ER receptor.	39
Figure 19 Main metabolic pathway of androgens leading to activation of AR receptor. On yellow marked the most potent ligands of AR receptor.....	41
Figure 20 SDS-PAGE showing the homogenated bacteria lysate fractions from purification process of Bl21DE3 bacteria expressing human HSD17B5_GST fussion gene product. 1- protein marker; 2- not induced bacteria pellet; 3- IPTG induced bacteria pellet; 4- not induced bacteria supernatant; 5- IPTG induced bacteria supernatant; 6- aliquot from suspension after incubation the with GT-sepharose (after 3x washing with PBS : 500rpm, 5min) ; 7- first elution of cleaved from GST enzyme (after incubation with thrombin); 8- second elution; 9- third elution; 10- forth elution; 11-	

Appendix

concentrated from all elutes human 17 β -HSD5; 12- filtered human 17 β -HSD5; 13- molecular mass	50
Figure 21 The letters are corresponding to the following aliquots (asterix and the appropriate number is the reference to the SDS-PAGE above): A)- Intact bacteria suspension in PBS; B) – supernatant after bacteria lysis and centrifugation 4500rpm, 15min; C) - supernatant after lysis and subsequent centrifugation at 14000rpm, 30min; D) - suspension after incubation supernatant with GT-sepharose; E) - filtered eluat after GT-elution; F) - filtered eluat after incubation with thrombine; G) - aliquot of purified h17 β -HSD5 (after incubation with thrombine). Samples for given purification fraction were normalized by having the same part (1:250) of the first bacteria suspension in each final volume.	50
Figure 22 <i>In vitro</i> screening results of inhibitory effect of 15 tested substances (2 μ M) on human 17 β -HSD3 (blue) and 17 β -HSD5 (red) in reduction the androstene-3,14-dione to testosterone. In the graphics the inhibition is expressed as a percent (%) of enzymatic activity in the control assay without inhibitor (1%DMSO).	52
Figure 23 <i>In vitro</i> screening results of inhibitory effect of 20 tested substances from the second batch (2 μ M) on human 17 β -HSD3 and 17 β -HSD5 in reduction the androstene-3,14-dione to testosterone. In the graphics the inhibition is expressed as a percent (%) of enzymatic activity in the control assay without inhibitor (1%DMSO). The source of enzyme in assays for 17 β -HSD3 was stable transfected HEK293 cell pellets, while in case of 17 β -HSD5 homogenated bacteria lysates...54	54
Figure 24 Estimation of IC ₅₀ values for the strongest 17 β -HSD5 inhibitors selected from performed screenings. Curves on plots where fitted by use Sigma-Plot 'One site saturation' module. A) Compound concentration dependent inhibitory effect (%) on conversion of androstenedione to testosterone by 17 β -HSD5. B) The plot as above demonstrated in logarithmic scale. C) Calculated IC ₅₀ values for selected 17 β -HSD5 inhibitors (Sigma plot program).	56
Figure 25 Selectivity of 2-9 inhibitor among chosen 17--HSDs types. There was checked the inhibitory activity of 17 β -HSD3 and 17 β -HSD5 in conversion of androstenedione to testosterone, 17 β -HSD1 and 17 β -HSD7 in reduction of estradiol to estrone and in the case of 17 β -HSD2 and 17 β -HSD4 of estrone to estradiol.	57
Figure 26 A: Changes in absorbation (OD340) at growing NADH concentrations create a linear curve. B: Changes in fluorescence intensity (RFU) at growing NADH concentrations create a parabolic line.	58
Figure 27 Spectrum of NADH/NAD UV-Vis light absorption (left). NADH fluorescence emission spectrum at λ_{exc} 340nm (right).	59
Figure 28 Spontaneous oxidation of NADH during 1h incubation in water solution at 37 $^{\circ}$ C monitored as fluorescence signal depletion (λ_{exc} = 340nm, λ_{em} =450nm). A) Time progress plot for various NADH concentrations. B) Calculated loss of fluorescence intensity in % during incubation for various NADH concentrations.	60
Figure 29 Time progress curves during the oxidation of androstanediol to androsterone at the presence of NADP+ as cofactor by purified form of human 17 β -HSD5. A: Detection of NADPH growing absorbance at 340nm; B: Detection of the fluorescence intensity (λ_{exc} 340nm/ λ_{em} 450nm) is corresponding to the growing NADPH.	61
Figure 30 Michealis-Menten substrate saturation plot for oxidation the androstanediol to androsterone by purified human recombinant 17 β -HSD5 (55 μ g per sample). Km and Vmax values were calculated here manually by use Lineweaver-Burke plot. Initial velocities were calculated from linear time progress curves of 15min incubation.	61

Appendix

Figure 31 Time progress plots for various concentrations of substrate (5-100 μ M) in oxidation of androstenediol to androsterone in the presence of NADP ⁺ as cofactor (200 μ M) by purified form of 17 β -HSD5 (8,25 μ g) and homogenated lysate from IPTG induced bacteria expressing 17 β -HSD5 enzyme.....	62
Figure 32 IC ₅₀ estimated for assay with artificial substrate for HSD17B5. Picture adopted from [121].....	63
Figure 33 IC ₅₀ estimated for assay with artificial substrate for HSD17B5	64
Figure 34 Lineveaver-Burk-plot for the evaluation of K _i . Conversion of 8-acetyl-2,3,5,6-tetrahydro-1H, 4H-11-oxa-3a-aza-benzo[de]anthracen-10-one to fluorescent product catalysed by purified recombinant human 17 β HSD5 was monitored in the presence of inhibitory substance 2-9. Data were fitted by Sigma-Plot Kinetics module.....	65
Figure 35 The best fit for competitive model of inhibition. A: competitive model; B: uncompetitive model of inhibition. Sigma Plot calculations utilizing the one site saturation plots mechanism of inhibition determination.....	65
Figure 36 Western blot confirming the overexpression of human HSD17B5 in used for assay stable or transiently transfected HEK293 cell and no detectable endogenous expression.....	67
Figure 37 <i>In vitro</i> conversion of radio-labeled androstenedione to testosterone during 1h of incubation at 37°C at the presence of NADPH as cofactor and for used various cell pellets of different cell lines types expressing human HSD17B5.....	68
Figure 38 Optimization the amount of cells (HSD17B5 stable transfected MCF7) for 30% conversion <i>in vivo</i> during 24h incubation with radio-labeled androstenedione.....	69
Figure 39 HPLC chromatogram of radio-labeled substrate/product extracted form enzymatic assay with HSD17B5 stable transfected HEK293 cell lines converting androstenedione to testosterone..	70
Figure 40 HPLC chromatogram of radio-labeled substrate/product extracted form enzymatic assay with HSD17B5 stable transfected MCF7 cell lines converting androstenedione to testosterone.	70
Figure 41 Cell Titer-Glow 24h viability test with not transfected HEK293 cell.....	72
Figure 42 MTT 48h test with stable transfected HEK293 cells.....	72
Figure 43 Recombinant human HSD17B8 expressed in BL21DE (3) bacteria as GST-fusion protein. a)SDS-PAGE, b) Western blot. Arrows show human GST-HSD17B8 fusion protein. P+ bacteria pellet induced, P- bacteria pellet not induced, S+ supernatant induced, S- supernatant not induced. Human HSD17B8 appear to be insoluble in a supernatant from lysed bacteria in the where the most of recombinant protein remains in the pellet after centrifugation.....	74
Figure 44 Protein expression in Rossetta2Lys, isolation and purification. Coomassie-stained PAGE. Arrow shows the recombinant SDR-O_GST fusion protein.....	75
Figure 45 Protein expression in Rossetta2Lys, isolation and purification. Commasie-stained PAGE. Arrow shows the recombinant HSDL2_GST fusion protein.....	76
Figure 46 Amino acid sequences of human HSD17B8 with marked SDR specific motifs in the context of recognized secondary structure (available at PDB, SGC; entry code: 2PD6).....	77
Figure 47 Amino acid sequences of human SDR-O with marked SDR specific motifs in a context of recognized secondary structure deduced from primary amino acid sequence by use of Psiprep program http://bioinf.cs.ucl.ac.uk/psipred/	78
Figure 48 Amino acid sequences of human HSDL2 with marked SDR specific motifs in a context of recognized secondary structure for SDR domain of the protein (available at PDB, SGC; entry code: 3KVO). Legend see table below.	78
Figure 49 Fragment of multiple alignment. The secondary structure is corresponding to deduced one of SDR-O. Marked on lila: acidic key residues.....	81

Appendix

Figure 50 Fragment of multiple alignment. The secondary structure is corresponding to HSDL2. Marked on blue: basic key residues.....	82
Figure 51 Amino acid sequences with identified chosen domain by Pro Dom program.....	86
Figure 52 Cytoplasmatic distribution of pcDNA4_C'MycHis (a) and pcDNA3_C'Flag (b) control vectors without insert (Green). Nuclear DNA was stained with Hoechst 3433 (blue). Subcellular localization was revealed with anti-Myc (monoclonal) and anti -Flag antibodies (polyclonal), respectively and subsequently with Alexa Fluor 488 secondary antibodies.	88
Figure 53 Intracellular localization of HSD17B8_C'myc tagged fusion protein. a) nucleus, b) stained mitochondria, c) mitochondria co-localization of HSD17B8_C'myc, d) overlay of pictures b) and c).	89
Figure 54 Intracellular localization of HSD17B8_N'flag tagged fusion protein. a) nucleus, b) stained mitochondria, c) delocalized in the cytoplasm HSD17B8_N'flag tagged fusion protein, d) overlay of pictures b) and c).....	89
Figure 55 Representative subcellular localization of SDR-O expressed as N- or C- tagged protein in HeLa cells.	90
Figure 56 Counterstaining with the endoplasmatic reticulum (red) human N'Flag_SDR-O (green)..	90
Figure 57 Counterstaining with early endosome markers (green); human SDR0_N'Myc (red).....	91
Figure 58 Counterstaining with peroxisomes markers (red); human SDR0_N'Myc (green).	91
Figure 59 Counterstaining with mitochondria: N' Flag_SDR-O.....	92
Figure 60 Subcellular localization of human HSDL2 recombinant protein in HeLa cells: co-localization of human recombinant N'tagged HSDL2with human HSD17B4 in peroxisomes. Red – HSD17B4 (in peroxisomes), green – N'myc-HSDL2.....	92
Figure 61 Counterstaining with mitochondria: red-mitochondria; green – C'Myc-HSDL2.....	93
Figure 62 cDNA synthesis from mRNA expression control in pcDNA3_SDR-O or pcDNA3_HSDL2 transiently transfected HEK293 cells.....	94
Figure 63 Comparison of all-trans-retinal conversion into all-trans-retinol at the presence of NADH by SDR-O in bacteria cell lysate and transfected HEK293 cells.....	97
Figure 64 Results of conversion or all-trans-retinal or all-trans-retinol by transfected with HSDL2 or SDR-O HEK293 cells or bacteria in the presense of NADH/NADPH or NAD/NADP, respectively (F. Haller, HMMG, IEG).....	98
Figure 65 Western-blot layer composition.....	110
Figure 66 Graphical visualization of IC ₅₀ determination.....	131
Figure 67 Reduction of androstendione to testosterone by human 17β-HSD3 and 17β-HSD5.....	146
Figure 68 Catalyzed by human 17β-HSD5 oxidation of 3α-androstanediol to androsterone. NADP(H) is more preferable cofactor than NAD(H) for 17β-HSD5. However by use of sensitive measurement methods the conversion by use of NAD(H) may be also detected.	149
Figure 69 The keto-form of the substrate 8-acetyl-2,3,5,6-tetrahydro-1H,4H-11-oxa-3a-aza-benzo[de]anthracen-10-one is effectively reduced by 17β-HSD5 in the presence of NADPH as cofactor to its hydroxy-form that gives a fluorescence signal with a maximum at λ=510nm when excited at λ=450nm (Figure adapted from [121].....	150
Figure 70 Mechanism of catalysis by 17β-HSD5. Picture modified on base of the scheme <i>Byrns et al</i> [128].....	155
Figure 71 Workflow of the BioNetWorks inhibitor project. Picture modified after [126].	161
Figure 72 Structure of human 17β-HSD8. Picture adapted from PDB database (PDB: 2pd6).....	163
Figure 73 Few examples of numerous captures showing the subcelular pattern of human SDR-O counterstained with ER markers: A: N'Flag-SDR-O, B: Second column depict endoplasmatic	

Appendix

reticulum (pDsRed_ER from Clontech which contains a fused with red fluorescent marker ER signaling sequence of carleticulin); Third column shows overlay images of SDR-O (green), ER (red) and nucleus (blue).....	169
Figure 74 Staining pattern for SDR-O antibodies in three various human cell lines: A) U-251, B) A-431 C) U-2 OS. Pictures adapted from http://www.proteinatlas.org/ENSG00000170426/subcellular [152].	170
Figure 75 Resolved homodimeric crystal structure of HSDL2 SDR catalytic domain in complex with NADP cofactor. Picture adopted from PDB database. PDB code: 3KVO [155].	174
Figure 76 Two reported alternative splicing products of human HSDL2 gene: isoform1 and isoform2 UniProt. <i>Genome Research "The status, quality, and expansion of the NIH full-length cDNA: the Mammalian Gene Collection (MGC)", The MGC Team Project, 2004.</i> Fragment of amino acid sequence marked on green is excised in alternative splicing isoform 2. Yellow marked amino acid are putative catalytic triad S-Y-K.	177

7.3 List of Tables

Table 1 Conserved sequence motifs of SDR family [9].	3
Table 2 Main differences between particular SDR subfamilies (<i>Persson et al., 2003</i>); [9].	4
Table 3 Examples of substrates catalyzed by human SDR enzymes.	5
Table 4 Examples of intracellular receptors and corresponding ligands being metabolites of SDR substrates	13
Table 5 Types of hormone intracellular action and activation of nuclear receptor. Table modified after [34] and [35].	14
Table 6 List of example human SDR enzymes involved in retinoid metabolism.	31
Table 7 List of example human SDR enzymes involved in fatty acid metabolism.	34
Table 8 Examples of diseases associated with impaired activity of SDR enzymes.	36
Table 9 Cancers and other disorders involved with up-regulated expression of 17-HSDs.	42
Table 10 Values of inhibitions results (%) for the first batch of compounds tested <i>in vitro</i> as potent inhibitors against reductive activity of 17 β -HSD3 and 17 β -HSD5. Values marked on yellow indicates compounds with inhibition over 40%.	52
Table 11 Second round of BNW compounds numbered from 2-1 to 2-20 screening their potential inhibitory activity towards 17 β -HSD3 and 17 β -HSD5 in reduction of androstenedione to testosterone. Values marked on yellow indicate compounds with inhibition over 50%.	54
Table 12 IC ₅₀ values for different cell line assays with or without serum.	71
Table 13 Listed SDR characteristic motifs according to <i>Persson et al. 2003</i> [9].	79
Table 14 Blastp selected sequences, ClustalW2 alignment for homology and similarity search, multiple alignment.	83
Table 15 Blastp selected sequences, ClustalW2 alignment for homology and similarity search, multiple alignment.	83
Table 16 Amino acid sequence similarity and identity of chosen SDR proteins compared to full amino acid sequence of HSDL2 (red) and to SDR domain of HSDL2 (1-293aa)solely (black). http://www.ebi.ac.uk , EMBOSS Pairwise alignment algorithms (matrix: Blosum62, open gap penalty: 10.0,	

Appendix

gap extension penalty: 0.2, algorithm: 'water') Few sequences were additionally proven in 'needle' algorithm (Needleman-Wunsch algorithm).....	84
Table 17 Identified domains by ProDom program.....	85
Table 18 The list of ³ H radio-labeled steroid substrates used in assays for activity screening studies of human HSDL2, SDR-O and HSD17B8. The last three columns show screening results for three enzymes.....	95
Table 19 Retinoid substrates tested in assays with HEK293 cell pellets over-expressing human HSD17B8, SDR-O, and HSDL2. Results signed with a yellow star were repeated in assays with suspension of bacteria pellet.....	96
Table 20 List of used Flask for cell transfection.....	106
Table 21 Vector constructs for intracellular localization analysis of chosen SDR proteins.....	121
Table 22 Summary of organelle counterstaining.....	122
Table 23 Antibodies used for visualisation.....	123
Table 24 HPLC parameters of mobile phase for utilized substrate-product analytes.....	127
Table 25 List of utilized primary antibodies.....	134
Table 26 List of utilized secondary antibodies.....	134
Table 27 List of used primers.....	135
Table 28 List of selected the best inhibitory compounds against activity of 17 β -HSD5 from two screening rounds (results from repeated experiments).....	152
Table 29 Physiological and artificial human 17 β -HSD5 substrates of various affinity to the enzyme.....	155
Table 30 IC ₅₀ values for the same compound in various types of enzymatic assay.....	158
Table 31 Examples of 17 β -HSD5 inhibitors.....	159

7.4 List of publications and presentations

1. Kowalik, D. ; Haller, F. ; Adamski, J. & Möller, G.: In search for function of two human orphan SDR enzymes: Hydroxysteroid dehydrogenase like 2 (HSDL2) and short-chain dehydrogenase/reductase-orphan (SDR-O). *J. Steroid Biochem. Mol. Biol.* 117, 117-124 (2009)
2. Schuster, D. ; Kowalik, D. ; Kirchmair, J. ; Laggner, C. ; Markt, P. ; Aebischer-Gumy, C.; Ströhle, F. ; Möller, G. ; Wolber, G. ; Wilckens, T. ; Langer, T. ; Odermatt, A. ; Adamski, J. Identification of chemically diverse, novel inhibitors of 17 β -hydroxysteroid dehydrogenase type 3 and 5 by pharmacophore-based virtual screening. *J. Steroid Biochem. Mol. Biol.* 125, 148-161 (2011)
3. Möller, G. ; Husen, B. ; Kowalik, D. ; Hirvelä, L. ; Plewczynski, D. ; Rychlewski, L. ; Messinger, J. ; Thole, H. ; Adamski, J. Species used for drug testing reveal different inhibition susceptibility for 17beta-hydroxysteroid dehydrogenase type 1. *PLoS ONE* 5:e10969 (2010)
4. Möller G, Deluca D, Gege C, Rosinus A, Kowalik D, Peters O, Droescher P, Elger W, Adamski J, Hillisch A. : Structure-based design, synthesis and in vitro characterization of potent 17 β -hydroxysteroid dehydrogenase type 1 inhibitors based on 2-substitutions of estrone and d-homo-estrone. *Bioorg. Med. Chem. Lett.* 19, 6740-6744 (2009)

Appendix

Posters:

5. In search for function of two human orphan SDR enzymes: Hydroxysteroid dehydrogenase like 2 (HSDL2) and short-chain dehydrogenase/reductase-orphan (SDR-O). Kowalik, D. ; Haller, F. ; Adamski, J. & Möller, G.:18th International Symposium of the Journal of Steroid Biochemistry and Molecular Biology, September 18-21, 2008, Seefeld, Austria
6. Pharmacophore-based virtual screening for the identification of novel inhibitors of 17 β -hydroxysteroid dehydrogenases type 3 and 5. Schuster, D.; Kowalik, D.; Kirchmair, J.; Laggner, C.; Markt, P.; Aebischer-Gumy, C.; Möller, G.; Wolber, G.; Wilckens, T.; Langer, T.; Odermatt, A.; Adamski, J. Congress of Steroid Research, March 27-29, 2011, Chicago, USA